

# Discovery of antibodies with pH-dependent binding towards snake venom toxin

**Ej Efternavn, Tulika**

*Publication date:*
2023

*Document Version*
Publisher's PDF, also known as Version of record

# Discovery of antibodies with pH-dependent binding towards snake venom toxin

Tulika
PhD Thesis
Technical University of Denmark

# Discovery of antibodies with pH-dependent binding towards snake venom toxin

PhD thesis by
Tulika

Supervisor: Andreas H. Laustsen-Kiel
Co-supervisor: Alexander Kai Buell
Department of Biotechnology and Biomedicine
Technical University of Denmark
January 2023

# Table of Contents

# Preface

The work presented in this thesis was carried out from February 2020 to January 2023 at the Department of Biotechnology and Biomedicine at the Technical University of Denmark. The main supervisor for the thesis was Prof. Andreas H. Laustsen-Kiel and the co-supervisor was Prof. Alexander Kai Buell. The PhD project was funded by European Research Council (ERC) under the European Union's Horizon 2020 research and innovation programme (grant no. 850974).

The mice studies presented in manuscript I were conducted in Instituto Clodomiro Picado.

A significant part of the research outlined in manuscript III was carried out during an external stay at the Laboratory of Adaptive Immunity and Homeostasis at the University of Oslo, from May to October 2022. The project was supervised by Prof. Jan Terje Andersen and Dr. Fulgencio Ruso-Julve during this period.

The figures included in Chapter 1, Chapter 3, and Chapter 5 were created using Biorender.com.

## Acknowledgements

As I look back at the three years of my PhD journey, I can't help but feel grateful for the support and encouragement I received along the way. I would like to start by expressing my gratitude towards my PhD supervisor Andreas. Thank you, Andreas, for believing in me, especially in the times when I didn't have faith in myself. I am particularly referring to the last two extremely stressful months of my PhD. I remember sending you an email at midnight during the Christmas break, telling you how impossible it is for me to make it. And I remember your call the very next morning, and how calmly you debunked my concerns and helped me visualize a plan to finish my PhD in time. You must know that that conversation gave me the needed fresh wave of confidence to finish the last sprint of my PhD. I also want to thank you for the critical and often brutally straightforward feedback you have provided throughout my PhD. Although, they were a bit difficult for me to digest when I started my PhD with you, now when I look back, I can say that they have enabled the beginning of my transformation from (in your words), a 'little girl' to an 'Amazona warrior woman'!

I would also like to extend my gratitude towards my co-supervisor Prof. Alexander Kai Buell for the invaluable insights and suggestions he has provided in this project.

During my PhD, I had the privilege to carry out my external research stay at the amazing Laboratory of Adaptive Immunity and Homeostasis at the University of Oslo. I am truly thankful to Prof. Jan Terje Andersen and his research team for being such wonderful and welcoming hosts. I am grateful to Jan for all the inspiring meetings he held with me to discuss my project and for providing some of the most critical insights to this project. I am also thankful to Dr. Fulgencio Ruso Julve, or should I say Ful, for patiently answering all my questions, helping me with my day-to-day experiments, and keeping me company with fun conversations almost every day over lunch for the six months of my stay in Oslo.

This PhD would not have been possible without the support of the wonderful members of the Center of Antibody Technologies: Andreas, Markus, Anne, Rasmus, Shirin, Jack, Christoffer, Charlotte, Esperanza, Yessica, Giang, Anna, Line, Tim, Cecilie, Carol, Pelle, Selma, Arijit, Helen, Lorenzo, Camilla, and Tasja. You all have been so helpful, kind, and fun. I would also like to extend my gratitude to our collaborators at the National Biological Facility who have produced dozens of antibodies that were crucial for this PhD project.

To not lose sanity when stuck in the cycle of worry, it often becomes necessary to express and let out the built-up stress. Thank you, Jack, Charlotte, Shirin, Giang, Christoffer, and Markus for lending your ears and time to my rants on the bad days, and somehow redirecting me towards more hopeful thoughts.

For the corrections and feedback on this PhD thesis, I am immensely thankful to Andreas, Markus, Anne, Jack, Christoffer, Cecilie, and Pelle. I really appreciate all your critical feedback and how quickly you provided them. And a special thank you goes to Markus for teaching me the very important lesson of how not to vomit a rainbow on a crystal structure figure.

I would also like to thank Billy who has been my anchor during this challenging journey. Yes, your Indian cuisine culinary skills are still a work in progress, but you should know that your efforts to cook Indian food to bribe me to eat when I was too stressed or simply just grumpy, are highly appreciated. Finally, I am grateful to my family and my friend Pallavi, who despite being thousands of kilometres away from me, have extended their support in whatever way possible. I am truly overwhelmed by the amount of encouragement and love you have sent my way.

# Abstract

Snakebite envenoming is a neglected tropical disease that kills 81,000 to 138,000 people each year and leaves many more with permanent sequelae. The only specific treatment for snakebite envenoming relies on animal-derived (traditional) antivenoms. Although these antivenoms have saved countless lives, they are plagued with several drawbacks, such as eliciting adverse reactions, a requirement for high doses, and low therapeutic content. Consequently, researchers are working to develop alternative treatment strategies. Prominently featuring among them are oligoclonal recombinant antivenoms, which are based on mixtures of recombinantly produced (human) monoclonal antibodies targeting medically relevant snake venom toxins. Since such antivenoms will contain antibodies that are more compatible with the human immune system, they will have a lower risk of eliciting adverse reactions in the patients. Plus, with high therapeutic content, they are likely to require lower treatment doses than traditional antivenoms. Additionally, the cost of manufacturing oligoclonal recombinant antivenoms is estimated to be competitive or even lower in the future compared to traditional antivenoms, which may further reduce treatment costs. Indeed, both reduced dosing and cost are crucial for the successful implementation of recombinant antivenoms. A potential solution to achieving lower dosing requirements, and consequently reduced treatment costs, can be achieved by the application of monoclonal antibodies that bind their cognate antigen in a pH-dependent manner, also known as recycling antibodies. Such antibodies bind antigens at the neutral pH in the bloodstream and dissociate from them in the acidic environment of endosomes. This allows the antibodies to be recycled back into circulation via neonatal Fc receptor (FcRn)-binding, while the antigen is destined for lysosomal degradation. Thus, compared to a non-recycling antibody, that binds antigen only once per binding site, a single recycling antibody can bind and eliminate multiple antigens in its lifetime. This enables recycling antibodies to achieve therapeutic effects at lower doses than non-recycling antibodies, and may thus find utility for the development of low-cost recombinant antivenoms.

In this thesis, I have worked on discovering antibodies that target snake toxins in a pH-dependent manner using phage display technology. While histidine doping in the variable domains of antibodies is the most used strategy to introduce pH-dependent binding, I explored whether pH-dependent antigen-binding antibodies can be discovered directly from a naïve human antibody library that consists of naturally occurring variable domains. Indeed, an antibody with pH-dependent binding towards the α-cobratoxin (α-cbtx) was discovered and found to be entirely devoid of histidines in its paratope. The findings of the study demonstrate that pH-dependent antigen-binding antibodies can be discovered from antibody libraries with naturally occurring variable domains, and that pH-dependent interactions can, at least at times, be derived from non-histidine amino acid residues.

Next, it was investigated whether light-chain shuffling can be employed as a strategy to enhance the pH-dependent antigen-binding properties of pre-existing antibodies. Light-chain shuffled libraries of two myotoxin-II (M-II)-targeting antibodies and one α-cbtx-targeting antibody were generated and coupled to phage display for

selection of pH-dependent antigen-binding antibodies. This resulted in the discovery of an M-II- and an α-cbtx-targeting pH-dependent antibody, thus demonstrating the utility of the employed strategy.

For efficient performance of antibodies with pH-dependent antigen-binding properties, it is crucial that they are efficiently rescued via FcRn binding. However, it has been found that biophysical properties of the fragment antigen-binding region (Fab) and antigen-binding can influence the FcRn-mediated rescue of antibodies. Thus, the discovered pH-dependent antigen-binding antibodies were further studied for their interaction with FcRn and their behavior in a cellular assay, which revealed distinct effects of Fab and antigen-binding on the cellular transport properties of the antibodies. Finally, by employing cellular assays, the study demonstrated that the discovered antibodies with pH-dependent antigen-binding properties performed as recycling antibodies.

While recycling antibodies against snake venom toxins have been discovered in this project, it is important to note that snakebite envenoming involves complex toxicokinetics, and the utility of recycling antibodies in such a setting is not known. Nevertheless, this PhD thesis explored antibody libraries with natural domains, light-chain shuffling, phage display selection strategies, and cellular assays for the discovery and validation of pH-dependent antigen-binding antibodies. Additionally, the role of Fab and antigen-binding on the cellular transport properties of these antibodies were explored, which provided insights into factors that could affect their performance as recycling antibodies. Thus, it is my hope that the studies presented in this thesis can enable further understanding of how to discover and engineer pH-dependent antigen-binding antibodies, and that the methodologies developed in the work behind this thesis can find applications in snakebite envenoming as well as other indications, such as oncology, autoimmunity, infectious diseases, and general protein science.

# Sammenfatning

Forgiftning som resultat af bid fra en giftig slange, er en negligeret tropisk sygdom, der hvert år dræber 81,000 til 138,000 mennesker og efterlader mange flere med permanente følgesygdomme. Den eneste specifikke behandling af forgiftning er afhængig af (traditionel) modgift produceret i dyr. Selvom disse modgifte har reddet et utal af liv, er de plaget af ulemper, de kan udløse negative reaktioner, krav på høje doser, og lav terapeutisk værdi. Som konsekvens af disse ulemper, arbejder forskere på at udvikle alternative behandlings strategier. Fremstående af disse er oligoklonale rekombinante modgifte, som er baseret på en blanding af rekombinant-produceret (menneskelige) monoklonale antistoffer rettet mod medicinsk relevante slangegift toksiner. Eftersom disse modgifte består af antistoffer der er kompatible med det menneskelige immunforsvar, vil der være en lavere risiko for at udløse skadelige reaktioner i patienten. Derudover vil det høje terapeutiske indhold betyde at de sandsynligvis vil kræve en mindre dosering end traditionel modgift. Det er estimeret at prisen for at producere oligoklonale rekombinante modgifte i fremtiden vil kunne konkurrere med prisen på de traditionelle modgifte, hvilket vil medføre en reduktion i prisen for behandling af forgiftning. Reduceret dosering og pris vil være afgørende for at kunne implementere rekombinante modgifte succesfuldt. En potentiel løsning for at opnå reduceret doserings krav og derfor en lavere pris for behandling, kan være benyttelsen af monoklonale antistoffer som binder deres relaterede antigen i en pH-afhængig manér, også kendt som genbruglige antistoffer. Denne type antistoffer binder antigenet ved neutral pH i blodet og adskiller sig fra dem i endosomets syrlige miljø. Det vil tillade antistofferne at blive genindført i blodcirkulationen via neonatal Fc receptorer (FcRn)-binding, mens antigenet er øremærket til degradering i lysosomet. Sammenlignet med ikke-genbrugelige antistoffer, som kun binder antistoffet en enkelt gang per bindingspunkt, kan et enkelt genbrugeligt antistof binde og eliminere flere antigener i sin livstid. Genbrugelige antistoffer kan derfor opnå terapeutisk effekt ved lavere doser end ikke-genbrugelige antistoffer, og dermed give potentiale til at udvikle rekombinante antistoffer til en lavere pris.

I denne Ph.d-afhandling, har jeg arbejdet med at finde antistoffer der er rettet mod slange toksiner i en pH-afhængig manér, ved hjælp af fag display teknologi. Selvom den mest anvendte strategi til at introducere pH-afhængig binding er via histidine doping af antistoffers variable region, så har jeg udforsket muligheden for at finde antistoffer som binder med en pH-afhængig manér, direkte fra et naivt bibliotek af menneskelige antistoffer med naturligt forekommende variable regioner. Et antistof med pH-afhængig binding mod α-cobratoxin (α-cbtx) blev fundet og viste sig at være helt tomt for histidiner i dets paratope. Fundene i dette studie demonstrerer at det er muligt at finde pH-afhængig antigen-bindende antistoffer fra biblioteker med antistoffer med naturligt fremkommende variable regioner og at pH-afhængige interaktioner i nogle tilfælde kan stamme fra ikke-histidin aminosyrer.

Det blev også undersøgt om det var muligt at forøge de pH-afhængige antigen-bindings egenskaber på allerede eksisterende antistoffer ved at udføre light-chain shuffling. Light-chain shuffled biblioteker af to myotoxin-II (M-II)-bindende antistoffer og en α-cbtx-bindende antistof blev genereret og brugt til fag display til selektion af pH-afhængig

antigen-bindende antistoffer. Ud fra dette blev der fundet et M-II- og et α-cbtx-bindende pH afhængigt antistof, hvilket demonstrerer anvendeligheden af den brugte strategi.

Det er afgørende for præstationen af antistoffer med pH-afhængige antigen-bindings egenskaber at de effektivt kan blive reddet via FcRn binding. Det er blevet påvist at de biofysiske egenskaber af fragment antigen-bindende region (Fab) og antigen-binding kan have indflydelse på redningen af antistoffer gennem FcRn binding. De fundene pH-afhængige antigen-bindende antistoffer blev derfor undersøgt i en cellulær analyse, som afslørede at bindingen mellem Fab og antigenet har en tydelig effekt på de cellulære transportegenskaber af antistofferne. Ved hjælp af cellulære analyser blev det demonstreret at de fundene antistoffer med pH-afhængige antigen-binding optrådte som genbrugelige antistoffer.

Selvom der blev opdaget genbruglige antistoffer i dette projekt, er det vigtigt at understrege at slangebids forgiftning involverer komplekse toxicokinetics, og nytten af genbrugelige antistoffer i sådan et omfang ikke er kendt. I denne Ph.d-afhandling blev biblioteker bestående af antistoffer med naturlige domæner, ligth-chain shuffling, fag display selektions strategier, og cellulære analyser benyttet til at finde og validere pH-afhængige antigen-bindende antistoffer. Fab og antigen-bindingens rolle i den cellulære transport af antistoffer, blev udforsket, hvilket har givet indblik i faktorer som kunne have indflydelse på antistoffernes genanvendelighed. Det er mit håb at studierne i denne Ph.d-afhandling kan muliggøre en dybere forståelse for hvordan man kan opdage og designe pH-afhængige antigen-bindende antistoffer, og at metodologierne udviklet kan finde applikationer i slangebids forgiftninger såvel som andre felter, såsom onkologi, autoimmune sygdomme, infektionssygdomme og protein forskning som helhed.

# Publications

## Papers included in this thesis

**Paper I - Advances in antibody phage display technology.** Ledsgaard, L., Ljungars, A., Rimbault, C., Sørensen, C.V., Tulika, T., Wade, J., Wouters, Y., McCafferty, J. and Laustsen, A.H., 2022. *Drug Discovery Today.*

**Manuscript I - Antibody-dependent enhancement of toxicity of myotoxin II from Bothrops asper.** Sørensen, C.V., Fernández, J., Adams, A.C., Wildenauer, H.H.K., Schoffelen, S., Ledsgaard, L., Pucca, M.B., Fiebig, M., Cerni, F.A., Tulika, T., Karatt-Vellatt, A., Morth, J.P., Ljungars, A., Grav, L.M., Lomonte, B, Laustsen, A.H.
*Manuscript in preparation.*

**Manuscript II - Phage display assisted discovery of a pH-dependent anti-α-cobratoxin antibody from a natural variable domain library.** Tulika, T., Pedersen R.W., Rimbault, C., Ahmadi, S., Ledsgaard, L., Bohn, M-F., Ljungars, A., Voldborg B.G., Ruso-Julve, F., Andersen, J.T., Laustsen, A.H.
*Manuscript in preparation*

**Manuscript III – Discovery, engineering, and characterization of recycling antibodies targeting snake toxins.**
Tulika, T., Ruso-Julve, F., Ahmadi, S., Ljungars, A., Wade. J., Bohn. M-F., Sørensen C.V., Ledsgaard. L., Voldborg. B.G., Schoffelen. S., Lomonte. B., Andersen J.T., Laustsen, A.H.
*Manuscript in preparation*

## Papers not included in this thesis

**AHA: AI-guided tool for the quantification of venom-induced haemorrhage in mice.** Jenkins, T.P., Laprade, W.M., Sánchez, A., Tulika, T., O'Brien, C., Sørensen, C.V., Stewart, T.K., Fryer, T., Laustsen, A.H., Gutiérrez, J.M., *Accepted for publication in Frontiers in Tropical Diseases*.

**Deep mining of complex antibody phage pools.** Tulika, T. and Ljungars, A. *Accepted for publication in Methods in Molecular Biology*.

# Abbreviations

| | |
|---|---|
| 3FTx | Three-finger toxin |
| α-cbtx | α-cobratoxin |
| BLI | Bio-layer interferometry |
| CDRs | Complementarity determining regions |
| DELFIAs | Dissociation-enhanced lanthanide fluorescence immunoassays |
| ENC | Expression-normalized capture |
| Fab | Fragment antigen-binding |
| FcγRIIb | Fcγ receptor IIb |
| Fc region | Fragment crystallizable region |
| FcRn | Neonatal Fc receptor |
| FRs | Framework regions |
| HERA | Human endothelial cell-based recycling assay |
| Ig | Immunoglobulin |
| mAb | Monoclonal antibody |
| M-II | Myotoxin II |
| nAChR | Nicotinic acetylcholine receptor |
| $PLA_2$s | Phospholipase $A_2$ |
| scFvs | Single-chain variable fragment |
| SVMP | Snake venom metalloprotease |
| SVSP | Snake venom serine protease |
| WHO | World Health Organization |

## Project aim

The work behind this thesis aimed to discover antibodies with pH-dependent antigen-binding properties against snake venom toxins by using phage display technology in combination with two different library designs. In the first approach, the project explored whether pH-dependent antibodies can be discovered from a naïve antibody library containing naturally occurring variable domains. In the second approach, it was investigated whether light-chain shuffling could be used as a strategy to enhance pH-dependent antigen-binding properties of preexisting antibodies. Finally, the work behind this thesis investigated whether the pH-dependent antigen-binding properties of the discovered antibodies translated to their recycling behaviour in a cellular assay.

# Chapter 1 - Introduction

## 1.1. Snakebite envenoming and snake toxins

### 1.1.1 Snakebite envenoming: a neglected tropical disease

Snakebite envenoming is a serious public health problem in several developing world countries, especially in their rural and tropical areas. According to the World Health Organization (WHO), it is estimated that around the world, each year approximately 1.8 to 2.7 million people suffer from snakebite envenoming, of which 81,000 to 138,000 people lose their lives, while many of the survivors sustain permanent sequelae such as amputations and disfigurements[1,2]. However, the actual number of snakebite envenomings and their negative effects on the victims' quality of life are expected to be much higher than the above-mentioned estimates[3–5]. Lack of proper data maintenance in public health care systems, inaccessibility of effective treatments to snakebite victims, and societal unawareness of how to deal with snakebites are some of the reasons behind currently underreported numbers[1].

The burden of snakebite envenoming is most pronounced in sub-Saharan Africa, Southeast Asia, Latin America, and parts of Oceania, where often the socio-economically deprived sections of society are hit the hardest[6–8]. Snakebite envenoming is considered an occupational disease as it mostly affects agricultural workers who are predominantly males[9]. Consequently, this often leads to the loss of a breadwinner from a family, as even if the victim survives, he/she may not be able to return to work. Thus, snakebite envenoming not only exacerbates poverty for those affected but also imposes an economic burden on society as a whole[10,11]. To highlight the severely unmet challenges of snakebite envenomings, the WHO reinstated snakebite envenoming in its list of neglected tropical diseases in 2017[12].

### 1.1.2 Snake toxins

While there are four families of venomous snakes, namely Viperidae (viperids), Elapidae (elapids), Lamprophiidae (lamprophiids), and Colubroidae (colubroids), the snakes that inflict the most severe envenoming cases belong to the Viperidae (rattlesnakes, lance-headed pit vipers, and true vipers) and Elapidae (cobras, mambas, kraits, coral snakes, Australian sea snakes, and sea snakes)[9,13]. Injection of venoms upon snakebites can have both local (at the bite site) and systemic effects. The local clinical manifestations for viperid bites include intense pain, rapid swelling, blistering, inflammation, extended bleeding, and superficial soft tissue and muscle necrosis[2]. The systemic effects include temporary vision loss, low blood pressure, abnormal heart rate, and spontaneous systemic bleeding[2]. In the case of elapid bites, the local effects include burning sensation and local swelling, while the systemic effects include drowsiness, altered mental state, and flaccid paralysis which can lead to the inability to breathe, and death due to suffocation[2].

Each venomous snake species possesses a unique venom composition[14–17]. The venom composition may further vary between members of the same species, based on factors such as the age of the snake and its geographic location[18–21]. Despite the complexity of snake venoms, the toxins that make up the venom can be divided into different toxin families **(Figure 1)**, the most medically relevant of which include phospholipase $A_2$s ($PLA_2$s), three-finger toxins (3FTxs), snake venom metalloproteases (SVMPs), and snake venom serine proteases (SVSPs). $PLA_2$s exert a variety of toxic activities, including myotoxicity, cytotoxicity, neurotoxicity and hemotoxicity. Toxins from 3FTx family are known to cause neurotoxicity and cytotoxicity, while the toxins from both SVMPs and SVSPs families have hemotoxic effects[22].

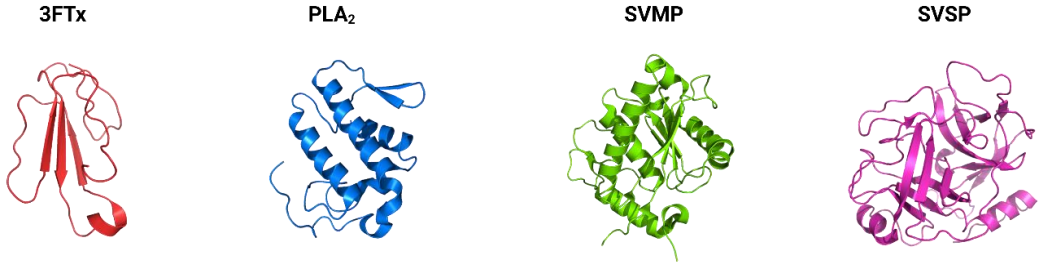


**Figure 1: Four main medically relevant toxin families.** Representative structures of a three-finger toxin (3FTx, PDB: 1CTX, from *Naja siamensis*), a phospholipase $A_2$ ($PLA_2$, PDB: 1CLP, from *Bothrops asper*), a snake venom metalloprotease (SVMP, PBD: 1ND1, from *Bothrops asper*), and a snake venom serine protease (SVSP, PDB: 1OP0, from *Agkistrodon acutus*). The toxins are not shown to scale i.e., their depicted sizes are not relative to each other.

In this thesis, I have worked with two snake toxins, α-cobratoxin (α-cbtx), which is a systemically acting neurotoxin derived from *Naja kaouthia*, and myotoxin-II (M-II), which is primarily a locally acting muscle degrading toxin derived from *Bothrops asper*[15,23–25]. Both these toxins are of high medical relevance but are known to belong to notoriously low immunogenic toxin families, hence creating a challenge for the animal's immune system to raise antibodies against them[26,27]. Thus, discovery of antibodies that specifically target these toxins would be beneficial for the treatment of the envenomings caused by them. The structures, lethality, and the mode of actions of these toxins are further described below.

α-cbtx belongs to the 3FTx family of non-enzymatic toxins of size 6-8 kDa and cause neurotoxicity. As suggested by the name, the toxins from 3FTx family have a structure that resembles that of three fingers, formed by three beta-stranded loops originating from a hydrophobic core with four conserved disulfide bonds[22]. Within the 3FTx family, α-cbtx belongs to the sub-group of long chain α-neurotoxins. These toxins bind nicotinic acetylcholine receptors (nAChRs) at the post-synaptic clefts with high affinity, which prevents the acetylcholine from binding and activating nAChRs. Inactive nAChRs are unable to transport sodium and potassium across the membrane, resulting in stalling of action-potential. Consequently, the signals from the neurons are prevented from reaching the muscles, which results in muscle paralysis[23,28] **(Figure 2(A-B))**.

M-II belongs to the enzymatically inactive sub-family of $PLA_2$s, known as $PLA_2$-like toxins[24,29]. However, both enzymatically active and inactive $PLA_2$s share a common

structural scaffold of four main helices with seven interchain disulfide bonds[22]. The $PLA_2$-like M-II is approximately 13 kDa in size and is known to cause severe muscle damage that often results in a need for amputations[30,31]. It has been proposed that the M-IIs form non-covalently bound homodimers to exert toxicity[32]. Two models for the homodimeric assembly of M-IIs have been proposed. The first model proposes a hinge formation between the two monomers, while the second model (that has recently gained more support) proposes a rather compact structure formation upon the homodimer assembly[32] **(Figure 2(C))**. While the M-II homodimeric structures greatly differ in the two models, the mode of M-II action described by the two models is similar. It is proposed that the cationic C-terminal regions of M-II homodimers interact with sarcolemma (skeletal muscle plasma membrane) and destabilize it. This can result in an uncontrolled influx of calcium ions into the cells that induces a series of cell-damaging events leading to cell death and muscle necrosis[24,30–34] **(Figure 2(C))**.

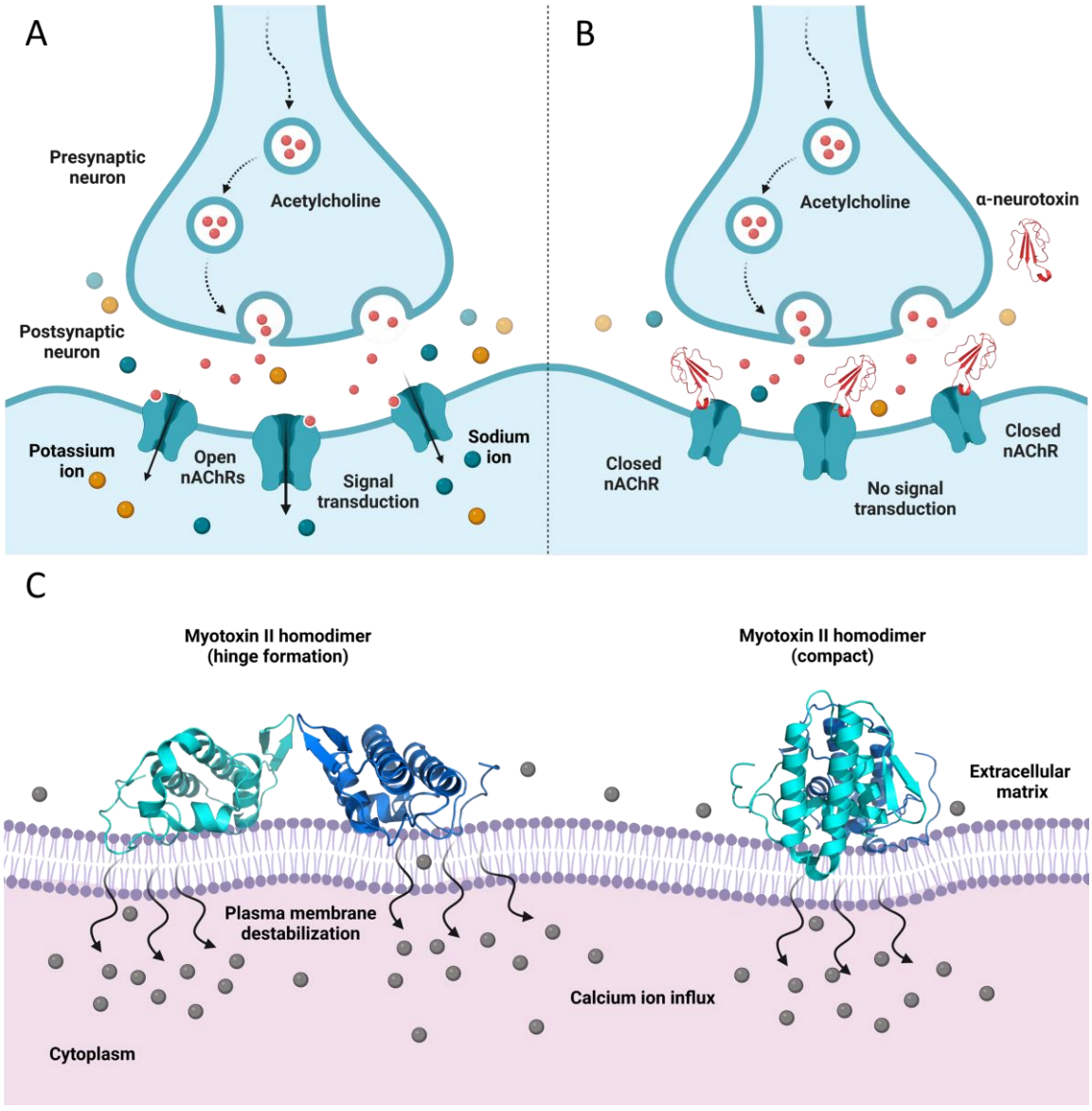


**Figure 2: Mode of action of α-neurotoxin and $PLA_2$s-like myotoxin II (M-II). (A)** Acetylcholine-mediated activation of nicotinic acetylcholine receptor (nAChR) of post synaptic

neurons. **(B)** Binding of α-neurotoxin (PDB: 1CTX, shown in red) to nAChR prevents acetylcholine-mediated activation of nAChR and consequently prevents signal transduction from neurons to muscles. Adapted from figure made by Line Ledsgaard. **(C)** Destabilization of a plasma membrane by C-terminal region of M-II homodimers (PDB: 1CLP, shown in cyan and blue). This causes an influx of calcium ions inside the cells and consequently results in irreversible cell damage and cell death. The model for hinge forming M-II homodimer is shown on the left, and the compact homodimeric M-II assembly is shown on the right. The M-II monomers are shown in cyan and blue. Adapted from Lomonte et al., 2023[32].

## 1.2. Traditional antivenom

Severe snakebites need acute medical intervention to save the life and limbs of the victim. However, the only specific treatments currently available for snakebite envenoming are the traditional plasma-derived antivenoms. These antivenoms are produced by repeated immunization of large animals, such as horses or sheep, with increasing amounts of snake venoms over a long time, typically months or even years[35]. The venom contains both toxic and non-toxic proteins, however, since they all can be immunogenic, the animal's immune system generates antibodies against both kinds of venom proteins. Once the immunization process is finished, blood is drawn from the animal, and plasma is separated from the blood cells. The animal-produced antibodies are purified from the plasma and used as antivenom to treat snakebite victims[36,37] (**Figure 3**). Traditional antivenoms can be either monovalent targeting one snake species, or polyvalent targeting multiple snake species, depending on the immunization strategy.

Traditional antivenoms save countless lives every year, however, they suffer from several drawbacks, and have seen little scientific advancement since their invention over a century ago[38–41]. Given the heterologous nature of the antivenoms, they often elicit early or late adverse reactions in the patients[42,43]. Furthermore, only a small percentage (5-36%) of the antibodies obtained from the animal blood target the snake venom toxins, which results in the need to administer high doses of antivenom to neutralize a given amount of toxins[41,44]. Consequently, high doses result in high treatment costs as well as increase the risk of adverse reactions. Further, the unique immune response of the immunized animals combined with the variation in snake venom composition between snakes, cause the produced antivenoms to often exhibit batch-to-batch variations[45].

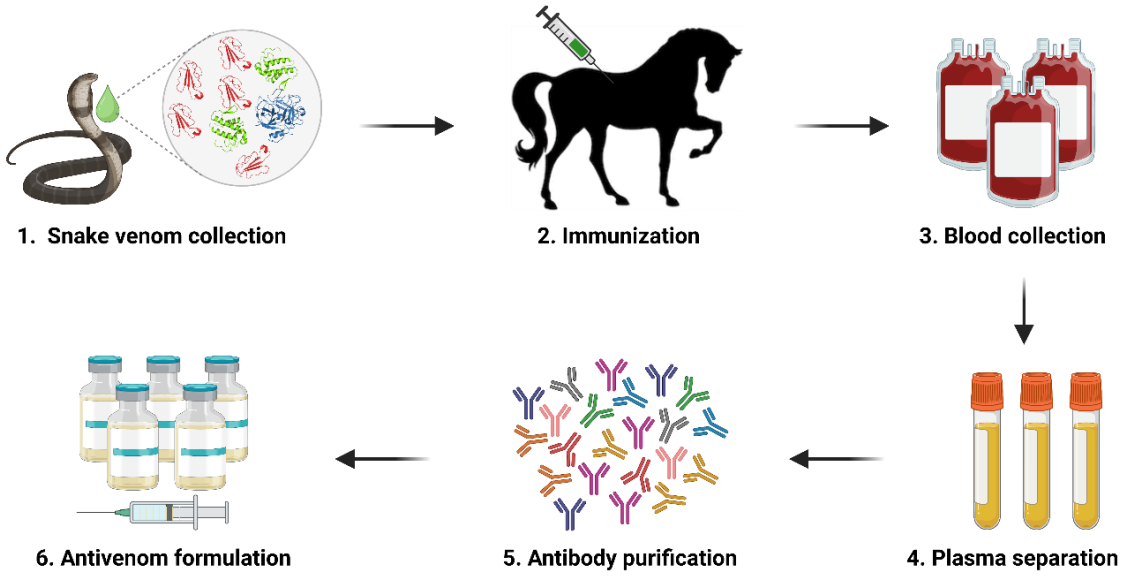


**Figure 3: Traditional antivenom production. (1)** Snake venom is collected. **(2)** A large mammal, like a horse, is immunized with the venom. **(3)** Blood is drawn from the immunized mammal. **(4)** Plasma is separated from the blood. **(5)** Antibodies are purified from the plasma. **(6**) The antibodies are formulated and used as antivenoms to treat snakebite victims.

## 1.3. Recombinant antivenoms

The need for advancement in the field of antivenoms has given rise to promising new treatment strategies using recombinantly produced monoclonal antibodies, i.e., recombinant antivenoms. Recombinant antivenoms can be either polyclonal or oligoclonal based on the underlying design approach[46]. Polyclonal recombinant antivenoms follow a "top-down" approach, where an undefined pool of antibodies obtained from the immunized animals are recombinantly expressed[46]. On the other hand, for oligoclonal recombinant antivenoms a "bottom-up" approach is taken, where a carefully selected panel of antibodies with known specificity to the most medically relevant toxins are included in the antivenom[27,47–50]. In this thesis, in **manuscript I, II, and III**, a "bottom-up" approach was taken to discover antibodies targeting snake venom toxins **(Figure 4)**. It has been hypothesized that compared to traditional antivenoms, oligoclonal recombinant antivenoms based on human recombinant antibodies potentially have lower risks of eliciting adverse reactions due to their compatibility with the human immune system[41,51]. Since the traditional antivenoms can result in adverse reactions, they are only administered when the snakebite victim show clinical manifestations and has reached the hospital[49,52]. This delay results in compromising the treatment. Thus, with better safety profiles than traditional antivenoms, oligoclonal recombinant antivenoms can be quickly administered to the victim, for example, during transportation to the hospital and thus possibly result in better treatment outcome[49]. Further, by employing already well established CHO-cell based systems to express and produce monoclonal antibodies, oligoclonal recombinant antivenoms can be produced with lower batch-to-batch variation than traditional antivenoms[44]. In addition, it has been estimated that oligoclonal recombinant antivenoms

can be manufactured at low cost, which is a crucial factor for treatment of the neglected disease of snakebite envenoming[44,53].

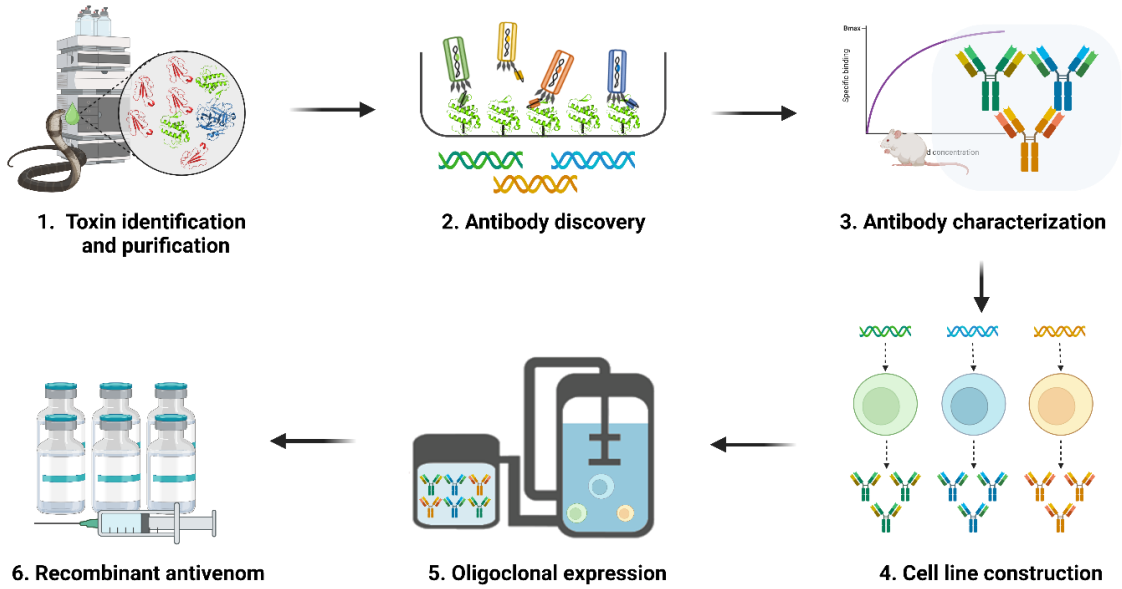


**Figure 4: Oligoclonal recombinant antivenom development and production. (1)** Medically relevant toxins are identified and purified from whole snake venom. **(2)** Antibodies targeting the toxins of interest are discovered, and the genes encoding toxin-binding antibodies are identified. **(3)** Antibodies are characterized for their therapeutic potential and selected. **(4)** Stable cell lines are generated for the production of antibodies. **(5)** Antibodies are expressed and purified from oligoclonal cell culture. **(6)** The purified antibodies constitute oligoclonal recombinant antivenom.

## 1.4. Antibodies and their discovery

### 1.4.1 Antibodies

The key ingredients for effective antivenoms are toxin-neutralizing antibodies. Antibodies, also known as immunoglobulins (Igs) are produced by B-cells and form an important part of the adaptive immune system with their ability to recognize and neutralize a wide variety of disease-causing molecules. In humans, five isotypes of antibodies, namely IgG, IgD, IgE, IgA, and IgM are found, of which IgG is found to be the most abundant isotype in blood, and will be discussed further in context to this PhD thesis[54].

IgGs are approximately 146 kDa in size and have a symmetrical structure consisting of four polypeptide chains. Two identical heavy chains (HCs) and two identical light chains (LCs) are covalently linked to each other via disulfide bonds. HCs consist of four domains, three of which are constant ($C_{H1}$, $C_{H2}$, and $C_{H3}$) and one of them is variable ($V_H$), while LCs comprise one constant ($C_L$) and one variable ($V_L$) domain. The CH2 and CH3 form the homodimeric fragment crystallizable (Fc) region of the IgG that is involved in Fc-effector functions. The antigen-binding part of the antibody, known as fragment antigen-binding (Fab) region is comprised of $C_{H1}$ and $V_{H1}$ domains of HC and $C_L$ and $V_L$ domains of LC. Together, one pair of $V_H$ and $V_L$ forms one antigen-binding site, resulting in two antigen-binding sites per IgG. Both $V_H$ and $V_L$ consist of three complementarity-determining regions (CDRs)

separated from each other by four framework regions (FRs). The CDRs are highly diverse in their amino acid sequence, especially CDR3 in $V_H$, which exhibits the highest sequence diversity[55]. Besides the IgG antibody, several other antibody formats have been engineered for various therapeutic applications. The antibody formats that are relevant to this thesis are IgGs, Fabs, and single-chain variable fragments (scFvs) as illustrated in **Figure 5.**

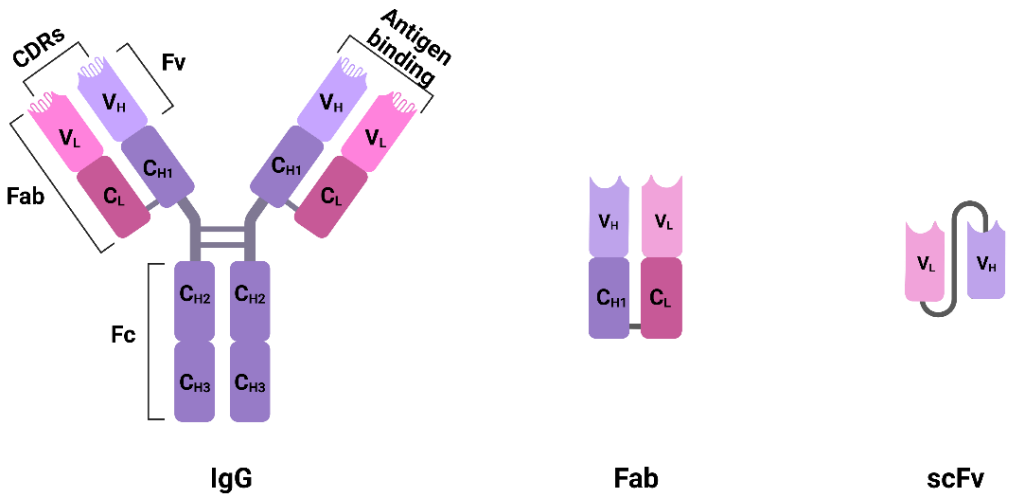


**Figure 5: Antibody formats relevant to this thesis.** Antibody formats of immunoglobulin G (IgG), fragment antigen-binding (Fab), and single-chain variable fragment (scFv) are illustrated to show their constant and variable domains, antigen-binding sites and disulfide bonds.

### 1.4.2 IgG and FcRn: the long half-life of IgG explained

Most of the antibodies that are used as therapeutic agents are of the IgG isotype due to their long plasma half-life[56]. Four subclasses of IgG namely, IgG1, IgG2, IgG3, and IgG4, are found in humans, of which three subclasses (IgG1, IgG2, and IgG4) have an average plasma half-life of 3 weeks, while that of IgG3 is 1 week[57–59]. Although three of the IgG subclasses have similar plasma half-life, so far IgG1 has been the most used subclass for therapeutics due to its higher stability and ability to trigger effector functions[56,60,61].

The reason behind the long half-lives of IgGs lies in the pH-dependent interaction between their Fc region and a widely expressed molecule in the body called neonatal Fc receptor (FcRn)[62–68]. FcRn is a non-classical major histocompatibility complex class 1 (MHC-1)-related heterodimeric receptor consisting of a transmembrane α heavy chain which is non-covalently associated with a soluble β2-microglobulin subunit ($\beta_2$m)[69,70]. The FcRn-mediated recycling pathway that is responsible for the extended half-life of IgGs is illustrated in **Figure 6**. Briefly, IgGs in the bloodstream are taken up by cells via fluid-phase pinocytosis and enter endosomes where the FcRn is predominantly expressed. The core interaction between the Fc and FcRn involves three key amino acid residues – I253, H310, and H435 – that are present at the $C_{H2}$-$C_{H3}$ domain interface of the Fc region. Given that the $pK_a$ of histidine is ~6.0, i.e. the pH below which the amino acid residue will be protonated, the low pH endosomal environment results in rendering a positive charge to histidines and facilitate salt-bridge formation with negatively charged amino acids that are

present on the heavy chain of FcRn[65,67,68,71]. For example, a strong salt bridge formation has been reported between Fc H310 and FcRn E115[72]. Upon binding to the FcRn, the IgGs are recycled back to the cell surface where exposure to the physiological pH, which is around 7.4, results in dissociation of the Fc from FcRn, and the IgGs are released back into circulation[73–78]. Thus, the IgGs are rescued by FcRn from lysosomal degradation and enjoy a long plasma half-life. As a result, several Fc-engineering strategies have been explored to enhance the binding between Fc and FcRn in a manner that can result in extended IgG half-life[66,79–83]. Studies have shown that enhanced binding between Fc and FcRn at low pH (~pH 6) can translate into extended plasma half-life of the IgG[80,81,84,85]. When incorporating increased binding between Fc and FcRn at low pH, it is however important that the increased affinity between the two molecules does not compromise release of the IgG from FcRn at physiological pH at the cell surface[79,86–88]. An Fc engineering strategy that leads to increased plasma half-life and is also used in this thesis, involves three amino acid substitutions Met252Tyr, Ser254Thr, and Thr256Glu, in combination also referred to as a YTE substitution. Introducing a YTE substitution leads to approximately 10-fold stronger binding to FcRn at pH 6.0 and 4-fold increase in the IgG plasma half-life in humans[80,85,89].

Although, the Fc-FcRn interaction is key for IgG recycling, it has been found that the half-life varies between IgGs of the same isotype[90–92]. Given that the Fc region is identical, this implies that the variation in half-life stems from the variable domain. Indeed, several recent studies have provided evidence for the influence of Fab arms on the interaction between Fc and FcRn[93–98]. Some of the ways by which Fabs may affect the interaction between Fc and FcRn include steric hindrance caused by the Fab arms, the influence of charge profile in the Fab region, and possibly by making direct contacts with FcRn[94,95,99,100]. Additionally, it has been found that Fc-FcRn interaction and IgG recycling can alter when the Fab is bound to an antigen[93,94,101]. In **Manuscript III,** we investigated such effects of Fabs and antigen-binding on the interaction between Fc and FcRn and how it affected the FcRn-mediated recycling of IgGs. Gaining a deeper insight into factors that may affect IgG and FcRn interaction may help in engineering IgGs with desirable pharmacokinetic profiles.

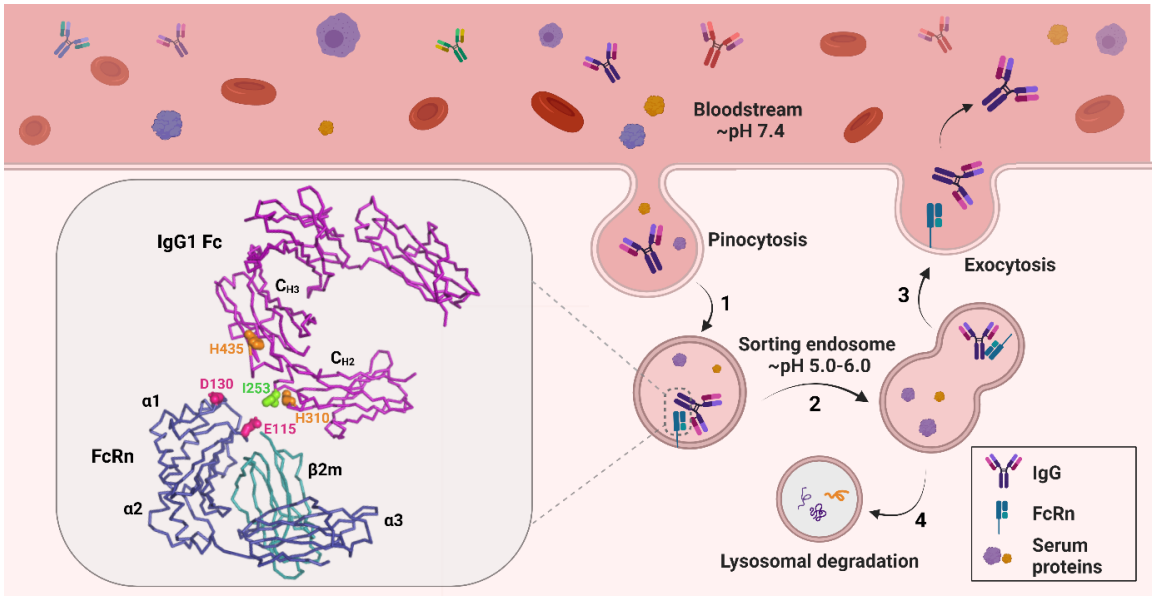


**Figure 6: FcRn-mediated recycling of IgG. (1)** IgGs and other serum proteins are pinocytosed by cells and enter acidified endosomes. **(2)** The Fc region of the IgG binds to the neonatal Fc receptor (FcRn) in the low pH environment of endosomes and sorted for recycling to the cell surface. **(3)** The exposure to near neutral pH environment at the cell surface disrupts the binding between Fc and FcRn and releases the IgG back into circulation. **(4)** Serum proteins unable to bind FcRn are sorted for lysosomal degradation. Illustration of a solved crystal structure of an IgG1 Fc and FcRn complex is shown as ribbon in the pop-up box (PDB: 4N0U). Homodimeric Fc is shown in magenta, and the α- and β-chain of FcRn are shown in dark blue and light blue, respectively. The key residues involved in the pH-dependent interaction between Fc and FcRn are indicated as orange (positively charged), pink (negatively charged), and green (hydrophobic) sticks.

### 1.4.3 Recycling antibodies

Various engineering strategies have been applied to antibodies to optimize their therapeutic effectivity in different diseases[56,84,88,102]. High affinity of antibodies for their cognate antigen is a common desired feature of therapeutic antibodies as it enables efficient neutralization[56,103,104]. However, in disease conditions such as snakebite envenoming, where high amounts of antigens need to be eliminated from the system, high affinity antibodies that remain bound to the antigen throughout the endosomal pH gradient, are required to be administered frequently and/or at high doses[105]. This is because when the antibody remains bound to the antigen in the endosome, it can either undergo antigen-mediated degradation or recycle back into circulation via the FcRn-mediated pathway in complex with the antigen, where the antigen continues to occupy the antigen-binding sites of the antibody[105]. In either case, an antibody can bind its cognate antigen only once in its lifetime. To lower the dose/dosing frequency of the antibody treatment, an antibody would need to neutralize multiple antigens sequentially requiring a decoupling of the fates of antigen and antibodies upon entering the endosome. This will allow the antibody to be rescued from the endosomes as a free antibody and bind multiple antigens in its lifetime, and thus achieve therapeutic efficacy at a lower dose/dosing frequency than the conventional antibodies[105–108].

To achieve this, Igawa et al., engineered a recycling antibody, that binds its cognate antigen with high affinity at neutral pH in the bloodstream but dissociates from it at low pH in the endosomes. This enabled the antibody to be rescued via FcRn binding, while the antigen is destined for lysosomal degradation[105] **(Figure 7)**. Following Igawa et al., several studies have been conducted to engineer antibodies with pH-dependent antigen-binding properties against various targets[109–112]. Additionally, antibodies that show altered binding to the antigen, driven by differences in the calcium concentration between the plasma (high) and the endosomes (low), have been explored as a strategy to achieve recycling antibody properties[113]. Further, to improve the performance of recycling antibodies, their Fcs can be engineered for increased binding to Fc receptors like FcRn and Fcγ receptor IIb (FcγRIIb) at neutral pH, and enhance the cellular uptake of antibody-antigen complexes[106,109,114,115]. Such antibodies are called sweeping antibodies. However, the majority of recycling/sweeping antibodies that have been studied are specific to disease-driven, overly expressed endogenous antigens, in the cases of cancer, autoimmune diseases, and chronic inflammatory diseases[105,109,111,112,115–117]. The recycling ability of such antibodies that allows them to achieve therapeutic efficacy at reduced doses, which may also lead to lower treatment costs can be potentially useful for the treatment of other diseases where high dose and low cost are limiting factors, such as infectious diseases and snakebite envenoming[116,118,119]. In this thesis, we have focused on the discovery of antibodies with pH-dependent antigen-binding properties against snake venom toxins namely, α-cbtx and M-II. While all the three manuscripts share similar methods to discover pH-dependent antigen-binding antibodies, the discovery and characterization of such antibodies are presented in **manuscript II and III**.

A common method for engineering antibodies with pH-dependent antigen-binding properties is through histidine doping in the antibody variable domains[106]. However, this approach may result in compromised binding between the antibody and antigen at neutral pH[106,107]. Additionally, modifying the antibody sequence through mutations may introduce unintended consequences such as developability and immunogenicity challenges[120,121]. As an alternative strategy, we have in **manuscript I, II, and III** employed naïve scFv libraries with naturally occurring variable domains to discover pH-dependent antibodies against snake venom toxins.

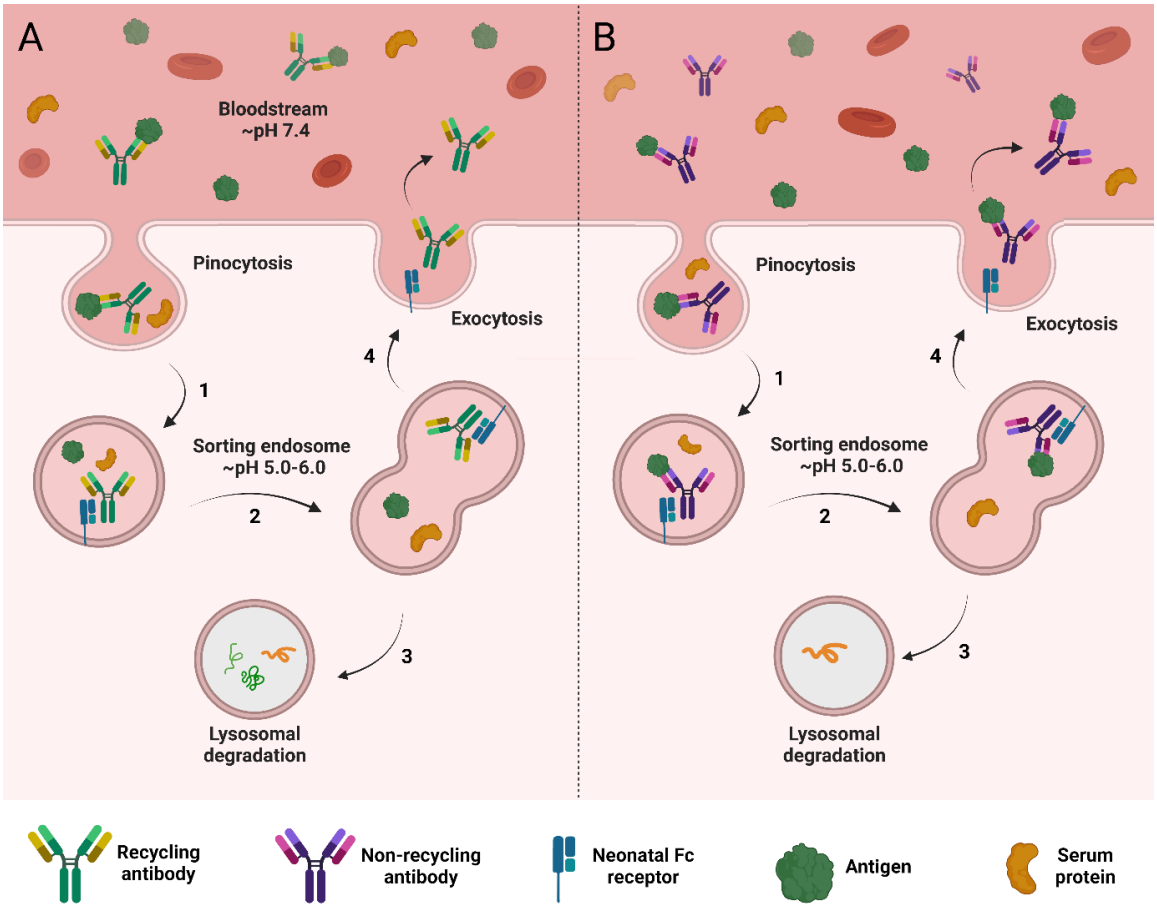


**Figure 7: Recycling versus non-recycling antibodies. (A)** The recycling pathway for a recycling antibody (antibody with pH-dependent antigen-binding properties). **(1)** The antibody-antigen complex enters endosome via pinocytosis. **(2)** The antibody dissociates from the antigen in the low pH environment of endosome. **(3)** The released antigen is degraded in the lysosome, and **(4)** the antibody is transported to the cell surface and released into circulation via the FcRn-mediated recycling pathway. Consequently, the antibody can bind and eliminate multiple antigens in its lifetime. **(B)** The recycling pathway for a non-recycling antibody (antibody without pH-dependent antigen-binding properties). **(1)** Upon pinocytosis, the antibody-antigen complex enters the endosome and **(2)** remains bound together throughout the endosomal gradient. **(3)** As a result, the antigen escapes lysosomal degradation and **(4)** is co-recycled with the antibody via the FcRn-mediated recycling pathway. The antibody can thus bind only one antigen per binding site in its lifetime.

### 1.4.4 Antibody discovery

Multiple methods exist to discover antibodies, such as *in vitro* display, single B-cell, and hybridoma technologies. The choice of which methodology to use depends on the characteristics of the antigen itself, the desired properties of the antibodies, and the accessibility of the method. In this thesis, we used phage display technology to discover antibodies for several reasons. Firstly, selections with phage display technology are, unlike immunizations strategies, not susceptible to antigen liabilities such as high toxicity and poor immunogenicity, which are the traits of the antigens of interest (snake toxins) relevant in this thesis. Secondly, I was interested in antibodies that bind antigens in a pH-dependent

manner. The selection of such antibodies can be facilitated by an *in vitro* display technology as it allows for easy manipulation of the selection criteria, which may not be possible using *in vivo* hybridoma technology. Thirdly, an scFv phage display library containing human antibody variable domains and has been proven to be successful in selecting for antibodies that bind to snake toxins was made available and could be utilized for the work in this thesis[27,48,122].

Phage display is a Nobel Prize-winning technology invented by G. Smith in 1985 as a method for presenting foreign peptides on the surface of M13 phages[123]. This was achieved by introducing a foreign peptide-encoding DNA into the M13 genome, such that the expressed foreign peptides were fused to the G3P coat proteins of the M13 phage[123]. The phage display technology was further modified by McCafferty et al., who were able to integrate an entire scFv gene to that of G3P, thus resulting in the expression scFv fused G3P coat protein, which enabled the first antibody phage display selection[124]. Briefly, in phage display selections, a library of scFv-displaying phages (or other antibody formats) is incubated with the antigen of interest, thus allowing the scFv-displaying phages to bind to the antigen. Next, unbound phages are washed away, while the bound phages are eluted, amplified in *Escherichia coli*, and subjected to another round of antigen-binding. This is repeated 2-3 times to enrich the antigen-specific scFv-displaying phages (**Figure 8**). Thereafter, the scFv encoding genes from the phages are extracted, subcloned into expression vectors, and individual clones are characterized for their binding to the antigen[125,126]. Antibody phage display technology is a versatile platform that has been adapted for selection of a wide variety of antibodies by employing various antigen presentation and selection strategies coupled with different library designs[122,126]. Such aspects of antibody phage display technology are reviewed in detail in **paper I**.

Further, in **manuscripts I, II, and III**, phage display selection strategies for antibodies that bind their antigen in a pH-dependent manner were employed. In **manuscript I and II**, the phages were allowed to bind the antigens at neutral pH and eluted using low pH buffer (pH 5.5−6.0). In **manuscript III** an additional deselection step prior to the selection was introduced where the phages that bind antigens at pH 5.5 were removed from the library.

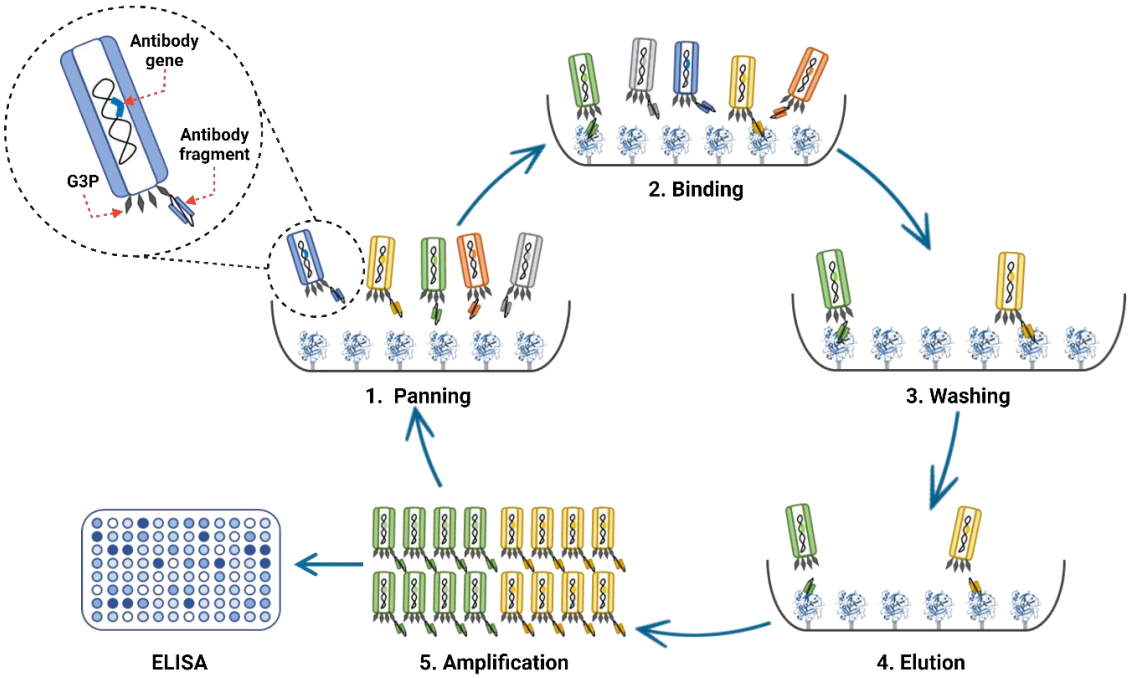


**Figure 8: Antibody phage display technology. (1)** An antibody phage display library, which comprises of genes encoding antibodies and displays the corresponding antibodies on its surface, is panned against the antigen of interest. **(2)** The phages are incubated with the antigen to allow binding. **(3)** Unbound phages and phages not specific to the antigen are washed away. **(4)** The bound phages are eluted. **(5)** Eluted phages are amplified and used as the input for the next round of panning. The process of panning to amplification is repeated 2-3 times to enrich for antigen-specific phages. After selections, the phages are evaluated for antigen-binding in ELISA.

The fundamental background for this PhD thesis has now been introduced. A description of snakebite envenoming, its impact on the world, and the challenges of its current treatment have been provided. Additionally, the concept of recombinant antivenoms, antibodies with pH-dependent antigen-binding properties, and antibody discovery via phage display technology have been described. An in-depth introduction to antibody discovery by phage display technology will be further provided in Chapter 2. Together Chapter 1 and 2 will provide the background needed to comprehend the research work presented in Chapters 3, 4 and 5 of this PhD thesis.

# Chapter 2 – Paper I

**Advances in antibody phage display technology**

The review article presented in this chapter serves as an extension to the introduction of this PhD thesis. The article covers four key aspects of antibody phage display technology that can be optimized to discover antibodies with desired binding characteristics against antigens of interest. First, the review discusses various antibody formats that can be presented on phages, along with their advantages and disadvantages. Second, different antigen presenting strategies, which are primarily dictated by the nature of the antigen, are described. Third, the article provides insight into the various phage display selection strategies that can be employed to select antibodies with desired binding properties, such as deselection strategies, selection with competition, selection of cross-reactive and environment sensing antibodies, and *in vivo* phage display selection. Fourth, different antibody library designs and their applications are described. Two of the aspects presented in the article, phage display selection strategies and library design are explored in the context of discovering pH-dependent antigen-binding antibodies in this PhD thesis.

This manuscript has been published in Drug Discovery Today. 2022 Aug;27(8):2151-2169.

ELSEVIER



# Advances in antibody phage display technology

**Line Ledsgaard [a,*], Anne Ljungars [a], Charlotte Rimbault [a], Christoffer V. Sørensen [a], Tulika Tulika [a], Jack Wade [a], Yessica Wouters [a], John McCafferty [b,c], Andreas H. Laustsen [a,*]**

[a] Department of Biotechnology and Biomedicine, Technical University of Denmark, DK-2800 Kongens Lyngby, Denmark
[b] Department of Medicine, Addenbrookes Hospital, Box 157, Hills Road, Cambridge CB2 0QQ, UK
[c] Department of Medicine, Cambridge Institute of Therapeutic Immunology and Infectious Disease, University of Cambridge, Addenbrooke's Hospital, Hills Road, Cambridge CB2 0QQ, UK

**Phage display technology can be used for the discovery of antibodies for research, diagnostic, and therapeutic purposes. In this review, we present and discuss key parameters that can be optimized when performing phage display selection campaigns, including the use of different antibody formats and advanced strategies for antigen presentation, such as immobilization, liposomes, nanodiscs, virus-like particles, and whole cells. Furthermore, we provide insights into selection strategies that can be used for the discovery of antibodies with complex binding requirements, such as targeting a specific epitope, cross-reactivity, or pH-dependent binding. Lastly, we provide a description of specialized phage display libraries for the discovery of bispecific antibodies and pH-sensitive antibodies. Together, these methods can be used to improve antibody discovery campaigns against all types of antigens.**

**Keywords: Phage display; Antibody discovery; Antigen presentation; Selection strategy; Library design**

Line Ledsgaard Line Ledsgaard has a BSc Eng. (2016) and MSc Eng. (2018) in biotechnology from the Technical University of Denmark (DTU). She holds a PhD from the Department of Biotechnology and Biomedicine at DTU, and her research centers on the discovery of antibodies against snake venom toxins with the aim of replacing current antivenoms with next-generation antivenoms, based on human recombinant monoclonal antibodies. Her work especially focuses on using phage display technology to discover broadly neutralizing antibodies with the ability to bind and neutralize the toxic effects of groups of similar toxins from different snake species.

Andreas Hougaard Laustsen-Kiel Andreas Hougaard Laustsen-Kiel heads the Center for Antibody Technologies in the Department of Biotechnology and Biomedicine at DTU and is specialized in antibody technologies. He is also the CTO of Bactolife ApS, where he is responsible for nanobody technology and discovery. Andreas is a Fellow of the Danish Academy of Technical Sciences, the Young Academy of Denmark, and the Young Academy of Europe. He holds a PhD from the University of Copenhagen (2016) and an M.Sc.Eng. from DTU (2012). Andreas is a co-founder of the companies, Biosyntia, VenomAb, Antag Therapeutics, Chromologics, VenomAid Diagnostics, and Bactolife.

John McCafferty John McCafferty was one of the founders of Cambridge Antibody Technology (CAT) and a co-inventor of antibody phage display. In 2012, he formed IONTAS, an innovative biotechnology company using phage display to develop novel antibody therapeutics. During this period John developed IONTAS's proprietary mammalian display technology. John is also an inventor of a novel molecular fusion format (KnotBody™), wherein naturally occurring, venom-derived cysteine-rich peptides are inserted into peripheral CDR loops of an antibody. He recently formed Maxion Therapeutics to take advantage of this drug development opportunity with a particular focus on modulation of ion channels and GPCRs. Interspersed within this company formation John has held academic positions at the Wellcome Trust Sanger Institute and the University of Cambridge. This includes establishment in 2022 of a group in the Department of Medicine to develop recombinant antivenoms.

* *Corresponding authors.Ledsgaard, L. (liljen@dtu.dk), Laustsen, A.H. (ahola@bio.dtu.dk).*

1359-6446/
https://doi.org/10.1016/j.drudis.2022.05.002

## Introduction

Phage display technology was first invented in 1985[1] for the display of peptides and, later, in 1990, the first antibody fragment was displayed on phages.[2] Since then, the technology has been used successfully for the discovery of many hundreds of antibodies for research, diagnostic, and therapeutic applications, including more than 14 antibodies that are clinically approved.[3] All aspects of the phage display methodology have been refined and advanced to enable the discovery of antibodies against challenging targets and antibodies with certain binding properties. One of the advantages of phage display, compared with other display technologies, such as ribosome,[4,5] yeast,[6] or mammalian display,[7,8] is that large libraries (diversity of $> 10^{11}$ unique clones) can be created and stored ready for selections, which allows for high-affinity antibodies to be discovered against a wide range of antigens. In this review, we address four major parameters that can be optimized to improve the outcome of antibody discovery campaigns: the choice of antibody display format, antigen presentation, selection strategy, and library construction.

## Antibody formats used in phage display libraries

Phage display libraries can be designed using different bacteriophages, such as filamentous M13, fd, and f1 bacteriophages,[9] to display a variety of different antibody formats. The two most commonly used formats are single-chain variable fragments (scFvs) and antigen-binding fragments (Fabs).[10,11] ScFvs are small (25–27 kDa) monovalent antibody fragments comprising $V_H$ and $V_L$ domains connected by a short peptide linker.[12] Fabs are 50 kDa in size[13] and comprise $V_H$, $V_L$, $C_L$, and $C_H1$ domains.[14] There is potential for loss of affinity on conversion of scFv to the Fab/IgG format,[11,15] which might be less of an issue for antibodies discovered in the Fab format.[11,15,16] However, Fabs generally do have lower expression yields than scFvs[17] and typically exhibit lower display levels on phages,[18,19] making scFvs a more robust format for libraries, particularly naïve libraries.

Other antibody formats have also been used for the construction of antibody phage display libraries, including human single-domain antibodies (human $V_H$) and camelid and shark single-domain antibodies ($V_HH$ and $V_{NAR}$, respectively). $V_HH$s are small (12–15 kDa[13]) and comprise the antigen-binding fragment from heavy-chain-only antibodies. With conventional antibodies, the interface that mediates pairing of $V_H$ and $V_L$ incorporates hydrophobic residues that are buried in the interface. In $V_HH$s, these are substituted with more hydrophilic residues, which results in increased water solubility and a decreased tendency to form aggregates.[20] The complementarity-determining region 3 (CDR3) loop in the $V_HH$ is often elongated compared with conventional antibodies, which allows the $V_HH$ to bind antigens that would be inaccessible for conventional antibodies, such as catalytic clefts of enzymes or receptor domains.[21,22] The $V_{NAR}$ antibody fragments are similar to the $V_HH$ antibody fragments in size, with the notable exception that they only have two CDR loops because of a deletion of a large portion of the Fr2-CDR2 region.[23]

Which of the antibody formats to choose for a phage display campaign is dependent on the final application of the discovered antibody. If the application is therapeutic and a long half-life is beneficial or engagement of effector cells is needed, an scFv or Fab library might be optimal, because they allow for easy reformatting to the commonly therapeutically used IgG format. For research reagents and diagnostic applications, or when the cost of large-scale manufacture is a major concern, a format such as the $V_HH$ might be most optimal, although this format can also be fused to an Fc-region to create a $V_HH$-Fc molecule with similar properties as an IgG in terms of half-life and effector cell engagement. Taken together, it is vital to delineate the requirements for the final antibody product to select the most suitable type of library.

## Antigen presentation strategies

For a successful phage display-based antibody discovery program, it is crucial that the conformation of the included antigens resembles the conformation that the antigens will have in the final application. Otherwise, the discovered antibodies could end up only recognizing the antigen in an altered conformation. Therefore, an initial and critical step for a phage display campaign is to determine the optimal strategy for antigen presentation.[24]

### *Antigen presentation through direct or indirect immobilization*

The most widely used antigen presentation strategy is to directly or indirectly immobilize the antigen on a surface (Fig. 1a). In direct immobilization, the antigen is coated on the surface using passive adsorption. This strategy is by far the simplest for antigen presentation; however, it is not well suited for many types of antigen that alter their native conformation upon adsorption.[25] It can be particularly more problematic for small antigens that might not exhibit enough intermolecular attraction forces to exert passive adsorption.[26] For some of these antigens, indirect immobilization can be used instead of direct immobilization.

Through indirect immobilization, the antigen is captured on the surface using a capture molecule. The most popular technique exploits the strong binding between streptavidin/neutravidin and biotin, whereby the surface is coated with streptavidin/neutravidin, and the antigen is conjugated to biotin via a linker or tag.[27,28] This enables an indirect, yet stable, attachment of the antigen to the surface.[27,28] The antigen is more likely to retain its native conformation through indirect immobilization because the antigen is raised from the selection surface. However, it is crucial not to overbiotinylate the antigen, because this can obscure important epitopes or result in antigen aggregation.[29]

Two different strategies for biotinylation exist: site-specific or random biotinylation. Site-specific biotinylation can be achieved using biotinylation acceptor peptides (BAPs) comprising an enzymatic biotinylation site.[30,31] One of the most widely used BAPs is the AviTag, which requires recombinant expression of the target antigen fused to the 15-amino acid peptide tag.[32] The AviTag sequence is biotinylated at its lysine residue by the *Escherichia coli* biotin ligase, BirA.[33] The AviTagged antigen can be co-expressed with BirA in bacterial cells, yeast, and mammalian cells to achieve *in vivo* biotinylation.[34,35] Alternatively, purified AviTagged antigen can be incubated with purified BirA and biotin to achieve *in vitro* biotinylation.[36] Biotinylation using BAPs

results in site-specific addition of a single biotin per antigen, thus controlling the antigen-to-biotin ratio and avoiding overbiotinylation. Nevertheless, it might not be possible to use the AviTag system in all cases, especially when it is difficult/unpractical to express the target antigen recombinantly, or when the AviTag would interfere with a potentially important (terminal) epitope of the antigen.

As an alternative to BAP biotinylation, random chemical biotinylation can be used. In this method, purified antigen and biotinylation reagents, using a variety of possible reaction chemistries, are mixed to achieve a covalent linkage between the antigen and biotin. A variety of linkers are available, making it possible to biotinylate antigens at the primary amines (N terminus or side chain of lysine residues[37]) or sulfhydryl and carboxyl groups.[38,39] Although faster and cheaper than enzymatic biotinylation (by the *E. coli* biotin ligase), chemical biotinylation needs titration to achieve the desired 1:1 antigen-to-biotin ratio.

Indirect immobilization of an antigen can also be used based on different peptide tags and tag-specific capture molecules. This requires the recombinant expression of the antigen in fusion with a peptide tag and the selection surface to be coated with the fusion tag-specific capture molecule. Binding between the tag and the capture molecule results in immobilization of the antigen. Although less popular than the biotin–streptavidin system, His-tags and anti-His antibodies or other His-capturing molecules have been exploited for antigen presentation in phage display selections.[40] Recently, a peptide–protein ligand pair, known as SpyTag/SpyCatcher, derived from fibronectin-binding protein in *Streptococcus pyogenes,* was used for antigen presentation in phage display selections.[41,42] The binding between SpyTag and SpyCatcher occurs via an isopeptide bond and has been reported to be irreversible, specific, and robust to various conditions, such as pH, temperature, and buffer.[41].

### *Antigen presentation through whole-cell panning*

Even though indirect immobilization is suitable for displaying many antigens, it is often not optimal when it comes to presenting antigens such as membrane proteins. Membrane proteins typically contain hydrophobic transmembrane regions and might be a part of a multisubunit protein complex; as a result,

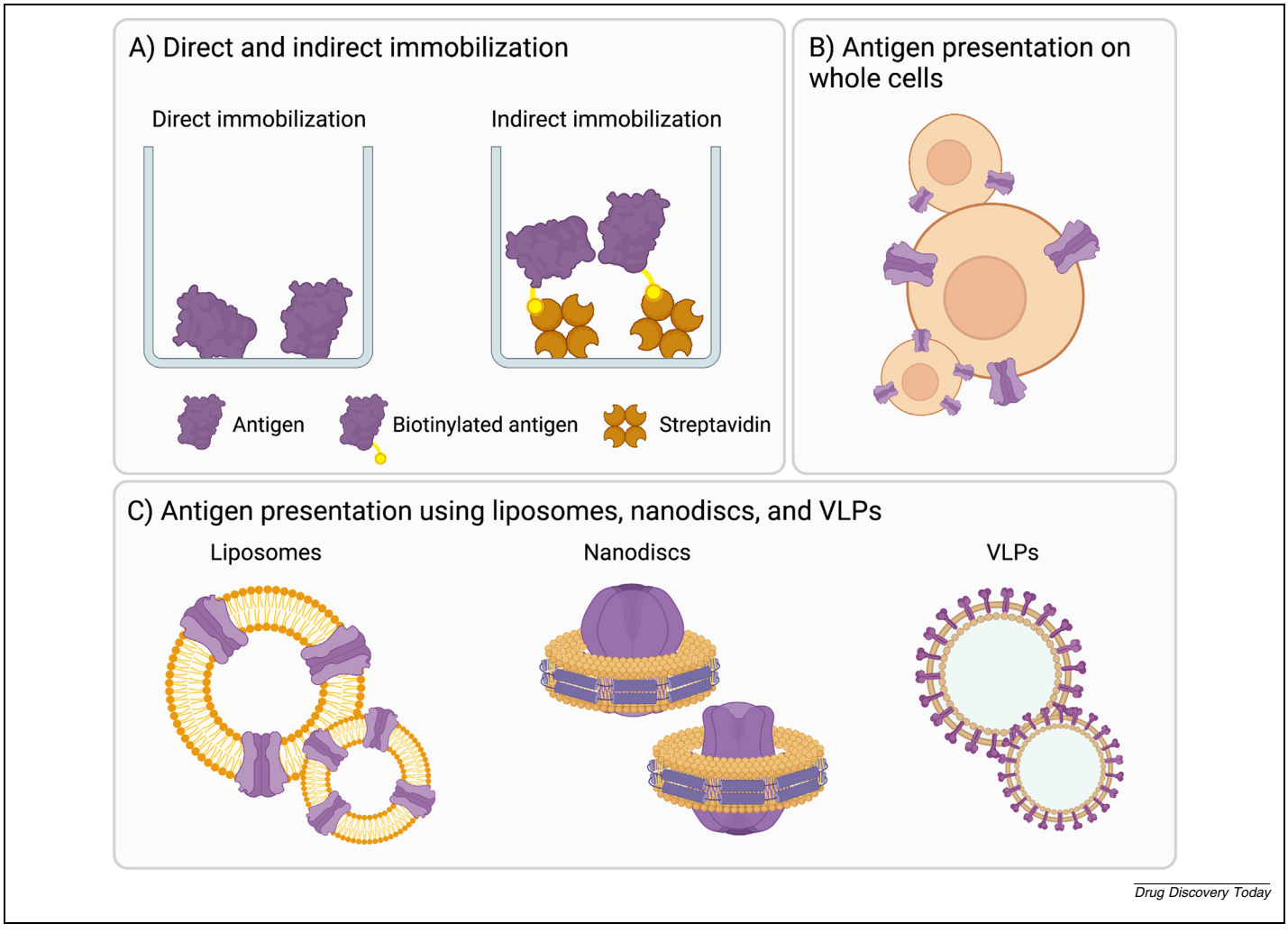


**FIG. 1**

Antigen presentation strategies. **(a)** Direct and indirect immobilization. **(b)** Antigen presentation on whole cells. **(c)** Antigen presentation on liposomes, nanodiscs, and virus-like particles (VLPs).

they lose their native conformation when isolated from their natural environment.[43] To conserve their conformation, membrane proteins can be expressed on a cell membrane (Fig. 1b). Mammalian cell lines, such as human embryonic kidney (HEK) cells or Chinese hamster ovary (CHO) cells, can be either transiently or stably transfected with a target protein to overexpress it and obtain a high density on the cell surface, while retaining the native conformation of the antigen.[43–46] Although selections are sometimes performed using cultured primary cells, it has been shown that cultured cells can alter their protein expression levels compared with primary cells[47]; to overcome this potential issue,[48] primary cells without culturing can be used for selection.[49] Other cell expression systems, including *E. coli*, yeast, and insect cells, can also be used to express and present membrane proteins.[50–52].

One problem with phage display selection on whole cells is that the target antigen, whether endogenous or recombinantly expressed, will represent only a small proportion of the total protein milieu presented to the library. To overcome this, deselection techniques can be used as described below. In addition, when transfected cells are used, the host cell can be altered between the selection rounds to focus selection on the recombinant antigens present on both cells.[43] Another challenge is that phage particles can nonspecifically adsorb to the cell surface via their coat protein (independently of their displayed antibody fragment). To counteract this, washing using low pH can be applied.[43,53] Furthermore, some phages can bind nonspecifically to dead cells and cell debris in the cell suspension used for panning. To reduce enrichment of such nonspecific binders, it is important to ensure that most of the cells used for selection are viable.[43,54]

### *Antigen presentation through liposomes, nanodiscs, and VLPs*

Membrane proteins can also be presented on amphiphilic structures, such as liposomes, nanodiscs, and virus-like particles (VPLs) (Fig. 1c). Liposomes are spherical vesicles comprising a volume of aqueous solution enclosed by one or more lipid bilayer membranes, usually composed of phospholipid molecules. The phospholipid bilayer membrane mimics the environment of a plasma membrane and creates a suitable platform to present membrane proteins.[55,56] Presenting antigens on liposomes requires the formation of the liposomes, extraction of the antigen from its native membrane environment (whether isolated from natural source or recombinantly expressed), and finally transferring the extracted antigen to the preformed liposomes. When recombinantly expressed, the antigen can be fused with a tag, which can be used later for purification.[57]

Membrane proteins can also be presented on nanodiscs, which are nanometer-sized discoidal structures comprising phospholipid bilayers encircled by two amphipathic helical protein belts, termed 'membrane scaffold proteins' (MSPs).[58] Purified membrane protein can be mixed with phospholipids and MSPs to obtain membrane protein-carrying nanodiscs[59,60] (Fig. 1c). The protein belts constrain the size of the bilayers, resulting in a more monodispersed and consistent size distribution of nanodiscs compared with liposomes. Furthermore, nanodiscs provide a more stable environment for the membrane proteins and can be stored for a longer period compared with liposomes.[61,62] Moreover, because of their discoidal structure, proteins incorporated in the nanodiscs are accessible from both sides of the membrane. This is beneficial when access to both the extracellular and intracellular domains of membrane proteins is required. Both liposomes and nanodiscs can be used to present ion channels and multitransmembrane proteins, such as ion channels and G-protein-coupled receptors, which have until recently proved difficult to express/purify. However, both liposomes and nanodiscs rely on detergents to extract membrane proteins, which can alter the structure of the protein. As an alternative, a detergent-free approach, using styrene maleic acid (SMA) copolymer, can solubilize membranes into lipid nanodiscs, which are nanometer-sized discoidal structures comprising a phospholipid bilayer encircled by SMA copolymer resulting in a structure called a 'styrene maleic acid–lipid particle' (SMALP).[57,63,64] The detergent-free extracted protein can also then be incorporated into liposomes for antigen presentation.[57].

Cytotoxic proteins can cause growth retardation and toxicity to the host cells when overexpressed, making them difficult to express.[65] Cytotoxic and membrane proteins can be synthesized in a cell-free manner in a reaction comprising modified cell lysates, which provide a suitable environment for the target protein expression,[66] potentially combined with membrane-mimicking structures, such as liposomes and nanodiscs, which capture and present the newly synthesized proteins.[67] Membrane protein presentation on nanodiscs has been successfully implemented for phage display.[62,68].

VLPs are another alternative for presentation of membrane proteins suitable for phage display.[69] VLPs are non-infectious, virus-like multiprotein structures that lack the viral genome, but contain the viral capsid proteins.[70,71] Target membrane proteins can be transiently overexpressed on the surface of the capsid-expressing host cell. The self-assembling viral capsid protein directs the budding of the plasma membrane, resulting in the formation of VLPs studded with target antigens (Fig. 1c). It is also possible to first synthesize the VLPs and then covalently attach the target proteins to their surface.[72] Compared with liposomes, VLPs are more stable and can present antigens at higher density. However, VLPs have a high cost, because commercially available VLPs are expensive, and their production in the lab can be laborious.[72].

## Advanced phage display selection strategies

An antibody discovery campaign using phage display selection can be conducted using various strategies and protocols. These strategies should be carefully selected to maximize the chance of discovering an antibody with the desired characteristics. Here, we present different strategies that can be used to discover antibodies with binding characteristics, such as cross-reactivity, high selectivity, or pH dependence.

### *Deselection strategies: Antigen tags and carrier material*

During a selection process, binders will potentially be selected against all antigens, including tags or fusion partners, as well support matrices, such as streptavidin beads. To overcome this, a deselection step using a nontarget is typically included to limit

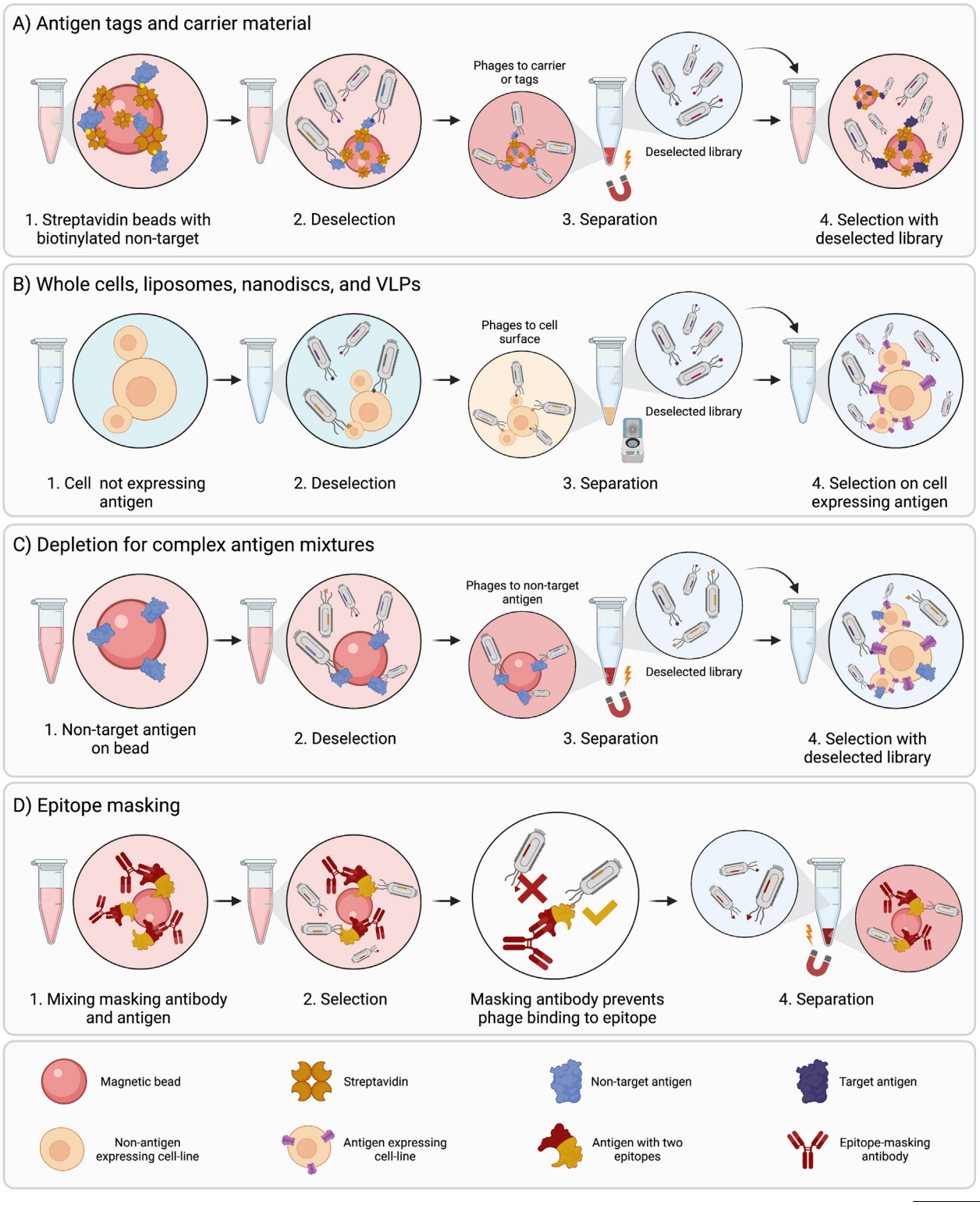


**FIG. 2**

Deselection strategies. **(a)** Deselection of antibodies against antigen tags or carrier material. **(b)** Deselection when presenting antigens on cells, liposomes, nanodiscs, and virus-like particles (VLPs). **(c)** Depletion of phages when selecting on complex antigen mixtures. **(d)** Using antibodies for masking specific epitopes.

enrichment of antibodies against antigens other than the target. For example, selection on a biotinylated protein using streptavidin beads can be preceded by exposing the library to a biotinylated nontarget protein coupled to streptavidin beads to reduce the proportion of such unwanted binders progressing to the selection step on the intended target[73–75] (Fig. 2a).

### *Deselection strategies: Whole cells, liposomes, nanodiscs, and VLPs*

The same principle can be applied to more complex targets, such as whole cells, liposomes, nanodiscs, or VLPs. When panning on whole cells, a cell transfected to express e.g. a surface receptor of interest is used to display the antigen, and antibodies specific to the receptor can be enriched using a mock-transfected cell or possibly an untransfected cell for deselection.[43,44,54] Moreover, for discovery of antibodies against viral targets, selection can be performed using an infected host cell as antigen and lysate of uninfected host cells for deselection.[76] When cells with an endogenous expression of the target are used, ideally, the same cell knocked down or knocked out for the antigen of interest can be used for deselection (Fig. 2b). For liposomes, nanodiscs, and VLPs, a similar strategy can be used, in which deselection is performed using the particle used for presentation without the antigen embedded, before selection on the antigen-displaying particle.[77]

A more complex scenario is when whole cells are used without knowing the target *a priori* in a phenotypic discovery campaign using mammalian[49] or bacterial cells.[78] Under such circumstances, deselection can be performed on a nontarget cell similar to the target cell to avoid enrichment against common cell surface antigens. However, the perfect match, as in the example with transfected cells, is impossible.[49,79] An example includes deselection on T cells when the goal is to identify antibodies targeting B cells.

### *Deselection strategies: Depletion for complex antigen mixtures*

Deselection through depletion can be used for complex targets, such as whole cells or impure protein samples, also when the target is unknown. An example is selection on whole cells without knowing the target beforehand. In such cases, even though the target antigen is unknown, the nontarget antigens might be known, which allows for protein depletion to be performed. During protein depletion, the phage display library is incubated with recombinant proteins corresponding to nontarget antigens coated or captured on immunotubes or beads. Thereafter, the unbound phages are transferred to the target antigen and used for selection[80–82] (Fig. 2c).

### *Deselection strategies: epitope-specific deselection*

For therapeutic antibodies, it is often crucial which epitope of a target antigen an antibody binds, because this can determine whether the antibody is of therapeutic value. To direct antibody binding to a specific part of the antigen, different techniques can be applied. To find binders against the ligand-binding site of a receptor, the elution step can be performed by adding high concentrations of the ligand, which will elute only antibodies competing with the ligand for binding.[83] However, a major drawback with this strategy is that mainly low-affinity antibodies are eluted, which makes it possible to use the method specifically for the reduction of the amount of low-affinity binders.[84] Antibody blocking,[81] also called epitope masking,[85–88] is another strategy for directing antibodies against a specific part of an antigen. During the selection, previously discovered antibodies binding undesirable epitopes of the antigen are included for blocking. These antibodies bind and block certain epitopes of the antigen, making some epitopes nonaccessible for new antibodies displayed on phages during the selection step. Thereby, antibodies binding new epitopes can be enriched (Fig. 2d). In addition to antibodies, receptor–ligand complexes can also be used in a similar way to deselect binders that do not recognize the same site as the receptor or ligand does.[89]

### *Selection with competition*

In many cases, it is desirable to reduce binding to antigens that are related to the target antigen. Thus, the goal is to focus selections on epitopes that are unique to the target antigen and reduce the proportion of binders to epitopes shared with related antigens. This is achieved by prior deselection on the related antigen.[74] However, deselection is not 100% efficient and is related to the target concentration and the affinity of the binding to the shared epitope. The binding between an antibody and an antigen is an equilibrium reaction following the law of mass action. Therefore, not all antibodies are bound to their antigens at a given time point. Thus, in all deselection strategies, several antibodies that have specificity for an antigen used for deselection will not be bound to the antigen at the time point at which deselection is concluded. Consequently, these antibodies with specificity to the antigen used for deselection will be carried through to the selection phase and might bind the target antigen here. To circumvent this, as an alternative to (or in combination with) deselection, selections can be performed in the presence of competing antigens (selection with competition).

In a selection with competition, target and nontarget antigens are mixed with the antibody library, allowing for competition for antibody binding between the target and nontarget. Use of a large excess of the nontarget antigen drives binding to epitopes shared between target and nontarget antigen, increasing the fraction of recovered antibodies that bind target-specific epitopes. Therefore, after the selection step, antibodies binding to the target antigen are enriched. Strategies to collect the target with binding antibodies include labeling the target with, for example, biotin, while leaving the nontarget unlabeled (Fig. 3a). This strategy can be used both for whole cells and purified proteins.[75] Another alternative is to present the target and nontarget antigens in different ways, such as having the target antigen immobilized or coated on a plastic surface and adding nontarget antigen in solution[90] (Fig. 3b). For whole-cell selections, the nontarget cells can also be presented as membrane particles, resulting in different densities of target and nontarget antigens, which allows for separation through centrifugation.[91].

Antigens that are upregulated in diseased tissue, cells, and fluids compared with healthy samples commonly serve as relevant targets for therapy or diagnosis.[92] An alternative for discovery of both such targets and antibodies targeting these is to use phenotypic discovery. However, in this case, a classical deselection strategy using healthy samples is suboptimal, because binders

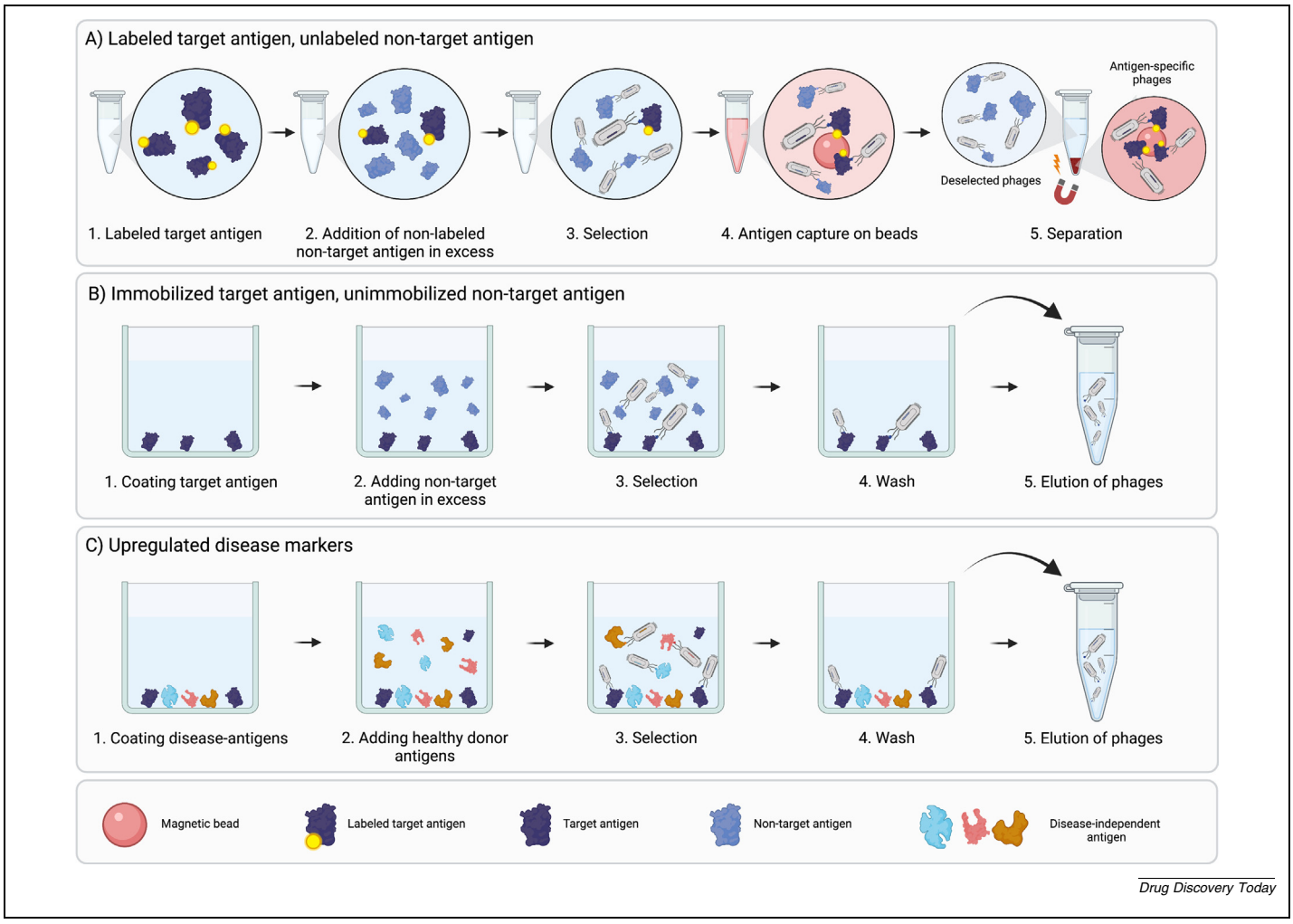


**FIG. 3**

Selection with competition. **(a)** Competitive selection using labeled target antigen and unlabeled nontarget antigen. **(b)** Competitive selection using immobilized target antigen and non-immobilized nontarget antigen. **(c)** Selecting for upregulated disease markers using competitive selection.

against all antigens present in the deselection step (on the healthy sample) will be reduced. Instead, including a competition during selection allows for the discovery of antibodies against these types of upregulated targets, not only the ones uniquely expressed. By varying the amount of added nontarget antigen for competition, the selection can be guided for the discovery of antibodies against a target that is upregulated to a certain degree.[93] Antibodies will compete for binding to the antigen present on both target and nontarget antigens, and the expression levels will determine whether antibodies are mainly collected and enriched or removed (Fig. 3c).

## Strategies to generate cross-reactive antibodies

Antibodies are highly specific molecules, and selections are typically designed to find specific antibodies against one target antigen and avoid any binding to other molecules. However, in many circumstances, although the antibodies must be highly specific for their target, they should preferably also bind homologs or different mutated versions of the same target. For example, preclinical studies of a therapeutic antibody binding a human target will be significantly easier to conduct if the antibody also recognizes the murine and simian version of the antigen. Other examples are infectious diseases and antivenom development, where it is beneficial if broadly neutralizing antibodies recognizing several different viruses, bacteria, or toxins can be discovered.[94]

### *Cross-panning*

A way to achieve cross-reactivity is to perform cross-panning, in which antigens are alternated between the different rounds in the selection process[95] (Fig. 4a). This technique has been used to find antibodies against conserved epitopes of HIV,[96] Influenza A strains,[97] and against cytotoxins in snake venoms from multiple species.[98] Success depends on the degree of conservation between related targets. A requirement for broad cross-reactivity against orthologs or paralogs with low conservation might result in finding low-affinity antibodies, nonspecific binders, or no antibodies.

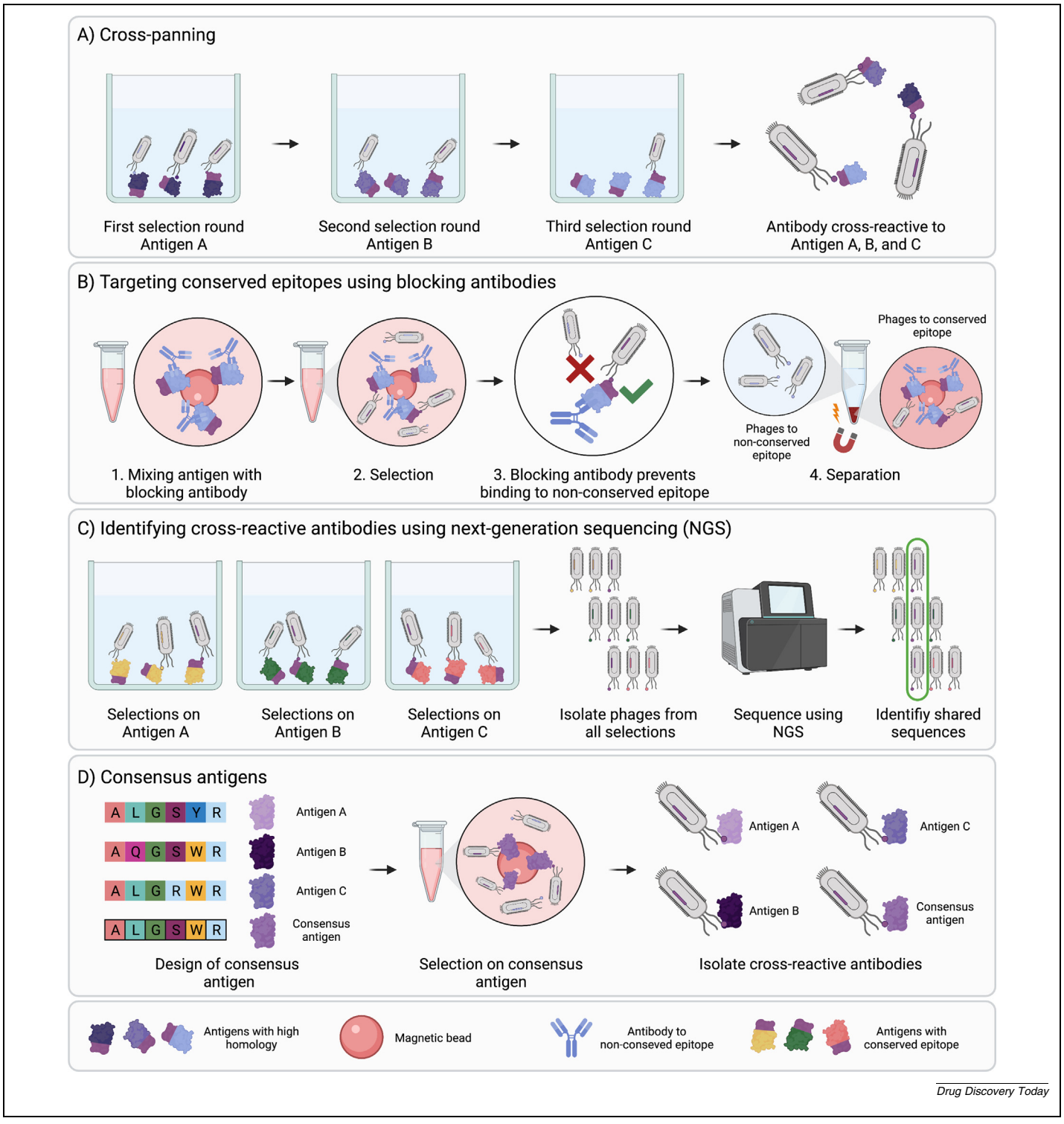


**FIG. 4**

Strategies to generate cross-reactive antibodies. **(a)** Cross-panning. **(b)** Targeting conserved epitopes using blocking antibodies. **(c)** Using next-generation sequencing (NGS) for identification of cross-reactive antibodies. **(d)** Consensus antigens.

### *Antibody blocking and next-generation sequencing*

For the discovery of cross-reactive antibodies when the same antigen is used in repetitive selection rounds, selections can be guided towards conserved epitopes of the antigen using antibody blocking, as described above (Fig. 4b). Another alternative is to evaluate the output from parallel pannings on different homologous proteins, with next-generation sequencing (NGS) to identify antibodies that are enriched and found in all output pools (Fig. 4c). This has been used to identify binders against serum albumin.[99]

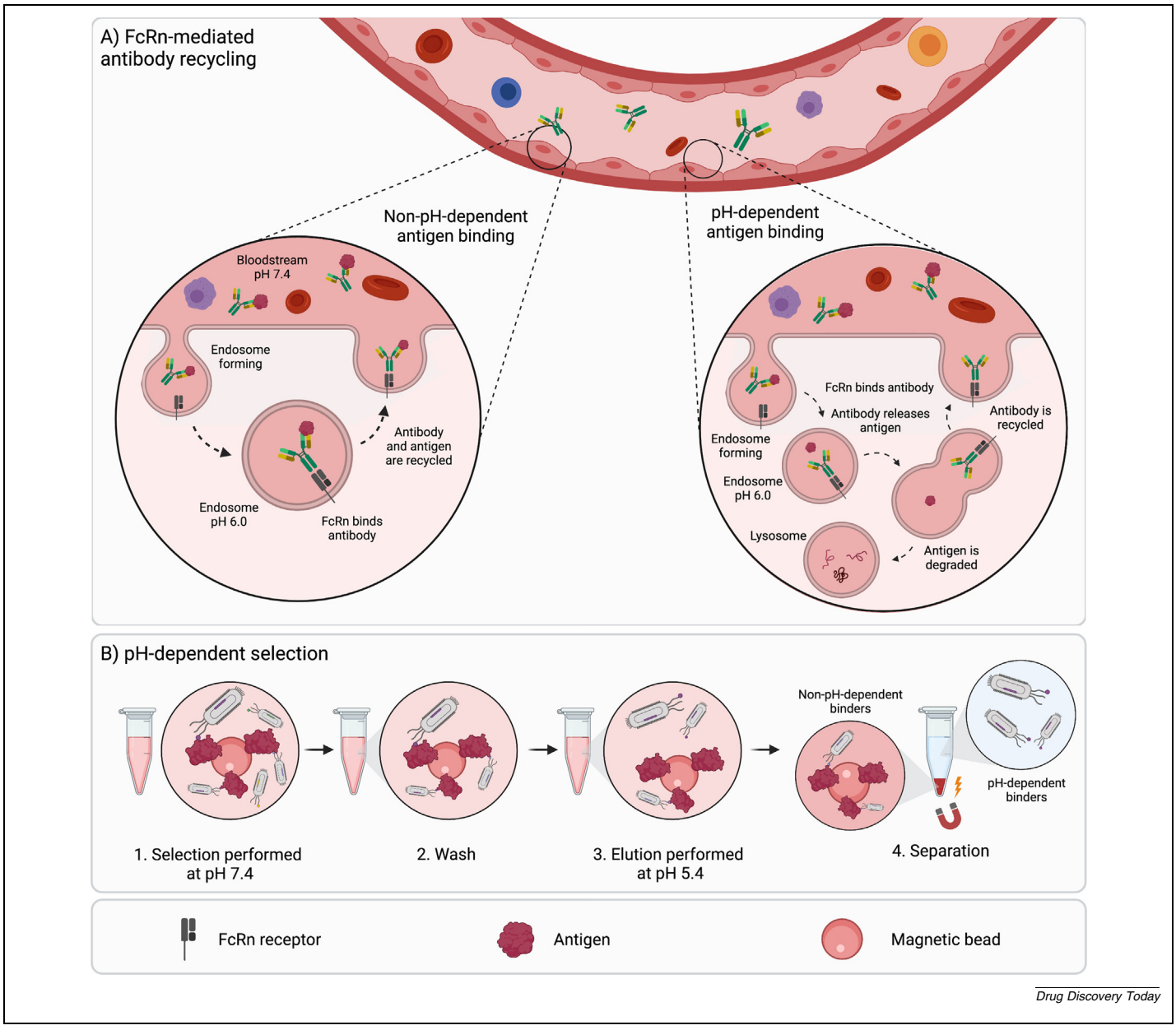


**FIG. 5**

Environment-sensing antibodies. **(a)** Neonatal Fc receptor (FcRn)-mediated recycling mechanism shown with and without pH-dependent binding to antigen. **(b)** Selection strategy for isolation of antibodies with pH-dependent binding.

### *Consensus antigens*

Another alternative to identify cross-reactive antibodies is to use consensus antigens in the selections (Fig. 4d). A consensus antigen is designed by sequence alignment of multiple homologous antigens and construction of an 'average' consensus antigen, containing the most abundant amino acid in each position. In positions where multiple alternatives exist, different approaches can be taken, such as selecting amino acids based on similar chemical properties or the one with the greatest predicted immunogenicity.[100] Polyclonal broadly neutralizing antibodies against short neurotoxins from various snakes have successfully been generated using consensus toxins for immunization of horses,[101,102] and it has been hypothesized that the use of consensus antigens might also be useful in phage-display-based antibody discovery campaigns.[103]

### *Selection of environment-sensing antibodies*

When administering therapeutic antibodies, the antibodies remain in circulation until they are endocytosed by cells. After endocytosis, the antibodies are directed to the lysosomes, where they can be recycled to the circulation via binding to the neonatal Fc receptor (FcRn). This significantly increases the half-lives of the antibodies.[104] However, when an antibody is bound to an antigen, the antigen-antibody complex is internalized and either degraded in the lysosomal compartment or recycled. To avoid recycling of the antigen as well as unnecessary antibody degrada-

tion, antibodies can be engineered to dissociate from their antigens within the acidic endosomes, allowing the antigen to be degraded while the antibody is recycled[105] (Fig. 5a). For a therapeutic antibody, this enables the antibody to be administered less frequently and/or at a lower dose to the patient. Given that the pH differs between circulation (pH 7.4) and inside endosomes (pH 5.8), antibodies binding their antigens with different affinities at different pH are desirable when the antibody is to be recycled without its cargo. It has been shown that the plasma antigen concentration was decreased by using a pH-dependent antibody, also engineered to have increased FcRn affinity, compared with a conventional antibody.[106,107] In addition, pH-dependent binding can enhance the cytotoxicity of antibody-drug conjugates[108,109] and possibly promote antibody transcytosis across the blood-brain barrier.[109] For discovery of pH-dependent antibodies, the phage selection protocol can be modified to enrich for this property. During the selection, binding is allowed to occur at neutral pH, following elution of pH-dependent binders by decreasing the pH to 5.4.[110] To optimize the chances of finding pH-dependent binders, libraries enriched for histidines can be used, which are described in more detail below.

Another strategy for increasing the half-life of antibodies is to have antibodies with binding properties dependent on the presence of ions. The calcium concentration differs between the environments in the endosomes and the plasma. Therefore, similar to pH dependence, calcium dependence can be used to recycle antibodies from the endosomes. As an example, selections against IL-6R in a calcium-containing buffer, followed by addition of EDTA to chelate $Ca^{2+}$ and thereby elute calcium-dependent antibodies, resulted in the discovery of an antibody with accelerated clearance of the antigen from plasma.[111]

Depending on the final use of the antibodies, enrichment for additional requirements, such as improved stability, or slow off rates, can be achieved during selection. One way to increase the stability is to increase the temperature[112] or add proteases[113] during the selection step for enrichment of antibodies stable to those conditions. For discovery of antibodies with slow off rates, the antigen concentration is typically reduced in consecutive selection rounds,[114] and additional wash steps are added.[115]

## *In vivo* phage display selection

As described previously, using whole cells as antigens for phage display selection is a valid strategy that accommodates many aspects, such as correct folding, post-translational modifications, and functionality of an antigen. However, the complexity and pharmacology of the antigen in a living organism remain lacking. Similar cell types might have completely different expression profiles or post-translational modifications because of variations in tissue microenvironments, both in healthy[116] and diseased tissues.[117]

To fully mimic the *in vivo* profile of the antigen, *in vivo* phage display technology was developed.[118] Here, a phage display library is usually administered intravenously and allowed to circulate, followed by intracardiac perfusion to remove unbound phages. Finally, the phages are rescued from the harvested, homogenized, or lysed target tissues and analyzed by sequencing. If the target of interest is known, the antibodies can be analyzed for binding before sequencing. Enrichment of phages is determined by comparing sequences present in the target tissues

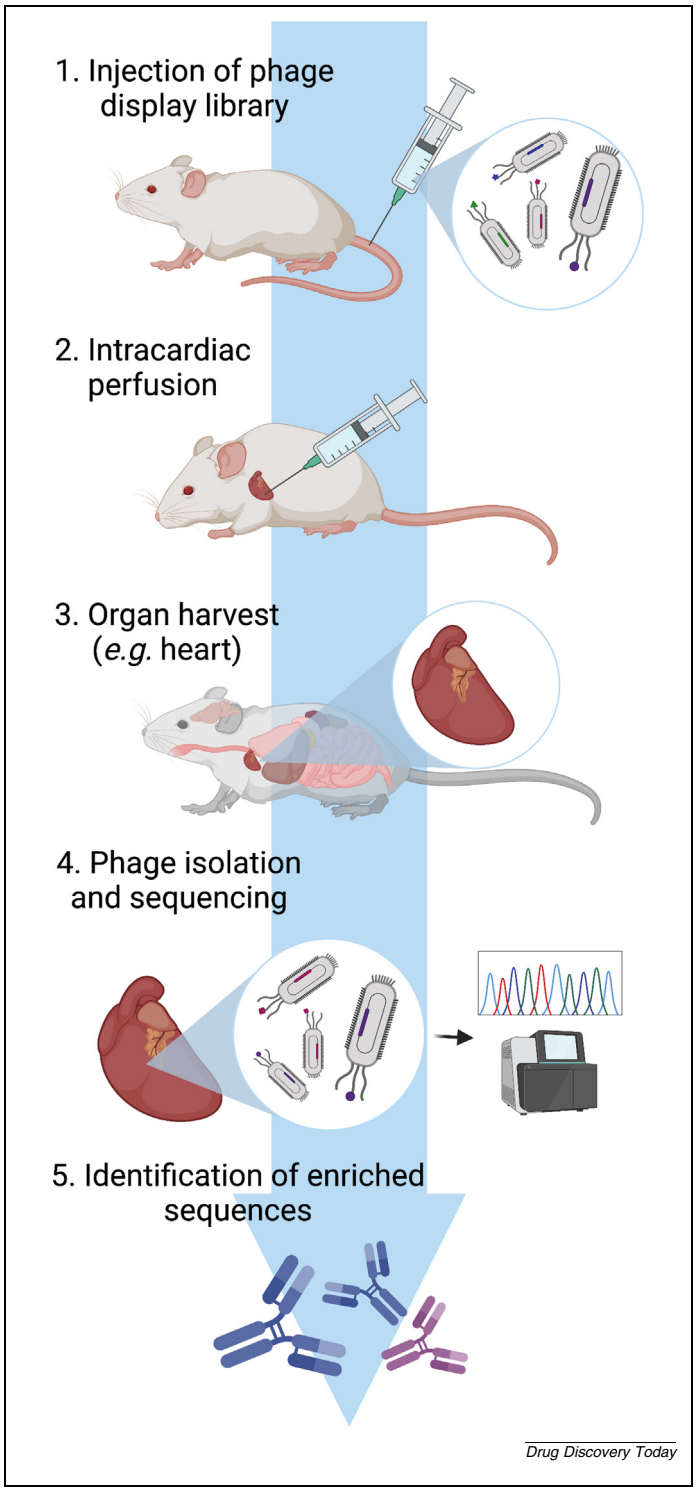


**FIG. 6**

*In vivo* phage display selection. (1) Phage display library is injected into the mouse. (2) Intracardiac perfusion is performed before (3) harvesting the organ in question. (4) Phages are isolated from the organ and the DNA is sequenced. (5) Sequences are compared to sequences from phages isolated from other organs or the input to identify enriched sequences.

with sequences present in the input or irrelevant tissues, and enriched sequences are selected for further characterization (Fig. 6).

In the original study describing *in vivo* phage display selection, peptide-based phage display libraries were used for identification of peptides that specifically bound to either brain or kidney blood vessels.[118] Antibodies in the form of scFvs[119,120] and single-domain antibodies (sdAbs)[121,122] have also been discovered using this technology. *In vivo* phage display has mainly been performed using mice or rats, although, a few studies also describe the use of this technology in humans.[123–125] However, it is not possible to perform the intracardiac perfusion step in humans because it leads to the death of the subject. To assign sequences specifically targeting the tissue of interest, phages present in the blood stream are analyzed and used for comparison.

## Design of antibody phage display libraries

As described above, selections can be performed using different selection strategies dependent on the final requirements for the desired antibody. In addition to the selection methodologies used, various phage display libraries can also be used to optimize the chances of identifying an antibody with the desired characteristics. Libraries can be based on different antibody formats, on natural or synthetic antibody sequences, and can even be tailored to contain antibodies with specific biophysical or binding characteristics. Different cloning strategies, such as sequential cloning of the light and heavy chain repertoires,[126,127] splicing by overlap extension PCR,[128] or golden gate cloning,[11,129] can be conducted to link $V_H$ and $V_L$ during library construction. Here, we describe some of the general library types, as well as more advanced tailored library designs.

Overall, antibody phage display libraries are divided into two main classes: natural and synthetic libraries, based on the origin of the antibody sequences used for library construction. The sequences are either obtained directly from B cells[73,130,131] or synthetically created using *de novo* synthetic technologies.[131,132]

### *Natural libraries*

Natural libraries capture the antibody repertoire of a donor and can be derived from specifically immunized or non-immunized ('naïve') donors. The immune response following an antigen challenge is accompanied by antibody class-switching from naïve IgM to secreted IgG. Therefore, naïve libraries are typically generated from the IgM repertoire of healthy donors to capture a diverse population of antibodies. By contrast, the IgG repertoire, reflecting the recent immune history of the donor, is used for immune libraries. The immune response is further driven by somatic hypermutations, resulting in improved affinity, expression levels, and antibody specificity.[133] Therefore, on average, antibodies discovered from an immune library have higher affinity than do those directly isolated from naïve libraries. However, antibody-engineering techniques enable optimization of antibodies from naïve libraries to the same or even better performance level compared with antibodies discovered directly from immune libraries.[134] Another difference is that immune libraries are typically smaller in size and can only be effectively used for discovery of antibodies against the antigen used for immunization or closely related antigens, whereas naïve libraries have broader application. For both naïve and immune natural libraries, the diversity of the library goes beyond the natural diversity,[135] because heavy and light chains,[73,127,136] as well as sometimes CDR regions,[137] are combined randomly without consideration for the natural pairing.

### *Synthetic libraries*

Synthetic libraries can be created *de novo* with multiple frameworks and random CDRs[138] or based on natural antibody sequences with synthesis of specific regions of interest in an antibody, typically the CDR loops most likely to be involved in antigen binding.[139] Both synthetic and natural libraries have their pros and cons for use in antibody discovery, some of which will be highlighted below.

### *Antigen immunogenicity requirements*

The creation of an immune library requires immunization with the antigen in question. This requires that the antigen is immunogenic, which is why immune libraries based on human donors cannot be efficiently created against human antigens unless B cells are taken from (naturally) infected patients.[140,141] Therefore, the creation of useful immune libraries against human antigens typically requires the use of orthologous species. For therapeutic purposes, such heterologous antibodies must be 'humanized'[142,143] following discovery. However, humanization can lead to a trade-off with potency, because residues crucial for binding in the original antibody cannot be removed entirely. Alternatively, fully human libraries for self-antigens can now be constructed through immunization of human immunoglobulin transgenic animals.[134]

Naïve libraries, alongside synthetically made libraries, have no antigen immunogenicity requirements and can be used to discover antibodies against all types of antigens, including highly conserved self antigens,[144] as well as those that are toxic to the host.[98]

### *Library design*

Throughout the years, numerous therapeutic antibodies have been discovered through phage display selection campaigns using mainly natural naïve libraries.[145,146] Requirements for a therapeutic antibody include having high stability and a low propensity to aggregate. These traits allow the antibody to be formulated at high concentration, which is often required for administration, and lower the risk of aggregate formation, which is associated with immunogenicity.[147–149] Collectively, biophysical properties of an antibody, that can be used to predict how easy it is to be developed into a therapeutic, are often referred to as the 'developability' of the antibody.[150]

To an extent, the process of B cell maturation eliminates poorly behaved antibodies, because B cell viability is maintained by tonic signaling proportional to the level of surface-expressed B cell receptors.[151] However, the fact that an antibody is from an immune source does not guarantee good developability. Nature does not require individual antibodies to be produced in serum to the level that might be required in antibody drug formulation, where concentrations around 100 mg/ml are typically required. Thus, irrespective of the origin of the antibody, biophysical lia-

bilities sometimes emerge during preclinical/clinical development when higher concentrations are required.[30]

During library construction, developability might be increased through amplification of certain germlines from donor lymphocytes based on the selected primers. However, primer overlap with unfavorable germlines can still occur. In synthetic libraries, developability can be improved by including clinically validated scaffolds and well-paired $V_H$-$V_L$ germlines.[152] Additionally, germline frameworks not conserved in all humans, such as the VH4b[153], can be omitted in the design.[154]

Finally, removal of sequence liabilities that might influence the antibody homogeneity and downstream manufacturing can be beneficial.[155] Sequence liabilities include NXS glycosylation sites; deamidation NG, NS, and NA motifs; DG isomerization; and M/C oxidation sites.[155] Naturally, the risk that a sequence liability will be important for the binding and functionality of an antibody increases with the number of sequence liabilities that are contained within the antibody paratope. Site-specific control of amino acids within synthetic libraries allow to minimize the occurrence of these motifs relative to natural libraries, which can save time on downstream engineering.

### *Library diversity*

Central to the prospects of discovering a therapeutic antibody against a desired epitope is maximizing the sequence diversity captured within a phage display library. Immune libraries use the natural diversity and affinity maturation process *in vivo* and are enriched for binders specific to the antigen used for immunization, but their use is limited to antibody discovery campaigns directed against only that and closely related antigens. By contrast, unbiased naïve and synthetic libraries can, if they are large enough, be used for discovery of binders against any antigen of interest.[73]

First-generation naïve libraries conventionally approached maximizing diversity by increasing the number of donors used as input into the library. The existence of public clones, antibody sequences that are shared between humans,[156] affects the true diversity of such first-generation naïve libraries. Consequently, the library size, determined by the number of unique sequences, is orders of magnitudes lower than how phage display diversity is measured conventionally (by counting the number of colonies following library transformation).[157] To increase the library size, not only the number of donors used for library construction is of importance, but also simply the amount of genetic starting material used.[158]

When working with synthetic libraries, the researcher has complete control over the input sequences, which means that germlines known to present poorly on phages can be omitted. Furthermore, the use of synthetic technologies can reduce clonal dominance and result in a higher sequence diversity, typically containing > 95% unique clones.[132,154]

Although synthetic libraries are better placed to fill the theoretical sequence space of a phage library with unique clones, it is unknown whether they contain the same level of structural diversity as natural libraries. In particular, the CDR-H3 loop, the most complex and major determinant for antigen specificity,[159] is typically fixed to a narrow loop length in synthetic libraries,[160] which can be a disadvantage for certain targets. Therefore, the theoretical larger size of synthetic libraries might not translate into a more functionally diverse antibody repertoire than those obtained from naïve natural libraries.

### *Specialized antibody phage libraries*

The choice of an appropriate library for a phage display selection campaign is one of the most crucial steps for identifying optimal antibody binders. Factors affecting the library choice include application of the end product, nature of the antigen, and the library availability in the laboratory. The emergence of new molecular methods has allowed laboratories to construct their own combinatorial antibody phage libraries to replicate the natural antibody repertoire offered by the immune system. Many of these libraries are designed with structural and sequence diversity with early-stage drug discovery in mind. However, some applications need libraries comprising antibodies with particular structural- or sequence-based characteristics.

### *Bispecific antibody libraries*

Compared with standard human antibodies, in which both binding sites are directed against the same epitope, bispecific antibodies (bsAbs) are engineered with two binding sites directed to different epitopes. These two binding sites can be directed to the same antigen (biparatopic bsAbs) or two different antigens. In the latter, one paratope could be used to target a specific region or cell, whereas the other one could bind the antigen of interest. The archetypical application of bsAb is T cell redirection in cancer immunotherapy[161] (i.e., the redirection of the cytotoxic activity of effector T cells to specifically eliminate tumor cells), but other disease areas outside cancer are also being explored, such as inflammatory disorders, diabetes, viral and bacterial infections, and Alzheimer's disease.[162]

A huge variety of bispecific antibody formats exists, including bispecific IgGs (bsIgGs), heterodivalent $V_HH$ dimeric constructs, and BiTEs.[162–165] However, some of these antibody formats are not simple to manufacture, such as bsIgGs, which are challenging to produce in a single host cell because co-expression of the heavy and light chains from two different antibodies results in random pairing of the chains and a complex mixture of IgG molecules. Ultimately, this reduces the overall yield of the bsIgG of interest, and the relatively low concentration of the bsIgG among the byproducts (including the incorrectly chain-paired IgGs) results in the need for elaborate purification techniques. To simplify the expression and purification processes, several strategies for chain pairing have been developed, including specialized phage display libraries with common light or heavy chains.[166] This approach allows for the concomitant expression of three different chains (instead of four) in the same cell and results in a mixture containing only two monoclonal antibodies (mAbs) and one bsAb (instead of ten different molecules) (Fig. 7a–c). Moreover, libraries with common light or heavy chains could also be used for the discovery of binding domains that can be used as building blocks to create new antibody formats.[163,167]

### *Chain pairing with common heavy chains*

ScFv-based phage display libraries with a common heavy chain ($V_H$) and different repertoires of light-chain variable genes ($V_L$)

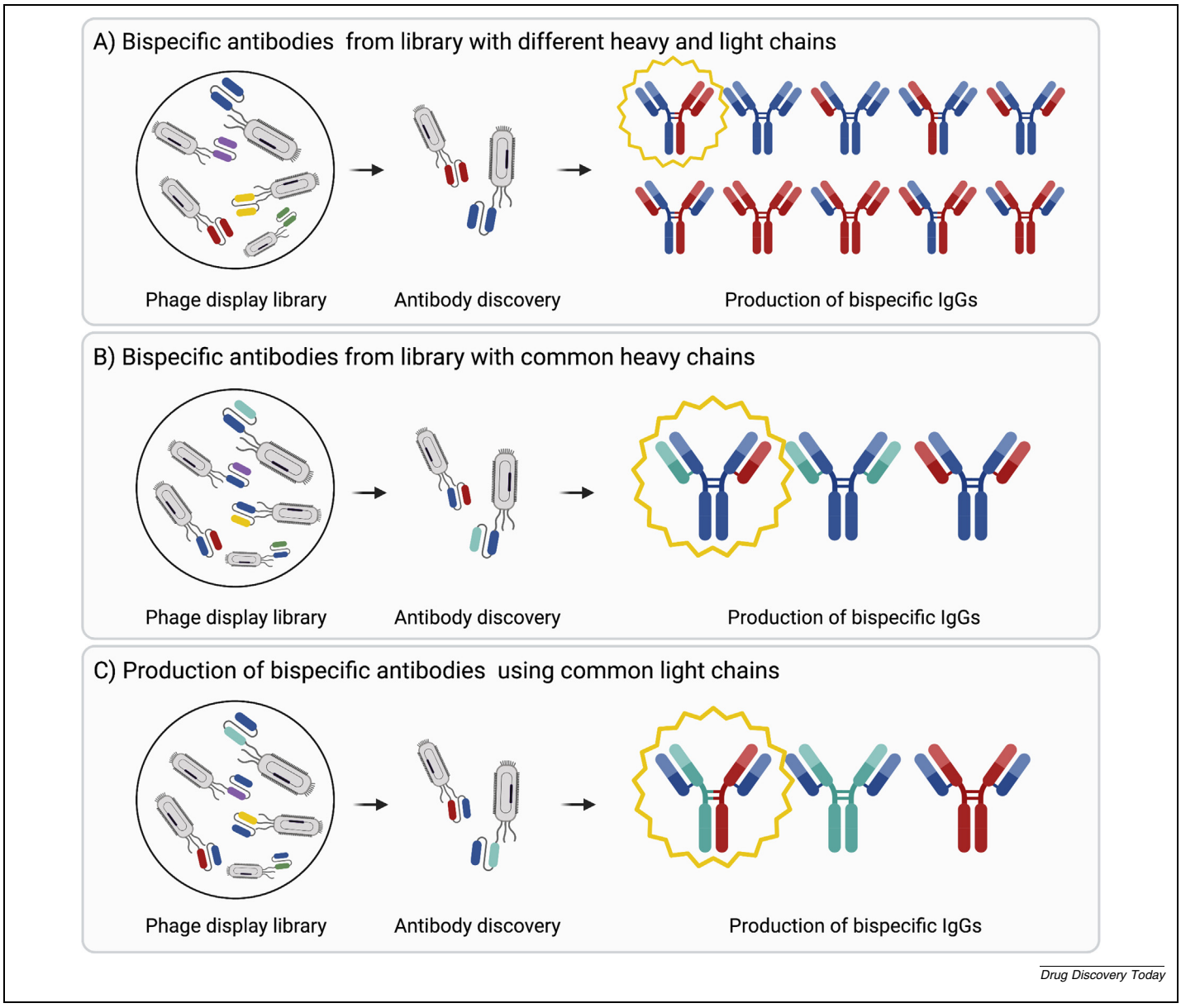


**FIG. 7**

Production of bispecific antibodies. **(a)** From libraries with different heavy and light chains, resulting in one bispecific antibody and nine incorrect antibody species. **(b)** From libraries with common heavy chains, resulting in one bispecific and only two incorrect antibody species. **(c)** From libraries with common heavy chains, resulting in one bispecific and only two incorrect antibody species.

can be created and used to select antibodies against two different antigens. The fixed $V_H$ could be chosen for its favorable properties for *in vitro* display technologies, its occurrence in natural human antibody repertoires, or intrinsic stability. Alternatively, the $V_H$ could be derived from an already existing mAb. The $V_L$ sequences could either be isolated from circulating B cells from healthy individuals or patients, or diversity could be generated *in vitro* using advanced mutagenesis strategies.[168] This allows for the isolation of candidates with different target specificities that share the same heavy chain but carry either κ or λ light chains. Based on its structure, such a fully human bsIgG format, carrying both a κ and a λ light chain, is referred to as a κλ-body.[168] These specialized libraries have been successfully developed and used against several soluble and cell surface human antigens, resulting in the discovery of high-affinity IgGκ and IgGλ. This confirms that the light chain can be sufficient to drive antibody specificity and has enabled the isolation of high-affinity antibodies that can be used for construction of functional bsIgG for several antigen combinations.[168]

### *Chain pairing with common light chains*

The most common strategy of chain pairing relies on the use of common light chains and distinct diversified heavy chains. This takes advantage of the high diversity in CDR-H3, which tends to dominate binding interactions in many cases.[169,170] Although the first scFv-based phage display libraries with common light chains appeared during the 1990 s,[171,172] subsequent use in bispecifics is more complicated than the corresponding heavy-

light chain pairing with a common heavy chain. Indeed, modification of the heavy chain in the Fc region is necessary to force the heterodimerization of two different heavy chains (e.g., 'knobs-into-holes' technology,[156,172,173] use of opposite electrostatic charges,[174–176] or grafting a heterodimeric interface onto the homodimeric interface of the IgG[177]). However, this strategy has been successfully applied with scFv and Fab libraries, with common light chains extracted from naïve or immune repertoires, as well as from existing therapeutic antibodies.[172,178,179] More recently, complexity has further increased with the generation of bispecific antibodies with histidine-enriched common light chains, allowing the antibody to bind its targets in a pH-dependent manner,[180] as further described below.

### *Libraries focused on CDR-H3*

The CDR3 of the immunoglobulin heavy and light chains are the most important regions involved in antigen contacts in antibody–antigen complexes. In particular, CDR-H3 shows the largest diversity of the CDRs, both in terms of sequence and length,[169] and this diversity is often sufficient for driving the specificity of an antibody.[169,170,181] Therefore, small libraries with relatively large structural diversity can be created by focusing on diversity in the CDR-H3 residues alone.[182]

Researchers have shed light on structural differences in CDR-H3s between antibodies from different species. For example, it was found that the CDR-H3s in antibodies from galline, camelid, and bovine species are longer than the corresponding loop of human antibodies, although examples of long CDR-H3s in humans exist.[183] Galline antibodies contain a high proportion of small amino acids that are associated with flexibility,[184] and high-affinity binding galline antibodies typically have an increased cysteine content, which creates long loops with complex, disulfide-constrained structures. Using yeast display technology,[185] or immunization followed by sorting and NGS of antigen binding B cells,[186] bovine antibodies with CDR-H3s specific against epidermal growth factor receptor (EGFR) and complement component C5, respectively, have been discovered. This highlights the likelihood that long loop binders can also be discovered from bovine antibody libraries using phage display technology. In camelids, the $V_HHs$ tend to bind with protruding loops into concave cavities on the surface of the antigen, whereas, in bovines, ultralong CDR-H3 regions form a 'stalk and knob' independently folding mini domain, similar to a knottin domain, which projects far out from the surface of the antibody and is diverse in both its sequence and disulfide pattern.[187] This 'minifold' has a general shape and dimension similar to several small disulfide-bonded protein families, including protease inhibitors, ion-channel blockers, venom toxins, and G-protein-coupled receptor ligands.[188–190] Thus, these atypical paratopes could provide the ability to interact with different epitopes, particularly recessed or concave surfaces, as exist in many enzymes, pores, and channels, compared with traditional antibodies.[191,192] As a proof of concept, an antibody format, 'KnotBodies', which are similar to the peculiar bovine antibodies and display knottin domains in place of the CDR2 loops,[193] was recently developed. These knottins, which are difficult to engineer and have short *in vivo* half-lives on their own,[194] benefit from the increased stability and extended half-life of the antibody scaffold. Both the knottin and the antibody loop sequences could be engineered and used in phage display selections to optimize binding selectivity and, as an example, the blocking potency of an antibody against an ion-channel.

Altogether, elucidation of other structural features of antibodies from other species has revealed eccentricities that can be used to bind new types of difficult-to-target epitopes, and new specialized phage display libraries with these features are coming to light.[195–198].

### *Side-and-loop libraries*

SdAbs and antibody mimics typically bind antigen clefts via their CDR loops.[199,200] As a consequence, when the antigen epitope is different (i.e., rather convex), it is less likely that an sdAb with a convex paratope will be able to bind. Hence, researchers have generated a new recognition surface on single immunoglobulin-like scaffolds by tailoring the location of amino acid diversity to residues outside the conventional loop positions.

Koide *et al*. observed that an FN3 monobody (an antibody mimic selected from a diversified library of the tenth FN3 domain of human fibronectin), was forming a binding surface via the longest loop and the face of a β-sheet.[201] Based on this observation, they created a monobody 'side-and-loop' library,[201] in which the longest loop and the adjacent β-sheet were carrying diversity. This corresponds, by structural homology, to the CDR3 loop and the β-sheet of an immunoglobulin that mediates heterodimerization between the variable domains of the heavy and light chains. After a few rounds of phage and yeast display selection, using a 'side-and-loop' and a 'loop only' library in parallel, it was demonstrated that the two libraries performed differently against different targets. Indeed, for one target (GFP), the side library clones had higher affinity than the counterparts from the loop library, whereas, for another target (hSUMO1), the trend was the opposite. This demonstrated that alternative library designs focused on the side-and-loop surface could be more effective than conventional loop-based strategies in recognizing epitopes with distinct topography.[202–205]

### *Histidine-enriched libraries*

The pH dependence of antibody–antigen interactions has an effect on subcellular trafficking dynamics and antibody recycling,[206] as described above. The literature has numerous examples of effective engineered antibodies with pH-sensitive binding derived from existing antibodies.[107,207–210] The principle is relatively simple and relies on the incorporation of histidine residues in the binding interface, which are ionizable at pH lower than 6. Upon protonation of these residues in the acidic endosome, structural transitions, caused by altered electrostatic interactions, account for a loss of binding to the antigen. Moreover, the total number of ionizable histidine residues involved in antigen binding impacts the degree of pH sensitivity.[208]

Whereas most examples of engineered antibodies with pH-sensitive binding used histidine scanning alone or combinatorial histidine scanning libraries derived from existing antibodies, there are only a few attempts of *de novo* isolation of pH-dependent antibodies from naïve libraries. The first example took advantage of a synthetic scFv-based phage display library

enriched in histidine residues to find pH-dependent binders to the human chemokine CXCL10.[110] The library was constructed to be histidine enriched by alternating YAT and NHT codons in 8–15 amino acid positions in the CDR-H3. However, after three rounds of selection, the pH dependency of the best clone was too low, and new libraries enriched for histidine in all the CDRs from the light and heavy chains were created. These new scFv-based libraries led to a final reformatted IgG clone with a low nanomolar affinity at pH 7.2 and a 22-fold faster dissociation rate at pH 6.0. Another recent study used a histidine-enriched and CDR3-diversified $V_{NAR}$ domain yeast display library against EpCAM, in which only one pH-dependent binder was found.[211]

The upfront selection of optimal conformations or sequences rather than the re-engineering of an antibody that was not initially selected for pH-dependent binding properties appears an attractive idea. Indeed, it is understandable that already existing antibodies are not always amenable to transformation into pH-dependent antibodies. However, the only two examples of *de novo* isolation of pH-sensitive antibodies might be an indication of the process difficulty, including the need to generate additional sublibraries for pH dependence and affinity maturation. Furthermore, the histidine-mediated pH-dependent binding restricts the number of suitable epitopes because they need to have positively charged, or proton donating residues. In other words, a negatively charged or proton-acceptor epitope is theoretically a difficult target for a pH-dependent binding antibody.

## Concluding remarks

In this review, four major parameters that can be altered to tailor an antibody discovery campaign using phage display selections have been presented: antibody format, antigen presentation, selection strategy, and design of phage display library. The information provided in this review can be used individually or in combination for designing an antibody discovery campaign, dependent on the requirements of the desired antibodies.

### Declaration of interests

The authors declare that they have no competing interests.

### *CRediT authorship contribution statement*

**Line Ledsgaard:** Conceptualization, Investigation, Visualization, Writing – original draft, Writing – review & editing. **Anne Ljungars:** Conceptualization, Investigation, Writing – original draft, Writing – review & editing. **Charlotte Rimbault:** Investigation, Writing – original draft, Writing – review & editing. **Christoffer V. Sørensen:** Investigation, Writing – original draft, Writing – review & editing. **Tulika Tulika:** Investigation, Writing – original draft, Writing – review & editing. **Jack Wade:** Investigation, Writing – original draft, Writing – review & editing. **Yessica Wouters:** Investigation, Writing – original draft, Writing – review & editing. **John McCafferty:** Investigation, Writing – review & editing. **Andreas H. Laustsen:** Conceptualization, Investigation, Writing – review & editing.

## Acknowledgments

Figures were created using BioRender (BioRender.com). The authors gratefully acknowledge the following sources of funding: Villum Foundation grant 00025302, Wellcome (221702/Z/20/Z), The European Research Council (ERC) under the European Union's Horizon 2020 research and innovation programme grant no. 850974, The Novo Nordisk Foundation (NNF16OC0019248), and The Hørslev Foundation (203866) to A.H.L.; Olsens Mindefold, Marie og M.B. Richters Fond, Niels Bohr Fondet, Torben og Alice Fritmodts Fond, William Demant Fonden, Otto Mønsteds Fond, Knud Højgaards Fond, Rudolph Als Fondet, Augustinus Fonden, and Tranes Fond to L.L.

## References

1. G.P. Smith, Filamentous fusion phage: novel expression vectors that display cloned antigens on the virion surface, Science. 228 (1985) 1315–1317.
2. J. McCafferty, A.D. Griffiths, G. Winter, D.J. Chiswell, Phage antibodies: filamentous phage displaying antibody variable domains, Nature. 348 (1990) 552–554.
3. M.A. Alfaleh, H.O. Alsaab, A.B. Mahmoud, A.A. Alkayyal, M.L. Jones, S.M. Mahler, et al., Phage display derived monoclonal antibodies: from bench to bedside, Front Immunol. 11 (2020) 1986.
4. J. Hanes, A. Plückthun, *In vitro* selection and evolution of functional proteins by using ribosome display, Proc Natl Acad Sci USA 94 (1997) 4937–4942.
5. L.C. Mattheakis, R.R. Bhatt, W.J. Dower, An *in vitro* polysome display system for identifying ligands from very large peptide libraries, Proc Natl Acad Sci USA 91 (1994) 9022–9026.
6. E.T. Boder, Wittrup KD Yeast surface display for screening combinatorial polypeptide libraries, Nat Biotechnol. 15 (1997) 553–557.
7. K. Parthiban, R.L. Perera, M. Sattar, Y. Huang, S. Mayle, E. Masters, et al., A comprehensive search of functional sequence space using large mammalian display libraries created by gene editing, mAbs 11 (2019) 884–898.
8. R.R. Beerli, M. Bauer, R.B. Buser, M. Gwerder, S. Muntwiler, P. Mauer, et al., Isolation of human monoclonal antibodies by mammalian cell display, Proc Natl Acad Sci USA 105 (2008) 14336–14341.
9. J.W. Kehoe, B.K. Kay, Filamentous phage display in the New Millennium, Chem. Rev. 105 (2005) 4056–4072.
10. C.E.Z. Chan, A.H.Y. Chan, A.P.C. Lim, Hanson BJ Comparison of the efficiency of antibody selection from semi-synthetic scFv and non-immune Fab phage display libraries against protein targets for rapid development of diagnostic immunoassays, J Immunol Methods 373 (2011) 79–88.
11. K. Chockalingam, Z. Peng, C.N. Vuong, L.R. Berghman, Chen Z Golden Gate assembly with a bi-directional promoter (GBid): a simple, scalable method for phage display Fab library creation, Sci Rep. 10 (2020) 2888.
12. K. Li, K.A. Zettlitz, J. Lipianskaya, Y. Zhou, J.D. Marks, P. Mallick, et al., A fully human scFv phage display library for rapid antibody fragment reformatting, Protein Eng Des Sel. 28 (2015) 307–316.
13. R. Ahamadi-Fesharaki, A. Fateh, F. Vaziri, G. Solgi, S.D. Siadat, F. Mahboudi, et al., Single-chain variable fragment-based bispecific antibodies: hitting two targets with one sophisticated arrow, Mol. Ther. Oncolytics 14 (2019) 38–56.
14. D. Röthlisberger, A. Honegger, A. Plückthun, Domain interactions in the Fab fragment: a comparative evaluation of the single-chain Fv and Fab format engineered with variable domains of different stability, J Mol Biol. 347 (2005) 773–789.
15. M. Steinwand, P. Droste, A. Frenzel, M. Hust, S. Dübel, T. Schirrmann, The influence of antibody fragment format on phage display based affinity maturation of IgG, mAbs 6 (2014) 204–218.
16. V. Quintero-Hernández, V.R. Juárez-González, M. Ortíz-León, R. Sánchez, L.D. Possani, B. Becerril, The change of the scFv into the Fab format improves the stability and *in vivo* toxin neutralization capacity of recombinant antibodies, Mol Immunol. 44 (2007) 1307–1315.
17. A. Frenzel, M. Hust, T. Schirrmann, Expression of recombinant antibodies, Front Immunol. 4 (2013) 217.
18. J.T. Koerber, M.J. Hornsby, J.A. Wells, An improved single-chain Fab platform for efficient display and recombinant expression, J Mol Biol. 427 (2015) 576–586.

19. R.H. Reader, R.G. Workman, B.C. Maddison, K.C. Gough, Advances in the production and batch reformatting of phage antibody libraries, Mol Biotechnol. 61 (2019) 801–815.
20. C. Vincke, R. Loris, D. Saerens, S. Martínez-Rodriguez, S. Muyldermans, K. Conrath, General strategy to humanize a camelid single-domain antibody and identification of a universal humanized nanobody scaffold, J Biol Chem. 284 (2009) 3273–3284.
21. D. Könning, S. Zielonka, J. Grzeschik, M. Empting, B. Valldorf, S. Krah, C. Schröter, et al., Camelid and shark single domain antibodies: structural features and therapeutic potential, Curr. Opin. Struct. Biol. 45 (2017) 10–16.
22. S. Jähnichen, C. Blanchetot, D. Maussang, M. González-Pajuelo, K.Y. Chow, L. Bosch, et al., CXCR4 nanobodies (VHH-based single variable domains) potently inhibit chemotaxis and HIV-1 replication and mobilize stem cells, Proc. Natl. Acad. Sci. U. S. A. 107 (2010) 20565–20570.
23. H. Dooley, M.F. Flajnik, A.J. Porter, Selection and characterization of naturally occurring single-domain (IgNAR) antibody fragments from immunized sharks by phage display, Mol. Immunol. 40 (2003) 25–33.
24. H. Ebersbach, S. Geisse, Antigen generation and display in therapeutic antibody drug discovery – a neglected but critical player, Biotechnol. J. 7 (2012) 1433–1443.
25. J.E. Butler, L. Ni, R. Nessler, K.S. Joshi, M. Suter, B. Rosenberg, et al., The physical and functional behavior of capture antibodies adsorbed on polystyrene, J. Immunol. Methods 150 (1992) 77–90.
26. Z. Duan, H. Siegumfeldt, An efficient method for isolating antibody fragments against small peptides by antibody phage display, Comb. Chem. High Throughput Screen. 13 (2010) 818–828.
27. C.M. Dundas, D. Demonte, S. Park, Streptavidin-biotin technology: improvements and innovations in chemical and biological applications, Appl. Microbiol. Biotechnol. 97 (2013) 9343–9353.
28. V.S. Ivanov, Z.K. Suvorova, L.D. Tchikin, A.T. Kozhich, V.T. Ivanov, Effective method for synthetic peptide immobilization that increases the sensitivity and specificity of ELISA procedures, J. Immunol. Methods 153 (1992) 229–233.
29. L. Ledsgaard, M. Kilstrup, A. Karatt-Vellatt, J. McCafferty, A.H. Laustsen, Basics of antibody phage display technology, Toxins 10 (2018) 236.
30. A.P. Sibler, E. Kempf, A. Glacet, G. Orfanoudakis, D. Bourel, E. Weiss, *In vivo* biotinylated recombinant antibodies: high efficiency of labelling and application to the cloning of active anti-human IgG1 Fab fragments, J. Immunol. Methods 224 (1999) 129–140.
31. E. de Boer, P. Rodriguez, E. Bonte, J. Krijgsveld, E. Katsantoni, A. Heck, et al., Efficient biotinylation and single-step purification of tagged transcription factors in mammalian cells and transgenic mice, Proc. Natl. Acad. Sci. USA 100 (2003) 7480–7485.
32. D. Beckett, E. Kovaleva, Schatz PJA minimal peptide substrate in biotin holoenzyme synthetase-catalysed biotinylation, Protein Sci. 8 (1999) 921–929.
33. M.G. Cull, P.J. Schatz, Biotinylation of proteins *in vivo* and *in vitro* using small peptide tags, Methods Enzymol. 326 (2000) 430–440.
34. B.K. Kay, S. Thai, V.V. Volgina, High-throughput biotinylation of proteins, Methods Mol. Biol. 498 (2009) 185–196.
35. M.D. Scholle, F.R. Collart, B.K. Kay, *In vivo* biotinylated proteins as targets for phage-display selection experiments, Protein Expr. Purif. 37 (2004) 243–252.
36. M. Fairhead, M. Howarth, Site-specific biotinylation of purified proteins using BirA, Methods Mol. Biol. 1266 (2015) 171–184.
37. O. Azim-Zadeh, A. Hillebrecht, U. Linne, M.A. Marahiel, G. Klebe, K. Lingelbach, et al., Use of biotin derivatives to probe conformational changes in proteins, J. Biol. Chem. 282 (2007) 21609–21617.
38. Luna EJ. Biotinylation of proteins in solution and on cell surfaces. *Curr. Protoc. Protein Sci.* 2001; Chapter 3, Unit 3.6.
39. Luna EJ. Biotinylation of proteins in solution and on cell surfaces. *Curr. Protoc. Protein Sci.* 1996; 6; 3.6.1–3.6.15.
40. A. Koide, J. Wojcik, R.N. Gilbreth, A. Reichel, J. Piehler, S. Koide, Accelerating phage-display library selection by reversible and site-specific biotinylation, Protein Eng. Des. Sel. 22 (2009) 685–690.
41. B. Zakeri, J.O. Fierer, E. Celik, E.C. Chittock, U. Schwarz-Linek, V.T. Moy, et al., Peptide tag forming a rapid covalent bond to a protein, through engineering a bacterial adhesin, Proc. Natl. Acad. Sci. USA 109 (2012) E690–E697.
42. J.K. Fierle, J. Abram-Saliba, M. Brioschi, M. deTiani, G. Coukos, S.M. Dunn, Integrating SpyCatcher/SpyTag covalent fusion technology into phage display workflows for rapid antibody discovery, Sci. Rep. 9 (2019) 12815.
43. M.L. Jones, M.A. Alfaleh, S. Kumble, S. Zhang, G.W. Osborne, M. Yeh, et al., Targeting membrane proteins for antibody discovery using phage display, Sci. Rep. 6 (2016) 26240.
44. B.D. Lipes, Y.-H. Chen, H. Ma, H.F. Staats, D.J. Kenan, M.D. Gunn, An entirely cell-based system to generate single-chain antibodies against cell surface receptors, J. Mol. Biol. 379 (2008) 261–272.
45. K.H. Khan, Gene expression in mammalian cells and its applications, Adv. Pharm. Bull. 3 (2013) 257–263.
46. A.D. Bandaranayake, S.C. Almo, Recent advances in mammalian protein production, FEBS Lett. 588 (2014) 253–260.
47. E. Urich, S.E. Lazic, J. Molnos, I. Wells, P.O. Freskgård, Transcriptional profiling of human brain endothelial cells reveals key properties crucial for predictive *in vitro* blood-brain barrier models, PLoS ONE 7 (2012) e38149.
48. P. Uva, A. Lahm, A. Sbardellati, A. Grigoriadis, A. Tutt, E. de Rinaldis, Comparative membranome expression analysis in primary tumors and derived cell lines, PLoS ONE 5 (2010) e11742.
49. A. Ljungars, L. Mårtensson, J. Mattsson, M. Kovacek, A. Sundberg, U.-C. Tornberg, et al., A platform for phenotypic discovery of therapeutic antibodies and targets applied on chronic lymphocytic leukemia, NPJ Precis. Oncol. 2 (2018) 18.
50. K. Kanonenberg, J. Royes, A. Kedrov, G. Poschmann, F. Angius, A. Solgadi, et al., Shaping the lipid composition of bacterial membranes for membrane protein production, Microb. Cell Factories 18 (2019) 131.
51. S.J. Routledge, L. Mikaliunate, A. Patel, M. Clare, S.P. Cartwright, Z. Bawa, et al., The synthesis of recombinant membrane proteins in yeast for structural studies, Methods 95 (2016) 26–37.
52. C. Trometer, P. Falson, Mammalian membrane protein expression in baculovirus-infected insect cells, in: I. Mus-Veteau (Ed.), Heterologous Expression of Membrane Proteins: Methods and Protocols, Totowa; Humana Press, 2010, pp. 105–117.
53. Tur MK, Huhn M, Sasse S, Engert A, Barth S. Selection of scFv phages on intact cells under low pH conditions leads to a significant loss of insert-free phages. *BioTechniques* 2010; 30: 404–408, 410, 412–413.
54. Y. Stark, S. Venet, A. Schmid, Whole cell panning with phage display, Methods Mol. Biol. 1575 (2017) 67–91.
55. A. Jesorka, O. Orwar, Liposomes: technologies and analytical applications, Annu. Rev. Anal. Chem. 1 (2008) 801–832.
56. L.K. Jespersen, A. Kuusinen, A. Orellana, K. Keinänen, J. Engberg, Use of proteoliposomes to generate phage antibodies against native AMPA receptor, Eur. J. Biochem. 267 (2000) 1382–1389.
57. I.A. Smirnova, P. Ädelroth, P. Brzezinski, Extraction and liposome reconstitution of membrane proteins with their native lipids without the use of detergents, Sci. Rep. 8 (2018) 14950.
58. T. Ravula, N.Z. Hardin, A. Ramamoorthy, Polymer nanodiscs: advantages and limitations, Chem. Phys. Lipids 219 (2019) 45–49.
59. I.G. Denisov, S.G. Sligar, Nanodiscs for structural and functional studies of membrane proteins, Nat. Struct. Mol. Biol. 23 (2016) 481–486.
60. T.H. Bayburt, Y.V. Grinkova, S.G. Sligar, Self-assembly of discoidal phospholipid bilayer nanoparticles with membrane scaffold proteins, Nano Lett. 2 (2002) 853–856.
61. A. Nath, W.M. Atkins, S.G. Sligar, Applications of phospholipid bilayer nanodiscs in the study of membranes and membrane proteins, Biochemistry 46 (2007) 2059–2069.
62. M. Pavlidou, K. Hänel, L. Möckel, D. Willbold, Nanodiscs allow phage display selection for ligands to non-linear epitopes on membrane proteins, PLoS ONE 8 (2013) e72272.
63. T.J. Knowles, R. Finka, C. Smith, Y.-P. Lin, T. Dafforn, M. Overduin, Membrane proteins solubilized intact in lipid containing nanoparticles bounded by styrene maleic acid copolymer, J. Am. Chem. Soc. 131 (2009) 7484–7485.
64. K.S. Simon, N.L. Pollock, S.C. Lee, Membrane protein nanoparticles: the shape of things to come, Biochem. Soc. Trans. 46 (2018) 1495–1504.
65. L. Thoring, D.A. Wüstenhagen, M. Borowiak, M. Stech, A. Sonnabend, S. Kubick, Cell-free systems based on CHO cell lysates: optimization strategies, synthesis of 'difficult-to-express' proteins and future perspectives, PLoS ONE 11 (2016) e0163670.
66. S.K. Dondapati, M. Stech, A. Zemella, S. Kubick, Cell-free protein synthesis: a promising option for future drug development, BioDrugs 34 (2020) 327–348.
67. C.E. Hodgman, M.C. Jewett, Cell-free synthetic biology: thinking outside the cell, Metab. Eng. 14 (2012) 261–269.
68. P.K. Dominik, M.T. Borowska, O. Dalmas, S.S. Kim, E. Perozo, R.J. Keenan, et al., Conformational chaperones for structural studies of membrane proteins using antibody phage display with nanodiscs, Structure. 24 (2016) 300–309.
69. B. van der Woning, G. De Boeck, C. Blanchetot, V. Bobkov, A. Klarenbeek, M. Saunders, et al., DNA immunization combined with scFv phage display identifies antagonistic GCGR specific antibodies and reveals new epitopes on the small extracellular loops, mAbs 8 (2016) 1126–1135.

70. Z. Shirbaghaee, A. Bolhassani, Different applications of virus-like particles in biology and medicine: vaccination and delivery systems, Biopolymers 105 (2016) 113–132.
71. A. Zeltins, Construction and characterization of virus-like particles: a review, Mol. Biotechnol. 53 (2013) 92–107.
72. R. Huang, M.M. Kiss, M. Batonick, M.P. Weiner, B.K. Kay, Generating recombinant antibodies to membrane proteins through phage display, Antibodies 5 (2016) 11.
73. D.J. Schofield, A.R. Pope, V. Clementel, J. Buckell, S.D.J. Chapple, K.F. Clarke, et al., Application of phage display to high throughput antibody generation and characterization, Genome Biol. 8 (2007) R254.
74. A. Roghanian, I. Teige, L. Mårtensson, K.L. Cox, M. Kovacek, A. Ljungars, et al., Antagonistic human FcγRIIB (CD32B) antibodies have anti-tumor activity and overcome resistance to antibody therapy *in vivo*, Cancer Cell 27 (2015) 473–488.
75. M. Yeboah, C. Papagregoriou, D.C. Jones, H.T.C. Chan, G. Hu, J.S. McPartlan, et al., LILRB3 (ILT5) is a myeloid cell checkpoint that elicits profound immunomodulation, JCI Insight 5 (2020) 141593.
76. M.I. Kirsch, B. Hülseweh, C. Nacke, T. Rülker, T. Schirrmann, H.-J. Marschall, et al., Development of human antibody fragments using antibody phage display for the detection and diagnosis of Venezuelan equine encephalitis virus (VEEV), BMC Biotechnol. 8 (2008) 66.
77. P.K. Dominik, A.A. Kossiakoff, Phage display selections for affinity reagents to membrane proteins in nanodiscs, Methods Enzymol. 557 (2015) 219–245.
78. A. DiGiandomenico, P. Warrener, M. Hamilton, S. Guillard, P. Ravn, R. Minter, et al., Identification of broadly protective human antibodies to Pseudomonas aeruginosa exopolysaccharide Psl by phenotypic screening, J. Exp. Med. 209 (2012) 1273–1287.
79. J.B. Ridgway, E. Ng, J.A. Kern, J. Lee, J. Brush, A. Goddard, P. Carter, Identification of a human anti-CD55 single-chain Fv by subtractive panning of a phage library using tumor and nontumor cell lines, Cancer Res. 59 (1999) 2718–2723.
80. G.S. Williams, B. Mistry, S. Guillard, J.C. Ulrichsen, A.M. Sandercock, J. Wang, et al., Phenotypic screening reveals TNFR2 as a promising target for cancer immunotherapy, Oncotarget 7 (2016) 68278–68291.
81. A. Ljungars, C. Svensson, A. Carlsson, B. Birgersson, U.-C. Tornberg, B. Frendéus, et al., Deep mining of complex antibody phage pools generated by cell panning enables discovery of rare antibodies binding new targets and epitopes, Front. Pharmacol. 10 (2019) 847.
82. C.C. Lim, P.C.Y. Woo, T.S. Lim, Development of a phage display panning strategy utilizing crude antigens: isolation of MERS-CoV nucleoprotein human antibodies, Sci. Rep. 9 (2019) 6088.
83. S.U. Eisenhardt, M. Schwarz, N. Bassler, K. Peter, Subtractive single-chain antibody (scFv) phage-display: tailoring phage-display for high specificity against function-specific conformations of cell membrane molecules, Nat. Protoc. 2 (2007) 3063–3073.
84. H. Thie, B. Voedisch, S. Dübel, M. Hust, T. Schirrmann, Affinity maturation by phage display, Methods Mol. Biol. 525 (2009) 309–322.
85. H.J. Ditzel, Rescue of a broader range of antibody specificities using an epitope-masking strategy, in: P.M. O'Brien, R. Aitken (Eds.), Antibody Phage Display: Methods and Protocols, Humana Press, Totowa, 2002, pp. 179–186.
86. H.J. Ditzel, J.M. Binley, J.P. Moore, J. Sodroski, N. Sullivan, L.S. Sawyer, et al., Neutralizing recombinant human antibodies to a conformational V2- and CD4-binding site-sensitive epitope of HIV-1 gp120 isolated by using an epitope-masking procedure, J. Immunol. 1995 (154) (1950) 893–906.
87. P.P. Sanna, R.A. Williamson, A.D. Logu, F.E. Bloom, D.R. Burton, Directed selection of recombinant human monoclonal antibodies to herpes simplex virus glycoproteins from phage display libraries, Proc. Natl. Acad. Sci. USA 92 (1995) 6439–6443.
88. K. Even-Desrumeaux, D. Nevoltris, M.N. Lavaut, K. Alim, J.-P. Borg, S. Audebert, et al., Masked selection: a straightforward and flexible approach for the selection of binders against specific epitopes and differentially expressed proteins by phage display, Mol. Cell. Proteomics 13 (2014) 653–665.
89. X. Zeng, L. Li, J. Lin, X. Li, B. Liu, Y. Kong, et al., Isolation of a human monoclonal antibody specific for the receptor binding domain of SARS-CoV-2 using a competitive phage biopanning strategy, Antib. Ther. 3 (2020) 95–100.
90. B. Stausbøl-Grøn, T. Wind, S. Kjaer, L. Kahns, N.J.V. Hansen, P. Kristensen, et al., A model phage display subtraction method with potential for analysis of differential gene expression, FEBS Lett. 391 (1996) 71–75.
91. J. Fransson, U.-C. Tornberg, C.A.K. Borrebaeck, R. Carlsson, B. Frendéus, Rapid induction of apoptosis in B-cell lymphoma by functionally isolated human antibodies, Int. J. Cancer 119 (2006) 349–358.
92. P. Carter, L. Smith, M. Ryan, Identification and validation of cell surface antigens for antibody targeting in oncology, Endocr. Relat. Cancer 11 (2004) 659–687.
93. Frendéus B. Bioinvent International. Method for screening anti-ligand libraries for identifying anti-ligands specific for differentially and infrequently expressed ligands. WO/2004/023140.
94. A.H. Laustsen, How can monoclonal antibodies be harnessed against neglected tropical diseases and other infectious diseases?, Expert Opin Drug Discov. 14 (2019) 1103–1112.
95. A.R.M. Bradbury, S. Sidhu, S. Dübel, J. McCafferty, Beyond natural antibodies: the power of *in vitro* display technologies, Nat. Biotechnol. 29 (2011) 245–254.
96. M.-Y. Zhang, Y. Shu, S. Phogat, X. Xiao, F. Cham, P. Bouma, et al., Broadly cross-reactive HIV neutralizing human monoclonal antibody Fab selected by sequential antigen panning of a phage display library, J. Immunol. Methods 283 (2003) 17–25.
97. D.C. Ekiert, A.K. Kashyap, J. Steel, A. Rubrum, G. Babha, R. Khayat, et al., Cross-neutralization of influenza A viruses mediated by a single antibody loop, Nature. 489 (2012) 526–532.
98. S. Ahmadi, M.B. Pucca, J.A. Jürgensen, R. Janke, L. Ledsgaard, E.M. Schoof, et al., An *in vitro* methodology for discovering broadly-neutralizing monoclonal antibodies, Sci. Rep. 10 (2020) 10765.
99. K.A. Henry, J. Tanha, G. Hussack, Identification of cross-reactive single-domain antibodies against serum albumin using next-generation DNA sequencing, Protein Eng. Des. Sel. 28 (2015) 379–383.
100. A.S. Kolaskar, P.C. Tongaonkar, A semi-empirical method for prediction of antigenic determinants on protein antigens, FEBS Lett. 276 (1990) 172–174.
101. G. de la Rosa, L.L. Corrales-García, X. Rodriguez-Ruiz, E. López-Vera, G. Corzo, Short-chain consensus alpha-neurotoxin: a synthetic 60-mer peptide with generic traits and enhanced immunogenic properties, Amino Acids 50 (2018) 885–895.
102. G. de la Rosa, F. Olvera, I.G. Archundia, B. Lomonte, A. Alagón, G. Corzo, Horse immunization with short-chain consensus α-neurotoxin generates antibodies against broad spectrum of elapid venomous species, Nat. Commun. 10 (2019) 3642.
103. M. Hamza, C. Knudsen, C.A. Gnanathasan, W. Monteiro, M.R. Lewin, A.H. Laustsen, et al., Clinical management of snakebite envenoming: future perspectives, Toxicon X 11 (2021) 100079.
104. D.C. Roopenian, A.S. FcRn, the neonatal Fc receptor comes of age, Nat. Rev. Immunol. 7 (2007) 715–725.
105. T. Igawa, K. Haraya, K. Hattori, Sweeping antibody as a novel therapeutic antibody modality capable of eliminating soluble antigens from circulation, Immunol. Rev. 270 (2016) 132–151.
106. T. Igawa, A. Maeda, K. Karaya, T. Tachibana, Y. Iwayanagi, F. Mimoto, et al., Engineered monoclonal antibody with novel antigen-sweeping activity *in vivo*, PLoS ONE. 8 (2013) e63236.
107. T. Igawa, S. Ishii, T. Tachibana, A. Maeda, Y. Higuchi, S. Shimaoka, et al., Antibody recycling by engineered pH-dependent antigen binding improves the duration of antigen neutralization, Nat. Biotechnol. 28 (2010) 1203–1207.
108. J.C. Kang, W. Sun, P. Khare, M. Karimi, X. Wang, Y. Shen, et al., Engineering a HER2-specific antibody–drug conjugate to increase lysosomal delivery and therapeutic efficacy, Nat. Biotechnol. 37 (2019) 523–526.
109. H. Sade, C. Baumgartner, A. Hugenmatter, E. Moessner, P.-O. Freksgård, J. Niewoehner, A human blood-brain barrier transcytosis assay reveals antibody transcytosis influenced by pH-dependent receptor binding, PLoS ONE 9 (2014) e96340.
110. P. Bonvin, S. Venet, G. Fontaine, U. Ravn, F. Gueneau, M. Kosco-Vilbois, et al., De novo isolation of antibodies with pH-dependent binding properties, mAbs 7 (2015) 294–302.
111. N. Hironiwa, S. Ishii, S. Kadono, F. Mimoto, K. Habu, T. Igawa, et al., Calcium-dependent antigen binding as a novel modality for antibody recycling by endosomal antigen dissociation, mAbs 8 (2015) 65–73.
112. S. Jung, A. Honegger, A. Plückthun, Selection for improved protein stability by phage display, J. Mol. Biol. 294 (1999) 163–180.
113. V. Sieber, A. Plückthun, F.X. Schmid, Selecting proteins with improved stability by a phage-based method, Nat. Biotechnol. 16 (1998) 955–960.
114. Ledsgaard L, Laustsen AH, Puš U, Wade J, Villar P, Boddum K, *et al.* In vitro discovery and optimization of a human monoclonal antibody that neutralizes neurotoxicity and lethality of cobra snake venom. *BioRxiv*. Published online September 7, 2021. http://dx.doi.org/10.1101/2021.09.07.459075.
115. S. Steidl, O. Ratsch, B. Brocks, M. Dürr, E. Thomassen-Wolf, *In vitro* affinity maturation of human GM-CSF antibodies by targeted CDR-diversification, Mol. Immunol. 46 (2008) 135–144.

116. E. Durr, J. Yu, K.M. Krasinska, L.A. Carver, J.R. Yates, J.E. Testa, et al., Direct proteomic mapping of the lung microvascular endothelial cell surface *in vivo* and in cell culture, Nat. Biotechnol. 22 (2004) 985–992.
117. P. Oh, J. Yu, E. Durr, K.M. Krasinska, L.A. Carver, J.E. Testa, et al., Subtractive proteomic mapping of the endothelial surface in lung and solid tumours for tissue-specific therapy, Nature. 429 (2004) 629–635.
118. R. Pasqualini, E. Ruoslahti, Organ targeting *In vivo* using phage display peptide libraries, Nature. 380 (1996) 364–366.
119. K. Deramchia, M.-J. Jacobin-Valat, A. Vallet, H. Bazin, X. Santarelli, S. Sanchez, et al., *In vivo* phage display to identify new human antibody fragments homing to atherosclerotic endothelial and subendothelial tissues, Am. J. Pathol. 180 (2012) 2576–2589.
120. P. Valadon, J.D. Garnett, J.E. Testa, M. Bauerle, P. Oh, J.E. Schnitzer, Screening phage display libraries for organ-specific vascular immunotargeting *in vivo*, Proc. Natl. Acad. Sci. USA 103 (2006) 407–412.
121. P. Stocki, J. Szary, C.L.M. Rasmussen, M. Demydchuk, L. Northall, D.B. Logan, et al., Blood-brain barrier transport using a high affinity, brain-selective VNAR antibody targeting transferrin receptor 1, FASEB J. 35 (2021) e21172.
122. S.A.M. van Lith, I. Roodink, J.J.C. Verhoeff, P.I. Mäkinen, J.P. Lappalainen, S. Ylä-Herttuala, et al., *In vivo* phage display screening for tumor vascular targets in glioblastoma identifies a llama nanobody against dynactin-1-p150 Glued, Oncotarget 7 (2016) 71594–71607.
123. W. Arap, R. Pasqualini, E. Ruoslahti, Cancer treatment by targeted drug delivery to tumor vasculature in a mouse model, Science 279 (1998) 377–380.
124. F.I. Staquicini, M. Cardó-Vila, M.G. Kolonin, M. Trepel, J.K. Edwards, D.N. Nunes, et al., Vascular ligand-receptor mapping by direct combinatorial selection in cancer patients, Proc. Natl. Acad. Sci. USA 108 (2011) 18637–18642.
125. D.N. Krag, G.S. Shukla, G.-P. Shen, S. Pero, T. Ashikaga, S. Fuller, et al., Selection of tumor-binding ligands in cancer patients with phage display libraries, Cancer Res. 66 (2006) 7724–7733.
126. D.J. Schofield, A.R. Pope, V. Clementel, J. Buckell, S.D.J. Chapple, K.F. Clarke, et al., Application of phage display to high throughput antibody generation and characterization, Genome Biol. 8 (2007) R254.
127. J. Kügler, S. Wilke, D. Meier, F. Tomszak, A. Frenzel, T. Schirrmann, et al., Generation and analysis of the improved human HAL9/10 antibody phage display libraries, BMC Biotechnol. 15 (2015) 10.
128. R.S. Nelson, Valadon PA universal phage display system for the seamless construction of Fab libraries, J. Immunol. Methods 450 (2017) 41–49.
129. C. Sellmann, L. Pekar, C. Bauer, E. Ciesielski, S. Krah, S. Becker, et al., A one-step process for the construction of phage display scFv and VHH libraries, Mol. Biotechnol. 62 (2020) 228–239.
130. G. Bullen, J.D. Galson, G. Hall, P. Villar, L. Moreels, L. Ledsgaard, et al., Cross-Reactive SARS-CoV-2 Neutralizing Antibodies From Deep Mining of Early Patient Responses, Front. Immunol. 12 (2021) 2049.
131. J.C. Almagro, M. Pedraza-Escalona, H.I. Arrieta, S.M. Pérez-Tapia, Phage display libraries for antibody therapeutic discovery and development, Antibodies 8 (2019) 44.
132. L. Frigotto, M.E. Smith, C. Brankin, A. Sedani, S.E. Cooper, N. Kanwar, et al., Codon-precise, synthetic, antibody fragment libraries built using automated hexamer codon additions and validated through next generation sequencing, Antibodies 4 (2015) 88–102.
133. N.J. Kräutler, A. Yermanos, A. Pedrioli, S.P.M. Welten, D. Lorgé, U. Greczmiel, et al., Quantitative and qualitative analysis of humoral immunity reveals continued and personalized evolution in chronic viral infection, Cell Rep. 30 (2020) 997–1012.
134. A.H. Laustsen, V. Greiff, A. Karatt-Vellatt, S. Muyldermans, T.P. Jenkins, Animal immunization, *in vitro* display technologies, and machine learning for antibody discovery, Trends Biotechnol. 39 (2021) 1263–1273.
135. C.A.K. Borrebaeck, M. Ohlin, Antibody evolution beyond Nature, Nat. Biotechnol. 20 (2002) 1189–1190.
136. L.J. Schwimmer, B. Huang, H. Giang, R.L. Cotter, D.S. Chemla Vogel, F.V. Dy, et al., Discovery of diverse and functional antibodies from large human repertoire antibody libraries, J. Immunol. Methods 391 (2013) 60–71.
137. E. Söderlind, L. Strandberg, P. Jirholt, N. Kobayashi, V. Alexeiva, A.-M. Åberg, et al., Recombining germline-derived CDR sequences for creating diverse single-framework antibody libraries, Nat. Biotechnol. 18 (2000) 852–856.
138. T. Tiller, I. Schuster, D. Deppe, K. Siegers, R. Strohner, T. Herrmann, et al., A fully synthetic human Fab antibody library based on fixed VH/VL framework pairings with favorable biophysical properties, mAbs 5 (2013) 445–470.
139. R.J. Johnston, L.J. Su, J. Pickney, D. Critton, E. Boyer, A. Krishnakumar, et al., VISTA is an acidic pH-selective ligand for PSGL-1, Nature 574 (2019) 565–570.
140. R.M. Hoet, E.H. Cohen, R.B. Kent, K. Rookey, S. Schoonbroodt, S. Hogan, et al., Generation of high-affinity human antibodies by combining donor-derived and synthetic complementarity-determining-region diversity, Nat. Biotechnol. 23 (2005) 344–348.
141. Y. Pan, J. Du, J. Liu, H. Wu, F. Gui, N. Zhang, et al., Screening of potent neutralizing antibodies against SARS-CoV-2 using convalescent patients-derived phage-display libraries, Cell Discov. 7 (2021) 57.
142. P.T. Jones, P.H. Dear, J. Foote, M.S. Neuberger, G. Winter, Replacing the complementarity-determining regions in a human antibody with those from a mouse, Nature 321 (1986) 522–525.
143. L. Riechmann, M. Clark, H. Waldmann, G. Winter, Reshaping human antibodies for therapy, Nature 332 (1988) 323–327.
144. A. Ascione, C. Arenaccio, A. Mallano, M. Flego, M. Gellini, M. Andreotti, et al., Development of a novel human phage display-derived anti-LAG3 scFv antibody targeting CD8+ T lymphocyte exhaustion, BMC Biotechnol. 19 (2019) 67.
145. A. Frenzel, T. Schirrmann, M. Hust, Phage display-derived human antibodies in clinical development and therapy, mAbs 8 (2016) 1177–1194.
146. R.-M. Lu, Y.-C. Hwang, I.-J. Liu, C.-C. Lee, H.-Z. Tsai, H.-J. Li, et al., Development of therapeutic antibodies for the treatment of diseases, J. Biomed. Sci. 27 (2020) 1.
147. K.D. Ratanji, J.P. Derrick, R.J. Dearman, I. Kimber, Immunogenicity of therapeutic proteins: influence of aggregation, J. Immunotoxicol. 11 (2014) 99–109.
148. M. Nabhan, M. Pallardy, I. Turbica, Immunogenicity of bioproducts: cellular models to evaluate the impact of therapeutic antibody aggregates, Front. Immunol. 11 (2020).
149. M. Sauerborn, V. Brinks, W. Jiskoot, H. Schellekens, Immunological mechanism underlying the immune response to recombinant human protein therapeutics, Trends Pharmacol. Sci. 31 (2010) 53–59.
150. T. Jain, T. Sun, S. Durand, A. Hall, N.R. Houston, J.H. Nett, et al., Biophysical properties of the clinical-stage antibody landscape, Proc. Natl. Acad. Sci. 114 (2017) 944–949.
151. S. Yasuda, Y. Zhou, Y. Wang, M. Yamamura, J.-Y. Wang, A model integrating tonic and antigen-triggered BCR signals to predict the survival of primary B cells, Sci. Rep. 7 (2017) 14888.
152. J. Glanville, W. Zhai, J. Berka, D. Telman, G. Huerta, G.R. Mehta, et al., Precise determination of the diversity of a combinatorial antibody library gives insight into the human immunoglobulin repertoire, Proc. Natl. Acad. Sci. USA 106 (2009) 20216–20221.
153. P.H. Sudmant, T. Rausch, E.J. Gardner, R.E. Handsaker, A. Abyzov, J. Huddleston, et al., An integrated map of structural variation in 2,504 human genomes, Nature 526 (2015) 75–81.
154. W. Zhai, J. Glanville, M. Fuhrmann, L. Mei, I. Ni, P.D. Sundar, et al., Synthetic antibodies designed on natural sequence landscapes, J. Mol. Biol. 412 (2011) 55–71.
155. W.R. Strohl, L.M. Strohl, Therapeutic Antibody Engineering, Woodhead Publishing, Sawston, 2012, pp. 377–595.
156. J.B. Ridgway, L.G. Presta, P. Carter, 'Knobs-into-holes' engineering of antibody CH3 domains for heavy chain heterodimerization, Protein Eng. 9 (1996) 617–621.
157. J. Glanville, S. D'Angelo, T.A. Khan, S.T. Reddy, L. Naranjo, F. Ferrara, et al., Deep sequencing in library selection projects: what insight does it bring?, Curr Opin. Struct. Biol. 33 (2015) 146–160.
158. M.F. Erasmus, S. D'Angelo, F. Ferrara, L. Naranjo, A.A. Teixeira, R. Buonpane, et al., A single donor is sufficient to produce a highly functional *in vitro* antibody library, Commun. Biol. 4 (2021) 1–16.
159. J.L. Xu, M.M. Davis, Diversity in the CDR3 region of VH is sufficient for most antibody specificities, Immunity 13 (2000) 37–45.
160. W. Zhai, J. Glanville, M. Furhmann, L. Mei, I. Ni, P.D. Sundar, et al., Synthetic antibodies designed on natural sequence landscapes, J. Mol. Biol. 412 (2011) 55–71.
161. R.E. Kontermann, U. Brinkmann, Bispecific antibodies, Drug Discov. Today 20 (2015) 838–847.
162. A.F. Labrijn, M.L. Janmaat, J.M. Reichert, P.W.H.I. Parren, Bispecific antibodies: a mechanistic review of the pipeline, Nat. Rev. Drug Discov. 18 (2019) 585–608.
163. U. Brinkmann, R.E. Kontermann, The making of bispecific antibodies. *mAbs* 9 (2017) 182–212.
164. J. Ma, Y. Mo, M. Tang, J. Shen, Y. Qi, W. Zhao, et al., Bispecific antibodies: from research to clinical application, Front. Immunol. 12 (2021) 626616.
165. S. Wang, K. Chen, Q. Lei, P. Ma, A.Q. Yuan, Y. Zhao, et al., The state of the art of bispecific antibodies for treating human malignancies, EMBO Mol. Med. 13 (2021).
166. S. Krah, C. Sellmann, L. Rhiel, C. Schröter, S. Dickgiesser, J. Beck, et al., Engineering bispecific antibodies with defined chain pairing, New Biotechnol. 39 (2017) 167–173.

167. A. Ljungars, T. Schiött, U. Mattson, J. Steppa, B. Hambe, M. Semmrich, et al., A bispecific IgG format containing four independent antigen binding sites, Sci. Rep. 10 (2020) 1546.
168. N. Fischer, G. Elson, G. Magistrelli, E. Dheilly, N. Fouque, A. Laurendon, et al., Exploiting light chains for the scalable generation and platform purification of native human bispecific IgG, Nat. Commun. 6 (2015) 6113.
169. V. Kunik, Y. Ofran, The indistinguishability of epitopes from protein surface is explained by the distinct binding preferences of each of the six antigen-binding loops, Protein Eng. Des. Sel. 26 (2013) 599–609.
170. J.L. Xu, M.M. Davis, Diversity in the CDR3 region of V(H) is sufficient for most antibody specificities, Immunity 13 (2000) 37–45.
171. E.S. Ward, VH shuffling can be used to convert an Fv fragment of anti-hen egg lysozyme specificity to one that recognizes a T cell receptor V alpha, Mol. Immunol. 32 (1995) 147–156.
172. A.M. Merchant, Z. Zhu, J.Q. Yuan, A. Goddard, C.W. Adams, L.G. Presta, et al., An efficient route to human bispecific IgG, Nat. Biotechnol. 16 (1998) 677–681.
173. S. Atwell, J.B. Ridgway, J.A. Wells, P. Carter, Stable heterodimers from remodeling the domain interface of a homodimer using a phage display library, J. Mol. Biol. 270 (1997) 26–35.
174. K. Gunasekaran, M. Pentony, M. Shen, L. Garrett, C. Forte, A. Woodward, et al., Enhancing antibody Fc heterodimer formation through electrostatic steering effects: applications to bispecific molecules and monovalent IgG, J. Biol. Chem. 285 (2010) 19637–19646.
175. C. De Nardis, L.J.A. Hendriks, E. Poirier, T. Arvinte, P. Gros, A.B.H. Bakker, et al., A new approach for generating bispecific antibodies based on a common light chain format and the stable architecture of human immunoglobulin G1, J. Biol. Chem. 292 (2017) 14706–14717.
176. P. Strop, W.-H. Ho, L.M. Boustany, Y.N. Abdiche, K.C. Lindquist, S.E. Farias, et al., Generating bispecific human IgG1 and IgG2 antibodies from any antibody pair, J. Mol. Biol. 420 (2012) 204–219.
177. D. Skegro, C. Stutz, R. Ollier, E. Svensson, P. Wassmann, F. Bourquin, et al., Immunoglobulin domain interface exchange as a platform technology for the generation of Fc heterodimers and bispecific antibodies, J. Biol. Chem. 292 (2017) 9745–9759.
178. J. Jackman, Y. Chen, A. Huang, B. Moffat, J.M. Scheer, S.R. Leong, et al., Development of a two-part strategy to identify a therapeutic human bispecific antibody that inhibits IgE receptor signaling, J. Biol. Chem. 285 (2010) 20850–20859.
179. S. Krah, C. Schröter, C. Eller, L. Rhiel, N. Rasche, J. Beck, et al., Generation of human bispecific common light chain antibodies by combining animal immunization and yeast display, Protein Eng. Des. Sel. 30 (2017) 291–301.
180. J.P. Bogen, S.C. Hinz, J. Grzeschik, A. Ebening, S. Krah, S. Zielonka, et al., Dual function pH responsive bispecific antibodies for tumor targeting and antigen depletion in plasma, Front. Immunol. 10 (2019) 1892.
181. M. Zemlin, M. Klinger, J. Link, C. Zemlin, K. Bauer, J.A. Engler, et al., Expressed murine and human CDR-H3 intervals of equal length exhibit distinct repertoires that differ in their amino acid composition and predicted range of structures, J. Mol. Biol. 334 (2003) 733–749.
182. C.M. Mahon, M.A. Lambert, J. Glanville, J.M. Wade, B.J. Fennell, M.R. Krebs, et al., Comprehensive interrogation of a minimalist synthetic CDR-H3 library and its ability to generate antibodies with therapeutic potential, J. Mol. Biol. 425 (2013) 1712–1730.
183. K. Sankar, K.H. Hoi, I. Hötzel, Dynamics of heavy chain junctional length biases in antibody repertoires, Commun. Biol. 3 (2020) 207.
184. L. Wu, K. Oficjalska, M. Lambert, B.J. Fennell, A. Darmanin-Sheehan, D.N. Shuílleabhaín, et al., Fundamental characteristics of the immunoglobulin VH repertoire of chickens in comparison with those of humans, mice, and camelids, J. Immunol. 188 (2012) 322–333.
185. L. Pekar, D. Klewinghaus, P. Arras, S.C. Carrara, J. Harwardt, S. Krah, et al., Milking the cow: cattle-derived chimeric ultralong CDR-H3 antibodies and their engineered CDR-H3-only knobbody counterparts targeting epidermal growth factor receptor elicit potent NK cell-mediated cytotoxicity, Front. Immunol. 12 (2012) 742418.
186. A. Macpherson, A. Scott-Tucker, A. Spiliotopoulos, C. Simpson, J. Staniforth, A. Hold, et al., Isolation of antigen-specific, disulphide-rich knob domain peptides from bovine antibodies, PLoS Biol. 18 (2020) e3000821.
187. F. Wang, D.C. Ekiert, I. Ahmad, W. Yu, Y. Zhang, O. Bazirgan, et al., Reshaping antibody diversity, Cell 153 (2013) 1379–1393.
188. J.J. Smith, J.M. Hill, M.J. Little, G.M. Nicholson, G.F. King, P.F. Alewood, et al., Unique scorpion toxin with a putative ancestral fold provides insight into evolution of the inhibitor cystine knot motif, Proc. Natl. Acad. Sci. USA 108 (2011) 10478–10483.
189. J. Silverman, Q. Lu, A. Bakker, W. To, A. Duguay, B.M. Alba, et al., Multivalent avimer proteins evolved by exon shuffling of a family of human receptor domains, Nat. Biotechnol. 23 (2005) 1556–1561.
190. D.J. Craik, N.L. Daly, C. Waine, The cystine knot motif in toxins and implications for drug design, Toxicon 39 (2001) 43–60.
191. A. Desmyter, T.R. Transue, M.R. Ghahroudi, M.-H.-D. Thi, F. Poortmans, R. Hamers, et al., Crystal structure of a camel single-domain V H antibody fragment in complex with lysozyme, Nat. Struct. Biol. 3 (1996) 803–811.
192. T. Liu, Y. Liu, Y. Wang, M. Hull, P.G. Schultz, F. Wang, Rational design of CXCR4 specific antibodies with elongated CDRs, J. Am. Chem. Soc. 136 (2014) 10557–10560.
193. D.C. Bell, A. Karratt-Vellatt, S. Surade, T. Luetkens, E.W. Masters, N.M. Sørensen, et al., Knotbodies: a new generation of ion channel therapeutic biologics created by fusing knottin toxins into antibodies, Biophys. J. 114 (2018) 203a.
194. Z. Miao, G. Ren, H. Liu, R.H. Kimura, L. Jiang, J.R. Cochran, et al., An engineered knottin peptide labeled with 18F for PET imaging of integrin expression, Bioconjug. Chem. 20 (2009) 2342–2347.
195. W. Lee, A. Syed Atif, S.C. Tan, C.H. Leow, Insights into the chicken IgY with emphasis on the generation and applications of chicken recombinant monoclonal antibodies, J. Immunol. Methods 447 (2017) 71–85.
196. U.S. Diesterbeck, Construction of bovine immunoglobulin libraries in the single-chain fragment variable (scFv) format, Methods Mol. Biol. 1701 (2018) 113–131.
197. H. Matz, H. Dooley, Shark IgNAR-derived binding domains as potential diagnostic and therapeutic agents, Dev. Comp. Immunol. 90 (2019) 100–107.
198. H. English, J. Hong, M. Ho, Ancient species offers contemporary therapeutics: an update on shark VNAR single domain antibody sequences, phage libraries and potential clinical applications, Antib. Ther. 3 (2020) 1–9.
199. H. Akiba, H. Tamura, M. Kiyoshi, S. Yanaka, K. Sugase, J.M.M. Caaveiro, et al., Structural and thermodynamic basis for the recognition of the substrate-binding cleft on hen egg lysozyme by a single-domain antibody, Sci. Rep. 9 (2019) 15481.
200. K.A. Henry, C.R. MacKenzie, Antigen recognition by single-domain antibodies: structural latitudes and constraints, mAbs 10 (2018) 815–826.
201. A. Koide, J. Wojcik, R.N. Gilbreth, R.J. Hoey, S. Koide, Teaching an old scaffold new tricks: monobodies constructed using alternative surfaces of the FN3 scaffold, J. Mol. Biol. 415 (2012) 393–405.
202. J. Wojcik, A.J. Lamontanara, G. Grabe, A. Koide, L. Akin, B. Gerig, et al., Allosteric inhibition of Bcr-Abl kinase by high affinity monobody inhibitors directed to the Src homology 2 (SH2)-kinase interface, J. Biol. Chem. 291 (2016) 8836–8847.
203. T. Kükenshöner, N.E. Schmit, E. Bouda, F. Sha, F. Pojer, A. Koide, et al., Selective targeting of SH2 domain-phosphotyrosine interactions of Src family tyrosine kinases with monobodies, J. Mol. Biol. 429 (2017) 1364–1380.
204. G. La Sala, C. Michiels, T. Kükenshöner, T. Brandstoetter, B. Maurer, A. Koide, et al., Selective inhibition of STAT3 signaling using monobodies targeting the coiled-coil and N-terminal domains, Nat. Commun. 11 (2020) 4115.
205. E.J. Petrie, R.W. Birkinshaw, A. Koide, E. Denbaum, J.M. Hildebrand, S.E. Garnish, et al., Identification of MLKL membrane translocation as a checkpoint in necroptotic cell death using monobodies, Proc. Natl. Acad. Sci. USA 117 (2020) 8468–8475.
206. S.C. Devanaboyina, S.M. Lynch, R.J. Ober, S. Ram, D. Kim, A. Puig-Canto, et al., The effect of pH dependence of antibody-antigen interactions on subcellular trafficking dynamics, mAbs 5 (2013) 851–859.
207. J. Chaparro-Riggers, H. Liang, R.M. DeVay, L. Bai, J.E. Sutton, W. Chen, et al., Increasing serum half-life and extending cholesterol lowering *in vivo* by engineering antibody with pH-sensitive binding to PCSK9, J. Biol. Chem. 287 (2012) 11090–11097.
208. M.L. Murtaugh, S.W. Fanning, T.M. Sharma, A.M. Terry, J.R. Horn, A combinatorial histidine scanning library approach to engineer highly pH-dependent protein switches, Protein Sci. 20 (2011) 1619–1631.
209. C. Schröter, R. Günther, L. Rhiel, S. Becker, L. Toleikis, A. Doerner, et al., A generic approach to engineer antibody pH-switches using combinatorial histidine scanning libraries and yeast display, mAbs 7 (2014) 138–151.
210. B.J. Tillotson, L.I. Goulatis, I. Parenti, E. Duxbury, E.V. Shusta, Engineering an anti-transferrin receptor ScFv for pH-sensitive binding leads to increased intracellular accumulation, PLoS ONE 10 (2015) e0145820.
211. D. Könning, S. Zielonka, C. Sellmann, C. Schröter, J. Grzeschik, S. Becker, et al., Isolation of a pH-sensitive IgNAR variable domain from a yeast-displayed, histidine-doped master library, Mar. Biotechnol. 18 (2016) 161–167.

# Chapter 3 - Manuscript I

**Antibody-dependent enhancement of toxicity of myotoxin II from *Bothrops asper***

This manuscript describes the discovery of anti-M-II antibodies using phage display technology. The antibody selection strategy involved incubation of a naïve scFv-phage library with M-II at pH 7.4, followed by elution of the bound scFv-phages at pH 6.0. Upon discovery, six selected antibodies were assessed for *in vitro* M-II neutralization in a fibroblast viability assay. Thereupon, three antibodies that demonstrated the highest neutralization ability were further tested in a preincubation experiments in a mouse model, where two antibodies showed complete neutralization of the myotoxic effects of M-II. One of the neutralizing antibodies was then tested for neutralization of whole venom from *B. asper*, where its neutralization abilities were found to be equally effective as polyvalent antivenom. Next, the antibody was tested in combination with polyvalent antivenom, where almost complete neutralization of the whole venom was observed, thus, demonstrating the possibility of achieving better neutralization of venoms by fortification of polyvalent antivenom with recombinant human monoclonal antibody. However, when this antibody was assessed in a rescue model, which better mimicked a real life envenoming case, it showed antibody-dependent enhancement (ADE) of myotoxicity of whole venom. In the following *in vivo* rescue experiments, various antibody engineering strategies were employed to investigate the ongoing phenomenon of ADE, which revealed that reducing FcRn-mediated recycling lowered the myotoxic effects. Further, the Fab format of the antibody significantly neutralized myotoxicity, although the mice died the next day. Several hypotheses to explain these quizzical observations are discussed in the manuscript, and further investigations are ongoing.

Additionally, given that the antibodies presented in this manuscript were discovered through a pH-dependent antigen-binding phage display selection strategy, some of these antibodies were assessed for their pH-dependent binding to M-II in the work behind manuscript III.

This manuscript is still in preparation.

# Antibody-dependent enhancement of toxicity of myotoxin II from *Bothrops asper*

Christoffer V. Sørensen[1], Julián Fernández[2], Anna Christina Adams[3], Helen H. K. Wildenauer[1], Sanne Schoffelen[1], Line Ledsgaard[1], Manuela B. Pucca[1,4], Michael Fiebig[5], Felipe A. Cerni[1,4], Tulika Tulika[1], Aneesh Karatt-Vellatt[6], J. Preben Morth[1], Anne Ljungars[1], Lise M. Grav[1], Bruno Lomonte[2]*, Andreas H. Laustsen[1]*

[1]Department of Biotechnology and Biomedicine, Technical University of Denmark, DK-2800 Kongens Lyngby, Denmark

[2]Instituto Clodomiro Picado, Facultad de Microbiologia, Universidad de Costa Rica, San Jose, Costa Rica

[3]The Novo Nordisk Foundation Center for Biosustainability, Technical University of Denmark, DK-2800 Kongens Lyngby, Denmark

[4]Medical School, Federal University of Roraima, Boa Vista BR-69310-000, Brazil

[5]Absolute Antibody Ltd, Wilton Centre, Redcar, Cleveland, TS10 4RF, United Kingdom

[6] IONTAS Ltd.; Cambridgeshire CB22 3FT, United Kingdom

*To whom correspondence should be addressed:
ahola@bio.dtu.dk
bruno.lomonte@ucr.ac.cr

**One Sentence Summary**

The first reported example of antibody-dependent enhancement of the toxic effects exerted by a toxin from the animal kingdom.

**Abstract**

Improved therapies are needed against snakebite envenoming, which kills and permanently disables thousands of people each year. Recently developed neutralizing monoclonal antibodies against several snake toxins have shown promise in preclinical rodent models. However, here we present conflicting data that call for caution. Using phage display technology, we discovered a human monoclonal antibody that causes antibody-dependent enhancement (ADE) of the toxic effects exerted by myotoxin II from *Bothrops asper* when tested in a mouse model of envenoming followed by intravenous treatment. This first report of ADE of a toxin from the animal kingdom highlights the necessity of assessing even well-known antibody formats in representative preclinical models to evaluate their therapeutic utility against toxins or venoms, to avoid potential deleterious effects as exemplified in the present case.

## Introduction

Snakebite envenoming is a devastating neglected tropical disease that kills and permanently disables hundreds of thousands of people each year *(1–3)*. In Central America and northern South America, the venomous pit viper *Bothrops asper* is known for causing a large number of bites that result in mortality and morbidity *(4)*. The venom of *B. asper* contains a significant amount of potent myotoxic phospholipases $A_2$ ($PLA_2$s) and $PLA_2$-like proteins, one of which is myotoxin II *(5, 6)*. Myotoxin II and other myotoxic $PLA_2$s are responsible for serious clinical effects, such as tissue loss, disability, and amputation *(7)*. It is therefore considered a key toxin to be neutralized for treatments to be efficacious in patients having fallen victim to envenoming by *B. asper (8)*. The mainstay treatments against snakebite envenomings are antivenoms derived from the plasma of hyperimmunized animals *(9)*. While effective, these treatments are also associated with several drawbacks, such as the risk of causing adverse reactions *(10, 11)*, high costs *(12)*, and low concentrations of therapeutically active antibodies *(13)*. To avoid these drawbacks, a novel type of snakebite therapeutics known as recombinant antivenoms, based on human monoclonal antibodies, is under development. A number of human monoclonal immunoglobulin G (IgG) antibodies have been reported to neutralize snake toxins *in vivo*, and it has been speculated that such types of antibodies could find broad therapeutic utility in the neutralization of different families of snake toxins *(14–17)*. However, common for all these previously reported human monoclonal IgG antibodies is that they target neurotoxins, which exert their function extracellularly by interacting specifically with cellular receptors.

In this work, we directed focus on a different type of toxin, namely the membrane-disrupting toxin myotoxin II from the notorious *Bothrops asper*. Using a similar workflow as previously described *(14, 16–18)*, we developed a human monoclonal antibody in both the IgG and Fab format and tested these in two different rodent models: One model involving preincubation of venom and antibody prior to intramuscular (i.m.) administration (preincubation assay), and the other model involving i.m. administration of venom, followed by intravenous (i.v.) administration of the antibody upon a time delay (rescue assay). While the IgG antibody showed superior neutralizing effects in the preincubation model, we observe a striking phenomenon in the rescue assays, namely that the IgG antibody enhances the myotoxic effects of *B. asper* venom. Moreover, some mice receiving both the antibody in Fab format and venom die a day after the experiment, both in the preincubation and rescue assay, despite the Fab is able to neutralize myotoxicity. To our knowledge, this is the first time that antibody-dependent enhancement (ADE) of the toxic effects exerted by a toxin from the animal kingdom has been observed. Based on the observations in this study, we hypothesize that the ADE of toxicity stems from the endocytosing and/or half-life extension of this membrane-disrupting toxin by the IgG, leading to potentiated myotoxicity, and that the Fab may entirely change the pharmacology of the toxin. These findings thus highlight the necessity of assessing even well-known antibody formats in representative preclinical models, such as rescue models mimicking a snakebite envenoming case, to evaluate their therapeutic utility, as well as the need for

careful design and engineering of monoclonal antibodies to ensure that they can neutralize toxins without causing ADE of toxicity.

## Resutls

### Phage display selection and initial screening of monoclonal scFvs

Using the IONTAS antibody phage display library λ *(19)*, single-chain variable fragment (scFv) displaying phages were selected against myotoxin II from *B. asper*. Three rounds of panning against myotoxin II were carried out to enrich for phages displaying scFvs with specificity to myotoxin II. To assess the success of the selection, the polyclonal outputs were investigated for their binding to myotoxin II by determining the number of colony-forming units (CFU) after each panning. Following the third round of panning, the specificity of the scFv-displaying phages was tested and confirmed (Fig. 1A, 1B).

Upon confirmation of successful accumulation of myotoxin II binders, DNA encoding the scFvs was amplified from the polyclonal phage outputs, and the genes were subcloned and expressed. Characterization of 276 scFv-producing monoclonal cultures using ELISA yielded 188 scFvs binding to myotoxin II (Fig. 1C). These 188 scFvs were screened for their specificity to myotoxin II by including milk proteins, streptavidin, neutravidin, and a $PLA_2$ from *Naja mossambica* as controls. Results demonstrated that all 188 scFvs of interest were binding specifically to myotoxin II and not to any of the controls (Data not shown). The genes encoding the $V_H$ and $V_L$ for all clones were sequenced, revealing 123 scFv sequences with unique CDR regions, of which 59 showed unique $V_H$ CDR3 regions (Fig. 1D).

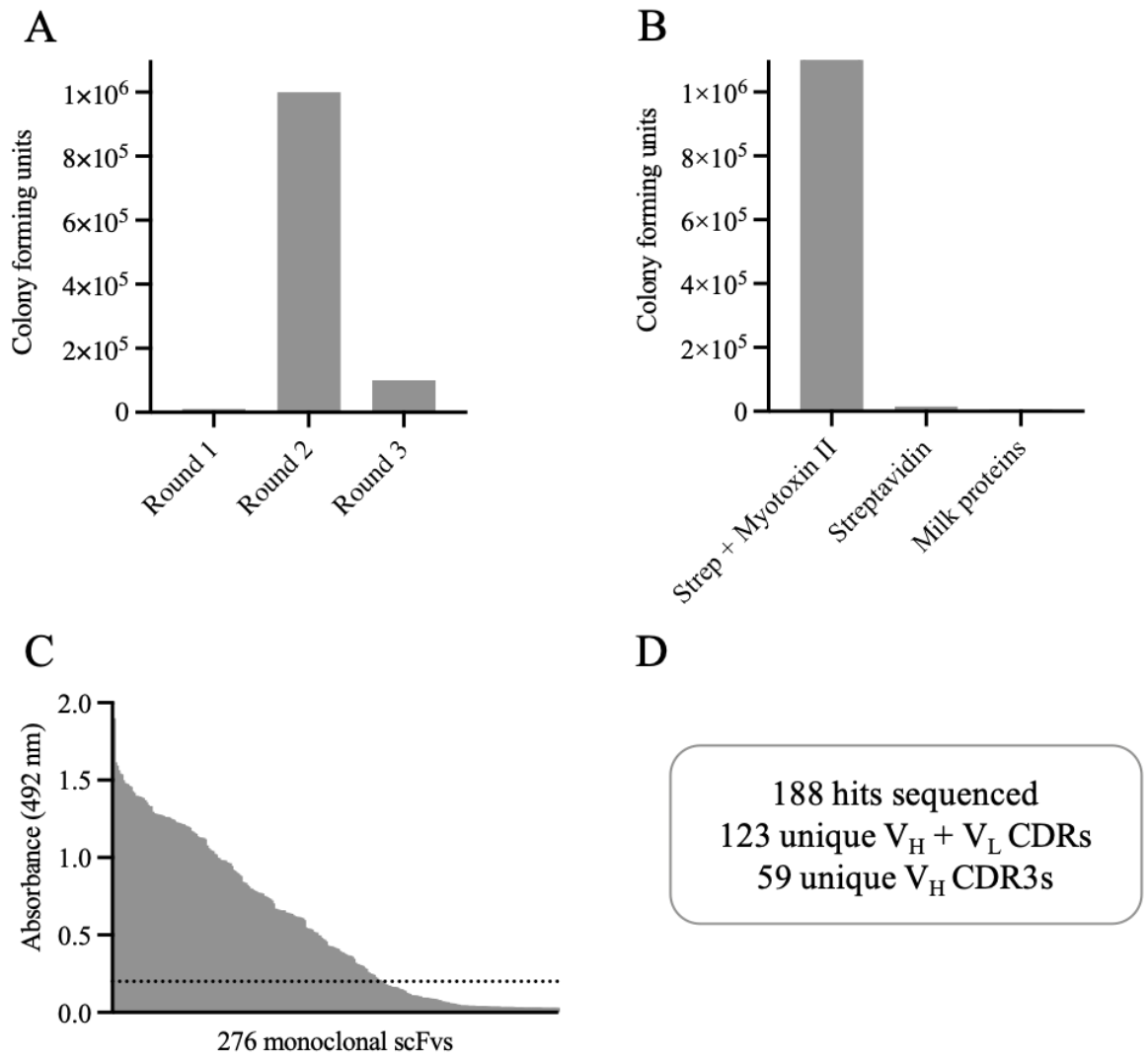


**Fig. 1. Overview of results from the discovery process**. (**A)** Phage display panning results reported as colony forming units (CFUs) for each of the outputs from the three rounds of panning. (**B)** Assessment of the specificity of the third round polyclonal phage output reported as CFU counts when panned against either myotoxin II or controls (streptavidin and milk proteins). **(C)** Monoclonal scFv ELISA signals against myotoxin II. **(D)** Summary of DNA sequencing results.

### Ranking of scFv binding and affinity assessment of IgG-reformatted clones

To rank the clones based on binding affinity, an expression-normalized capture (ENC) assay was performed (Data not shown). The six scFvs displaying the highest binding signals (TPL0039_05_E02, TPL0039_05_B12, TPL0039_05_F04, TPL0039_05_G08, TPL0039_05_B04, and TPL0039_05_A03) were selected for reformatting to the IgG format, expressed, purified, and their binding to myotoxin II was confirmed for all six IgGs through ELISA (Fig. 2A). Following confirmation of retained binding ability, the functional affinity (avidity) of the six IgGs were measured using octet, yielding functional affinities ranging from 9 nM to <1 pM (no dissociation observed) as seen in Fig. 2B. To test how the functional affinity (avidity) compared to the affinity of the individual binding

sites, a single clone (TPL0039_05_E02) was expressed as Fab and its affinity assessed by Octet. The KD of the Fab format was measured as 2.4 nM, where the IgG version of the clone was measured as <1 pM.

A

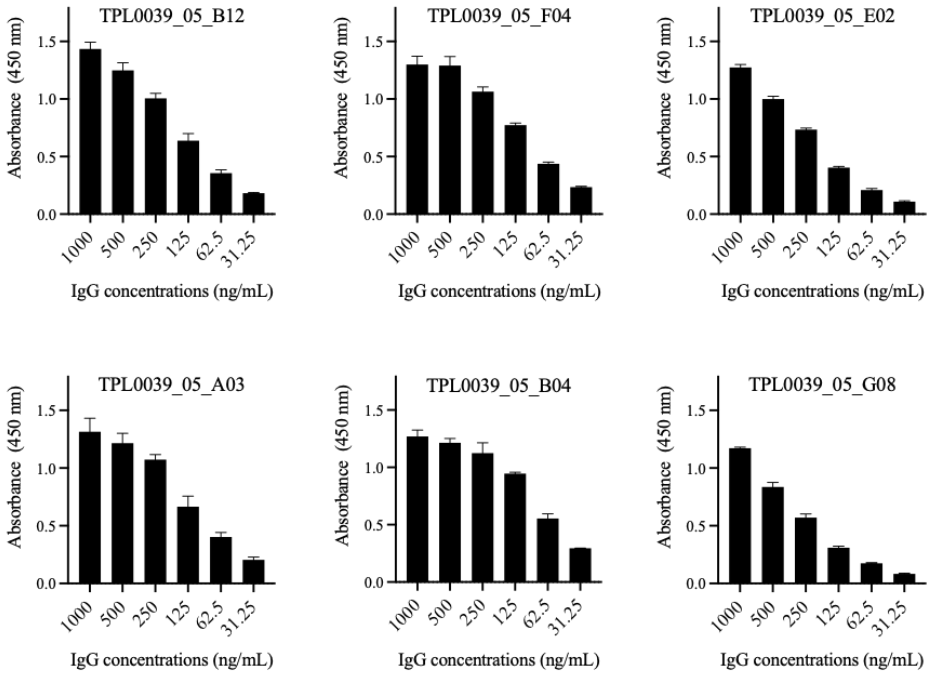


B

| Antibody | Functional affinity |
|---|---|
| TPL0039_05_B12 | <1 pM* |
| TPL0039_05_F04 | 18 pM |
| TPL0039_05_E02 | <1 pM* |
| TPL0039_05_A03 | <1 pM* |
| TPL0039_05_B04 | 75 pM |
| TPL0039_05_G08 | 9 nM |
| TPL0039_05_E02_Fab | 2.4 nM |

**Fig. 2. IgG binding assessment**. **(A)** ELISAs showing binding to myotoxin II by the converted IgGs tested in a dilution series. **(B)** Functional affinity (avidity) of the six IgGs and one Fab. * <1 pM means that the IgG was not observed to dissociate from myotoxin II, thereby obtaining the minimum value possible.

## Investigating neutralization of cytotoxic effects of myotoxin II using a fibroblast-based assay

To test the functional neutralization of the cytotoxic effects of myotoxin II by the six IgGs *in vitro*, a fibroblast viability assay was carried out (Fig. 3). In this assay, four molar ratios of toxin:IgG were tested; 1:0.5, 1:1, 1:1.5, and 0:1.5. The included controls were: a negative

control (PBS), a positive control (toxin challenge without IgG), and a non-myotoxin II binding IgG at toxin:IgG ratios of 1:3 and 0:3. The negative control showed no influence on cell viability, whereas the positive control resulted in ~80% reduction in viability. The irrelevant IgG displayed no significant change in viability when compared to the positive control, suggesting that any neutralization observed in the assay for other IgGs is caused by the specificity to myotoxin II.

The *in vitro* neutralization of the six IgGs can be divided into three patterns. The neutralization of the two IgGs, TPL0039_05_E02 and TPL0039_05_F04, were at all concentrations significantly lower than the negative control, and furthermore resulted in decreased cell viability with increasing IgG amounts. For TPL0039_05_G08 and TPL0039_05_B04, the neutralization capacity was observed to be slightly dose-dependent, with increasing IgG ratios leading to an increase in cell viability. TPL0039_5_G08 showed full neutralization (non-significant change from negative control) at 1:1 toxin:IgG ratio. Finally, TPL0039_05_B12, TPL0039_05_B04, and TPL0039_05_A03 displayed full neutralization at the lowest tested 1:0.5 toxin:IgG ratio, and showed no dose-response increase with increasing IgG ratios.

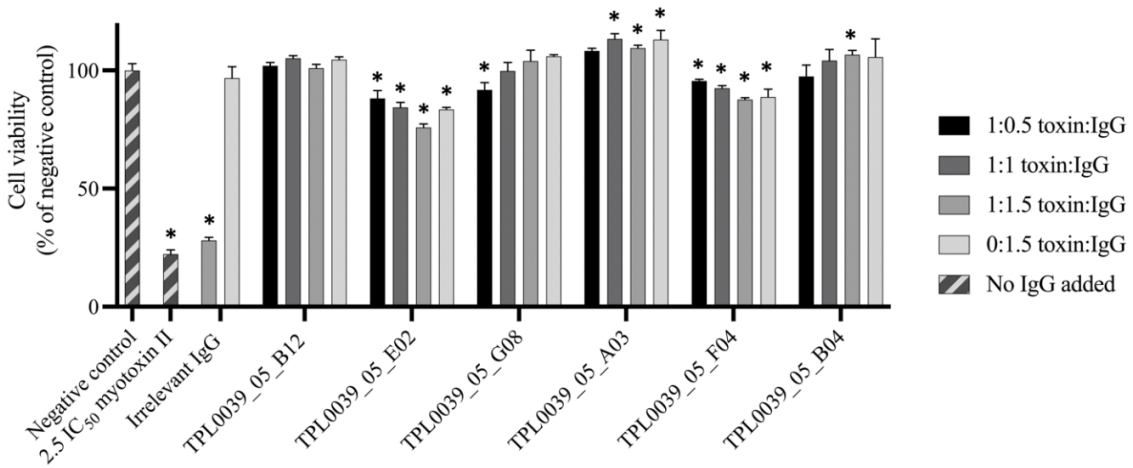


**Fig. 3. Toxin:IgG ratios for full myotoxin II neutralization by six different IgGs.** Six IgGs were tested in four toxin:IgG ratios to check for myotoxin II neutralizing abilities in an in vitro fibroblast viability assay. Assay controls included a negative control (PBS), a positive control (toxin challenge without IgG), and a non-myotoxin II binding IgG at toxin:IgG ratios of 1:3 and 0:3. Experiments were performed in triplicates and reported as means normalized to the negative control. Asterisks (*) notes statistical difference ($p < 0.05$) compared to the negative control (PBS). Statistics were carried out by comparing each column to the negative control (PBS) using a one-way ANOVA, followed by Dunnett's multiple comparison test.

## IgG provides full *in vivo* neutralization of myotoxin II toxicity at low dose

From the shown data obtained for the six IgGs, TPL0039_05_B12, TPL0039_05_E02, and TPL0039_05_G08 were evaluated to be the most promising and were selected for investigation of *in vivo* neutralization of myotoxin II (Fig. 4). Mice were injected i.m. with preincubated mixtures of myotoxin II and IgG in a 1:1 molar ratio. Control mice were

injected with either PBS, myotoxin II, myotoxin II and ICP polyvalent equine antivenom, or myotoxin II and a non-myotoxin II binding IgG. After three hours, the mice were bled, and the plasma creatine kinase (CK) levels were measured as an indicator of muscle damage. Injection of myotoxin II caused a large increase in CK activity levels compared to the PBS-injected control group. Injection of the IgGs without myotoxin II resulted in slight increasing trends in the CK levels, although without any statistical increase. When tested, the currently used antivenom for *B. asper* bites, ICP polyvalent equine antivenom, showed neutralizing trends, although the CK level increase was still significantly larger compared to the levels observed for the negative control. When testing the three monoclonal IgGs, it was revealed that the IgG TPL0039_05_G08 was unable to prevent the CK increment caused by myotoxin II at a 1:1 toxin:IgG ratio, indicating that this antibody might bind a non-neutralizing epitope. However, both the TPL0039_05_B12 IgG and TPL0039_05_E02 IgG were able to fully neutralize the CK level increase caused by myotoxin II (toxin and IgG injection was not significantly higher than the negative controls) at a 1:1 toxin:IgG molar ratio.

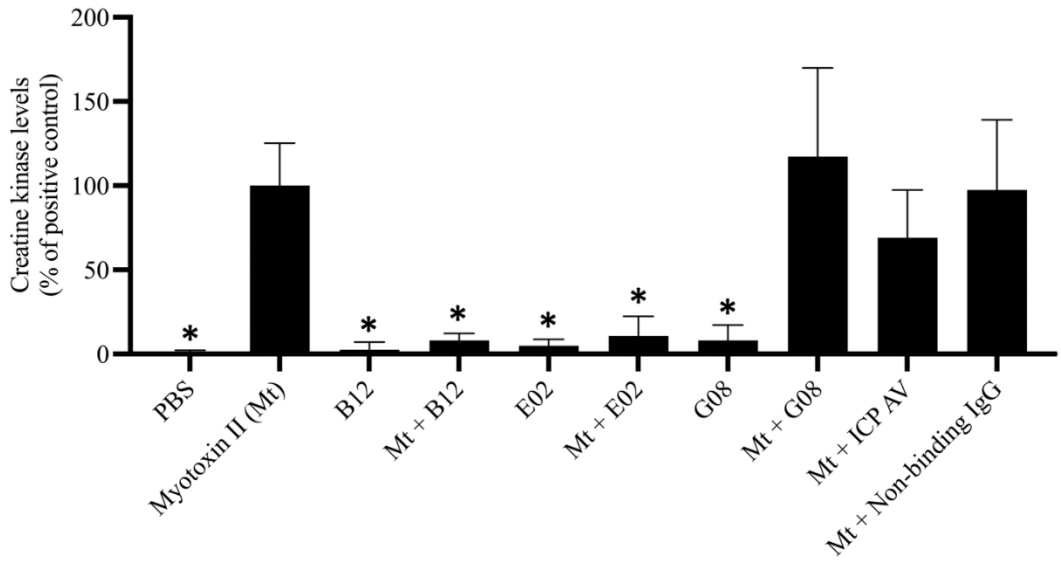


**Fig. 4. In vivo neutralization of myotoxin II.** The graph illustrates *in vivo* muscle damage caused by myotoxin II from *B. asper* measured as increased creatine kinase levels. Myotoxin II was preincubated with antibody/antivenom for 30 minutes and then injected i.m. in mice. After three hours, the mice were bled, and creatine kinase levels were measured. To accommodate for assays carried out on different days, the creatine kinase levels have been normalized to the positive control (Myotoxin II). Asterisks (*) notes significant statistical difference ($p < 0.05$) compared to the positive control. Statistics were carried out by comparing each column to the positive control using a one-way ANOVA, followed by Dunnett's multiple comparison test. For clearer visualization, the antibody names (TPL0039_05_XXX) have been abbreviated as XXX, and ICP antivenom has been abbreviated as ICP AV.

**A combination of TPL0039_05_B12 monoclonal IgG and ICP polyvalent equine antivenom neutralizes muscle damage caused by *B. asper* whole venom in preincubation assays**

Additionally, we wanted to assess whether our discovered human IgGs could be used in combination with the ICP polyvalent equine antivenom *in vivo* to reinforce its neutralizing ability. To assess this, we tested if the ICP antivenom supplemented with TPL0039_05_B12 IgG could neutralize the muscle damage caused by *B. asper* whole venom. In this experiment, mice were injected i.m. with preincubated mixtures of *B. asper* whole venom and ICP antivenom supplemented with TPL0039_05_B12 IgG. Control mice were injected with either PBS, *B. asper* venom, *B. asper* venom, and ICP polyvalent equine antivenom, or *B. asper* venom and TPL0039_05_B12 IgG. Injection of *B. asper* venom caused a large increase in CK activity levels compared to the PBS-injected control group (Fig. 5). Furthermore, the venom preincubated with TPL0039_05_B12 and venom preincubated with ICP antivenom controls showed partial neutralization of the increased CK levels. When tested together against *B. asper* venom, ICP antivenom and TPL0039_05_B12 IgG showed CK levels almost identical to the PBS only control, corresponding to full neutralization of the muscle-damaging effects caused by the whole venom.

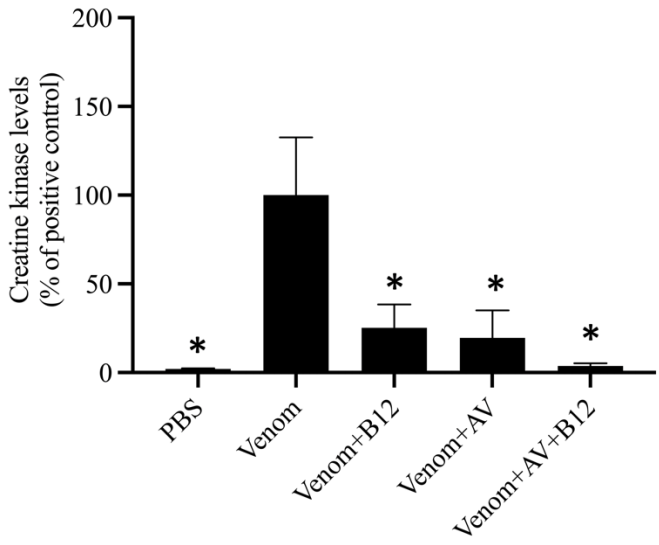


**Fig. 5. *In vivo* neutralization of the muscle damaging effects caused by *B. asper* venom.** The graph illustrates *in vivo* muscle damage caused by *B. asper* venom measured as increased creatine kinase levels. *B. asper* whole venom (Venom) was preincubated with antibody/antivenom (B12/AV) for 30 minutes and then injected i.m. in mice. After three hours, the mice were bled, and creatine kinase levels were measured. The creatine kinase levels have been normalized to the positive control (Venom) for graph consistency. Asterisks (*) notes significant statistical difference ($p < 0.05$) compared to the positive control. Statistics were carried out by comparing each column to the positive control using a one-way ANOVA, followed by Dunnett's multiple comparison test.

**The TPL0039_05_B12 IgG switches from toxin-neutralizing to toxin-enhancing when tested in rescue assays instead of preincubation assays**

Next, we tested the neutralizing capabilities of TPL0039_05_B12 IgG in a rescue assay since it closer resembles a real-life envenoming. As a positive control, injection of venom alone was used which resulted in an increase in CK levels, and the negative control (PBS) resulted in no increase in CK levels (Fig. 6A). Injection of venom followed by injection of the TPL0039_05_B12 IgG resulted in a significant increase in CK levels compared to the positive control. The ICP polyvalent antivenom decreased the CK level compared to the venom only, although when combined with TPL0039_05_B12 IgG, the CK levels were increased compared to using ICP polyvalent antivenom alone to treat the venom. This increase of CK levels when treating the venom with TPL0039_05_B12 IgG was thus observed both when used alone and in combination with the ICP polyvalent antivenom, but when tested without venom, the TPL0039_05_B12 IgG caused no CK level increase.

To investigate this unexpected switch from toxin-neutralizing to toxin-potentiating we modified the mutations of the TPL0039_05_B12 IgG to only contain the LALA mutation, instead of both the LALA and YTE as in all earlier experiments. This change in the IgG scaffold appeared to remove the CK increase that the TPL0039_05_B12 IgG caused when administered after venom injection, either in combination with the ICP polyvalent antivenom or alone (Fig 6B).

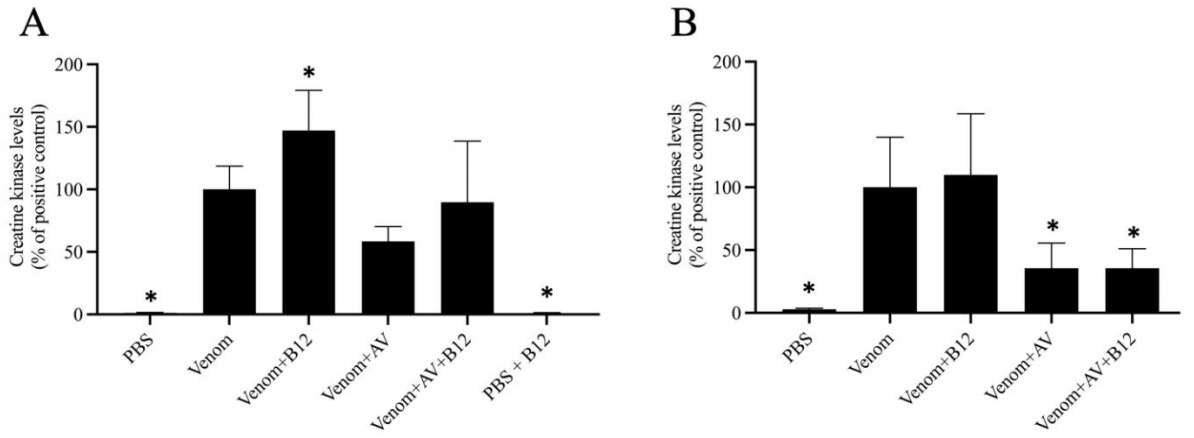


**Fig. 6. *In vivo* rescue assays.** The graph illustrates *in vivo* muscle damage caused by *B. asper* venom measured as increased creatine kinase levels. *B. asper* whole venom (Venom) was injected i.m. and 3 minutes later antibody/antivenom (B12/AV) or PBS was injected i.v. in mice. The IgG scaffold for B12 either had the **(A)** LALA+YTE mutations or **(B)** only the LALA mutation. After three hours, the mice were bled, and creatine kinase levels were measured. The creatine kinase levels have been normalized to the positive control (Venom) for graph consistency. Asterisks (*) denotes significant statistical difference ($p < 0.05$) compared to the positive control. Statistics were carried out by comparing each column to the positive control using a one-way ANOVA, followed by Dunnett's multiple comparison test.

**In the Fab format, TPL0039_05_B12 shows significant neutralization (~60%) of myotoxicity in rescue *in vivo* assays**

Lastly, an assessment of the TPL0039_05_B12 antibody in Fab format was performed using a preincubation *in vivo* assay, demonstrating that the Fab was able to significantly decrease the CK levels (Figure 7). Further, by assessing the Fab in a rescue assay (Figure 7), it was also shown that the Fab could significantly reduce the CK levels.

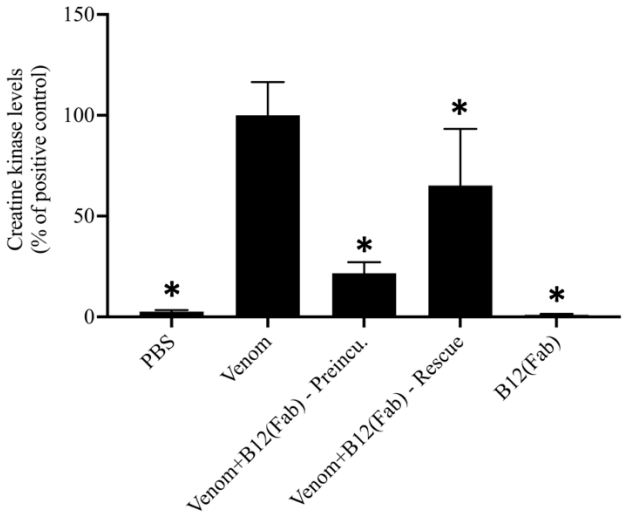


**Fig. 7. *In vivo* preincubation and rescue assays using Fabs.** The graph illustrates *in vivo* muscle damage caused by *B. asper* venom measured as increased creatine kinase levels. *B. asper* whole venom (Venom) was either preincubated for 30 minutes with B12(Fab) and injected i.m. or injected without preincubation i.m. followed by i.v. administration of B12(Fab) 3 minutes later in mice. As the first negative control, PBS alone was injected i.m., and as the second negative control, B12(Fab) alone was injected i.v. After three hours, the mice were bled, and creatine kinase levels were measured. The creatine kinase levels have been normalized to the positive control (Venom) for graph consistency. Asterisks (*) denotes significant statistical difference ($p < 0.05$) compared to the positive control. Statistics were carried out by comparing each column to the positive control using a one-way ANOVA, followed by Dunnett's multiple comparison test.

## Discussion

In this study, high affinity fully human recombinant monoclonal IgG antibodies targeting myotoxin II from *B. asper* venom were discovered using phage display technology directly from a naïve antibody library. A handful of these antibodies could neutralize myotoxin II *in vitro*, and two of the antibodies could fully neutralize the toxin in preincubation assays with i.m. administration in rodent models, even at a low toxin:antibody molar ratio of 1:1. One of the discovered antibodies (TPL0039_05_B12) was further assessed *in vivo* for its potential utility as a fortification agent for polyvalent antivenom. These experiments also involved a preincubation assay followed by i.m. injections and demonstrated that the human monoclonal antibody could be co-administered with the plasma-derived antivenom and improve the neutralization of myotoxicity (Fig 5). However, when instead using a rescue assay, it was observed that the i.v. administration of TPL0039_05_B12 following i.m. venom injection significantly increased myotoxicity (Fig 6A). This increased

myotoxicity was not caused by the antibody alone but only occurred when the antibody was administered i.v. after i.m. venom injection. These data thus constitute the first reported example of ADE of a toxin originating from the animal kingdom. Further assays indicated that the ADE of toxicity was likely partially connected to the recyclability of the antibody, since the removal of the half-life extending IgG1 scaffold mutation, YTE, decreased the ADE effects (Fig 6B). This finding is to some extent supported by the assessment of the antibody in Fab format, where the Fab showed significant neutralization of myotoxicity in the rescue assay (Figure 7). However, it is to be noted that surprising outcomes were observed the following day, where all mice receiving venom alone were alive, while some mice receiving the Fab and venom, both in preincubation and in rescue assays, were dead (data not shown). At the time of thesis hand in, observations were still ongoing, and final conclusion on the effect of the Fab on the toxin is therefore still pending.

A similar rescue assay setup was recently employed by Ledsgaard *et al. (16)*, where it was demonstrated that full neutralization of long-chain α-neurotoxins (LNTXs) administered subcutaneously could be achieved with i.v. administered human monoclonal IgG antibodies without any observed ADE effects. The explanation for the different outcomes observed in our study and the study by Ledsgaard *et al.* can possibly be found in the structural and functional differences of the targeted toxins. LNTXs function by binding extracellularly to nicotinic acetylcholine receptors (nAChRs) *(20)*, thereby blocking the binding of acetylcholine and inhibiting neuromuscular transmission. In contrast, myotoxin II interacts directly with cell membranes, which could possibly occur both intracellularly and extracellularly *(21, 22)*. In this relation, it is not unlikely that an endocytosed non-neutralized LNTX would be harmless to the endosome, whereas an endocytosed non-neutralized myotoxin II might destabilize the endosome and potentially damage the entire cell. Further, since LNTXs do not act through cellular degradation, but instead act through antagonistic binding to nAChR, they must remain attached to nAChR to exert their toxicity. Thereby, one toxin molecule can only affect one nAChR molecule. In contrast, since myotoxin II disrupts cell membranes, it might theoretically only need to affect the cell membrane until disruption and thereafter be able to affect additional cells. Thus, if myotoxin II was bound by an IgG antibody in a non-neutralizing fashion, the toxin might both be able to damage endosomes and obtain an extended half-life from the antibody, thereby increasing the overall exposure of the toxin to cells. However, in the IgG preincubation assays, it was observed that the antibody neutralizes myotoxin II upon binding (Fig 4, Fig 5).

Based on the findings in this study, two hypotheses emerge, which could explain how myotoxin II could appear neutralized in the preincubation assay, but exert toxicity in the rescue assay using IgG, and display puzzling pharmacology when the antibody is employed in the Fab format. Our first hypothesis is that antibodies and myotoxin II dimers form large immune complexes while being incubated with IgG in the preincubation assay. This could potentially occur if each IgG antibody engages with two different toxin molecules (one on each binding paratope) and if each myotoxin II dimer is bound by two antibodies, thereby allowing for continuous linking between antibodies and myotoxin II dimers (Fig. 8A). These large hypothetical immune complexes would likely possess

drastically altered pharmacokinetics than monomeric or dimeric myotoxin II, which may in effect abrogate the toxicity of the complexed toxins by steric hindrance *(23)*, or if the complex cannot escape the depot at the site of injection. Thereby, the observed neutralization of myotoxin II by the antibody might still occur even if the antibody binds to a non-neutralizing epitope. In comparison, the toxins and antibodies do not co-occur in high local concentrations when administered via two different routes of administration in the rescue assay. Therefore, the formation of large immune complexes may not occur in the rescue assays. Instead, the antibodies might bind myotoxin II without forming large immune complexes, which could potentially result in non-neutralized myotoxin II benefitting from the increased half-life of the antibody (Fig. 8B). This hypothesis may find some support from the results of both the preincubation and rescue assays performed with Fabs, as puzzling deaths were observed the day after the *in vivo* experiments (final conclusion pending). The second hypothesis is that the antibodies bind to neutralizing epitopes of myotoxin II, but that binding to neutralizing epitopes on both subunits of the myotoxin II dimers only occur in the preincubation assays (due to co-occurrence of toxin and antibody at high local concentrations during preincubation), while only one binding event between an antibody molecule and a myotoxin II dimer typically occurs in the rescue assay (Fig. 8C). In this scenario, one myotoxin II subunit in the dimer-antibody complex might still be able to exert toxicity *(24)* (Fig. 8D). The explanation for the difference between the Fab and IgG effects in the rescue assay could be partially connected to the much longer half-life of the IgG compared to the Fab *(25)*, as the IgG might retain the active myotoxin longer in the animal or in other ways increase the exposure of muscle tissue to the toxin. An alternative explanation is, that the myotoxin II can detach from the IgG or Fab in the endosomes. However, since the Fabs are not recycled by the neonatal Fc receptor (FcRn), they will remain in the endosome and can re-attach to myotoxin II. In contrast, if the IgG gets recycled through the FcRn, while myotoxin II is unattached to the IgG, then the active toxin will remain in the endosome, and the IgG will be recycled, preventing further binding between the two. As the IgG antibody may keep the toxin from being cleared in the kidneys, the net effect may be the observed enhancement of toxicity. When the antibody is preincubated with the venom toxins, this may not occur, as larger complexes may be prevented from entering circulation, thereby reducing overall exposure to the toxin, as earlier suggested in this discussion. However, when the antibody is delivered as Fab either in preincubation or in a rescue assay, completely different pharmacology might take place: We speculate that only smaller complexes can form due to the monomeric nature of the Fabs and that while the Fabs may neutralize myotoxicity, the Fab-toxin complexes may suddenly obtain altered toxicity. This could potentially happen if the Fab-toxin complexes find their way to the kidneys both in the preincubation and rescue model, where they might dissociate and cause nephrotoxicity, which may only manifest itself later, i.e., the puzzling deaths of some mice the day after the experiment. Further experiments are needed to uncover the underlying pharmacology, but previous work on amatoxins from poisonous mushrooms could lend credence to this speculations *(26)*. In addition to such potential altered anatomical site of action, other mechanisms could also be the cause of the observed ADE of toxicity, including altered mode of action, obscure synergistic effects, or other pharmacological effects. To fully elucidate the underlying

pharmacology, further experiments are needed, as well as the reason of the delayed deaths of some mice would be relevant to uncover.

Regardless of the underlying mechanisms at play in the rodent models employed here, our findings clearly highlight limitations of the preincubation assay as the current golden standard for assessing preclinical efficacy in the field of antivenom research. It seems evident that while the preincubation model may still be highly useful, it cannot alone be used to evaluate next-generation antivenom products, such as human monoclonal antibodies. With this in mind, we recommend antivenom researchers to carefully consider the utility of their preclinical model(s) for evaluating the potential of new therapeutic agents, and possibly include more advanced models, such as the rescue assay, to better assess preclinical efficacy *(27, 28)*

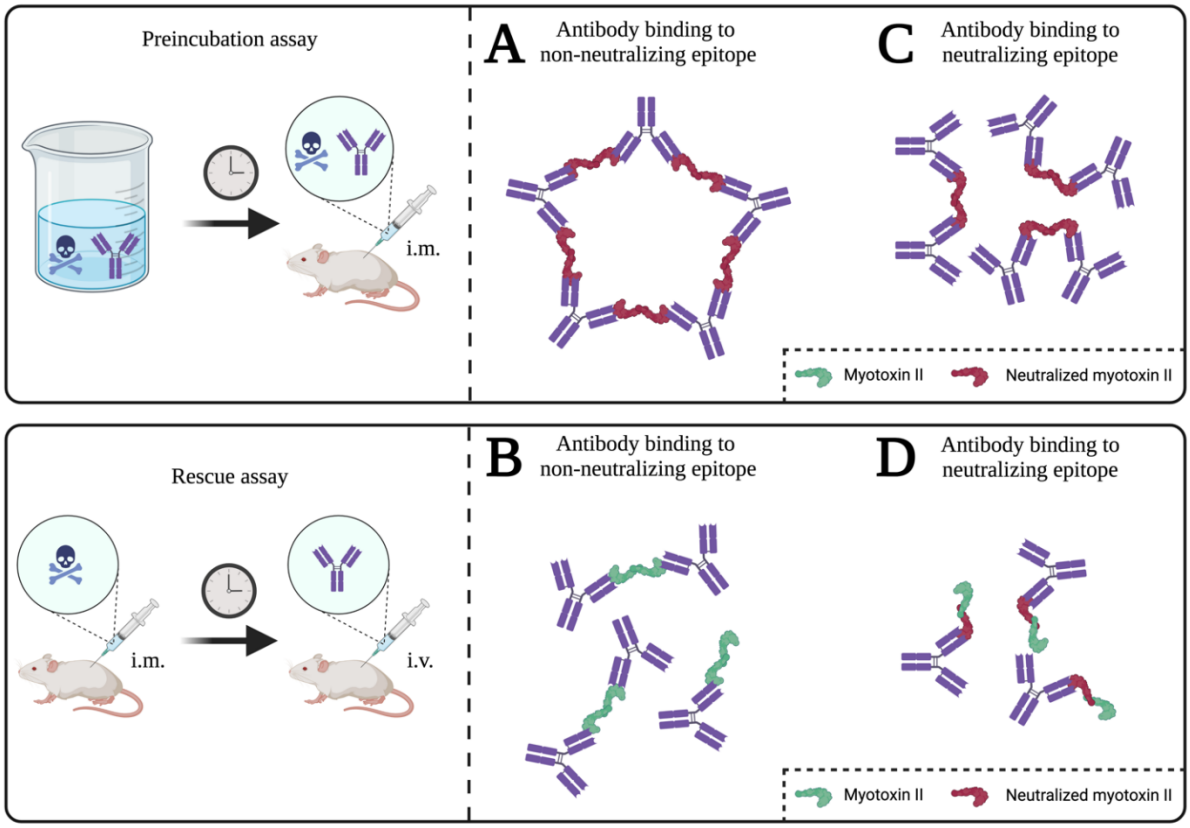


**Fig. 8. Schematic of *in vivo* assays and hypotheses that might explain the observed differences between preincubation and rescue assays. (Top)** In the preincubation assay, the toxin/venom is incubated with antibodies/antivenom for 30 minutes before the mixture is injected i.m. in mice. **(Bottom)** In the rescue assay, the venom is injected alone i.m., followed by an i.v. injection of the antibody/antivenom i.v.3 minutes later. **(A)** Antibodies bind to non-neutralizing epitopes of dimeric toxins and form large immune complexes. Neutralization could happen through drastic changes to the pharmacokinetics compared to the monomeric or dimeric toxins. **(B)** In the rescue assay the toxins and antibodies do not co-occur in high local concentrations when administered via two different routes of administration in the rescue assay. Thus immune complex formation may not occur. **(C)** Antibodies bind to both neutralizing epitopes. (D) In the rescue assay the toxins and antibodies do not co-occur in high local concentrations therefore the majority of myotoxin II dimers are only bound on one neutralizing epitope.

## Materials and Methods

*Purification of myotoxin II*

Myotoxin II (Uniprot P24605) was purified from the venom of *Bothrops asper* by cation-exchange chromatography on CM-Sephadex C25, followed by reverse-phase HPLC on $C_{18}$, as described previously *(5, 7)*.

*Biotinylation of myotoxin II*

Lyophilized myotoxin II was solubilized in phosphate buffered saline (PBS) and mixed with biotin linked to *N*-hydroxysuccinide (NHS) via a $PEG_4$ linker (EZ-LinkTM NHS-$PEG_4$-Biotin, Thermo Scientific, #A39259) in a molar ratio of 1:1.5 (toxin:biotin) according to Ahmadi *et al. (18)*. Purification of the biotinylated toxins was also carried out by buffer exchange according to Ahmadi *et al. (18)*.

*Phage display selection and assessment of polyclonal output*

For phage display selection, the IONTAS phage display library λ was employed, which is a human antibody phage display library with a clonal diversity of $1.6 \times 10^{10}$. The displayed antibodies come in the form of scFvs and have been constructed from B lymphocytes collected from 43 non-immunized human donors *(19)*.

Phage display selection was carried out as earlier described *(19)*, with the following modifications described briefly: For selections, biotinylated myotoxin II (10 µg/mL) was indirectly immobilized using streptavidin-coated (10 µg/mL) Maxisorp vials, employing a streptavidin-biotin capture system. In the second and third selection round, neutravidin was used instead of streptavidin to prevent accumulation of streptavidin-recognizing antibodies. Elution in the third round was carried out by incubating with a 10 mM glycine-HCL solution at pH 6 for 15 minutes instead of eluting with trypsin.

After three rounds of phage display selection, antigen specificity of the phage output was evaluated. This was carried out according to Føns *et al. (29)*, using a similar protocol to the phage display selections. The phage output was purified utilizing polyethylene glycol precipitation *(19)*, and binding was tested against Maxisorp vials coated with either (i) biotinylated myotoxin II indirectly immobilized using streptavidin, (ii) streptavidin, or (iii) 3% (w/v) skimmed milk in PBS (M-PBS). Biotinylated myotoxin II and streptavidin were used at a concentration of 10 µg/mL.

*Sub-cloning, primary screening, and sequencing of scFvs*

To facilitate expression of soluble scFvs, the scFv genes from the third selection round were sub-cloned from the phage display vector (pIONTAS1) into the pSANG10-3F expression vector using *NcoI* and *NotI* restriction endonucleases. The expression vectors

were then transformed into *E. coli* BL21(DE3) cells (New England Biolabs), following protocols from Martin *et al. (30)*. Individual scFv-producing monoclonal colonies (276 colonies) were picked and expressed in 96-well format using auto-induction media *(31)*. To determine the binding of the scFvs to myotoxin II, a monoclonal scFv ELISA was carried out. 96-well Maxisorp plates with biotinylated myotoxin II (5 µg/mL) indirectly immobilized using streptavidin (10 µg/mL) were used. For detection of binding, a 1:20,000 dilution of Anti-FLAG M2-Peroxidase (HRP) (Sigma Aldrich, #A8592) antibody in 3% M-PBS and an OPD solution (Sigma-Aldrich, P5412) was used as substrate according to the manufacturer's protocol. A biotinylated HPLC fraction from *Naja mossambica* containing $PLA_2$ was included as a negative control. Further controls included wells coated with streptavidin/neutravidin (10 µg/mL) and 3% M-PBS. Results were measured as absorbance at 492 nm using an Epoch spectrophotometer from Biotek (15020518) with the Gen5 2.07 software.

The genes encoding scFvs binding specifically to myotoxin II with absorbance (492 nm) values above a pre-set threshold of 0.2 were sequenced (Eurofins and Macrogen genomics sequencing service) using the S10b primer (GGCTTTGTTAGCAGCCGGATCTCA). The antibody framework and CDR regions were annotated and analysed using the Jalview 2.10.5 program and Abysis.org to identify unique scFvs.

*Expression-Normalized Capture (ENC) assay*

123 unique scFvs were tested in an ENC assay, which was carried out as earlier described *(14)*, with the exception of using an antigen molar concentration of 10 nM.

*Conversion from scFv to antigen-binding fragment (Fab) format*

$V_L$ and $V_H$ sequences from TPL0039_05_E2 were codon optimized for expression in human cells and synthesized by Integrated DNA Technologies (IDT). The $V_L$ was cloned using *NheI* and *NotI*, and the $V_H$ was cloned using *NcoI* and *Xho*I restriction endonucleases into mammalian expression vector pINT12 containing the gene for the CH1 antibody domain. The $C_L$ antibody domain sequence and heavy chain promoter were cloned in a stuffer fragment using *NotI* and *NcoI* restriction endonucleases. Following ligation of the four fragments, the construct was transformed into DH10B *E. coli* cells and sequence verified. For sequencing, pINT $V_H$ Seq Fwd (TGGAGCTGTATCATCCTCTTCTTGG) and pINT VL lambda seq R (ACTCCGGCTTTCACTGGGGAGCTGTCTGCCTTC) were used.

*Expression, purification, and buffer exchange of Fab*

The Fab was expressed by transient transfection of the constructed expression plasmid in Expi293F™ cells (Life Technologies™, A14527) using the Expi293™ transfection system (Life Technologies™, A14525) according to the manufacturer's instructions. The

Fabs were purified using CH1 CaptureSelect™ IgG-CH1 Affinity Matrix (Thermo scientific, 194320010) resin beads, and Proteus '1 step batch' midi spin column (Generon, NB-45-00080). The Fabs were eluted using 0.2 M Glycine at pH 2.6, and the eluate was immediately neutralized using 1 M Tris buffer at pH 8.0. The eluted Fabs were buffer exchanged into PBS using Illustra™ NAP™ 10 columns according to manufacturer's instructions.

*Conversion from scFv to IgG format*

Antibody variable domains were converted from scFv to IgG format prior to expression in CHO-S cells. The variable chains ($V_L$ and $V_H$) were extracted from the pSANG10-3F vector by PCR and were cloned into a single expression vector using the NEBuilder® cloning technique. The expression vector contained the constant domain sequences of the respective human IgG heavy chain (with LALA *(32)* and YTE *(33)* mutation) and human kappa light chain. After cloning, expression vectors were sequence verified (Eurofins), and plasmids were purified using NucleoBond Xtra Midi EF (Macherey-Nagel) according to the manufacturer's instructions. A CHO-S cell line with pre-established landing pad suitable for recombinase-mediated cassette exchange with the IgG expression vector were cultivated in CD CHO medium (Gibco), supplemented with 8 mM L-Glutamine (Thermo Fisher Scientific) and 2 uL/mL anti-clumping agent (Gibco) at 37°C, 5% $CO_2$ at 120 rpm (shaking diameter 25 mm). The cell line was transfected with IgG expression vector and Cre-recombinase vector in 3:1 ratio (w:w) in 6-well plates (BD-biosciences) at a concentration of $10^6$ cells/mL using FreeStyle MAX transfection reagent (Thermo Fischer Scientific) according to the manufacturer's recommendation. Stable cell pools were generated by adding 5 µg/mL blasticidin five days post-transfection, continuing until cell death of untransfected cells and complete recovery of transfected cells (>95% viability). IgG producing cell pools were seeded at $3x10^5$ cells/mL in FortiCHO or CD CHO medium supplemented with 8 mM glutamine and 2 µL/mL anti-clumping reagent. The pools were cultivated in Batch mode (CD CHO) for 5 days or in Fed-batch mode (Forti-CHO) for 7 to maximum 13 days, feeding glutamine, glucose, and feeding supplements cell boost 7a and 7b (VWR) starting on either day 3, 4, or 5. Cultures were harvested by centrifuging the cell suspension at 300 g for 10 minutes followed by 4700 g for 15 minutes, removing cells and cell debris. Clarified supernatants were stored at -80 °C until the time point of purification.

*Purification of IgGs*

Supernatants were thawed overnight, either at 4 or 10 °C, cleared once more by centrifugation at 4500 g for 15 minutes, and loaded on a column packed with 25 mL MabSelect PrismA proteinA chromatography resin (Cytiva). An aqueous solution of 20 mM sodium phosphate and 150 mM NaCl (pH 7.2) was used for equilibration and washing of the column. Elution was performed with 0.1 M sodium citrate (pH 3). Elution fractions were neutralized by having 1 M Tris (pH 9) in the collection plate, using 0.2 mL per 1 mL of elution fraction. Fractions of interest were pooled and loaded on a HiPrep 26/10 desalting column for exchange of elution buffer to PBS. Fractions containing the protein were

concentrated by centrifugal filtration using an Amicon® Ultra-15 centrifugal filter unit (30 kDa NMWL), aiming for a minimum concentration of 20 mg/mL. Upon collection from the centrifugal filter unit, protein solutions were filter sterilized. The final concentration was determined by measuring the absorbance at 280 nm on a Nanodrop2000 instrument. Proteins were stored at 4 $^{o}$C.

*Monoclonal IgG ELISA*

A monoclonal IgG ELISA was set up to test whether the binding properties of the scFv were retained through reformatting to the IgG1 format. The monoclonal IgG ELISA was carried out according to Føns *et al. (29),* with the exception that the biotinylated myotoxin II was immobilized in streptavidin coated (10 µg/mL) wells and supernatants of IgG expression were used instead of purified IgGs. Absorbance was measured at 450 nm in a Multiskan FC Microplate Photometer (Thermo Scientific).

*Human fibroblast assay*

A functional *in vitro* neutralization assay was carried out using human dermal fibroblasts (neonatal; 106-05N, Sigma Aldrich) based on the CellTiter-Glo® Luminescent Cell Viability Assay (Cat.# G7571, Promega, USA) Firstly, the $IC_{50}$ of myotoxin II was determined in fibroblasts (72.5 µg/mL) and subsequently all IgGs were assessed for their neutralizing abilities. The level of neutralization was tested at toxin:IgG molar ratios of 1:0.5, 1:1, and 1:1.5.

The assay was carried out according to the manufacturer's protocol over a span of three consecutive days and all experiments were run in triplicates: On the first day, 100 µL of cells (400,000 cells/ mL in fibroblast culture medium) were seeded in 96-well plates and grown for 24h at 37°C/ 5% $CO_2$. After 24 hours of incubation, the toxin, or toxin-IgGs mixtures (preincubated 30 minutes at 37°C) were added to their respective wells. Following 24 hours of incubation (37°C/ 5% $CO_2$), the wells were emptied and 100 uL CellTiter-Glo® Reagent (room temperature) was added to each well and the plates were incubated 5-10 minutes on an orbital shaker. After 10 minutes at room temperature the luminescence was recorded (Victor Nivo, Perkin Elmer).

*Octet measurement*

1x Kinetic Buffer (KB, ForteBio) prepared in PBS was used as the running buffer in the octet experiment. Immediately prior to the assay, the streptavidin (SAX) biosensors were pre-wet for 10 min in 1X KB. Kinetic assay was performed by first capturing biotinylated-MII using SAX biosensors followed by a 120 s baseline step in 1X KB. The MII-captured biosensors were then dipped in wells containing increasing concentrations of Fab or IgGs – 0nM, 1 nM, 10 nM and 100 nM for a 600 s of association step, followed by a dissociation step in 1X KB for 600 s. The experiment was performed at 30°C with a shaking at 1000 rpm. FroteBio's data analysis software was used to fit the curve using 1:1 binding model

to determine the $k_a$, $k_d$ and KD (except for TPL0039_05_G08 which used a 2:1 binding model).

*In vivo mouse assay for myotoxicity neutralization*

Myotoxin II was preincubated for 30 min at room temperature with either (a) phosphate-buffered saline (0.12 M NaCl, 0.04 M sodium phosphate; PBS, pH 7.2), (b) monoclonal antibody (TPL0039_05_B12, TPL0039_05_E02, and TPL0039_05_G08) at 1:1 molar ratio, or (c) polyvalent equine antivenom (batch 6720721, Instituto Clodomiro Picado) at 1.6 mg toxin/mL antivenom ratio. Subsequently the preincubated mixtures were injected by intramuscular (gastrocnemius) route, in a total volume of 100 μL (containing 75 μg of toxin as challenge dose), in groups of five CD-1 mice. As a control, a group of mice received an identical injection of 100 μL of PBS alone. Monoclonal antibody alone, in equal amount as in the myotoxin-preincubated mixture, was injected in a group of 5 mice as an additional control. All mice were bled 3 h after injection and the plasma creatine kinase (CK) activity was determined using a UV-kinetic commercial assay (CK-Nac, Biocon Diagnostik), as an indicator of skeletal muscle necrosis*(34)*.

Using the same mouse assay, it was evaluated whether monoclonal antibody TPL0039_05_B12 (153 ug), TPL0039_05_B12 Fab format (102 ug), polyvalent equine antivenom (batch 6720721, Instituto Clodomiro Picado) (29 uL), or polyvalent equine antivenom (29 uL) mixed with monoclonal antibody TPL0039_05_B12 (125 ug), could neutralize the myotoxic effects of whole *B. asper* venom. Venom and antibodies were preincubated for 30 min at room temperature, and then the mixtures were intramuscularly injected in groups of 5 mice (100 μL, containing 50 μg of whole venom as challenge dose), using as a control group of mice receiving PBS alone. Plasma CK activity after 3 h was determined as above.

Mouse experiments followed ethical guidelines of the Institutional Committee for the Use and Care of Animals (CICUA, #084-17) of the University of Costa Rica. Statistical significance of the difference between each group and the positive control (Venom) was determined by one-way ANOVA followed by Dunnet's multiple comparisons test using Graphpad Prism version 9.2.0 for macOS.

*In vivo mouse rescue assays for myotoxicity neutralization*

A rescue assay using TPL0039_05_B12, polyvalent equine antivenom (batch 6720721, Instituto Clodomiro Picado) or polyvalent equine antivenom mixed with monoclonal antibody TPL0039_05_B12 was performed. *B. asper* venom (50 μg in 100 μL of PBS) was injected in the right gastrocnemius of groups of 5 mice. After 3 minutes, mice were intravenously injected with either TPL0039_05_B12 (1085 μg) , polyvalent equine antivenom (200 μL), or polyvalent equine antivenom (150 μL) mixed with monoclonal antibody TPL0039_05_B12 (760 ug). A control group was injected intramuscularly with *B. asper* venom (50 μg in 100 μL of PBS) with no rescue injection after 3 min. Two other

control groups were injected intramuscularly with PBS (100 μL), one group received an intravenous injection of TPL0039_05_B12 (1085 μg) and the other group did not receive a rescue injection. Plasma CK activity after 3 h was determined in all mice groups as above.

Another rescue assay was performed using the same methodology as above, in groups of 5 mice, but instead using the Fab format of TPL0039_05_B12 or different scaffold mutations for the TPL0039_05_B12 IgG1, meaning that the scaffold in all above experiments contained both LALA and YTE mutations, but in this experiment it only contained the LALA mutation. *B. asper* venom (50 μg in 100 μL of PBS) was injected in the right gastrocnemius of groups of 5 mice. After 3 minutes, mice were intravenously injected with modified TPL0039_05_B12 IgG LALA (985 μg), TPL0039_05_B12 Fab (664 μg), polyvalent equine antivenom (batch 6720721, Instituto Clodomiro Picado) (200 μL), or polyvalent equine antivenom (150 μL) mixed with modified TPL0039_05_B12 IgG LALA (690 ug). A control group was injected intramuscularly with *B. asper* venom (50 μg in 100 μL of PBS) with no rescue injection after 3 min. A second control group was injected intramuscularly with PBS (100 μL) and did not receive a rescue injection. A third control group was injected intramuscularly with PBS (100 μL), and after 3 minutes, mice were intravenously injected with TPL0039_05_B12 Fab (664 μg). Plasma CK activity after 3 h was determined in all mice groups as described previously.

**References**


1. J. M. Gutiérrez, J. J. Calvete, A. G. Habib, R. A. Harrison, D. J. Williams, D. A. Warrell, Snakebite envenoming. *Nat. Rev. Dis. Primer* **3**, 17063 (2017).

2. A. Kasturiratne, A. R. Wickremasinghe, N. de Silva, N. K. Gunawardena, A. Pathmeswaran, R. Premaratna, L. Savioli, D. G. Lalloo, H. J. de Silva, The global burden of snakebite: a literature analysis and modelling based on regional estimates of envenoming and deaths. *PLoS Med.* **5**, e218 (2008).

3. N. L. S. Roberts, E. K. Johnson, S. M. Zeng, E. B. Hamilton, A. Abdoli, F. Alahdab, V. Alipour, R. Ancuceanu, C. L. Andrei, D. Anvari, J. Arabloo, M. Ausloos, A. F. Awedew, A. D. Badiye, S. M. Bakkannavar, A. Bhalla, N. Bhardwaj, P. Bhardwaj, S. Bhaumik, A. Bijani, A. Boloor, T. Cai, F. Carvalho, D.-T. Chu, R. A. S. Couto, X. Dai, A. A. Desta, H. T. Do, L. Earl, A. Eftekhari, F. Esmaeilzadeh, F. Farzadfar, E. Fernandes, I. Filip, M. Foroutan, R. C. Franklin, A. M. Gaidhane, B. G. Gebregiorgis, B. Gebremichael, A. Ghashghaee, M. Golechha, S. Hamidi, S. E. Haque, K. Hayat, C. Herteliu, O. S. Ilesanmi, M. M. Islam, J. Jagnoor, T. Kanchan, N. Kapoor, E. A. Khan, M. N. Khatib, R. Khundkar, K. Krishan, G. A. Kumar, N. Kumar, I. Landires, S. S. Lim, M. Madadin, V. Maled, N. Manafi, L. B. Marczak, R. G. Menezes, T. J. Meretoja, T. R. Miller, A. Mohammadian-Hafshejani, A. H. Mokdad, F. N. P. Monteiro, M. Moradi, V. C. Nayak, C. T. Nguyen, H. L. T. Nguyen, V. Nuñez-Samudio, S. M. Ostroff, J. R. Padubidri, H. Q. Pham, M. Pinheiro, M. Pirestani, Z. Quazi Syed, N. Rabiee, A. Radfar, V. Rahimi-Movaghar, S. J. Rao, P. Rastogi, D. L. Rawaf, S. Rawaf, R. C. Reiner, A. Sahebkar, A. M. Samy, M. Sawhney, D. C. Schwebel, S. Senthilkumaran, M. A. Shaikh, V. Y. Skryabin, A. A. Skryabina, A. Soheili, M. A. Stokes, R. Thapar, M. R. Tovani-Palone, B. X. Tran, R. S. Travillian, D. Z. Velazquez, Z.-J. Zhang, M. Naghavi, R. Dandona, L. Dandona, S. L. James, D. M. Pigott, C. J. L. Murray, S. I. Hay, T. Vos, K. L. Ong, GBD 2019 Snakebite Envenomation Collaborators, Global mortality of snakebite envenoming between 1990 and 2019. *Nat. Commun.* **13**, 6160 (2022).

4. R. Otero-Patiño, Á. Segura, M. Herrera, Y. Angulo, G. León, J. M. Gutiérrez, J. Barona, S. Estrada, A. Pereañez, J. C. Quintana, L. J. Vargas, J. P. Gómez, A. Díaz, A. M. Suárez, J. Fernández, P. Ramírez, P. Fabra, M. Perea, D. Fernández, Y. Arroyo, D. Betancur, Lady Pupo, E. A. Córdoba, C. E. Ramírez, A. B. Arrieta, A. Rivero, D. C. Mosquera, N. L. Conrado, R. Ortiz, Comparative study of the efficacy and safety of two polyvalent, caprylic acid fractionated [IgG and F(ab′)2] antivenoms, in Bothrops asper bites in Colombia. *Toxicon* **59**, 344–355 (2012).

5. B. Lomonte, J. Gutiérrez, A new muscle damaging toxin, myotoxin II, from the venom of the snake Bothrops asper (terciopelo). *Toxicon* **27**, 725–733 (1989).

6. A. Alape-Girón, L. Sanz, J. Escolano, M. Flores-Díaz, M. Madrigal, M. Sasa, J. J. Calvete, Snake Venomics of the Lancehead Pitviper Bothrops asper: Geographic, Individual, and Ontogenetic Variations. *J. Proteome Res.* **7**, 3556–3571 (2008).

7. D. Mora-Obando, C. Díaz, Y. Angulo, J. M. Gutiérrez, B. Lomonte, Role of enzymatic activity in muscle damage and cytotoxicity induced by Bothrops asper Asp49 phospholipase A2 myotoxins: are there additional effector mechanisms involved? *PeerJ* **2**, e569 (2014).

8. B. Lomonte, Identification of linear B-cell epitopes on myotoxin II, a Lys49 phospholipase A2 homologue from Bothrops asper snake venom. *Toxicon* **60**, 782–790 (2012).

9. A. H Laustsen, M. Engmark, C. Milbo, J. Johannesen, B. Lomonte, J. Maria Gutierrez, B. Lohse, From fangs to pharmacology: the future of snakebite envenoming therapy. *Curr. Pharm. Des.* **22**, 5270–5293 (2016).

10. D. J. Williams, A. G. Habib, D. A. Warrell, Clinical studies of the effectiveness and safety of antivenoms. *Toxicon* **150**, 1–10 (2018).

11. E. Alirol, S. K. Sharma, A. Ghimire, A. Poncet, C. Combescure, C. Thapa, V. P. Paudel, K. Adhikary, W. R. Taylor, D. Warrell, Dose of antivenom for the treatment of snakebite with neurotoxic envenoming: Evidence from a randomised controlled trial in Nepal. *PLoS Negl. Trop. Dis.* **11**, e0005612 (2017).

12. H. F. Williams, H. J. Layfield, T. Vallance, K. Patel, A. B. Bicknell, S. A. Trim, S. Vaiyapuri, The Urgent Need to Develop Novel Strategies for the Diagnosis and Treatment of Snakebites. *Toxins* **11**, 363 (2019).

13. Á. Segura, M. Herrera, M. Villalta, M. Vargas, J. M. Gutiérrez, G. León, Assessment of snake antivenom purity by comparing physicochemical and immunochemical methods. *Biologicals* **41**, 93–97 (2013).

14. A. H. Laustsen, A. Karatt-Vellatt, E. W. Masters, A. S. Arias, U. Pus, C. Knudsen, S. Oscoz, P. Slavny, D. T. Griffiths, A. M. Luther, In vivo neutralization of dendrotoxin-mediated neurotoxicity of black mamba venom by oligoclonal human IgG antibodies. *Nat. Commun.* **9**, 3928 (2018).

15. J. Glanville, J. C. Andrade, M. Bellin, S. Kim, S. Pletnev, D. Tsao, R. Verardi, R. Bedi, T. Friede, S. Liao, R. Newland, N. L. Bayless, S. Youssef, E. Tully, B. Zhang, T. Bylund, S. Kim, T. Liu, P. D. Kwong, *Venom protection by antibody from a snakebite hyperimmune subject* (Immunology, 2022; http://biorxiv.org/lookup/doi/10.1101/2022.09.26.507364).

16. L. Ledsgaard, J. Wade, K. Boddum, I. Oganesyan, J. Harrison, T. P. Jenkins, P. Villar, R. A. Leah, R. Zenobi, J. McCafferty, B. Lomonte, J. M. Gutiérrez, A. H.

Laustsen, A. Karatt-Vellatt, Discovery of a broadly-neutralizing human antibody that can rescue mice challenged with neurotoxin-rich snake venoms, 2022.06.17.496531 (2022).

17. L. Ledsgaard, A. H. Laustsen, U. Pus, J. Wade, P. Villar, K. Boddum, P. Slavny, E. W. Masters, A. S. Arias, S. Oscoz, D. T. Griffiths, A. M. Luther, M. Lindholm, R. A. Leah, M. S. Møller, H. Ali, J. McCafferty, B. Lomonte, J. M. Gutiérrez, A. Karatt-Vellatt, In vitro discovery and optimization of a human monoclonal antibody that neutralizes neurotoxicity and lethality of cobra snake venom. *bioRxiv* , 2021.09.07.459075 (2021).

18. S. Ahmadi, M. B. Pucca, J. A. Jürgensen, R. Janke, L. Ledsgaard, E. M. Schoof, C. V. Sørensen, F. Çalışkan, A. H. Laustsen, An in vitro methodology for discovering broadly-neutralizing monoclonal antibodies. *Sci. Rep.* **10**, 1–7 (2020).

19. D. J. Schofield, A. R. Pope, V. Clementel, J. Buckell, S. D. Chapple, K. F. Clarke, J. S. Conquer, A. M. Crofts, S. R. Crowther, M. R. Dyson, Application of phage display to high throughput antibody generation and characterization. *Genome Biol.* **8**, 1–18 (2007).

20. S. Nirthanan, Snake three-finger α-neurotoxins and nicotinic acetylcholine receptors: molecules, mechanisms and medicine. *Biochem. Pharmacol.* **181**, 114168 (2020).

21. S. Vargas-Valerio, J. Robleto, S. Chaves-Araya, L. Monturiol-Gross, B. Lomonte, F. Tonello, J. Fernández, Localization of Myotoxin I and Myotoxin II from the venom of Bothrops asper in a murine model. *Toxicon* **197**, 48–54 (2021).

22. M. L. Massimino, M. Simonato, B. Spolaore, C. Franchin, G. Arrigoni, O. Marin, L. Monturiol-Gross, J. Fernández, B. Lomonte, F. Tonello, Cell surface nucleolin interacts with and internalizes Bothrops asper Lys49 phospholipase A2 and mediates its toxic activity. *Sci. Rep.* **8**, 1–14 (2018).

23. A. H. Laustsen, J. María Gutiérrez, C. Knudsen, K. H. Johansen, E. Bermúdez-Méndez, F. A. Cerni, J. A. Jürgensen, L. Ledsgaard, A. Martos-Esteban, M. Øhlenschlæger, U. Pus, M. R. Andersen, B. Lomonte, M. Engmark, M. B. Pucca, Pros and cons of different therapeutic antibody formats for recombinant antivenom development. *Toxicon* **146**, 151–175 (2018).

24. Y. Angulo, J. M. Gutiérrez, A. M. Soares, W. Cho, B. Lomonte, Myotoxic and cytolytic activities of dimeric Lys49 phospholipase A2 homologues are reduced, but not abolished, by a pH-induced dissociation. *Toxicon* **46**, 291–296 (2005).

25. A. P. Chapman, P. Antoniw, M. Spitali, S. West, S. Stephens, D. J. King, Therapeutic antibody fragments with prolonged in vivo half-lives. *Nat. Biotechnol.* **17**, 780–783 (1999).

26. H. Faulstich, K. Kirchner, M. Derenzini, Strongly enhanced toxicity of the mushroom toxin α-amanitin by an amatoxin-specific Fab or monoclonal antibody. *Toxicon* **26**, 491–499 (1988).

27. A. Silva, W. C. Hodgson, T. Tasoulis, G. K. Isbister, Rodent Lethality Models Are Problematic for Evaluating Antivenoms for Human Envenoming. *Front. Pharmacol.* **13** (2022) (available at https://www.frontiersin.org/articles/10.3389/fphar.2022.830384).

28. C. Knudsen, N. R. Casewell, B. Lomonte, J. M. Gutiérrez, S. Vaiyapuri, A. H. Laustsen, Novel Snakebite Therapeutics Must Be Tested in Appropriate Rescue Models to Robustly Assess Their Preclinical Efficacy. *Toxins* **12**, 528 (2020).

29. S. Føns, L. Ledsgaard, M. V. Nikolaev, A. A. Vassilevski, C. V. Sørensen, M. K. Chevalier, M. Fiebig, A. H. Laustsen, Discovery of a Recombinant Human Monoclonal Immunoglobulin G Antibody Against a-Latrotoxin From the Mediterranean Black Widow Spider (Latrodectus tredecimguttatus). *Front Immunol 11 587825 Doi 103389fimmu* (2020).

30. C. D. Martin, G. Rojas, J. N. Mitchell, K. J. Vincent, J. Wu, J. McCafferty, D. J. Schofield, A simple vector system to improve performance and utilisation of recombinant antibodies. *BMC Biotechnol.* **6**, 46 (2006).

31. F. W. Studier, Protein production by auto-induction in high-density shaking cultures. *Protein Expr. Purif.* **41**, 207–234 (2005).

32. D. Xu, M.-L. Alegre, S. S. Varga, A. L. Rothermel, A. M. Collins, V. L. Pulito, L. S. Hanna, K. P. Dolan, P. W. H. I. Parren, J. A. Bluestone, L. K. Jolliffe, R. A. Zivin, In Vitro Characterization of Five Humanized OKT3 Effector Function Variant Antibodies. *Cell. Immunol.* **200**, 16–26 (2000).

33. W. F. D. Acqua, R. M. Woods, E. S. Ward, S. R. Palaszynski, N. K. Patel, Y. A. Brewah, H. Wu, P. A. Kiener, S. Langermann, Increasing the Affinity of a Human IgG1 for the Neonatal Fc Receptor: Biological Consequences. *J. Immunol.* **169**, 5171–5180 (2002).

34. J. Gutiérrez, B. Lomonte, L. Cerdas, Isolation and partial characterization of a myotoxin from the venom of the snake Bothrops nummifer. *Toxicon* **24**, 885–894 (1986).

# Chapter 4 - Manuscript II

**Phage display-assisted discovery of a pH-dependent anti-α-cobratoxin antibody from a natural variable domain library**

This manuscript describes the discovery of an α-cbtx-targeting pH-dependent antibody from a naïve scFv-phage library consisting of naturally occurring variable domains. The selection strategy for pH-dependent antigen-binding antibodies involved incubating the phage library with the antigen for binding at pH 7.4, followed by elution of the bound phages using low pH (pH 5.5−6.0) buffer. Following screening of the selected clones for pH-dependent antigen-binding in expression normalized capture (ENC) dissociation-enhanced lanthanide fluorescence immunoassay (DELFIA), and bio-layer interferometry (BLI), one clone with a faster off-rate at pH 5.5 than 7.4 was identified. In Fab format, this antibody demonstrated an approximately 8-fold faster off-rate at pH 5.5 than at 7.4. Additionally, when sequenced, its variable domains, i.e., both CDRs and FRs were found to be entirely devoid of histidine residues. Since pH-dependent binding has been widely attributed to the presence of histidine residues, finding no histidine residues in the discovered antibody was surprising. Thus, we suggest that the observed pH-dependent binding between the discovered antibody and α-cbtx may be an effect of the molecular microenvironment that can alter the local $pK_a$ of the amino acid residues at the antibody-antigen interface. The findings of this study suggest that histidine doping may not be necessary and that pH-dependent antibodies can be discovered directly from antibody libraries with natural variable domains. Additionally, given that the employed library was naïve, it can potentially be used to discover antibodies with pH-dependent antigen-binding properties against many different targets.

This manuscript is still in preparation.

# Phage display assisted discovery of a pH-dependent anti-α-cobratoxin antibody from a natural variable domain library

**Tulika Tulika[1†], Rasmus W. Pedersen[1†]**, Charlotte Rimbault[1], Shirin Ahmadi[1], Line Ledsgaard[1], Markus-Frederik Bohn[1], Anne Ljungars[1], Bjørn G. Voldborg[1], Fulgencio Ruso-Julve[2,3], Jan Terje Andersen[2,3], Andreas H. Laustsen[1*]

[1]Department of Biotechnology and Biomedicine, Technical University of Denmark, Lyngby, Denmark

[2]Department of Immunology, Oslo University Hospital Rikshospitalet, N-0372 Oslo, Norway

[3]Department of Pharmacology, Institute of Clinical Medicine, University of Oslo, N-0372 Oslo, Norway

*Corresponding author: Andreas H. Laustsen, ahola@bio.dtu.dk
[†] Equal contribution

**Abstract**

Recycling antibodies can bind to their target antigen at neutral pH in the blood stream and release them upon endocytosis when pH levels drop, allowing the antibodies to be recycled into circulation via FcRn-mediated pathway, while the antigens undergo lysosomal degradation. This enables recycling antibodies to achieve the same therapeutic effect at lower doses than their non-recyclable counterparts. The development of such antibodies is typically achieved by histidine doping of the variable regions of specific antibodies or by performing *in vitro* antibody selection campaigns utilizing histidine doped libraries. While often successful, these strategies may introduce sequence liabilities, as they often involve mutations that may render the resultant antibodies to be non-natural. Here, we present a methodology that employs a naïve antibody phage display library, consisting of natural variable domains, to discover antibodies that bind α-cobratoxin from the venom of *Naja kaouthia* in a pH-dependent manner. Upon screening of the discovered antibodies with immunoassays and bioloyer interferometry, a pH-dependent antibody was discovered that exhibits an 8-fold higher dissociation rate at pH 5.5 than 7.4. Interestingly, the variable domains of the pH-dependent antibody were found to be entirely devoid of histidines, demonstrating that pH-dependency may not always be driven by this amino acid. Further, given the high diversity available in a naïve antibody library, the methodology presented here can likely be applied to discover pH-dependent antibodies against different targets *ab initio* without the need of histidine doping.

**Key words:** pH-dependent antigen-binding antibody, naïve antibody library, natural antibody variable domains, phage display technology, histidine, α-cobratoxin, snake venom

## Introduction

Monoclonal antibodies (mAbs) of the immunoglobulin G (IgG) class are a rapidly growing class of drugs used to treat a range of conditions including cancer and autoimmune diseases[1–3]. The major factors behind their clinical success, include their high specificity and affinity for cognate antigens combined with the ability to mediate effector functions[1,2]. In addition, IgG has a plasma half-life of 3 weeks on average in humans, which makes it an attractive choice for the development of mAbs for diseases where exposure over time is key. This hallmark is regulated by binding of the IgG fragment crystallizable (Fc) region to a broadly expressed cellular receptor named the neonatal Fc receptor (FcRn), which rescues IgGs from intracellular lysosomal degradation via recycling or transcytosis. Mechanistically, this happens in a strictly pH-dependent manner where IgG is entering cells via fluid-phase pinocytosis followed by engagement of FcRn, which predominantly resides in mildly acidified endosomes. The complex is then recycled back to the cell surface or transcytosed across polarized cells followed by exposure to the near neutral pH, which triggers dissociation and release of the IgG to the extracellular milieu[4,5]. As such, IgG antibodies are rescued from intracellular degradation via FcRn-directed transport routes.

However, when most IgGs are bound to their cognate antigen, this often occurs with high affinity throughout this endosomal pH gradient. Thus, the IgGs may undergo antigen-mediated clearance via lysosomal degradation or they may be recycled by FcRn along with the bound antigen. As a result, antibodies can bind the antigen only once in their lifetime. An attractive strategy is to engineer antibody binding to the antigen such that high affinity is kept at near neutral pH while binding becomes weaker when approaching the acidic environment of endosomes[6–15]. This allows the antigen to dissociate from the antibody in the acidic endosomes (~pH 5.0-6.5) and undergo lysosomes for degradation, while the antibody is rescued via FcRn-mediated pathway and released upon exposure to the near-neutral pH conditions (pH ~7.4) at the cell surface. This will allow the same IgG to be used multiple times, ready to engage new antigens in the blood stream[6,13,16]. Such engineering has shown to reduce the required dose and/or frequency of dosing to achieve therapeutic effect[14,17]. Importantly, this is an attractive approach for design of antibodies tailored for treatment regiments relying on high dosing and where cost is a limiting factor, such as snakebite envenoming and infectious diseases[18].

Specifically, the ability of antibodies to bind cognate antigens in a pH-dependent manner has largely been attributed to the presence of histidines (p*Ka* ~6.0) at the antibody-antigen binding interface[19,20]. Thus, the discovery of pH-dependent antibodies has predominantly been carried out using histidine scanning approaches or histidine-enriched libraries[8–12,21–26]. However, such strategies may not always be straightforward as histidine doping may compromise target binding properties at neutral pH[12,23,24]. In addition, histidine-mediated pH-dependent binding requires the epitope to have positively charged residues, which restricts the number of suitable epitopes[27]. Furthermore, histidine-enriched antibody libraries are designed, and therefore, the generated antibodies may have developability and immunogenicity risks that should be taken into consideration. Immunized libraries have also been explored but derived antibodies have needed to

undergo humanization[28,29]. Additional approaches for discovery of pH-dependent antibodies are thus attractive.

In this study, we demonstrate the utility of natural naïve human antibody libraries for discovery of fully human IgG1 antibodies with pH-dependent antigen binding properties. We show that this is possible even without having any histidines in the complementarity determining regions (CDRs). To achieve this, we employed phage display technology based on a naïve human antibody library consisting of naturally occurring variable domains for the discovery of pH-dependent antibodies against a long-chain α-neurotoxin, namely α-cobratoxin (α-cbtx). The results showcase that pH-dependency is not always driven by histidines, but instead can be due to other structural features at the antibody-antigen binding interface.

## Materials and Methods

### Biotinylation of antigen

Purified α-cobratoxin (α-cbtx) from *N. kaouthia* (Latoxan, France) was dissolved in 1X standard phosphate buffered saline (PBS) and biotinylated using 1:1.25 (toxin: biotin reagent) molar ratio as previously described[30]. The biotinylated toxins were purified using buffer exchange columns (Vivacon 500, Sartorius, 3000 Da Molecular Weight Cut-Off) using the manufacturer's protocol. Protein concentration was determined using the toxin's extinction coefficient and absorbance measurement with a NanoDrop One instrument. The degree of biotinylation was analyzed by MALDI-TOF in an Ultraflex II TOF/TOF spectrometer (Bruker Daltonics).

### Solution-based phage display pH selection

The protocol for carrying out solution-based phage display selections was adapted from previous work[8]. The libraries used were the IONTAS naïve single-chain variable fragment (scFv) phage display κ library[31]. Briefly, the phage display library was first blocked using 3% skimmed milk in PBS (MPBS) and then deselected using streptavidin-coated beads (DynaBeads M280, Thermo Fisher #11205D). 100 nM biotinylated α-cbtx was mixed with the deselected library and incubated for selection for one hour. This selection was carried out at pH 7.4. Phages bound to α-cbtx were then captured on streptavidin-coated beads, and non-specific phages were eliminated by washing thrice with PBS + 0.1% Tween (PBS-T), and twice with PBS. In the first round of phage display panning, all phages were eluted by trypsin digestion. In round two and round three, pH-dependent clones were eluted by adding citrate buffer at pH 5.5 for 15-60 min or by trypsin. For the phages eluted using citrate buffer, trypsin was subsequently added to the eluted phages. The eluted phages were then used to infect TG1 cells as described before[32].

### Sub-cloning and screening of scFvs

Sub-cloning of scFv genes from phage outputs into the pSANG10-3F vector and primary screening were performed as previously described[30]. In short, *NcoI* and *NotI* restriction

endonucleases sites were used to sub-clone scFv genes from phagemids into the pSANG10-3F vector, which was then transformed into *E. coli* strain BL21(DE3) (New England Biolabs). From each of the selection outputs, 184 colonies were picked, expressed in 96 well format and assessed for binding to 50 nM of biotinylated α-cobratoxin in an expression-normalized capture (ENC) assay as described earlier, with a few modifications[30].

First, Nunc MaxiSorp plates (Invitrogen, 44-2404-21) were coated overnight with 50 µL of 2.5 µg/mL anti-FLAG M2 antibody (Sigma Aldrich, F1804). Plates were washed thrice with PBS and blocked with 200 µL of 3% MPBS. Plates were washed thrice with PBS, and 60 µL of 0.5X unpurified scFv-containing culture supernatant in 3% MPBS was added before incubating for 1 hour at room temperature. Plates were washed thrice with PBS + 0.1% Tween and thrice with PBS before adding 50 µL of 50 nM biotinylated α-cbtx in MPBS to each well. After 1 hour of incubation, the plates were washed thrice with PBS + 0.1% Tween and thrice with PBS. Then, 1 µg/mL of Europium-labeled Streptavidin (Perkin Elmer, 1244–360) in dissociation-enhanced lanthanide fluorescence immunoassay (DELFIA) Assay Buffer (Perkin Elmer, 4002–0010) was added. Following 30 minutes of incubation, plates were washed thrice with PBS + 0.1% Tween and thrice with PBS, and DELFIA Enhancement Solution (Perkin Elmer, 4001–0010) was added for detection of binding. Clones that gave a signal above 5,000 counts were selected for further characterization.

**ENC pH DELFIA and sequencing**

To characterize the pH-dependency of the α-cbtx-binding scFv candidates, a modified ENC DELFIA assay was performed. The assay was carried out as described in the above section, with an additional pH-elution step. The ENC pH DELFIA was performed in duplicates until after the incubation and washing of α-cbtx, where 60 µL of citrate buffer at either pH 6.0 or pH 7.4 was added to each well. Following 60 minutes of incubation, plates were washed thrice with PBS + 0.1% Tween and thrice with PBS. Detection of biotinylated antigen was carried out as described in the above section.

**BLI off-rate screening of scFvs from bacterial culture supernatant**

Prior to the assay, streptavidin (SAX) biosensors were pre-wetted for at least 10 min in 1x Kinetics Buffer (KB, Forte Bio). Screening assay was performed by first loading 1µg/mL biotinylated α-cbtx on SAX biosensors, followed by a 120 s baseline step in 1x PBS pH 7.4. The toxin-loaded biosensors were then dipped in scFv-containing bacterial supernatant wells for 600 seconds of association step, followed by a dissociation step in 1x PBS pH 7.4 for 600 seconds. The tips were regenerated in regeneration buffer 10mM Glycine pH 2.0 and neutralization buffer (1x KB) for 5 seconds for a total of 5 cycles. The tips were then dipped into 1x PBS pH 5.4 for 120 s, followed by association in the scFv-containing bacterial supernatant wells for 600 seconds, and dissociation in 1x PBS pH 5.4 for 600 seconds. The experiment was performed at 25°C with shaking at 1000 rpm. ForteBio's data

analysis software was used to fit the curves using a 1:1 binding model to obtain dissociation rates for pH 7.4 and 5.4.

**Kinetics measurements with Fab**

The KD of the Fab was determined as described in 2.5, except that purified Fabs in 1x HEPES pH 7.4 were used for association at 200nM-3nM in a 2-fold dilution. ForteBio's data analysis software was used to global fit the curves using 1:1 binding model to determine kinetic constants.

**Production of IgGs**

The reformatting of scFv into IgG was performed as previously described[32], except that the IgG expression vector for TPL0197_01_C08 contained the human kappa light chain. ExpiCHO cells were cultured and transfected with expression vector according to the manufacturer's guidelines (Gibco™) following a protocol where ExpiFectamine™ CHO Enhancer and a single feed were added at Day 1 and cells were maintained at 37°C and 5% $CO_2$. The supernatant was collected at Day 7 by removal of the cells through centrifugation at 300 g for 5 min, followed by an additional centrifugation at 1000 g for 5 minutes. The supernatant was either used for purification on the same day or stored at -80$^{o}$C. Supernatant was thawed overnight at 4$^{o}$C, centrifuged, filtered and loaded on a MabSelect column (Cytiva). 20 mM sodium phosphate and 150 mM NaCl (pH 7.2) was used for equilibration and washing of the column and elution was performed with 0.1 M sodium citrate (pH 3). Elution fractions were immediately neutralized by 1 M Tris (pH 9) using 1/5 V of neutralization solution for 1 V of elution fraction. Fractions of interest were pooled and loaded on a HiPrep 26/10 desalting column for buffer exchange to Dulbecco's PBS. Protein fractions were sterile-filtered and concentrated by centrifugal filtration using an Amicon® Ultra-15 centrifugal filter unit (30 kDa NMWL). The final concentration was determined by measuring the absorbance at 280 nm on a Nanodrop2000 instrument. Purity was checked by SDS-PAGE. The purified protein was stored at 4$^{o}$C or -80$^{o}$C.

**Production of Fab**

The reformatting of scFvs to Fabs and expression of Fabs was carried out as described in section above except that expression vector of TPL0197_01_C08 contained the constant domain 1 sequence of heavy and human kappa light chain, while that of 2554_01_D11 contained human lambda light chain. After expression, the collected supernatant, centrifuged, and loaded on a 5-mL HisTrap Excel column (Cytiva), equilibrated with 20 mM sodium phosphate (pH 7.4), 500 mM NaCl. The column was washed with 10 column volumes of 10 mM imidazole in 20 mM sodium phosphate (pH 7.4), 500 mM NaCl. Elution was performed in up-flow mode with 20 column volumes of 500 mM imidazole in 20 mM sodium phosphate (pH 7.4), 500 mM NaCl. Protein containing fractions of interest were pooled and loaded on a HiPrep 26/10 desalting column for buffer exchange to Dulbecco's PBS. The protein was then concentrated by centrifugal filtration using an Amicon® Ultra-

15 centrifugal filter unit (10 kDa NMWL). The final concentration was determined by measuring the absorbance at 280 nm on a Nanodrop2000 instrument. Purity was checked by SDS-PAGE. The purified protein was stored at 4 ºC or -80ºC.

### pH-dependent binding properties in ELISA

96-well EIA/RIA 3590 microplates (Corning) were coated with 100µL of 0.5µg/mL α-cbtx (Latoxan, France) diluted in PBS overnight at 4˚C. The plates were blocked with 4% skimmed milk powder (M) (Sigma-Aldrich) dissolved in PBS for 1 h, followed by washing four times with PBS containing 0.05% Tween20 (PBS-T) (Sigma-Aldrich) (PBST). Unless stated, the following steps were carried out at pH 7.4 and 5.5, respectively, and the washing was conducted with PBS-T with the corresponding adjusted pH. Next, 100µL of titrated amounts (1-0.015 µg/mL) of the samples containing IgGs diluted in PBST-M were added to the plates and incubated at RT for one hour. After washing, 100µL of ALP-conjugated anti-human IgG Fc-ALP (Sigma-Aldrich) diluted 1:5000 in M-PBST was added and incubating for 1 hour. Thereafter, following washing with PBST, the bound proteins were detected by adding 100µL of 1 mg/mL p-nitropenylphosphate substrate tablets dissolved in diethanolamine buffer (pH 9.8) (Sigma-Aldrich). The absorbance was measured at 405 nm using the Sunrise spectrophotometer (Tecan).

## Results

### pH elution during antibody phage display selections enables discovery of pH-dependent binders

To enrich antibodies with a pH-dependent antigen-binding, three consecutive rounds of phage display selections were performed against biotinylated α-cbtx using a buffer with low pH or trypsin (as a control) for elution of binding scFv displayed on phages. Following reformatting to soluble scFv and expression in *E.coli*, 918 of the 1472 screened clones bound to α-cbtx in an ENC DELFIA[30,33] with a signal above the arbitrary cut-off value of 5000 (Figure 1(a)). To screen for pH dependent binding, 635 of the binding clones were randomly selected, re-expressed, and analyzed in an ENC pH DELFIA, where the clones were allowed to bind α-cbtx at pH 7.4 and thereafter either incubated in a buffer of pH 7.4 or pH 5.4 for an hour before adding the detection reagent. This revealed that 166 clones showed at least 50% decrease in the binding signal after incubation at pH 5.5 compared to 7.4, indicating a pH-dependent binding of the scFvs to the antigen (Figure 1(b))[8]. Further, sequencing of these 166 clones showed that ~99% of the clones were identical, resulting in 2 unique clones. Both clones came from the phage display selection where a low pH buffer was employed for elution of the bound phages.

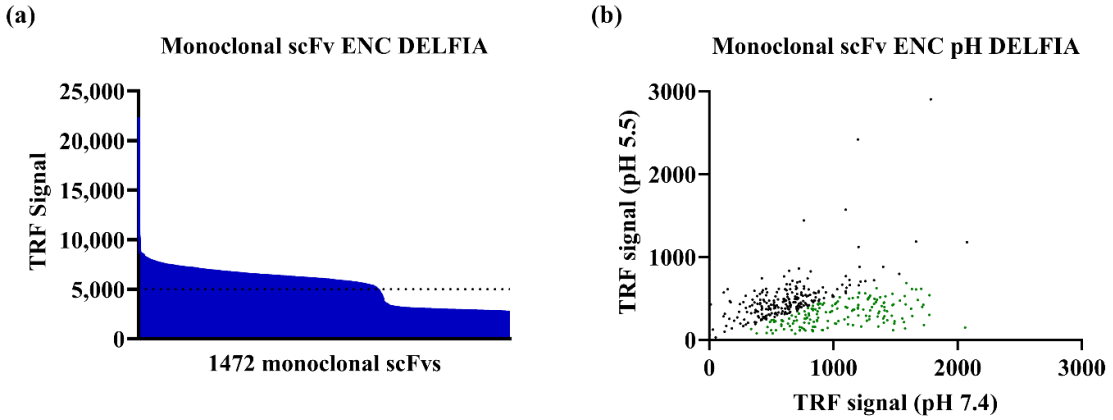


**Figure 1: Screening of binders. (a)** Binding signal of 1472 discovered monoclonal scFvs against α-cbtx in ENC DELFIA. **(b)** Scatter plot showing binding signal of a subset of selected α-cbtx binding monoclonal scFvs ENC pH DELFIA. The monoclonal scFvs showing at least 50% decrease in binding signal after being incubated at pH 5.5 than pH 7.4 buffer are colored in green.

## The most abundant pH-dependent clone contains no histidine residues in the variable domains

The two unique scFv clones were expressed in *E. coli*, and the bacterial supernatants containing the expressed scFvs were used in biolayer interferometry (BLI) to determine their pH dependent target dissociation. The most abundant clone, TPL0197_01_C08 (which will be referred to as C08 from here on) showed a faster off-rate at pH 5.5 compared to pH 7.4 (Figure 2 (a)). Sequence analysis of this clone showed that it contains no histidines in the variable regions- neither in the CDRs nor in the framework (Figure 2 (b)). This was surprising since histidines have been widely attributed as a major contributing factor of pH-dependence[6].

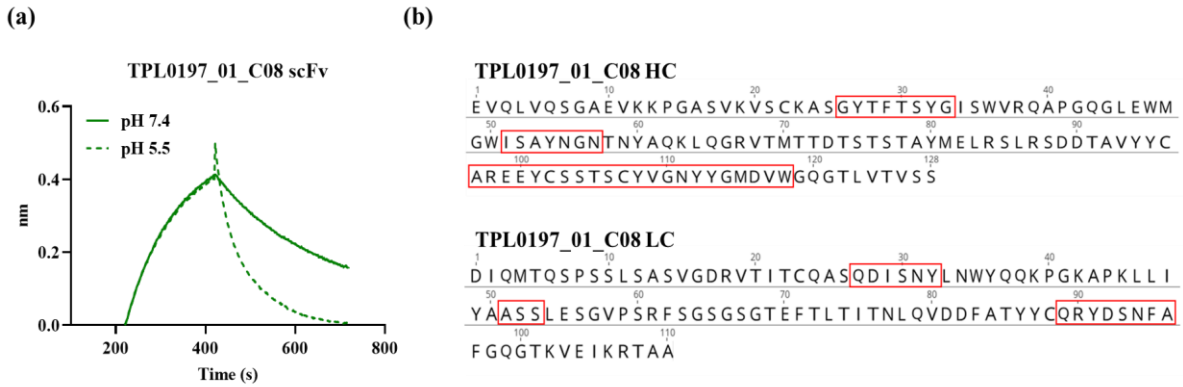


**Figure 2**: **BLI binding curves and sequence of the pH-dependent clone C08. (a)** BLI sensogram showing association at pH 7.4 and dissociation at pH 7.4 (solid line) and 5.5 (dashed line for scFv C08). **(b)** Amino acid sequences of heavy chain (HC) and light chain (LC) of clone C08. The CDRs are highlighted in red boxes.

**The pH dependent IgG, C08, shows less binding at pH 5.5 compared to pH 7.4 in ELISA**

To further characterize C08, it was reformatted to an IgG1 format, expressed in CHO cells, and purified. To validate IgG pH-dependent binding to α-cbtx, an ELISA-based binding assay was performed at pH 7.4 and 5.5 (Figure 3 (a)). A previously discovered high affinity (1.8 nM), α-cbtx targeting IgG 2554_01_D11 (which will be referred to as D11 in the following text) that previously was discovered through phage display without any pH-selection pressure, was included for comparison[34]. Both IgGs bound to α-cbtx at pH 7.4, however the signal at comparative concentrations was lower for C08 than D11, indicating a low affinity of C08 towards α-cbtx. At pH 5.5, C08 showed negligible binding to α-cbtx, while D11 bound with almost identical strength to α-cbtx as that observed at pH 7.4 (Figure 3(a), (b)). This showed that both binding and pH-dependency of C08 towards α-cbtx was retained after reformatting to an IgG format.

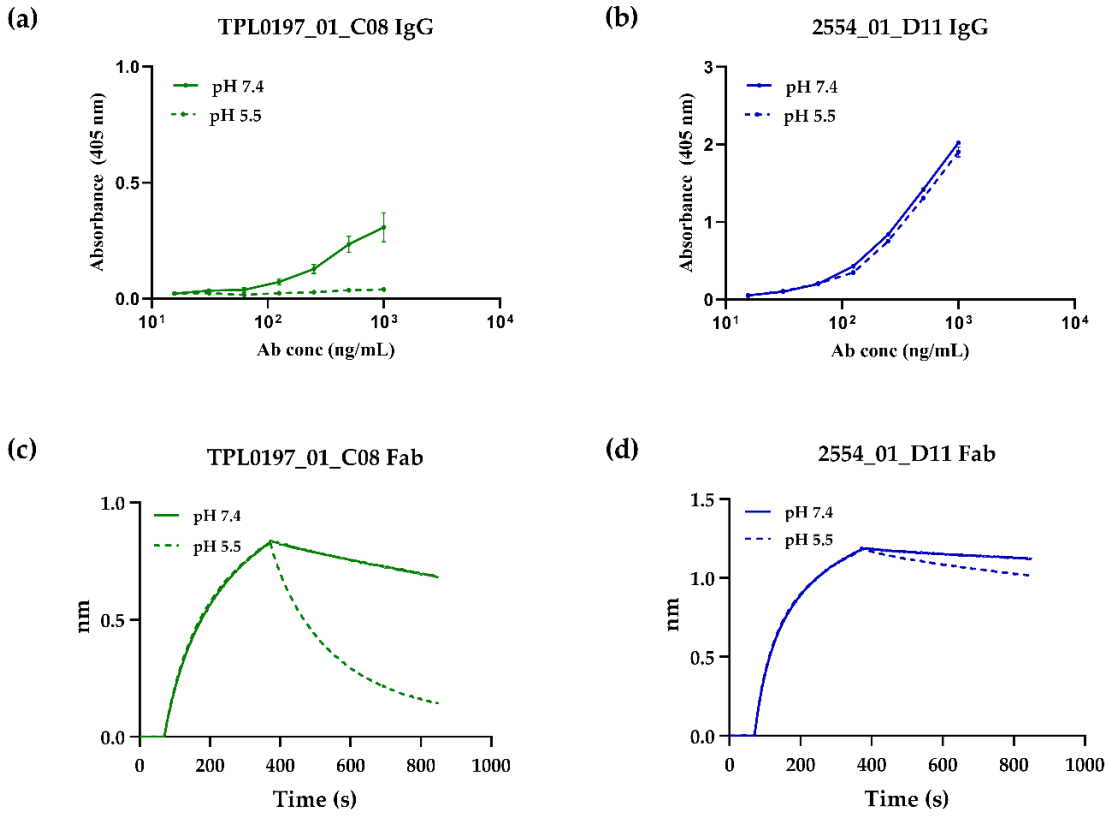


**Figure 3: Binding characterization of a pH-dependent and a non pH-dependent antigen-binding clone in IgG and Fab format.** ELISA binding curves to α-cbtx at pH 7.4 (solid line) and 5.5 (dashed line) of **(a)** pH-dependent IgG C08 and **(b)** non-pH dependent IgG D11. Biolayer interferometry (BLI) curves showing association at pH 7.4 and dissociation at pH 7.4 (solid line) and 5.5 (dashed line) for a **(c)** pH-dependent Fab C08 and **(d)** non-pH dependent Fab D11.

### pH-dependent antigen-binding Fab C08 shows increased rate of dissociation at pH 5.5

To determine the binding kinetics of the pH-dependent binder C08 while avoiding avidity effects, C08 was reformatted into a Fab, expressed in CHO cells, and His-tag purified. D11 in Fab format was included as a non pH-dependent antigen-binding control. Both Fabs were then characterized for their pH-dependent binding using BLI, on biotinylated α-cbtx loaded streptavidin biosensor tips. Fabs were allowed to associate at pH 7.4 followed by dissociation at either pH 7.4 or 5.5 (Figure 3(c), (d)). An 8-fold higher dissociation rate at pH 5.5 than 7.4 was observed for C08. In contrast, the difference between the dissociation rates at these pH values was negligible for D11 (Table 1). Thus, the pH-dependent binding of C08 towards α-cbtx was confirmed in both IgG and Fab formats using ELISA and BLI respectively.

| Fab | $k_d$ ($s^{-1}$) pH 7.4 | $k_d$ ($s^{-1}$) pH 5.5 | Fold difference (pH 5.5/7.4) |
|---|---|---|---|
| **TPL0197_01_C08** | $8.077 \times 10^{-4}$ | $6.634 \times 10^{-3}$ | 8.22 |
| **2554_01_D11** | $1.65 \times 10^{-3}$ | $1.59 \times 10^{-3}$ | 0.96 |

**Table 1**: Dissociation rates of pH-dependent and non pH-dependent Fab binders determined by BLI. The association of Fabs to the biotinylated α-cbtx loaded on streptavidin biosensors was performed at pH 7.4, while the dissociation was performed at pH 5.5.

### Discussion

In the recent years, recycling antibodies that engage with their target antigen in a pH-dependent manner have gained increased attention, as they retain high efficacy when administered at lower doses than their non-pH-dependent counterparts. This feature stems from the combination of pH-dependent antigen-binding properties and long plasma half-life deriving from FcRn-mediated recycling mechanism. Consequently, various strategies to discover and engineer pH-dependent recycling antibodies have been explored[7].

In this study, we employed a naïve human antibody phage display library consisting of naturally occurring variable domains and successfully discovered an antibody that binds its target antigen in a pH-dependent manner. While pH-dependent antibodies have previously been discovered using histidine doping of antibody libraries or the paratopes of a pre-existing antibodies[7], we here show that such strategies may not necessarily be required to discover antibodies with highly pH-dependent antigen-binding properties. Avoiding the incorporation of histidines in variable regions of antibodies may have several benefits. First, introduction of such mutations in antibody paratopes can be a time-consuming and laborious task, as it requires detailed analysis and validation of pH-dependency of the mutants and may still not provide an antibody with desirable features. For example, it has been reported that, occasionally, histidine mutations that were incorporated to reduce the binding between antibody and antigen at low pH also resulted

in reduced binding at neutral pH[7,12]. Second, the incorporation of mutations, particularly in antibody sequences deriving from natural sources, may come with a risk of introducing sequence liabilities in the antibody that could pose problems for the developability of the antibody, such as causing it to be immunogenic[35–38]. The employment of an antibody library with natural variable domains for the discovery of pH-dependent antibodies could potentially reduce this risk, since the variable domains of the antibodies have gone through the test for self-tolerance[31]. Third, given that a naïve natural antibody library can be used to find binders to a multitude of targets, the observation that histidine doping may not be necessary for the discovery of antibodies with pH-dependent antigen-binding properties indicates that such antibodies can possibly be found against many targets directly *ab initio*[39].

Besides originating from a naïve natural antibody library, the variable domains of the discovered pH-dependent antibody was surprisingly found to be entirely devoid of histidine residues. Although the presence of histidine is widely attributed to mediate pH-dependent binding[28], our findings suggest that antibodies can, at least at times, derive pH-dependent antigen-binding properties from different residues. A possible explanation for this could be the effect of the molecular microenvironment that can change the local pKa of amino acids at the antibody-antigen binding interface, which may influence the binding behavior between the two molecules[40,41].

So far, the utility of recycling antibodies that bind their target antigens in a pH-dependent manner has mostly been demonstrated against endogenous targets, such as IL-6, PCK9, CXCL10, and TNF-α[8–11]. In this study, an exogenous soluble antigen, α-cbtx from *N. kaouthia* venom, was used as the target antigen. Recycling antibodies that bind snake toxins in a pH-dependent manner could potentially find utility for the development of novel types of antivenoms, which could be administered to patients at lower doses compared to both current plasma-derived antivenoms and recombinant antivenoms which are based on non-recyclable antibodies. However, in the case of snakebite envenoming, both complex toxicokinetics and pharmacokinetics are at play[42]. While endogenous targets are often (semi-) constitutively produced within the body and therefore can be maintained at a concentration below certain thresholds by using recycling antibodies; toxins are instantaneously injected in a large dose into the body of the victim during a snakebite envenoming case, and thus, require an urgent intervention[18,42]. The effectiveness of recycling antibodies with pH-dependent binding to their target under such circumstances, where large amounts and often fast-acting toxins are required to be removed from circulation is not known. However, given that, in the majority of the cases of snakebite envenoming, the bite is either intramuscular or subcutaneous, the injection of toxins is followed by an initial absorption phase[42]. Further, for systemic toxins (such as α-cbtx), a likely depot effect might result in a delay in the onset of their toxic effects since the toxins first need to leave the bite site to enter the blood[18]. Under such circumstances, where the toxins are released over time from the bite site into circulation and not all at once, the antibodies would not be burdened with large amounts of toxins at once. Thus, we speculate that it would potentially be possible to neutralize the toxins using recycling antibodies at a lower dose and consequently at reduced cost, than the non-recyclable antibodies. However, to understand the overall effect of using recycling antibodies to neutralize toxins in a

snakebite envenoming case requires further investigation. Nevertheless, the methodologies presented in this study could find broad applicability beyond snakebite envenoming as a general approach for the discovery of pH-dependent antibodies against potentially any target using *in vitro* display technologies.

**Acknowledgments**

The authors are supported by a grant from the European Research Council (ERC) under the European Union's Horizon 2020 research and innovation programme (grant no. 850974); Villum Foundation under grant 00025302; Wellcome (221702/Z/20/Z); Novo Nordisk Foundation (NNF20SA0066621); and Research Council of Norway (287927). The authors would like to thank Sara Petersen Bjørn, Karen Kathrine Brøndum, and Daniel Duun from National Biologics Facility for the reformatting and production of Fabs and IgGs.

**Competing interests**

No conflict of interest.

**References**


1. Carter, P. J. & Lazar, G. A. Next generation antibody drugs: pursuit of the 'high-hanging fruit'. *Nat. Rev. Drug Discov.* **17**, 197–223 (2018).

2. Carter, P. J. & Rajpal, A. Designing antibodies as therapeutics. *Cell* **185**, 2789–2805 (2022).

3. Kaplon, H., Chenoweth, A., Crescioli, S. & Reichert, J. M. Antibodies to watch in 2022. *mAbs* **14**, 2014296 (2022).

4. Lencer, W. I. & Blumberg, R. S. A passionate kiss, then run: exocytosis and recycling of IgG by FcRn. *Trends Cell Biol.* **15**, 5–9 (2005).

5. Challa, D. K., Velmurugan, R., Ober, R. J. & Sally Ward, E. FcRn: from molecular interactions to regulation of IgG pharmacokinetics and functions. *Curr. Top. Microbiol. Immunol.* **382**, 249–272 (2014).

6. Klaus, T. & Deshmukh, S. pH-responsive antibodies for therapeutic applications. *J. Biomed. Sci.* **28**, 11 (2021).

7. Igawa, T., Haraya, K. & Hattori, K. Sweeping antibody as a novel therapeutic antibody modality capable of eliminating soluble antigens from circulation. *Immunol. Rev.* **270**, 132–151 (2016).

8. Bonvin, P. *et al.* De novo isolation of antibodies with pH-dependent binding properties. *mAbs* **7**, 294–302 (2015).

9. Schröter, C. *et al.* A generic approach to engineer antibody pH-switches using combinatorial histidine scanning libraries and yeast display. *mAbs* **7**, 138 (2015).

10. Igawa, T. *et al.* Antibody recycling by engineered pH-dependent antigen binding improves the duration of antigen neutralization. *Nat. Biotechnol.* **28**, 1203–1207 (2010).

11. Chaparro-Riggers, J. *et al.* Increasing Serum Half-life and Extending Cholesterol Lowering in Vivo by Engineering Antibody with pH-sensitive Binding to PCSK9 *. *J. Biol. Chem.* **287**, 11090–11097 (2012).

12. Devanaboyina, S. C. *et al.* The effect of pH dependence of antibody-antigen interactions on subcellular trafficking dynamics. *mAbs* **5**, 851–859 (2013).

13. Igawa, T. *et al.* Engineered Monoclonal Antibody with Novel Antigen-Sweeping Activity In Vivo. *PLOS ONE* **8**, e63236 (2013).

14. Lee, J. W. *et al.* Ravulizumab (ALXN1210) vs eculizumab in adult patients with PNH naive to complement inhibitors: the 301 study. *Blood* **133**, 530–539 (2019).

15. Sheridan, D. *et al.* Design and preclinical characterization of ALXN1210: A novel anti-C5 antibody with extended duration of action. *PLOS ONE* **13**, e0195909 (2018).

16. Roopenian, D. C. & Akilesh, S. FcRn: the neonatal Fc receptor comes of age. *Nat. Rev. Immunol.* **7**, 715–725 (2007).

17. Fukuzawa, T. *et al.* Long lasting neutralization of C5 by SKY59, a novel recycling antibody, is a potential therapy for complement-mediated diseases. *Sci. Rep.* **7**, 1080 (2017).

18. Laustsen, A. H. How can monoclonal antibodies be harnessed against neglected tropical diseases and other infectious diseases? *Expert Opin. Drug Discov.* **14**, 1103–1112 (2019).

19. Raghavan, M., Bonagura, V. R., Morrison, S. L. & Bjorkman, P. J. Analysis of the pH dependence of the neonatal Fc receptor/immunoglobulin G interaction using antibody and receptor variants. *Biochemistry* **34**, 14649–14657 (1995).

20. Tanokura, M. 1H-NMR study on the tautomerism of the imidazole ring of histidine residues. I. Microscopic pK values and molar ratios of tautomers in histidine-containing peptides. *Biochim. Biophys. Acta* **742**, 576–585 (1983).

21. Murtaugh, M. L., Fanning, S. W., Sharma, T. M., Terry, A. M. & Horn, J. R. A Combinatorial Histidine Scanning Library Approach to Engineer Highly pH-Dependent Protein Switches. *Protein Sci. Publ. Protein Soc.* **20**, 1619–1631 (2011).

22. Ito, W. *et al.* The His-probe method: Effects of histidine residues introduced into the complementarity-determining regions of antibodies on antigen-antibody interactions at different pH values. *FEBS Lett.* **309**, 85–88 (1992).

23. Laughlin, T. M. & Horn, J. R. Engineering pH-Sensitive Single-Domain Antibodies. in *Single-Domain Antibodies: Methods and Protocols* (eds. Hussack, G. & Henry, K. A.) 269–298 (Springer US, 2022). doi:10.1007/978-1-0716-2075-5_13.

24. Igawa, T., Mimoto, F. & Hattori, K. pH-dependent antigen-binding antibodies as a novel therapeutic modality. *Biochim. Biophys. Acta BBA - Proteins Proteomics* **1844**, 1943–1950 (2014).

25. Könning, D. *et al.* Isolation of a pH-Sensitive IgNAR Variable Domain from a Yeast-Displayed, Histidine-Doped Master Library. *Mar. Biotechnol. N. Y. N* **18**, 161–167 (2016).

26. Watkins, J. M. & Watkins, J. D. An Engineered Monovalent Anti–TNF-α Antibody with pH-Sensitive Binding Abrogates Immunogenicity in Mice following a Single Intravenous Dose. *J. Immunol.* **209**, 829–839 (2022).

27. Ledsgaard, L. *et al.* Advances in antibody phage display technology. *Drug Discov. Today* **27**, 2151–2169 (2022).

28. Sampei, Z. *et al.* Antibody engineering to generate SKY59, a long-acting anti-C5 recycling antibody. *PLOS ONE* **13**, e0209509 (2018).

29. Yang, D. *et al.* Maximizing in vivo target clearance by design of pH-dependent target binding antibodies with altered affinity to FcRn. *mAbs* **9**, 1105–1117 (2017).

30. Laustsen, A. H. *et al.* In vivo neutralization of dendrotoxin-mediated neurotoxicity of black mamba venom by oligoclonal human IgG antibodies. *Nat. Commun.* **9**, 3928 (2018).

31. Schofield, D. J. *et al.* Application of phage display to high throughput antibody generation and characterization. *Genome Biol.* **8**, R254 (2007).

32. Ledsgaard, L. *et al.* In vitro discovery of a human monoclonal antibody that neutralizes lethality of cobra snake venom. *mAbs* **14**, 2085536.

33. Martin, C. D. *et al.* A simple vector system to improve performance and utilisation of recombinant antibodies. *BMC Biotechnol.* **6**, 46 (2006).

34. Ledsgaard, L. Discovery and optimization of a broadly-neutralizing human monoclonal antibody against long-chain α-neurotoxins from snakes. Accepted. Nature Communiations.

35. Egli, J. *et al.* Enhanced immunogenic potential of cancer immunotherapy antibodies in human IgG1 transgenic mice. *mAbs* (2022).

36. 16 - Development issues: antibody stability, developability, immunogenicity, and comparability. in *Therapeutic Antibody Engineering* (eds. Strohl, W. R. & Strohl, L. M.) 377–595 (Woodhead Publishing, 2012). doi:10.1533/9781908818096.377.

37. Ausserwöger, H. *et al.* Non-specificity as the sticky problem in therapeutic antibody development. *Nat. Rev. Chem.* 1–18 (2022) doi:10.1038/s41570-022-00438-x.

38. Fernández-Quintero, M. L. Assessing developability early in the discovery process for novel biologics. Manuscript in preparation.

39. Laustsen, A. H., Greiff, V., Karatt-Vellatt, A., Muyldermans, S. & Jenkins, T. P. Animal Immunization, in Vitro Display Technologies, and Machine Learning for Antibody Discovery. *Trends Biotechnol.* **39**, 1263–1273 (2021).

40. Shan, J. & Mehler, E. L. CALCULATION OF pKa IN PROTEINS WITH THE MICROENVIRONMENT MODULATED-SCREENED COULOMB POTENTIAL (MM-SCP). *Proteins* **79**, 3346–3355 (2011).

41. Isom, D. G., Castañeda, C. A., Cannon, B. R. & García-Moreno E., B. Large shifts in pKa values of lysine residues buried inside a protein. *Proc. Natl. Acad. Sci.* **108**, 5260–5265 (2011).

42. Sanhajariya, S., Duffull, S. B. & Isbister, G. K. Pharmacokinetics of Snake Venom. *Toxins* **10**, 73 (2018).

# Chapter 5 - Manuscript III

**Discovery, engineering, and characterization of recycling antibodies targeting snake toxins**

This manuscript describes the coupling of light-chain shuffled libraries and phage display selection strategies to discover pH-dependent antibodies. The manuscript also explores the influence of Fab and antigen-binding on the antibody-FcRn interaction and the cellular transport properties of the antibodies. Finally, the manuscript investigates whether the pH-dependent antigen-binding properties of the antibodies translate to recycling properties in a cellular assay.

In this study, two anti-M-II antibodies (discovered in manuscript I) and an anti-α-cbtx antibody (discovered in manuscript II) were light-chain shuffled using a naïve human light-chain library with natural variable domains. The libraries were employed for selection of antibodies with pH-dependent antigen-binding properties using phage display technology. Upon discovery, an M-II- and an α-cbtx-targeting light-chain shuffled antibody, along with their parental antibodies, and previously reported pH-dependent and non-pH-dependent antigen-binding antibodies, were obtained in IgG1 formats with WT or YTE Fc mutations for further experiments. Using FcRn affinity chromatography, it was revealed that Fc engineering, Fab regions, and binding to the antigen had distinct effects on the antibody-FcRn interaction. The antibodies were further tested for their cellular transport properties in a human endothelial cell-based recycling assay (HERA), where again distinct influences from Fc engineering, Fab regions, and binding to the antigen were observed. Finally, the antibodies were assessed for their pH-dependent antigen-binding properties in HERAs, which revealed that the discovered light-chain shuffled antibodies performed as recycling antibodies. Additionally, the parental anti-α-cbtx antibody that was discovered in manuscript II, and the positive control included in the study for pH-dependent antigen-binding, also showed recycling characteristics in the cellular assay. This study demonstrates that light chain-shuffling combined with *in vitro* display technology can, at least in some cases, serve as a useful strategy for selection of antibodies with pH-dependent antigen-binding properties. The study further highlights the effects of Fabs and antigen-binding on the antibody-FcRn interaction and the cellular transport properties of antibodies, and how these may affect the performance of recycling antibodies.

This manuscript is still in preparation.

# Discovery, engineering, and characterization of recycling antibodies targeting snake toxins

Tulika Tulika[1], Fulgencio Ruso-Julve[2,3], Shirin Ahmadi[1], Anne Ljungars[1], Jack Wade[1], Markus-Frederik Bohn[1], Christoffer V. Sørensen[1], Line Ledsgaard[1], Bjørn G. Voldborg[1], Bruno Lomonte[4], Jan Terje Andersen[2,3]*, Andreas H. Laustsen[1]*

[1]Department of Biotechnology and Biomedicine, Technical University of Denmark, Lyngby, Denmark

[2]Department of Immunology, Oslo University Hospital Rikshospitalet, Oslo, Norway

[3]Department of Pharmacology, Institute of Clinical Medicine, University of Oslo, Oslo, Norway

[4]Instituto Clodomiro Picado, Facultad de Microbiologia, Universidad de Costa Rica, San Jose, Costa Rica

*Correspondence: Andreas H. Laustsen, ahola@bio.dtu.dk
Jan Terje Andersen, j.t.andersen@medisin.uio.no

**Abstract**

Recycling or pH-dependent antigen-binding antibodies release antigens in the endosomes for degradation and are recycled back into circulation via the FcRn-mediated pathway as free antibodies. As a result, recycling antibodies can bind and eliminate multiple antigens in their lifetime, which enables them to achieve therapeutic efficacy at a lower dose or dosing frequency than non-recycling antibodies. The most common strategy to engineer pH-dependent antigen-binding properties in the antibody is based on the incorporation of histidines in the antibody variable regions. However, using such strategies may introduce sequence liabilities as they involve incorporation of mutations in the antibody. In this study, we present light-chain shuffling based on natural antibody domains coupled to phage display selections as a strategy to increase the pH-dependent antigen-binding properties of pre-existing antibodies targeting snake venom toxins, myotoxin II (M-II), or α-cobratoxin (α-cbtx). The discovered clones were screened for pH-dependent off-rates and further assessed in a cellular assay, resulting in the identification of an M-II- and an α-cbtx-targeting pH-dependent antibody that recycled as free antibodies in the presence of their cognate antigens. Additionally, the study revealed that the cellular transport properties of the antibodies varied depending on the antibody variable region and antigen-binding, which can in turn affect the performance of the recycling antibodies. Thus, the study provides methodologies and findings that can be applied in the future discovery and engineering of recycling antibodies.

**Key words:** Recycling antibody, pH-dependent antigen-binding, light-chain shuffling, phage display technology, FcRn, HERA, Fab region, α-cobratoxin, myotoxin II, snake venom

## Introduction

Monoclonal antibodies (mAbs) are used as therapeutic agents to treat a variety of diseases because of their ability to target antigens with high specificity and affinity[1–3]. In addition, the most used format is built on immunoglobulin G1 (IgG1)[2,4], which has a plasma half-life of three weeks on average in humans due to pH-dependent binding between its fragment crystallizable (Fc) region and the neonatal Fc receptor (FcRn)[5–7]. Briefly, IgG in the bloodstream is taken up by cells via fluid-phase pinocytosis followed by entering of endosomes where the mildly acidic pH facilitates engagement of FcRn. The FcRn-IgG complex is then recycled back to the cell surface where exposure to the near-neutral pH of the extracellular environment triggers release of IgG from the receptor. As such, FcRn rescues IgG from lysosomal degradation in a strictly pH dependent manner, which explains its long half-life[8–11]. Insight into this biology has resulted in Fc-engineering strategies allowing for more favorable engagement of human FcRn translating into extended plasma half-life in human FcRn transgenic mice, non-human primates and humans[6,12–15]. One such Fc technology is based on three amino acid substitutions, M252Y/S254T/T256E: YTE, that improve FcRn binding at acidic pH without disrupting pH-dependency, which, impressively, has shown to extend half-life by 4-fold in non-human primates[6,14,16]. In addition, biophysical properties of the variable regions of the antigen-binding fragment (Fab) arms, such as surface charge patches and the isoelectric point (pI), can modulate plasma half-life in both an FcRn-dependent and independent manner[17,18]. Thus, to tailor IgGs for optimal pharmacokinetics there is a need to gain an in-depth understanding on how such factors affect cellular uptake and FcRn-mediated transport both in the absence and presence of cognate antigen.

Most IgGs bind their cognate antigen throughout the endosomal pH gradient. This means that IgG-antigen complexes remain intact in the acidified endosomes resulting in lysosomal degradation of complexes, or recycling of the IgG-antigen complex back to the cell surface membrane via FcRn when the antigen is soluble, followed by exocytosis and release[19]. In the latter scenario, the antigen continues to occupy the binding sites of the IgG upon recycling[20]. Thus, in both cases, an IgG can only bind antigen once per binding site, which means that high doses of IgGs are needed when many antigen molecules are to be bound[20]. To overcome this challenge, antigen-binding can be engineered such that high affinity is kept at near neutral pH while binding becomes weaker when approaching the acidic environment of endosomes[12,19–27]. Consequently, this allows the antigen to be released in the acidic endosomes followed by lysosomal degradation while IgG is recycled back to the circulation through the FcRn-mediated pathway, ready to bind new antigen molecules[20,21]. Thus, the same IgG molecule can be used multiple times to direct antigens for degradation. This strategy has been demonstrated to be effective in targeting of over-produced disease-driven endogenous antigens[12,19–29] at lower doses and/or more infrequent dosing intervals compared to their non-pH-dependent IgG counterparts[12,20,26]. Such pH-dependent antigen-binding IgGs (also known as recycling antibodies) are attractive when frequent dosing and/or high doses are required, which may also lead to lower costs, ideal for treatment of for instance chronic diseases, infectious diseases[30] and snakebite envenoming[31,32].

The most common approach employed to engineer pH-dependent antigen-binding antibodies is by incorporating histidine residues into the antibody variable domains[12,19,20,22,24]. The rationale is based on the fact that histidine has a $pK_a$ ~ 6.0, which enables its protonation at pH 6.0 and below, thereby potentially weakening the antibody-antigen interaction in acidified endosomes[33,34]. However, such histidine engineering must be tailored to not negatively affect binding to the antigen at neutral pH[24]. Additionally, introducing mutations may give rise to immunogenicity and developability risks[35–37]. However, the use of *in vitro* display technology based on naïve human antibody library has been demonstrated to circumvent this challenge by giving rise to a pH-dependent antigen-binding antibody entirely devoid of histidines[32].

In this study, we present a light-chain shuffling strategy that utilizes naturally occurring variable domain sequences to generate pH-dependent antigen-binding antibodies. We demonstrate the utility of this approach by increasing pH-dependent antigen-binding properties of existing antibodies targeting two snake venom toxins, α-cobratoxin (α-cbtx) from *Naja kaouthia* (monocled cobra from Southeast Asia) and myotoxin II (M-II) from *Bothrops asper* (Fer-de-Lance from Central America). Specifically, α-cbtx blocks nicotinic acetylcholine receptors (nAChRs) in synaptic clefts and disrupts neuromuscular transmission resulting in paralysis[38], while M-II is a phospholipase $A_2$ ($PLA_2$)-like protein that damages cell membranes, leading to severe tissue damage that often requires amputation[39,40]. Using human endothelial cell-based recycling assay (HERA), we found that these antibodies bound human FcRn (hFcRn) in a pH-dependent manner and were rescued from intracellular degradation, which could be enhanced by the YTE technology. Importantly, in the presence of antigen, the pH-dependent antigen-binding antibodies were recycled as free antibodies, while the non-pH-dependent antibodies were recycled in complex with their cognate antigen. However, distinct differences in the cellular transport properties of the antibodies were observed in the presence of the two different antigens. While the antibodies' cellular uptake, recycling, and accumulation were either reduced or not affected upon α-cbtx binding, these cellular parameters were enhanced for antibodies bound to M-II. This demonstrates a clear effect of antigen-binding on the cellular handling of the antibodies which can potentially affect the performance of the recycling antibodies.

## Methods

### Purification of myotoxin II

M-II (Uniprot P24605) was purified from the venom of *B. asper* by cation-exchange chromatography on CM-Sephadex C25, followed by reverse-phase HPLC on C18, as described previously[39].

### Biotinylation of toxin

Purified M-II and α-cbtx (Latoxan, France) was dissolved in 1 X standard phosphate buffered saline (PBS) and biotinylated using a 1:1.25 ) toxin to biotin molar ratio as

previously described[41]. The biotinylated toxins were purified using buffer exchange columns (Vivacon 500, Sartorius, 3000 Da Molecular Weight Cut-Off) using the manufacturer's protocol. Protein concentration was determined using the toxin's extinction coefficient and absorbance measurement with a NanoDrop One instrument.

**Light-chain shuffling**

Light-chain shuffling of scFvs TPL0197_01_C08 and TPL0039_05_B04 was carried out as previously described[42], except that pIONTAS1[43] vectors containing naïve lambda variable light ($V_L$) chain libraries were used. Briefly, the variable heavy (VH) regions of scFvs TPL0197_01_C08, TPL0039_05_B04, and TPL0039_05_B12 were PCR amplified from the pSANG10-3F plasmid with pSANG10 PelB FWD (CGCTGCCCAGCCGGCCATGG) and HLINK3 REV (CTGAACCGCCTCCACCACTCGA) primers using Platinum™ SuperFi II Green PCR Master Mix (Invitrogen). The PCR products were digested with NcoI and XhoI restriction endonucleases at 37$^o$C for 3 hours and purified using GeneJET PCR Purification Kit (Thermo Scientific) as per manufacturer's protocol. 160ng of restricted and purified product was ligated into 400ng pIONTAS1 vectors containing naïve variable light (VL) lambda and kappa chain libraries at 16$^o$C for 16 hours, followed by purification of ligation product using MinElute PCR Purification Kit (Qiagen). Electrocompetent TG1 cells (Lucigen) were thawed on ice and transformed with the purified ligation product, followed by immediate addition of 6 mL of recovery media (Lucigen), and incubated at 37$^o$C for 1 hour at 280 rpm shaking. Transformed cells were plated on 2TY agar plates supplemented with 2% glucose and 100 µg/mL ampicillin. Dilutions of cells were also plated to determine the library size, which was found to be 6.8 x $10^7$ for TPL0197_01_C08, 3.1 x $10^7$ for TPL0039_05_B04, and 3.6 x $10^7$ for TPL0039_05_B12, with more than 92% of the transformants being positive for insertion of heavy chain insert, as determined by colony PCR.

**Library rescue and solution-based phage display selection**

Phage rescue from the chain-shuffled libraries, deselection of streptavidin-specific phages, and three rounds of phage display selections were performed as described previously[42] with a few exceptions. To enrich for antibodies that bind the antigens in a pH-dependent manner, all three rounds of selections were started with the deselection of phages that bound the antigen at pH 5.5. To do this, phages were incubated with biotinylated antigen for 30 min in 3% milk PBS pH 5.5, followed by the addition of Dynabeads (Invitrogen, M-280) for 15 min to capture the biotinylated antigen-bound phage complexes that were formed at pH 5.5. The mix was then placed on a magnetic rack, whereupon Dynabeads (with the captured antigen-phage complex at its surface were separated and discarded, while the solution containing unbound phages (that did not bind the antigen at low pH) was collected. The pH of this unbound phage-containing solution (3% milk PBS) was adjusted to pH 7.4 using 1M Tris (pH 8.0). These phages, now in a neutral pH solution were employed for selection, where they were allowed to bind biotinylated antigen[42], followed by elution of the bound

phages using PBS at pH 5.5 for 15 min (Fig 1(a)). The eluted phages were trypsinated to ensure successful infection of the bacterial cells[44]. The concentrations of the α-cbtx and M-II during the deselection (antigen-binding at pH 5.5) and selection step ( antigen-binding at pH 7.4) in all three rounds were 10 nM and 1 nM, respectively.

**Primary assessment of polyclonal phage outputs (phage ELISA)**

The phage outputs from the second and third selection rounds were evaluated for antigen-binding. Phage ELISA was performed to assess the binding of selected phages to the corresponding biotinylated toxin (10 µg/mL) indirectly immobilized on streptavidin-coated MaxiSorp plates. For binding detection, a 1:2000 dilution of Anti-M13-HRP antibody (Sino Biological) and TMB (Thermo Scientific) were used according to the manufacturer's protocol.

**Sub-cloning, screening of scFvs, and sequencing**

Sub-cloning of scFv genes from the third round of phage output into the pSANG10-3F expression vector and primary screening was performed as previously described[41]. From each of the selection outputs, 184 colonies were picked, expressed in 96 well formats, and assessed for binding to 10 nM of their respective toxins in an expression normalized capture dissociation-enhanced lanthanide fluorescence immunoassay (ENC DELFIA) as described earlier[41]. Clones showing a binding signal 10 times above the background (10,000 RU) were designated as binding clones.

**Reformatting and production Fabs and IgG1s**

The reformatting of the scFvs to Fabs and IgG1s and their production was performed as described previously[32], except that the expression vectors containing human lambda light chain were used, and some IgG1s were also produced with WT Fc.

**Bio-layer interferometry (BLI) off-rate screening of Fab from crude expression media**

BLI experiments were performed on an OctetRed 96 system (ForteBio). Streptavidin (SAX) biosensors (Sartorius) were blocked for at least 10 min in 1 x Kinetics Buffer (PBS with 0.05% Tween-20 and 0.1% BSA, Forte Bio) before the assay. The screening assay was performed by loading biotinylated α-cbtx or M-II toxin (1 µg/mL) on SAX biosensors, followed by transferring the loaded biosensors into Fab-containing expression media for a 300 s. Dissociation was performed in 1x HEPES-MES, buffered to either pH 7.4 or pH 5.5, for 300 s. The biosensors were regenerated at the end of each cycle by iteratively dipping them into 10 mM Glycine pH 2.0 and 1 x KB (5 cycles, of 10 s). The experiment was performed at 25°C with shaking at 1000 rpm. ForteBio's data analysis software (12.2.2.4) was to fit the curves using a 1:1 binding model to obtain dissociation rates for pH 7.4 and 5.5 (local fitting model).

**Off-rates of purified Fabs over a range of pH values using BLI**

The off-rates of the purified Fabs over a range of pH values were obtained as described in 2.6, with a few variations. For association 700 nM of Fab was prepared in HEPES-MES buffer at pH 7.4. The association and dissociation steps were carried out for 180 s and 600 s respectively. A total of 8 association-dissociation rounds were performed, where in each round, association conditions were kept the same, while the pH of the dissociation buffer (HEPES-MES) was changed. The pH values of the HEPES-MES buffer used for dissociation from round 1 to round 8 were 7.4, 6.5, 6.0, 5.5, 5.0, 4.5, 4.0, and 3.5. The tips were regenerated 10 mM Glycine pH 2.0 for 10 s X 7 cycles in between the rounds. ForteBio's data analysis software (12.2.2.4) was used to fit the curves using a 1:1 binding model to obtain dissociation rates at the different pH values (local fitting model). The off-rates of IgGs at pH 7.4 and 5.5 were determined are described above except that 10 nM of the IgGs was used for association.

**Kinetics measurements of Fabs and IgGs using BLI**

The KD of the Fabs at pH 7.4 and 5.4 were determined as described in 2.6, except that purified Fabs were used for association at 3–250 nM in a 2-fold dilution. Both association and dissociation steps were performed in HEPES-MES buffer pH 7.4 for 300 s and 600 s respectively. ForteBio's data analysis software (12.2.2.4) was used to fit the curves using 1:1 binding model to obtain the kinetic measurements (global fitting model).

**IgG-hFcRn binding ELISA**

ELISA was performed to determine the pH-dependent binding between IgGs and hFcRn as described previously[45]. Briefly, ELISA plates were coated with 100 µL of serially diluted IgGs (1000-0.488 ng/mL) in PBS, overnight at 4 °C. Next, the plates were blocked with 250 µL of PBS supplemented with 4% (w/v) skimmed milk (Sigma-Aldrich) and incubated for 1 hour on a shaker at room temperature. Plates were washed 4 times with 200 µL PBS containing 0.05% Tween20 (T) (Sigma-Aldrich) (PBS-T) between all subsequent steps. Biotinylated truncated monomeric hFcRn (hFcRn-bio) (Immunitrack) was incubated with alkaline phosphatase-conjugated streptavidin (AP) (Roche) at a 1:1 molar ratio for 20 minutes and added to the plates at final concentrations of 0.25 ug/mL FcRn-bio and 3.36 µg/mL streptavidin-AP diluted in milk PBS-T (pH 5.5 or 7.4) for 1 hour. The ELISA signal was developed by adding 100 µL of 10 µg/mL p-nitrophenyl-phosphate substrate (Sigma-Aldrich) dissolved in diethanolamine solution to all wells. A Sunrise spectrophotometer (Tecan) was used to measure absorbance at 405 nm.

**Preincubation of the IgGs with cognate antigens**

For the experiments involving incubation of the IgGs with cognate antigen, preincubation was done by adding the specified ratios of antigen and IgG in a volume of 20 µL of the appropriate buffer, mixing thoroughly, and incubating at RT for 20 min before experiment

initiation. Where the injection of such samples is specified, the injection, preincubation, and running buffers were all the same.

### Analytical hFcRn affinity chromatography

Analytical hFcRn affinity chromatography was performed to quantify the hFcRn binding of the antibodies across a pH gradient using an ÄKTA Avant25 instrument (GE Healthcare), as described previously[18,46]. Briefly, 77 µL of a 1 mg/mL IgG solution was injected into an FcRn-coupled resin column (Roche) in a pH 5.5 buffer (20 mM MES, 140 mM NaCl; Sigma-Aldrich), and eluted by a linear gradient to pH 8.8 (20 mM Tris-HCl, 140 mM NaCl; Sigma-Aldrich) throughout 110 min. For the immune complex (IC) studies, IgG (1 mg/mL) and its cognate antigen (M-II or α-cbtx) were preincubated at a 1:2 molar ratio, in 20 mM MES, 140 mM NaCl buffer, before dilution into the specified injection volume and column application. pH elution values were determined by a pH detector (GE Healthcare).

### Human endothelial cell line stably overexpressing hFcRn

HMEC-1 cells stably expressing HA-FcRn-EGFP (HMEC-1-FcRn)[47] were cultured at 37°C and 8% CO2 in MCDB131 medium (Gibco) supplemented with 2 mM L-glutamine (Sigma), 25 µg/mL streptomycin/25 U/mL penicillin (Sigma-Aldrich), 10% FCS (Sigma-Aldrich), 10 ng/mL mouse epidermal growth factor (Gibco), 1 µg/mL hydrocortisone (Sigma-Aldrich), and 100 µg/mL G418 (Gibco) and 50 µg/mL blasticidin (Gibco) to maintain FcRn expression.

### Human endothelial cell-based recycling assay (HERA)

HERA experiments were performed to quantify the amount of IgG taken up, recycled, and retained in endothelial cells, as described elsewhere[46]. Briefly, 1.5 x 105 HMEC-1-FcRn cells were seeded in 250 µL of culturing medium per well in two 48-well plates (Costar) (Uptake and Recycling plate). 20-24 hours after seeding, the medium was removed from all wells, and the cells were washed twice in 250 µL of pre-warmed Hank's balanced salt solution (HBSS; ThermoFisher). Cells were starved at 37 °C for 1 hour in pre-warmed HBSS. Next, IgGs were prepared at a final concentration of 800 nM in pre-warmed HBSS and added to cells at a final volume of 125 µL in technical triplicates in both plates.

For the studies of the IgGs in the presence of cognate antigen, HERA experiments were performed to quantify the amounts of IC recycled in the endothelial cells, as described previously[17] with some modifications. Antibodies were prepared at a final concentration of 800 nM in HBSS either alone or following preincubation with a two-fold molar excess of their cognate biotinylated-Ag, then added to the cells at a final volume of 125 µL in technical triplicates in both plates. After a 3-hour incubation period, the samples were removed, and the cells were washed four times in 250 µL ice-cold HBSS. Uptake plates were frozen at -80°C following aspiration of washing medium, while 220 µL of pre-warmed serum-free growth medium supplemented with 1X MEM non-essential amino

acids (Gibco) were added to the recycling plates. After another 3-hour incubation period, recycling samples were harvested and frozen at -20°C. Residual plates were washed four times with ice-cold HBSS and frozen at -80°C on the day of analysis. Frozen cells were lysed by adding 220 µL RIPA buffer (ThermoFisher) supplemented with 1X complete protease inhibitor cocktail (Roche) and incubated on a shaker for 10 minutes on ice. Cellular debris was removed by 5 min centrifugation at 10,000 xg.

For IgG-detecting HERA, proteins present in the lysates and recycling medium were quantified by two-way anti-Fc ELISA. 96-well plates (Costar) were coated with anti-hIgG Fc (Sigma) diluted 1:1000 in PBS and incubated overnight at 4°C. The next day, plates were blocked by adding 250 µL of milk PBS-T and washed four times with PBS-T. Next, cell lysates (containing uptake and residual) and medium (containing recycled proteins) were added to the plates, in addition to serial dilutions from 350-0.122 ng/mL of the proteins tested diluted in PBST-M, which were used as standards to quantify protein levels. Following a 1.5-hour incubation period at room temperature, a goat anti-human Fc polyclonal antibody conjugated to alkaline phosphatase (Sigma-Aldrich) diluted 1:5000 in milk PBST was added and incubated for 1 hour at room temperature. The ELISA was developed, and absorbance was measured as indicated above.

For IC-detecting HERA, plates were coated with 10 ug/mL streptavidin in PBS overnight at 4°C. Plates were blocked with milk PBST and washed with PBST. Cell lysates and recycled proteins containing medium were added to the plates, in addition to serial dilutions of the ICs (as standards) as described above. After 1-hour incubation, bound proteins were detected by adding goat anti-human Fc polyclonal antibody conjugated to alkaline phosphatase (Sigma-Aldrich) diluted in PBST-S. The ELISA was developed, and absorbance was measured as indicated above.

HERA experiments were independent and numerical data were summarized as the mean ± SD using GraphPad Prism9 software (San Diego, CA). For the IC-detecting HERA, values were relative to the uptake values of each protein. Each global mean was compared using an unpaired Student's t-test. Two-tailed p-values $\leq 0.05$ were considered statistically significant.

**Analytical size-exclusion chromatography (SEC)**

Analytical SEC was performed using a Superdex 75 10/300 column coupled to an Äkta FPLC instrument (Cytvia). 10 µg of IgGs were injected 10 µL in PBS (Gibco). For studies of complex formation, 10 µg of IgGs were preincubated with the specified molar ratios of their cognate antigens in an end volume of 10 µl in PBS for 20-30 min at RT prior to injection.

**Sequence based net protein charge calculation**

Sequence based net charge of proteins at different pH values were calculated using the Emboss iep calculator (http://www.bioinformatics.nl/cgi-bin/emboss/iep?_pref_hide_optional=0). All cysteines were assumed to form disulfide

bridges. Whole Fvs were defined as the combined variable heavy chain (HC) and variable light chain (LC) sequences. Remaining residues were defined as the framework after removing CDRs and were assumed to have one N-terminal residue. CDRs were not assumed to have any terminal residues.

## Results

### Selection of pH-dependent antigen-binding antibodies by light-chain shuffling

Previously, four fully human IgG1 mAbs specifical to M-II were discovered using phage display technology, with a selection strategy that involved binding of M13 phages to M-II at pH 7.4, and elution of bound phages at pH 6.0[48]. To study if binding of these IgG1s to M-II was sensitive to pH alteration, BLI measurements were performed by adding the IgG1s to biotinylated M-II captured on streptavidin-coated biosensors at pH 7.4, followed by dissociation at either pH 7.4 or 5.5 (Table 1). The result revealed that two of the IgG1s, TPL0039_05_A03 (referred to as A03) and TPL0039_05_E02 were not pH-dependent, while TPL0039_05_B04 and TPL0039_05_B12 (referred to as B04 and B12) demonstrated a 5.8- and 650-fold faster off-rate at pH 5.5 than pH 7.4, although the off-rate of B12 was still in the order of $10^{-5}$ $s^{-1}$.

To investigate if chain shuffling can be used to engineer antibodies to exhibit more pronounced pH-dependent antigen-binding, B04 and B12 were employed to generate light-chain shuffled single-chain variable fragment (scFv) phage display libraries based on fusion of the scFvs to pIII on the M13 phage[43]. This yielded libraries with a clonal diversity of 6.8 x $10^7$ and 3.6 x $10^7$ for B04 and B12, respectively. With the same objective, a previously discovered anti-α-cbtx IgG1, TPL0197_01_C08[32] (referred to as C08), that was selected by phage display selection for pH-dependent antigen-binding, and showed an 8-fold faster off-rate at pH 5.5 than at neutral pH[32], was also light-chain shuffled. The clonal diversity of the C08 library was determined to be 3.1 x $10^7$.

**Table 1: Affinities and off-rates of anti-M-II IgG1 variants.**

| IgG | $K_D$ at pH 7.4 (pM)[48] | $k_{off}$ ($s^{-1}$) | | $k_{off}$ fold difference (pH 5.5/7.4) |
|---|---|---|---|---|
| | | pH 7.4 | pH 5.5 | |
| **TPL0039_05_A03** | < 1 | < 1.0 x$10^{-07}$ | < 1.0 x$10^{-07}$ | ND |
| **TPL0039_05_B04** | 75 | 6.5 x$10^{-05}$ | 3.8 x$10^{-04}$ | 5.8 |
| **TPL0039_05_B12** | < 1 | < 1.0 x$10^{-07}$ | 6.5 x$10^{-05}$ | 650 |
| **TPL0039_05_E02** | < 1 | < 1.0 x$10^{-07}$ | < 1.0 x$10^{-07}$ | ND |

Binding constants ($K_D$) of anti-M-II IgG1s at pH 7.4, their off-rates ($k_{off}$) at pH 7.4 and 5.5, and the fold difference between the off-rates at the two pH values. A $k_{off}$ of < 1.0 x $10^{-7}$ $s^{-1}$ implies that the IgG did not show any dissociation from M-II in the observed dissociation period. ND stands for not determined.

To select for scFvs with improved pH-dependent antigen-binding properties, the C08 library was panned against α-cbtx, and the B04 and B12 libraries against M-II. This

was done by performing three consecutive rounds of selection in solution, where each cycle started with a deselection step where phages and biotinylated antigens were incubated at low pH (~pH 5.5), followed by removal of the phages that bound the biotinylated antigens at low pH using streptavidin magnetic beads. The unbound phages were then employed for binding biotinylated antigen at pH 7.4, captured on streptavidin beads, and eluted using a low pH buffer (Fig 1 (a)). An ELISA was then used to assess the polyclonal phage outputs, which indicated enrichment of scFvs specific for the antigen, while negligible binding to the negative control (streptavidin) was detected (Fig S1(a-c)). The scFv gene sequences from the third selection round from each library were amplified by PCR, subcloned into the bacterial expression vector PSANG10-3F in frame of a gene segment encoding a FLAG-tag. 184 clones from each library were expressed as soluble FLAG-tagged scFvs in *E.coli.* As the expression levels between clones may vary, a normalized capture DELFIA was used to allow ranking based on binding affinity at pH 7.4. This was done by capturing the expressed FLAG-tagged scFvs on a limiting concentration of coated anti-FLAG antibody, followed by addition of biotinylated antigen to confirm scFv binding. Binders were defined by signals above a threshold value of 10,000 (10 times above the background). From the C08 library, 23 scFvs were shown to bind α-cbtx, while the numbers of M-II binders were 52 and 104 for the B04 and B12 libraries, respectively (Fig S1(d-f)). Subsequently, 10 α-cbtx-binding clones from the B02 library, and 33 and 49 M-II binding clones from the B04 and B12 libraries were sequenced. This resulted in identification of 1 unique α-cbtx-binding scFv, and 12 and 20 unique M-II-binding clones from B04 and B12 library, respectively.

Next, the variable heavy and light chains from the scFv clones were reformatted to Fabs by subcloning the corresponding gene sequences into in a combi-expression vector encoding both the lambda light chain and constant domain of the human IgG1 heavy chain in frame with a His-tag. CHO cells were transiently transfected with the generated expression vectors followed by harvesting of supernatants that were used in for BLI measurements. An off-rate screening against the toxins, was performed at both pH 7.4 and 5.5 as above. Surprisingly, the α-cbtx-targeting Fab, TPL0544_01_B01 (referred to as B01), showed a similar off-rate at both pH conditions (Fig 1(b)), while the M-II targeting Fab, TPL0552_02_A05 (referred to as A05) from the B04 library, showed a faster off-rate at pH 5.5 than pH 7.4 (Fig 1(c)). The binding of all other Fabs from the B04 and B12 libraries to M-II were found not be affected by pH alteration.

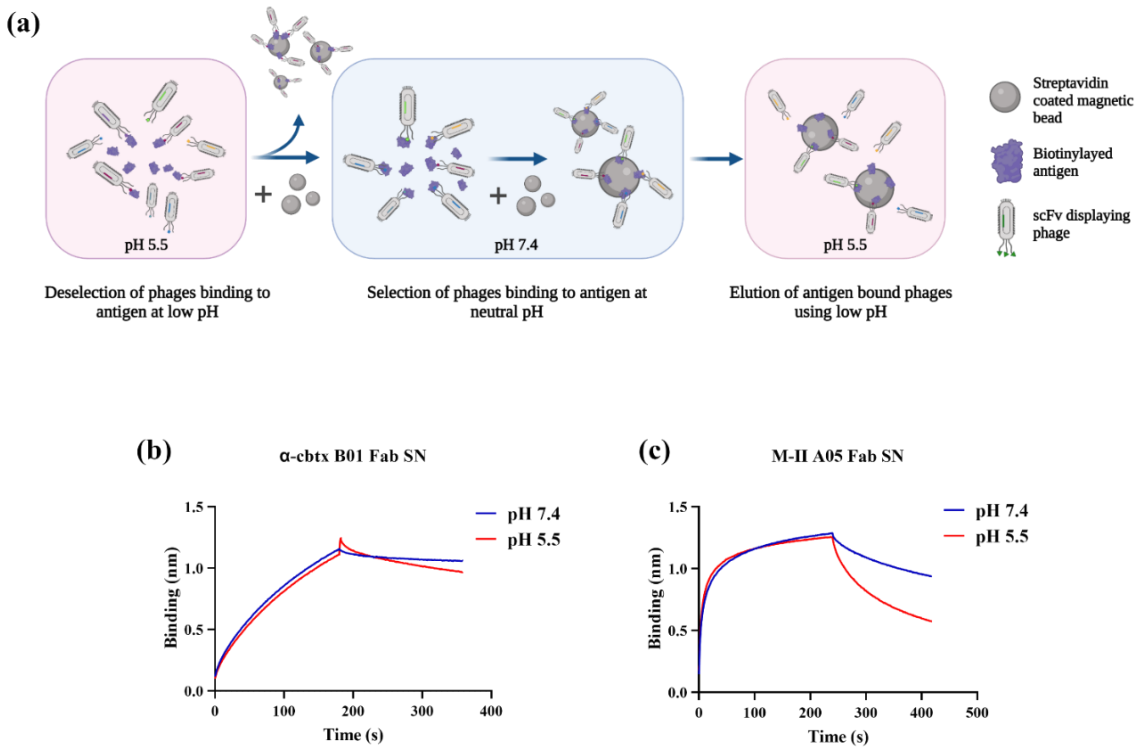


**Figure 1: Phage display selection strategy and BLI sensograms of crude Fab supernatants.** **(a)** Schematic diagram of the strategy employed during the phage display selection campaigns to select scFvs with pH-dependent antigen-binding properties. scFv-displaying phages were incubated with biotinylated antigen at pH 5.5, followed by capturing and removal of phages that bound the antigen at low pH using streptavidin coated magnetic beads. The unbound phages were then used to bind biotinylated antigen at pH 7.4, whereupon the bound phages were eluted using a pH 5.5 buffer. BLI sensograms of crude Fab samples from CHO cell expression medium supernatant of **(b)** TPL0544_01_B01 and **(c)** TPL0552_02_A05 showing binding to α-cbtx and M-II, respectively, at pH 7.4, followed by dissociation at pH 7.4 or 5.5. (SN = supernatant)

## Off-rate screening of Fabs over a pH gradient confirms pH-dependent antigen-binding of A05

To further investigate the pH-dependency of B01 and A05, we screened their off-rates across a broad pH range, from 7.5 to 3.5. Here, purified Fab fractions isolated by capturing on a Ni column via their His-tags (fused to the C-terminal of heavy chain) were used. For comparison, the parental Fabs C08 and B04, and an anti-M-II A03 Fab binding equally well at both 5.4 and 7.4 (Table 1) were included. Additionally, previously discovered α-cbtx targeting Fabs A01[49,50] and D11[49,50] were included as positive and negative control for pH-dependent binding respectively. As expected, the off-rate of all Fabs from the toxin-loaded biosensor increased with decreasing pH (Fig 2, Supplementary table 1). While Fab A01 and the parent Fab C08 showed increasing off-rates at pH 5.5 compared to pH 7.4 (Fig 2 (a-b), (g)), a drastically faster dissociation was measured for the light-chain shuffled Fab B01 at pH 4.5 and below (Fig 2(c), (g)). In comparison, Fab D11 showed slower off-rates over the pH range compared with the other Fabs (Fig 2 (d), (g)). In the case of M-II, the light-chain shuffled Fab A05 showed faster off-rates with decreasing pH than the parent

Fab B04 (Fig 2 (e-f)). In comparison, Fab A03 showed a slower off-rate at pH 7.4, with a pH-dependent off-rate profile that was very similar to the α-cbtx-targeting Fab B01 (Fig 2 (g-h)). Additionally, the affinities of the Fabs were also measured at pH 7.4 (Supplementary table 2).

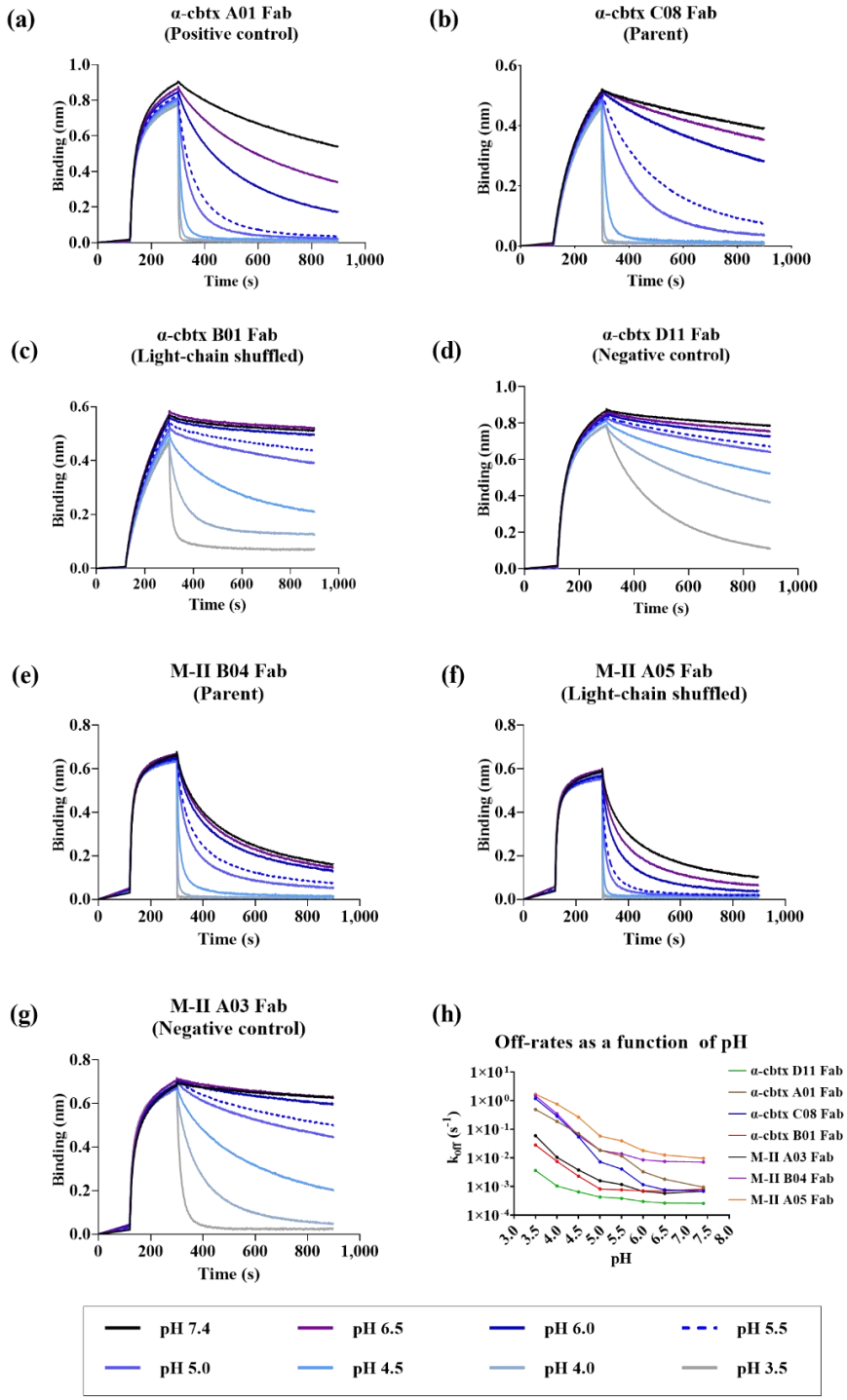


**Figure 2**: **BLI sensograms of Fabs showing their off-rate over a range of pHs (3.5–7.4).** Off-rate curves of α-cbtx targeting: **(a)** Fab A01 that is included as a positive control for pH-dependent antigen-binding antibody, **(b)** parental Fab C08, **(c)** light-chain shuffled Fab B01, and **(d)** Fab D11 that is included as a non-pH-dependent binding control for α-cbtx. Off-rate curves of M-II targeting: **(e)** parental Fab B04, **(f)** light-chain shuffled Fab A05, and **(g)** Fab A03 that is included as a non-

pH-dependent binding control for M-II. The off-rated of the Fabs are carried out at pH 3.5, 4.0, 4.5, 5.0, 5.5, 6.0, 6.5, and 7.4. The negative controls mean that the Fabs showed similar off-rates at pH 5.5 and 7.4. The legend for graphs (a) to (g) is provided at the bottom of the figure. **(f)** pH versus off-rate ($k_{off}$) plot of the assessed Fabs.

### Sequence analysis reveals presence of a histidine residue in the variable light chain of A05 and B01

To compare the variable sequence differences between the light-chain shuffled A05 and B01 and corresponding parental clones B04 and C08, respectively, sequence alignments were made. The results revealed that A05 had gained 6 amino acid changes compared to the parent B04 where a tyrosine residue in the light chain complementarity determining region 3 (CDRL3) of B04 was replaced with a histidine in A05 (Fig S2(a)), which may explain its pH-dependent antigen-bidning. In the case of B01, that showed similar off-rates at pH 5.5 and 7.4, the sequence analysis revealed 66 amino acid changes compared to the parent C08, where an asparagine residue in the framework region 2 was replaced with a histidine (Fig S2(b)). This change of several residues in the light chain sequence of B01 may be the reason behind its slower off-rate at low pH than the parent C08.

### Fc-engineering enhanced the interaction between IgG1 and hFcRn

To study the hFcRn binding properties of the antibodies, the Fabs were reformatted and expressed as IgG1 molecules in the CHO cells upon transient transfection of the encoding combi-vectors. All IgG1s were expressed with the YTE amino acid substitutions to address the effect of combining pH-dependent antigen-binding with Fc-engineering for enhanced hFcRn binding. Additionally, D11 and A03 were made with WT Fcs. A list of the designed IgG1 variants is given in Table 2.

To verify that the produced IgG1s exhibited pH-dependent binding to hFcRn, ELISA plates were coated with titrated amounts of the IgG1s followed by adding biotinylated recombinant hFcRn, pre-incubated with streptavidin-conjugated alkaline phosphatase (Fig 3(a)). The results revealed that all IgG1 variants bound hFcRn at pH 5.5 (Fig 3(b), (d)). In contrast, only the YTE-containing variants bound hFcRn at neutral pH (Fig 3(c), (e)).

To mimic pH-dependent Fc and FcRn binding-and-release taking place in the endosomal pathway, we took advantage of an hFcRn-coupled column by injecting the antibodies at pH 5.5 followed by a gradual increase in pH until 8.8[46]. The generated elution profiles revealed that the IgG1-YTE variants were retained for a longer time on the column, and as such, released from the receptor at higher pH than the WT counterparts (Fig 3(f-g) and Table 2). For anti-α-cbtx IgG1s, the four YTE-containing variants were shown to elute at similar pH (7.5) where C08 was released slightly before the other variants (Fig 3(f) and Table 2). More variation in elution profiles was measured for the anti-M-II IgG1-YTE variants, whereA03 was retained on the column the longest (pH 7.7), followed by B04 (pH 7.59), and A05 (H 7.55) (Fig 3(g) and Table 3). Furthermore, a striking difference was detected for the two D11 and A03 WT variants, as anti-M-II A03 was eluted at pH 7.21

compared with pH 6.95 for anti-α-cbtx D11 (Table 3). Thus, variable region differences can modulate the ability of IgG1 antibodies to be released from hFcRn, while Fc engineering for improved receptor engagement can further modulate the ability to be released as a function pH.

**Binding to antigen affects the interaction between Fc and FcRn in different ways**

To investigate the effect of immune complexes on FcRn binding, the stoichiometry for the IgG-antigen complex was determined using size exclusion chromatography (SEC). Formation of complexes at a molar ratio of 1:2 (IgG:antigen) was observed for anti-α-cbtx IgG1s (Fig S3(a-d)). However, clear data for complex formation for IgG1s and M-II could not be obtained, as the chromatogram signals were too low to be distinctly analyzed. Nevertheless, a preincubated mix of IgG1 and the cognate antigen at a 1:2 molar ratio was applied to the column to study the interaction between the immune complex (IC) and hFcRn (Fig 3(h-n)). It was observed that both WT and YTE variants of IgG1 D11 showed earlier elution i.e., at lower pH in the presence of the antigen than IgG1 alone (Fig 3(h)). For IgG1s A01-YTE and C08-YTE, the presence of α-cbtx resulted in low to no change in the retention time, while for B01-YTE a reduced retention time on the column was observed in the presence of α-cbtx (Fig 3(i-k)). In contrast, in the case of anti-M-II IgG1 A03, both WT and YTE variants were retained longer on the column in the presence of M-II, with the A03-YTE being retained the longest and the elution profile containing two peaks (Fig 3(l)). No effect of antigen was observed for IgG1 B04-YTE and A05-YTE (Fig 3(m-n)). In summary, the two antigens, α-cbtx and M-II exhibited distinct effects on the binding between ICs and hFcRn for some IgG1s.

**Table 2: hFcRn-binding capacities of IgG1s and immune complexes**

| Target | Antibody | Fc | Elution peak pH | |
|---|---|---|---|---|
| | | | IgG1 | IC |
| α-cbtx | 2554_01_D11 | WT | 6.95 | 6.84 |
| | 2554_01_D11 | YTE | 7.55 | 7.47 |
| | 2555_01_A01 | YTE | 7.56 | 7.54 |
| | TPL0544_01_B01 | YTE | 7.57 | 7.50 |
| | TPL0197_01_C08 | YTE | 7.53 | 7.51 |
| M-II | TPL0039_05_A03 | WT | 7.21 | 7.30 |
| | TPL0039_05_A03 | YTE | 7.73 | 7.88 |
| | TPL0039_05_B04 | YTE | 7.59 | 7.59 |
| | TPL0552_02_A05 | YTE | 7.55 | 7.55 |

Elution peak pH values from hFcRn chromatography of IgG1s and IgG1s preincubated with their cognate antigen at 1:2 molar ratio. IC: immune complex.

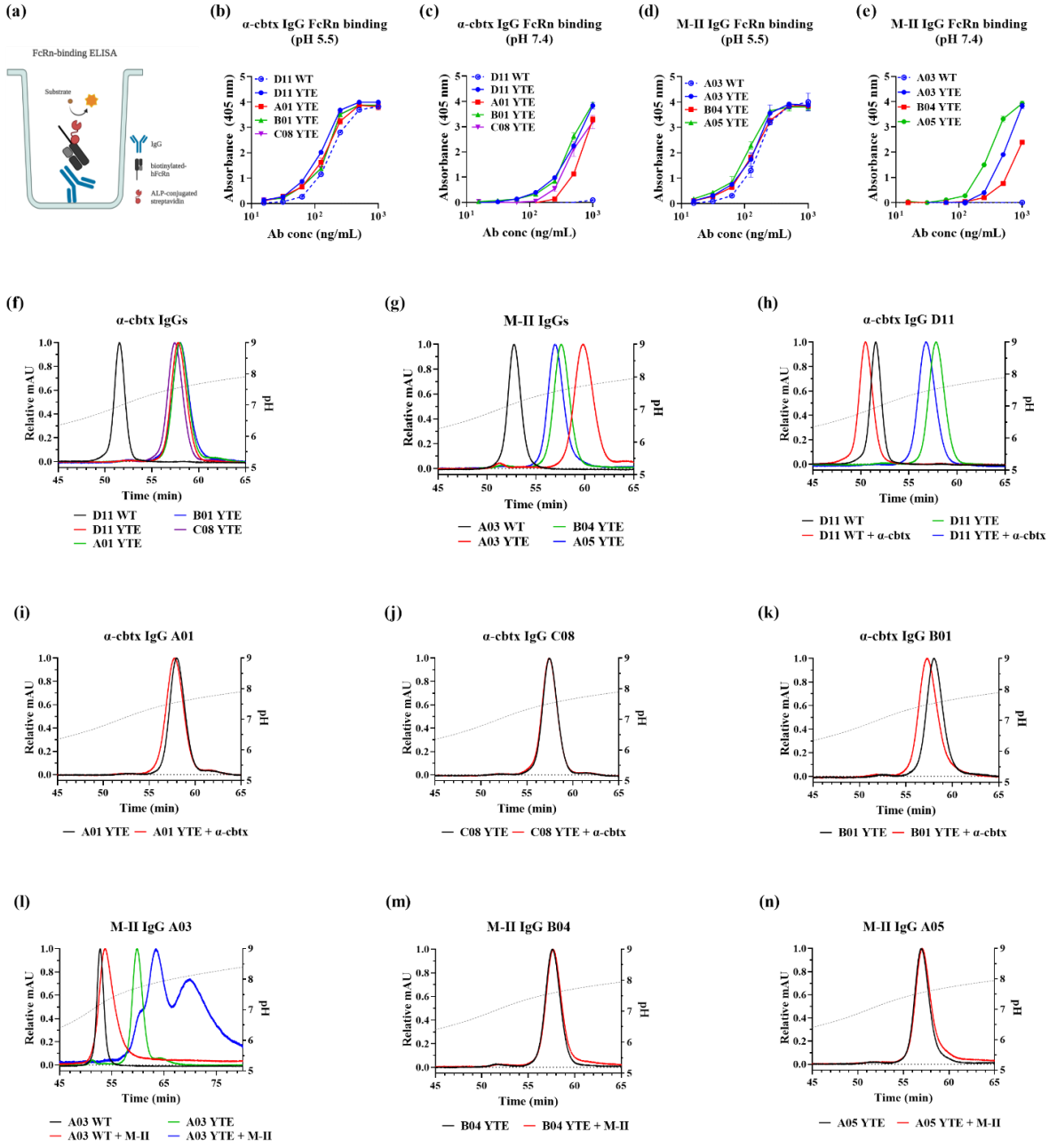


**Figure 3: IgG1-hFcRn interaction studies with ELISA and affinity chromatography.** (**a**) Schematic illustration of the ELISA setup to detect binding between IgG1 and biotinylated hFcRn (bio-hFcRn); created with Biorender. Binding curves to bio-hFcRn of the anti-α-cbtx (**b,c**) and anti-M-II (**d,e**) IgG1s, at pH 5.5 and pH 7.4, where the numbers represent the mean ± SD of duplicates. Elution profiles of the **(f)** anti-α-cbtx and **(g)** anti-M-II IgG1s from hFcRn affinity chromatography are shown as relative absorbance units throughout the pH gradient. Elution profiles from FcRn affinity chromatography of preincubated (**h-k**) IgG1 + α-cbtx and (**l-n**) IgG1 + M-II complex at pH 5.5, shown as relative absorbance units and as a function of pH. The pH is plotted on the right Y-axis (dotted line).

### Sequence-based charge differences in the Fv domains of the antibodies

It has been shown that the Fc-FcRn interaction can be influenced by biophysical properties, such as the net charge of the Fv[17,18,51]. Thus, based on the sequences the net charge of the Fvs, CDRs, and framework regions of the antibodies was calculated as a function of pH (Fig 3). It was observed that all antibodies possessed a net negatively charged Fv between pH 5.5-7.4, except the M-II targeting antibodies A03 and B04 which had a positive net charge at pH 5.5 (Fig 4(a), (d)). Further, the CDRs of all the antibodies had a negative net charge, while their framework regions had a net positive charge, except for the α-cbtx targeting antibody A01, which displayed a net negative charge at pH 5.5 and above (Fig 4(b-c), (e-f)).

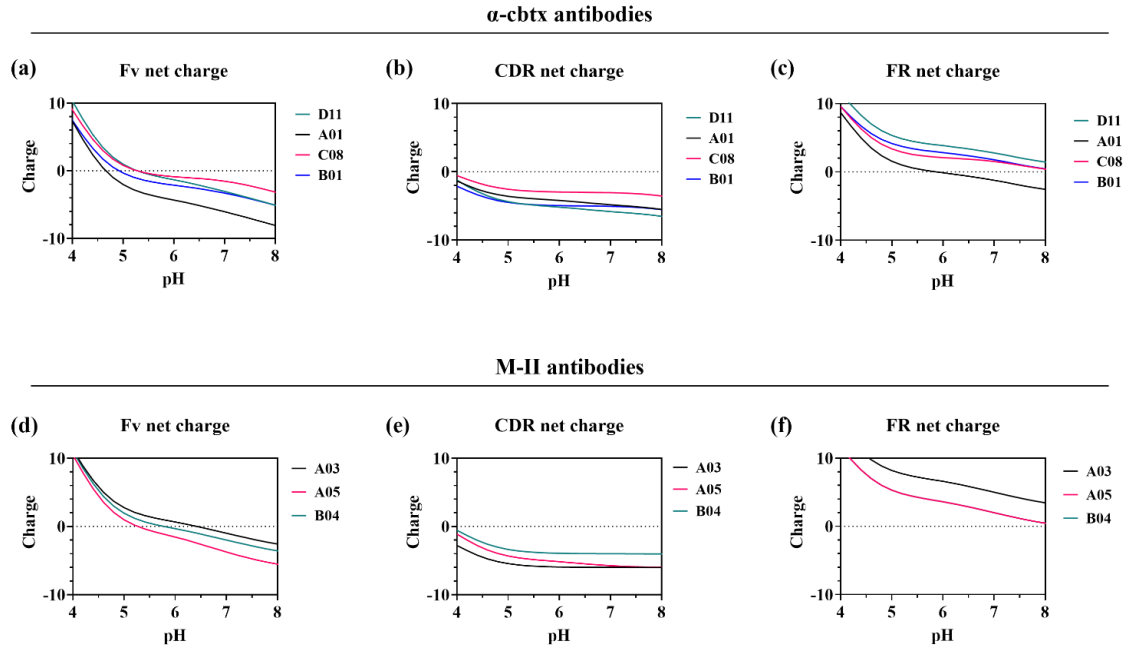


**Figure 4**: Sequence based net charge calculation of **(a)** Fv, **(b)** CDR, and **(c)** FR of α-cbtx targeting antibodies, and **(d)** Fv, **(e)** CDR, and **(f)** FR of M-II targeting antibodies through pH 4.0–8.0. (Fv = antibody variable fragment, CDR = complementarity-determining region, FR = framework region).

### Antigen-binding has distinct effects on the cellular transport properties of IgG1s

To address if the observed IgG1-hFcRn binding in hFcRn-column translated into the rescue of IgG1 from intracellular degradation, IgG1s alone and in complex with their biotinylated cognate antigen were assessed in a human endothelial cell-based recycling assay (HERA). An adherent human endothelial cell line stably overexpressing human hFcRn (HMEC1-hFcRn) was employed for the assay[46]. Equimolar amounts of the IgG1s were added to the cells in parallel with the same IgG1s preincubated with two times molar excess of their cognate biotinylated antigen. After 3-hour incubation, cells were either lysed to assess the amounts taken up or washed and placed in IgG1-depleted growth medium to allow for cell-internalized molecules to be recycled and released into the medium. After a final incubation, the medium was collected, and the cells lysed. To quantify the levels of cellular

uptake, recycling, and accumulation, samples were analyzed in an ELISA to detect the soluble IgG1s using anti-Fc antibodies for both capture and detection. Results showed that the YTE variants of both anti-α-cbtx and anti-M-II IgG1s showed higher uptake and recycling levels than the WT variants (Fig 5(a-b), 5(d-e)) as expected. However, amongst the YTE variants of α-cbtx IgG1s, lower level of recycling was observed for IgG1 C08 (Fig 5(b)). Interestingly, all anti-M-II IgG1s showed lower uptake, recycling, and residual amount than the anti-a-cbtx IgG1s.

When the IgG1s were studied in the presence of antigen, two distinct effects of α-cbtx were observed on the cellular handling of anti-α-cbtx IgG1s. It was found that when bound to α-cbtx, both YTE and WT variants of D11 and A01-YTE, showed reduced uptake, recycling, and residual amounts compared to IgG1 alone. As such, a 2-fold decrease in uptake and recycling was observed for D11-YTE, while for A01-YTE these processes were lowered by 2- and 1.5-fold respectively in the presence of α-cbtx. Moreover, when bound to α-cbtx, D11-WT could not be detected in the recycled sample. However, no such effect of α-cbtx was observed for C08-YTE and B01-YTE (Fig 5(a-b)).

On the contrary, in the case of anti-M-II IgG1s, binding to M-II resulted in an enhanced uptake, recycling, and residual amounts of all tested IgG1s (Fig 5(d-f)). When bound to M-II, approximately 5-, 7- and 2.5-fold higher uptake was observed for YTE variants of IgG1s A03, B04, and A05, while for A03-WT a 33-fold higher uptake was seen. For recycling, an increase by 3-, 3.5-, and 2-fold was observed for YTE variants of A03, B04, and A05. For IgG1 A03-WT, the recycling levels increased by 33-fold in the presence of M-II. An increase in cellular accumulation of the all anti-M-II IgG1s was also observed by 4 to 5-fold. However, the accumulation of A03-WT was approximately 3 times lower than for A03-YTE, albeit similar levels of uptake and recycling of the two IgG1s in the presence of M-II were observed. Overall, the results demonstrate a clear effect of antigen-IgG1 binding on the cellular transport properties of these antibodies.

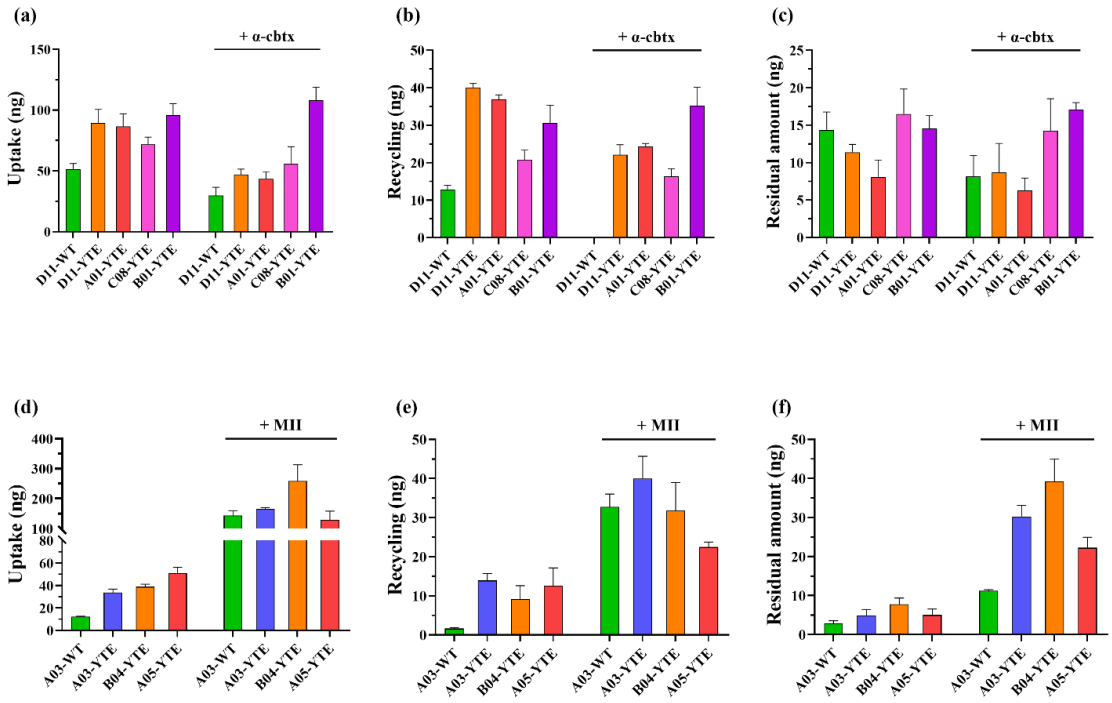


**Figure 5**: **Cellular transport properties of the IgG1s in HERA with or without antigen**. Observed **(a)** uptake, **(b)** recycled, and **(c)** residual amounts of the anti-α-cbtx IgG1s alone or in complex with α-cbtx. Observed **(d)** uptake, **(e)** recycled, **(f)** residual amounts of anti-M II IgG1s alone or in complex with M-II. Values correspond to one representative experiment (n=3 per data point). Data bars show mean± SD.

## Antibodies with pH-dependent antigen-binding properties are not recycled as antibody-antigen complex

To investigate whether the antibodies exhibited pH-dependent recycling in the cells, samples from HERA carried out with IgG1-(biotinylated) antigen complexes, were assessed to specifically detect the immune complexes in the cellular samples. This was done by capturing the complex via biotin (on antigen) and detecting it via Fc (on the IgG1) (Fig 6(a)). The recycling and residual levels were determined for each complex relative to its uptake value.

The immune complexes of all the anti-α-cbtx IgG1s were detected in the cellular uptake samples, but only the IgG1 D11-YTE complex was detected in the recycled sample, suggesting its non-pH-dependent antigen-binding nature (Fig 6(b)). No recycled complex of IgG1 D11-WT was observed, which is likely due to the non-detectable recycling of IgG1 D11-WT in the presence of α-cbtx as seen before (Fig 5(b), Fig 6(c)). Immune complexes of the pH-dependent positive control IgG1 A01-YTE and the parent IgG1 C08-YTE, were not detected in either the recycled or residual samples, which indicated that their pH-dependent antigen-binding properties translate to low or no recycling of the antigen (Fig 6(d-e)). For the light-chain shuffled IgG1 B01-YTE, no immune complex was observed in the recycled sample, although some accumulation of it was observed in the residual amounts (Fig 6(f)). The absence of IgG1 B01-YTE complex in the recycled sample was

surprising since B01 had displayed a much slower off-rate at pH 5.5 than A01 and C08 (Fig 2(h)).

Similar to anti-α-cbtx IgG1s, the immune complexes of all anti-M-II IgG1s, were detected in the cellular uptake samples. For IgG1s A03-YTE, A03-WT and the parent B04-YTE, their immune complexes were also observed in both the recycled and residual samples (Fig 6(g-i)). However, no immune complexes were observed for the light-chain shuffled IgG1 A05-YTE, again in correlation with its suggested pH-dependent antigen-binding nature (Fig 6(j)). In summary, this indicates that antibodies with pH-dependent antigen-binding properties are not recycled as immune complexes in the HERA assay.

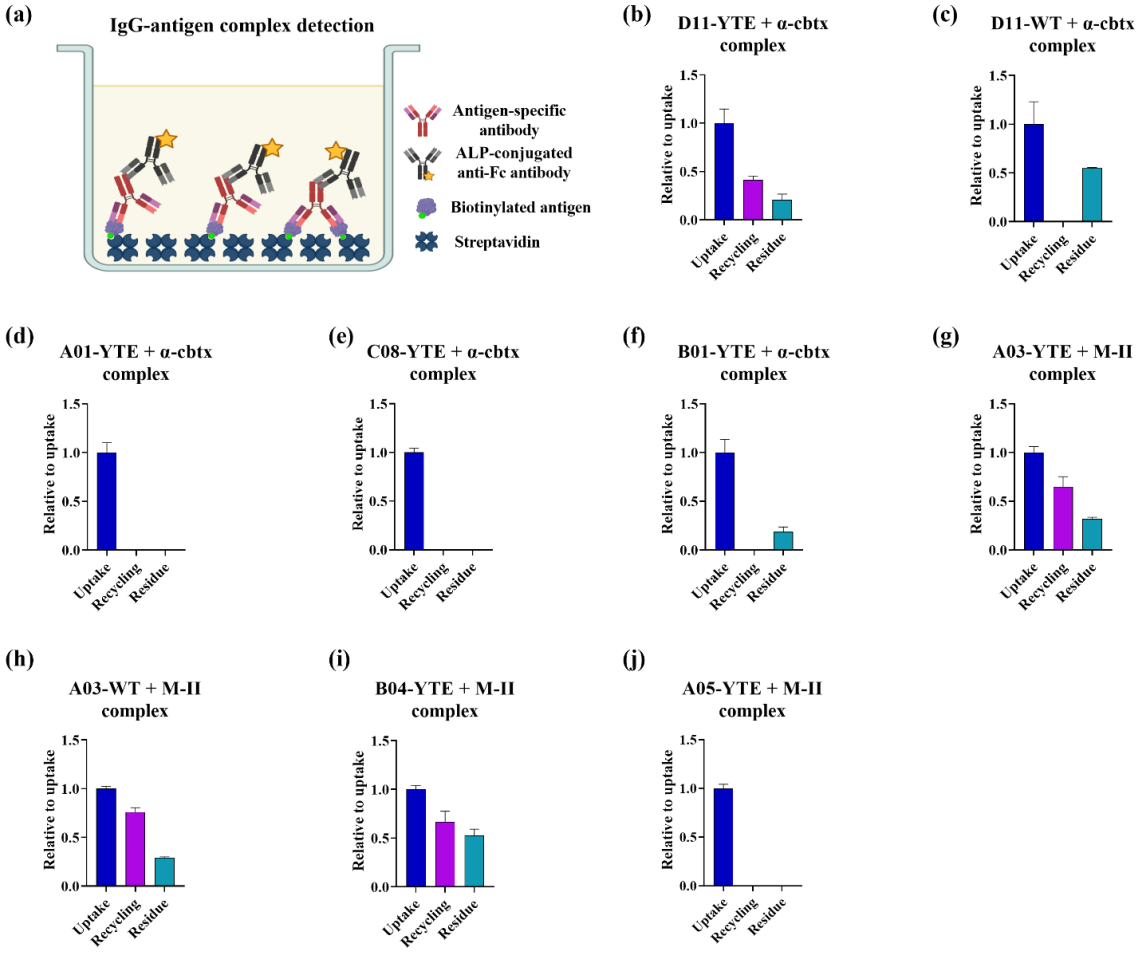


**Figure 6: Analysis of uptake, recycling and residual amounts of immune complexes using HERA. (a)** Illustration of the ELISA set-up employed to specifically detect immune complexes in the HERA obtained samples; created with Biorender. **(b-g)** Relative uptake, recycling, and residual amounts of the anti-α-cbtx IgG1 complexes. **(h-k)** Relative uptake, recycling, and residual amounts of the anti-M-II IgG1 complexes. For each IgG1-antigen complex, the relative uptake, recycling, and residue are normalized to the obtained uptake value of the complex. Data corresponds to one representative experiment (n=3 per data point). Data bars show mean ± SD.

## Discussion

In this study, we employed light-chain shuffling coupled to phage display selection as a new approach to increase the pH-dependency of the antibody-antigen interaction for three pre-existing antibodies B04, B12 (anti-M-II), and C08 (anti-α-cbtx) that already showed faster off-rates from their cognate antigen at pH 5.5 than at pH 7.4. This strategy resulted in the selection of a clone A05, that, when tested in the Fab format, bound its cognate antigen, M-II, in a more pH-dependent manner across a pH range (pH 3.5–6.0) compared to its parent Fab B04. In the case of selections from the C08 library, one anti-α-cbtx clone, B01, was discovered, which, in the Fab format, consistently bound its antigen in a less pH-dependent manner over the pH range (pH 3.5–6.0) compared to its parent Fab C08. Next, the parental and the discovered chain-shuffled antibodies, along with three antibody controls, A01 (anti-α-cbtx) as a positive control for pH-dependent antigen-binding, and two negative controls D11 (anti-M-II) and A03 (anti-M-II) as non-pH-dependent antigen-binding antibodies, were assessed in further analysis.

Efficient rescue of antibodies with pH-dependent antigen-binding properties via the FcRn-mediated recycling pathway is crucial for their function[7,12,14,52]. However, it has been shown that the interaction between Fc and FcRn can be influenced and/or modulated by the Fab regions of the antibody as well as bound antigen[17,18,51,53]. To investigate whether this was the case for the discovered antibodies, the Fabs were reformatted to IgG1s either with YTE substitutions in their Fc or without such mutations (wildtype, WT) and studied for their ability to interact with hFcRn in an hFcRn affinity chromatography column over a pH gradient. In agreement with the known function of YTE, which enhances the interaction between Fc and FcRn[6,14], it was observed that the IgG1s with YTE substitution in their Fc had longer retention times on the hFcRn-column than the IgG1s with WT Fc. Most IgG1s with the same Fc mutation showed similar retention times on the hFcRn-column, except for IgG1s A03-WT, A03-YTE, and B04-YTE, which eluted from the hFcRn-column at a higher pH than their respective Fc variant IgGs. These variations in the binding between IgG and hFcRn are possibly due to the differences in the charge profiles of their variable domains. It has been suggested that increased binding strength between IgG1s and FcRn may result from positive charges on Fabs that interact with the negatively charged patches on FcRn[18]. Although, the net Fv charge of all the IgG1s were found to be negative over the range of pH 5.5–8.0, Fv of A03 and B04 had the least net negative net charge, with their framework sequences displaying a higher net positive charge compared to the other antibodies. It is thus possible that IgG1s A03 and B04 may possess certain positively charged patches, which enabled their enhanced binding to the hFcRn.

The IgG1s were then studied in HERA to investigate how their hFcRn binding characteristics related to how they were handled by cells. In agreement with the observations made from the affinity chromatography experiments, IgG1s with YTE substitution in their Fc showed higher uptake and recycling than their WT counterparts. However, it was observed that IgG1 C08-YTE showed lower recycling than its light-chain shuffled offspring IgG1 B01-YTE, thus indicating that variable light chain region might modulate the FcRn interaction. This phenomenon has also been observed in other studies[18,54,55]. Interestingly, the M-II-targeting IgG1s A03-YTE, A03-WT, and B04-YTE

that had shown delayed release from the hFcRn affinity column at neutral pH did not show any striking differences in how they were handled by cells compared to the other anti-M-II-IgG1 A05-YTE. It should be noted, however, that in the cellular experiments, the IgG1 interacts with hFcRn embedded in cell membranes, which can result in the observed differences in the behaviour of the IgG1s between the chromatographic and cellular experiments[17,53].

Additionally, it was observed that all anti-M-II IgG1s showed lower levels of cellular uptake and recycling than the anti-α-cbtx IgG1s, while the residual amounts for all IgG1s were comparable. As these two sets of IgG1s target two different antigens, their distinct cellular behaviour could be a result of the influence of differences in Fvs. As such, the Fvs present in the anti-α-cbtx IgG1s may enable higher uptake and recycling, while the Fvs in the anti-M-II IgG1s may not have the same influence. Previous studies have correlated higher cellular IgG1 uptakes with net positively charged Fvs, which can facilitate unspecific interactions with the negatively charged cell membrane[17,18,51]. However, we did not find such correlations, as all the IgG1s had similar net Fv charge profiles. Moreover, in a recent study, Brinkhaus *et al.* showed that Fab arms can impose steric hindrance by clashing with the plasma membrane, which can impair the uptake of the IgG1 bound to membrane associated FcRn[53]. We thus speculate, that the Fab regions of the M-II-targeting IgG1s might create greater steric hindrance for the cellular uptake of IgG1s compared to the Fab regions of the anti-α-cbtx IgG1s.

Next, the effect of antigen on IgG1 and hFcRn interaction and cellular handling of IgG1s was investigated. When preincubated IgG1 and α-cbtx immune complexes were applied over the hFcRn affinity column, it was observed that the IgG1-α-cbtx complexes of D11-WT, D11-YTE, and B01-YTE eluted at a lower pH from the hFcRn affinity column than the IgG1s did in the absence of α-cbtx. A slight early release of A01-YTE was observed in the presence of α-cbtx, while no difference in the elution profile for C08-YTE was detected. Given that the samples for hFcRn affinity chromatography are prepared at pH 5.5, it is very likely that stable immune complexes of A01 and C08 were not formed since they exhibit fast off-rates at pH 5.5. Further, when studied in the cellular assays, it was found that IgG1s D11-WT, D11-YTE, and A01-YTE, which share the same variable heavy chain ($V_H$), showed a decrease in uptake and recycling in the presence of α-cbtx. On the other hand, α-cbtx had no detectable effects on the uptake and recycling of IgG1s C08-YTE and B01-YTE that possess the same $V_H$ (but different than that of A01 and D11). Thus, it appears that the effect of α-cbtx binding on the cellular handling of these IgG1s may be largely influenced by the residues present in their $V_H$s. For example, masking of positive charged patches in Fabs by antigen-binding has been speculated to reduce the unspecific interaction between the antibodies and negatively charged cell membrane[17,18,51], which consequently can result in reduced uptake of antibodies. Moreover, the interaction between hFcRn and IgG1s D11 and A01 might follow a two-way pronged binding mechanism[56], where both Fabs of the IgG1 could bend downward and interact with hFcRn. Thus, binding to α-cbtx may restrict the movement of Fabs in a manner that can potentially impair their interaction with FcRn[17,56]. It is, however, important to note that since IgG1

A01 is a recycling antibody, its reduced uptake in the presence of α-cbtx may hinder its effective functioning by possibly extending the half-life of the antigen[28].

In contrast to the effects of α-cbtx, M-II binding resulted in a delayed elution of both WT and YTE Fc variants of IgG1 A03 from the hFcRn-column. However, no effect of M-II was observed for the other two anti-M-II IgG1s B04-YTE and A05-YTE, which could be due to their inability to form a stable immune complex at pH 5.5, since both these antibodies displayed fast off-rates at pH 5.5. When studied in cellular assays, all anti-M-II IgG1s showed an increase in cellular uptake, recycling, and residual amounts in the presence of M-II. As M-II is postulated to form large complexes with IgG1s[48], this may result in multimerization of Fcs, thus enabling higher uptake and recycling through avidity-mediated enhanced FcRn binding[17]. Moreover, the increase in uptake of the IgG1s in the presence of M-II also resulted in higher accumulation inside the cells. Previous studies with HMEC-1 cells have shown that large immune complexes are more likely to be directed to lysosomal degradation than being recycled[18,47], which may be the case for M-II bound IgG1s. Additionally, since M-II itself interacts with plasma membranes, it may potentially increase the uptake of the bound IgG1s by bringing them in closer proximity to the cell membrane, where hFcRn resides[39,48]. Thus, our results show distinct effects of Fabs and antigen-binding on IgG1-FcRn interaction and IgG1 cellular behaviour.

Next, we characterized the pH-dependent antigen-binding properties of the IgG1s in HERA by specifically detecting the presence of antibody-antigen complexes in the cellular recycled samples. It was observed that the control IgG1s D11-YTE (anti-α-cbtx) and A03-YTE (anti-M-II) were recycled in complex with their cognate antigens, thus further demonstrating the absence of pH-dependence in their antigen-binding properties. In contrast, the immune complexes of anti-α-cbtx IgG1s A01-YTE, C08-YTE, and anti-M-II IgG1 A05-YTE were not detected in recycled and residual samples. Given that the IgG1s themselves were detected in the recycled and residual samples in the presence of their cognate antigens, this suggests that these IgG1s were able to dissociate from the cognate antigens inside the cells and get recycled as free IgG1s. Further, the absence of immune complexes of these IgG1s in the residual samples indicated that the antigens were degraded intracellularly. Additionally, the immune complex of the light-chain shuffled anti-α-cbtx IgG1 B01-YTE was also not detected in the recycled sample. This was surprising, since in BLI studies, B01 had shown similar off-rates at pH 7.4 and 5.5, with a sharp increase off-rate only being observed at pH 4.5. In order to be recycled as free antibodies, antibodies with pH-dependent antigen-binding properties are engineered to release their cognate antigen in the mildly acidic sorting endosomes (pH 5.5–6.0). However, it has been reported that the acidification of endosomes (pH 5.0 or below) can begin while the FcRn and its cargo (IgG1 in this case) are still being sorted[24,57]. Thus, it may be the case that IgG1 B01-YTE is able to dissociate from α-cbtx in a later endosomal stage and rescued as free IgG1. Hence, we speculate that despite showing comparable off-rates at pH 5.5 and 7.4, B01 may still function as an IgG1 with pH-dependent antigen-binding properties in the endosomes.

In contrast to the observed recycling behaviour of IgG1 B01, IgG1 A03 was found to be recycled in complex with its cognate antigen, which was surprising since both these antibodies displayed similar off-rate profiles throughout the assessed pH range (pH 3.5–

7.5) in BLI. A possible explanation behind the different recycling behaviour of these two IgG1s could be derived from the sizes of their immune complexes that involve two quite different antigens. As the formation of larger complexes of M-II and IgG1s has been speculated to occur[48], it may be unlikely that all IgG1s in the immune complex dissociate from the bound M-II molecules at the same time when the pH is lowered. In contrast, B01 likely does not form large immune complexes with α-cbtx, which may explain the observed differences in their ability to recycle as free IgG1. Moreover, antibodies with fast on-rates at low pH may also rebind the dissociated toxins in the endosomes[52]. Thus, studying the on-rates of the antibodies at low pH might shed light on the distinct pH-dependent antigen-binding behaviours of these two IgG1s.

## Conclusion

The currently widely used strategy to discover antibodies with pH-dependent antigen-binding properties is based on introducing histidines in the antibody Fab region, which comes with the risk of compromising antibody- antigen-binding at neutral pH[12,24]. Additionally, incorporation of mutations in antibody sequences may introduce sequence liabilities that can result in developability and immunogenicity issues[58]. Here, we demonstrate that light-chain shuffling coupled to *in vitro* display technologies can, in some cases, serve as a useful tool to generate pH-dependent antigen-binding properties of antibodies against soluble targets. Moreover, by performing light-chain shuffling with naturally occurring antibody variable domains the native origin of the antibodies is preserved. In this study, we further employed a panel of IgG1s to demonstrate that the FcRn binding and cellular handling properties of the IgG1s are not just governed by Fc engineering, but also modulated by differences in Fab regions and antigen-binding mode, which can result in reduction or increase in the cellular uptake of IgG1s. For the effective functioning of IgG1s with pH-dependent antigen-binding properties, it is thus important to consider the possible effects of biophysical attributes of the Fabs and cognate antigens on their cellular handling properties[28].

So far, antibodies with pH-dependent antigen-binding properties have mostly been studied to target endogenous antigens that are continuously produced in the body[12,19,20,22,23]. In this study, we used snake venom toxins α-cbtx and M-II as target antigens, which are exogenous to mammals and instantly delivered in very high quantities upon an envenoming[31]. Therefore, the current treatment of snakebite envenoming, which is currently based on animal-derived antivenoms, requires correspondingly very high doses for effective neutralization of the venom toxins[59]. In this relation, we speculate that recycling antibodies that target snake venom toxins could be used to develop novel recombinant antivenoms that could potentially be administered at even lower dose than antivenoms based on non-recycling antibodies, such as the currently widely used heterologous and $F(ab)_2$-based antivenoms[32]. In turn, this might help reduce the cost of treatment, which is a major limiting factor for the deployment of antivenoms to treat snakebite envenoming[31]. However, in contrast to continuously produced endogenous antigens, where instant neutralization may not be of high importance, (fast-acting) snake toxins are delivered in high quantities in the victim and must be neutralized relatively

quickly. As the *in vivo* recycling efficiency of snake toxin-neutralizing recycling antibodies is not known, it is difficult to state how efficient such antibodies would be in eliminating the antigens under circumstances where complex toxicokinetics is at play. Therefore, it would be beneficial in further studies to investigate the *in vivo* performance of recycling snake toxin-neutralizing antibodies. Nevertheless, the methodologies employed in this study can be utilized to discover antibodies with pH-dependent antigen-binding properties against other targets, as well as characterize them for their pH-dependent antigen-binding in a cellular setting. We thus hope that these methods may find broad applications in other fields, such as neutralization of toxins and virulence factors from other venomous animals and bacteria, as well as targeting of endogenous antigens.

**Acknowledgments**

The authors are supported by a grant from the European Research Council (ERC) under the European Union's Horizon 2020 research and innovation programme (grant no. 850974); Villum Foundation under grant 00025302; Wellcome (221702/Z/20/Z); Novo Nordisk Foundation (NNF20SA0066621); and Research Council of Norway (287927). The authors would like to thank Sara Petersen Bjørn, Karen Kathrine Brøndum, and Daniel Duun from National Biologics Facility for the reformatting and production of Fabs and IgG1s.

**Competing interests**

The authors declare no conflict of interest.

**References**


1. Kaplon, H., Chenoweth, A., Crescioli, S. & Reichert, J. M. Antibodies to watch in 2022. *mAbs* **14**, 2014296 (2022).

2. Carter, P. J. & Lazar, G. A. Next generation antibody drugs: pursuit of the 'high-hanging fruit'. *Nat. Rev. Drug Discov.* **17**, 197–223 (2018).

3. Carter, P. J. & Rajpal, A. Designing antibodies as therapeutics. *Cell* **185**, 2789–2805 (2022).

4. Lu, R.-M. *et al.* Development of therapeutic antibodies for the treatment of diseases. *J. Biomed. Sci.* **27**, 1 (2020).

5. Duivelshof, B. L. *et al.* Therapeutic Fc-fusion proteins: Current analytical strategies. *J. Sep. Sci.* **44**, 35–62 (2021).

6. Kang, T. H. & Jung, S. T. Boosting therapeutic potency of antibodies by taming Fc domain functions. *Exp. Mol. Med.* **51**, 1–9 (2019).

7. Roopenian, D. C. & Akilesh, S. FcRn: the neonatal Fc receptor comes of age. *Nat. Rev. Immunol.* **7**, 715–725 (2007).

8. Challa, D. K., Velmurugan, R., Ober, R. J. & Sally Ward, E. FcRn: from molecular interactions to regulation of IgG pharmacokinetics and functions. *Curr. Top. Microbiol. Immunol.* **382**, 249–272 (2014).

9. Gan, Z., Ram, S., Vaccaro, C., Ober, R. J. & Ward, E. S. Analyses of the recycling receptor, FcRn, in live cells reveal novel pathways for lysosomal delivery. *Traffic Cph. Den.* **10**, 600 (2009).

10. Lencer, W. I. & Blumberg, R. S. A passionate kiss, then run: exocytosis and recycling of IgG by FcRn. *Trends Cell Biol.* **15**, 5–9 (2005).

11. Ward, E. S. *et al.* From sorting endosomes to exocytosis: association of Rab4 and Rab11 GTPases with the Fc receptor, FcRn, during recycling. *Mol. Biol. Cell* **16**, 2028–2038 (2005).

12. Igawa, T., Haraya, K. & Hattori, K. Sweeping antibody as a novel therapeutic antibody modality capable of eliminating soluble antigens from circulation. *Immunol. Rev.* **270**, 132–151 (2016).

13. Lee, C.-H. *et al.* An engineered human Fc domain that behaves like a pH-toggle switch for ultra-long circulation persistence. *Nat. Commun.* **10**, 5031 (2019).

14. Acqua, W. F. D. *et al.* Increasing the Affinity of a Human IgG1 for the Neonatal Fc Receptor: Biological Consequences1. *J. Immunol.* **169**, 5171–5180 (2002).

15. Zalevsky, J. *et al.* Enhanced antibody half-life improves in vivo activity. *Nat. Biotechnol.* **28**, 157–159 (2010).

16. Dall'Acqua, W. F., Kiener, P. A. & Wu, H. Properties of human IgG1s engineered for enhanced binding to the neonatal Fc receptor (FcRn). *J. Biol. Chem.* **281**, 23514–23524 (2006).

17. Gjølberg, T. T. *et al.* Biophysical differences in IgG1 Fc-based therapeutics relate to their cellular handling, interaction with FcRn and plasma half-life. *Commun. Biol.* **5**, 1–17 (2022).

18. Grevys, A. *et al.* Antibody variable sequences have a pronounced effect on cellular transport and plasma half-life. *iScience* **25**, 103746 (2022).

19. Chaparro-Riggers, J. *et al.* Increasing Serum Half-life and Extending Cholesterol Lowering in Vivo by Engineering Antibody with pH-sensitive Binding to PCSK9 *. *J. Biol. Chem.* **287**, 11090–11097 (2012).

20. Igawa, T. *et al.* Antibody recycling by engineered pH-dependent antigen binding improves the duration of antigen neutralization. *Nat. Biotechnol.* **28**, 1203–1207 (2010).

21. Klaus, T. & Deshmukh, S. pH-responsive antibodies for therapeutic applications. *J. Biomed. Sci.* **28**, 11 (2021).

22. Bonvin, P. *et al.* De novo isolation of antibodies with pH-dependent binding properties. *mAbs* **7**, 294–302 (2015).

23. Schröter, C. *et al.* A generic approach to engineer antibody pH-switches using combinatorial histidine scanning libraries and yeast display. *mAbs* **7**, 138 (2015).

24. Devanaboyina, S. C. *et al.* The effect of pH dependence of antibody-antigen interactions on subcellular trafficking dynamics. *mAbs* **5**, 851–859 (2013).

25. Igawa, T. *et al.* Engineered Monoclonal Antibody with Novel Antigen-Sweeping Activity In Vivo. *PLOS ONE* **8**, e63236 (2013).

26. Lee, J. W. *et al.* Ravulizumab (ALXN1210) vs eculizumab in adult patients with PNH naive to complement inhibitors: the 301 study. *Blood* **133**, 530–539 (2019).

27. Sheridan, D. *et al.* Design and preclinical characterization of ALXN1210: A novel anti-C5 antibody with extended duration of action. *PLOS ONE* **13**, e0195909 (2018).

28. Sampei, Z. *et al.* Antibody engineering to generate SKY59, a long-acting anti-C5 recycling antibody. *PLOS ONE* **13**, e0209509 (2018).

29. Hori, Y. *et al.* Elimination of plasma soluble antigen in cynomolgus monkeys by combining pH-dependent antigen binding and novel Fc engineering. *mAbs* **14**, 2068213 (2022).

30. Kroetsch, A. *et al.* Engineered pH-dependent recycling antibodies enhance elimination of Staphylococcal enterotoxin B superantigen in mice. *mAbs* **11**, 411–421 (2018).

31. Laustsen, A. H. How can monoclonal antibodies be harnessed against neglected tropical diseases and other infectious diseases? *Expert Opin. Drug Discov.* **14**, 1103–1112 (2019).

32. Tulika, T. & Pedersen, R. *et al*. Phage display assisted discovery of a pH-dependent anti-α-cobratoxin antibody from a natural variable domain library. Manuscript II (in preparation).

33. Raghavan, M., Bonagura, V. R., Morrison, S. L. & Bjorkman, P. J. Analysis of the pH dependence of the neonatal Fc receptor/immunoglobulin G interaction using antibody and receptor variants. *Biochemistry* **34**, 14649–14657 (1995).

34. Tanokura, M. 1H-NMR study on the tautomerism of the imidazole ring of histidine residues. I. Microscopic pK values and molar ratios of tautomers in histidine-containing peptides. *Biochim. Biophys. Acta* **742**, 576–585 (1983).

35. Egli, J. *et al.* Enhanced immunogenic potential of cancer immunotherapy antibodies in human IgG1 transgenic mice. *mAbs* (2022).

36. 16 - Development issues: antibody stability, developability, immunogenicity, and comparability. in *Therapeutic Antibody Engineering* (eds. Strohl, W. R. & Strohl, L. M.) 377–595 (Woodhead Publishing, 2012). doi:10.1533/9781908818096.377.

37. Ausserwöger, H. *et al.* Non-specificity as the sticky problem in therapeutic antibody development. *Nat. Rev. Chem.* 1–18 (2022) doi:10.1038/s41570-022-00438-x.

38. Alkondon, M. & Albuquerque, E. X. alpha-Cobratoxin blocks the nicotinic acetylcholine receptor in rat hippocampal neurons. *Eur. J. Pharmacol.* **191**, 505–506 (1990).

39. Mora-Obando, D., Díaz, C., Angulo, Y., Gutiérrez, J. M. & Lomonte, B. Role of enzymatic activity in muscle damage and cytotoxicity induced by Bothrops asper Asp49 phospholipase A2 myotoxins: are there additional effector mechanisms involved? *PeerJ* **2**, e569 (2014).

40. Lomonte, B. & Gutiérrez, J. M. A new muscle damaging toxin, myotoxin II, from the venom of the snake Bothrops asper (terciopelo). *Toxicon Off. J. Int. Soc. Toxinology* **27**, 725–733 (1989).

41. Laustsen, A. H. *et al.* In vivo neutralization of dendrotoxin-mediated neurotoxicity of black mamba venom by oligoclonal human IgG antibodies. *Nat. Commun.* **9**, 3928 (2018).

42. Ledsgaard, L. *et al.* In vitro discovery of a human monoclonal antibody that neutralizes lethality of cobra snake venom. *mAbs* **14**, 2085536.

43. Schofield, D. J. *et al.* Application of phage display to high throughput antibody generation and characterization. *Genome Biol.* **8**, R254 (2007).

44. Ledsgaard, L., Kilstrup, M., Karatt-Vellatt, A., McCafferty, J. & Laustsen, A. H. Basics of Antibody Phage Display Technology. *Toxins* **10**, 236 (2018).

45. Wade, J. *et al.* Generation of Multivalent Nanobody-Based Proteins with Improved Neutralization of Long α-Neurotoxins from Elapid Snakes. *Bioconjug. Chem.* **33**, 1494–1504 (2022).

46. Grevys, A. *et al.* A human endothelial cell-based recycling assay for screening of FcRn targeted molecules. *Nat. Commun.* **9**, 621 (2018).

47. Weflen, A. W. *et al.* Multivalent immune complexes divert FcRn to lysosomes by exclusion from recycling sorting tubules. *Mol. Biol. Cell* **24**, 2398–2405 (2013).

48. Sørensen, C. V. *et al*. Antibody-mediated enhancement of toxicity of myotoxin II from Bothrops asper. Manuscript I (in preparation).

49. Wade, J. *et al*. Structure of a neurotoxin-neutralizing antibody reveals determinants for broad reactivity and a pH-responsive allosteric switch. Manuscript in preparation.

50. Ledsgaard, L. Discovery and optimization of a broadly-neutralizing human monoclonal antibody against long-chain α-neurotoxins from snakes. Accepted. Nature Communiations.

51. Schoch, A. *et al.* Charge-mediated influence of the antibody variable domain on FcRn-dependent pharmacokinetics. *Proc. Natl. Acad. Sci. U. S. A.* **112**, 5997–6002 (2015).

52. Ward, E. S. & Ober, R. J. Targeting FcRn to generate antibody-based therapeutics. *Trends Pharmacol. Sci.* **39**, 892–904 (2018).

53. Brinkhaus, M. *et al.* The Fab region of IgG impairs the internalization pathway of FcRn upon Fc engagement. *Nat. Commun.* **13**, 6073 (2022).

54. Piche-Nicholas, N. M. *et al.* Changes in complementarity-determining regions significantly alter IgG binding to the neonatal Fc receptor (FcRn) and pharmacokinetics. *mAbs* **10**, 81–94 (2018).

55. Jensen, P. F. *et al.* Investigating the Interaction between the Neonatal Fc Receptor and Monoclonal Antibody Variants by Hydrogen/Deuterium Exchange Mass Spectrometry *. *Mol. Cell. Proteomics* **14**, 148–161 (2015).

56. Jensen, P. F. *et al.* A Two-pronged Binding Mechanism of IgG to the Neonatal Fc Receptor Controls Complex Stability and IgG Serum Half-life *. *Mol. Cell. Proteomics* **16**, 451–456 (2017).

57. Ober, R. J., Martinez, C., Vaccaro, C., Zhou, J. & Ward, E. S. Visualizing the Site and Dynamics of IgG Salvage by the MHC Class I-Related Receptor, FcRn1. *J. Immunol.* **172**, 2021–2029 (2004).

58. Fernández-Quintero, M. L. Assessing developability early in the discovery process for novel biologics. Manuscript in preparation.

59. Ooms, G. I. *et al.* Availability, affordability and stock-outs of commodities for the treatment of snakebite in Kenya. *PLoS Negl. Trop. Dis.* **15**, e0009702 (2021).

## Supplementary material

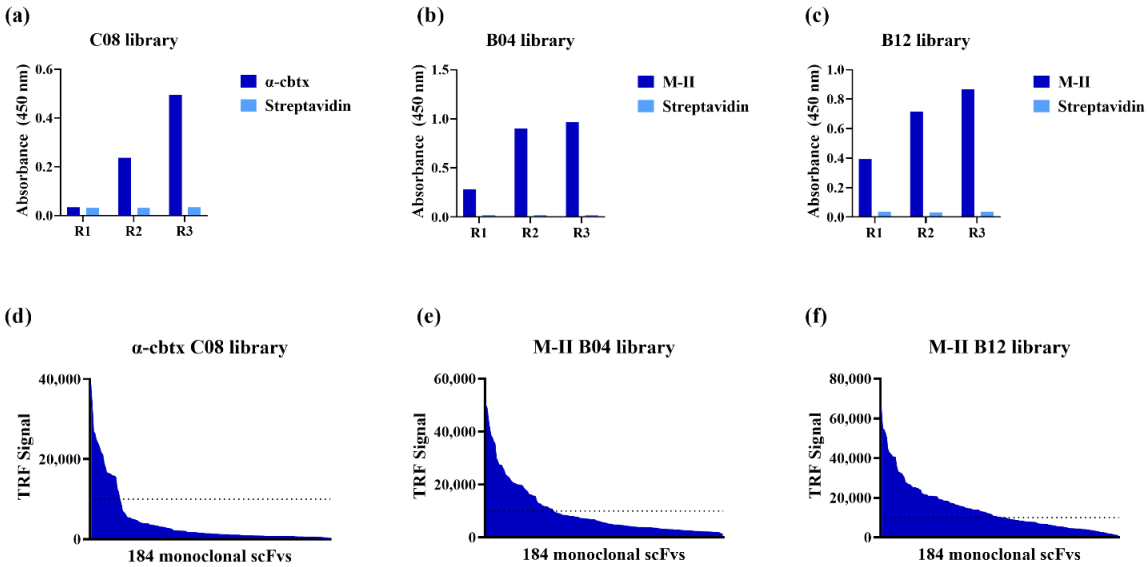


**Fig S1. Polyclonal phage ELISA and screening of binding clones obtained from phage display selections.** Polyclonal phage ELISA of selection outputs from three selection rounds of the chain-shuffled library **(a)** C08, **(b)** B04, and **(c)** B12 showing binding to their target antigen and negligible binding to streptavidin. Binding signal of 184 monoclonal scFvs from the library **(d)** C08, **(e)** B04 and, **(f)** B12 against their target antigen. Clones that gave a binding signal (TRF: time-resolved fluorescence) above the set threshold of 10,000 units (shown by dotted lines) were selected for further analysis.

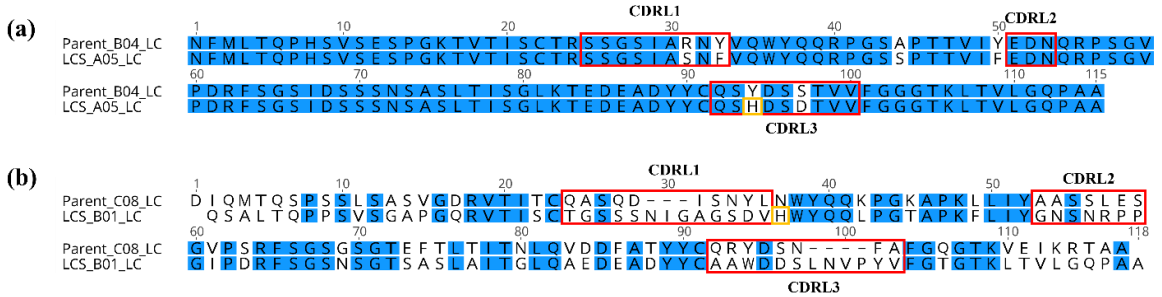


**Fig S2. Light chain sequence alignments of parental and light-chain shuffled antibodies. (a)** Sequence alignment of light chains of anti-M-II parent antibody B04 and the light-chain shuffled antibody A05. **(b)** Sequence alignment of light chains of the anti-α-cbtx parent antibody C08 and the light-chain shuffled antibody B01. Identical amino acid residues in the sequence alignments are marked with a blue background, while distinct amino acids are marked with a white background. The CDRLs are shown in red boxes and the histidine residues originating from light-chain shuffling are shown in yellow boxes. The sequence alignments were made using Geneious Prime. (LCS= Light-chain shuffled, LC=Light chain, CDRL= light chain complementarity-determining region)

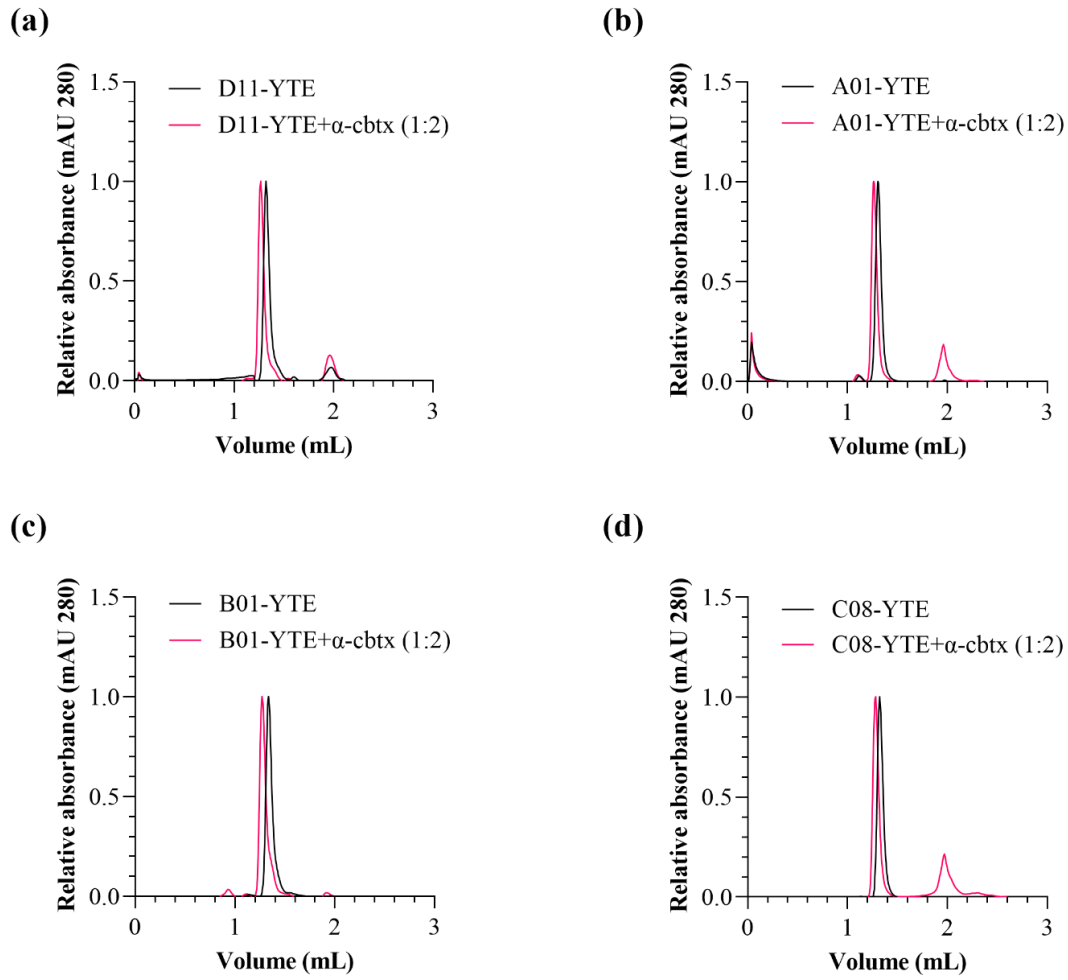


**Fig S3. Size exclusion chromatograms IgGs and IgG-antigen complexes.** Size exclusion chromatograms of IgGs and their preincubated immune complexes with α-cbtx at 1:2 molar ratio **(a)** D11-YTE, **(b)** A01-YTE, **(c)** B01-YTE, and **(d)** C08-YTE.

**Supplementary table 1:** Off-rates of Fabs at pH 7.4, 6.5, 6.0, 5.5, 5.0, 4.5, 4.0, and 3.5 as determined by BLI.

| pH | α-cbtx targeting Fabs | | | | M-II targeting Fabs | | |
|---|---|---|---|---|---|---|---|
| | **A01 (PC)** | **C08 (Parent)** | **B01 (LCS)** | **D11 (NC)** | **A05 (LCS)** | **B04 (Parent)** | **A03 (NC)** |
| **7.4** | 9.54E-04 | 6.94E-04 | 8.12E-04 | 2.61E-04 | 7.14E-03 | 9.69E-03 | 6.88E-04 |
| **6.5** | 1.81E-03 | 7.74E-04 | 7.08E-04 | 2.67E-04 | 7.51E-03 | 1.27E-02 | 5.84E-04 |
| **6.0** | 3.31E-03 | 1.16E-03 | 7.05E-04 | 3.03E-04 | 8.53E-03 | 1.81E-02 | 6.86E-04 |
| **5.5** | 1.17E-03 | 4.08E-03 | 7.75E-04 | 3.88E-04 | 1.39E-02 | 3.94E-02 | 1.18E-03 |
| **5.0** | 1.86E-03 | 7.28E-03 | 8.22E-04 | 4.33E-04 | 1.84E-02 | 5.78E-02 | 1.59E-03 |
| **4.5** | 7.02E-02 | 5.44E-02 | 2.32E-03 | 6.55E-04 | 6.03E-02 | 2.63E-01 | 3.78E-03 |
| **4.0** | 1.87E-01 | 2.85E-01 | 7.53E-03 | 1.05E-03 | 3.43E-01 | 7.56E-01 | 1.04E-02 |
| **3.5** | 4.93E-01 | 1.18E00 | 2.83E-02 | 3.65E-03 | 1.45E00 | 1.67E00 | 5.95E-02 |

(PC = Positive control, NC = Negative control, LCS= Light-chain shuffled)

**Supplementary table 2: Affinity measurements of the Fabs**

| Target | Fab | $k_{on}$ ($Ms^{-1}$) | $k_{off}$ ($s^{-1}$) | $K_D$ |
|---|---|---|---|---|
| **α-cbtx** | TPL0197_01_C08 (Parent)[32] | $1.06 \times 10^{4}$ | $8.50 \times 10^{-4}$ | 64 nM |
| | TPL0544_01_B01 (LCS) | $6.39 \times 10^{3}$ | $2.63 \times 10^{-4}$ | 41.1 nM |
| | 2555_01_A01[49] (PC) | $1.50 \times 10^{4}$ | $5.03 \times 10^{-4}$ | 33.8 nM |
| | 2554_01_D11 (NC)[32] | $1.05 \times 10^{4}$ | $8.06 \times 10^{-4}$ | 1.3 nM |
| **M-II** | TPL0039_05_B04 (Parent) | $4.40 \times 10^{5}$ | $9.19 \times 10^{-3}$ | 20.8 nM |
| | TPL0552_02_A05 (LCS) | $5.41 \times 10^{5}$ | $1.34 \times 10^{-2}$ | 24.8 nM |
| | TPL0039_05_A03 (NC) | $2.04 \times 10^{5}$ | $3.07 \times 10^{-4}$ | 1.5 nM |

The dissociation constants, on-rates ($k_{on}$), off-rates ($k_{off}$), and affinities ($K_D$) of the Fabs at pH 7.4 as determined by BLI. (LCS = light-chain shuffled clone, NC = negative control, PC= positive control). Positive control means the Fab showed an increased off-rate at pH 5.5 than 7.4. Negative control implies that the off-rates at pH 5.5 and 7.4 were similar.

# Chapter 6 - Conclusions and further perspectives

## 6.1. Discovering pH-dependent antibodies

Antibodies that bind their cognate antigen at neutral pH and dissociate from the antigen at acidic pH are known as recycling antibodies[105,113]. *In vivo*, such antibodies bind antigens in the bloodstream (pH 7.4) and release the antigen upon entering endosomes (pH 5.0−6.0), whereupon the antibodies are recycled back into the bloodstream, while the antigens are subjected to lysosomal degradation[105]. Consequently, recycling antibodies can bind and eliminate multiple antigens in their lifetime, which enables them to achieve therapeutic efficacy at a lower dose or frequency of dosing than their non-recycling counterparts[114,117]. As a result, recycling antibodies have gained increased attention in recent years[108,127].

The most common strategy to engineer antibodies that bind to their antigen in a pH-dependent manner is based on the incorporation of histidine residues in the variable regions of the antibody, by employing approaches such as histidine scanning and generation of histidine enriched libraries[106]. The reason for this is that histidine has a $pK_a$ of approximately 6.0, meaning that at pH levels below 6.0, the histidine side chain carries a positive charge. Consequently, an antibody-antigen interaction involving a histidine residue may be stable at neutral pH but get destabilized when the histidine residue gets protonated in the acidic environment of endosomes[105]. However, this approach does not come without a series of drawbacks. Firstly, given that histidine-mediated pH-dependent binding relies on the electrostatic repulsion between the protonated histidine paratope and the positively charged epitope at low pH, this feature of histidine may be restricted when targeting negatively charged epitopes[113]. Further, it has been shown that histidine-mediated reduction in the antibody-antigen-binding can also result in compromised binding between the two molecules at neutral pH[107]. Additionally, incorporation of mutations in the antibody sequence may come with the risk of introducing potential sequence liabilities that may negatively impact the developability and immunogenicity of the antibody[120].

In the work described in this thesis, I have explored the possibility of discovering antibodies with pH-dependent antigen-binding properties from antibody libraries consisting of naturally occurring variable domains. To do this, I used *in vitro* (phage) display technology, as it allows for easy manipulation of selection strategies that can enable selection of antibodies with desired antigen-binding properties. Indeed, the studies presented in **manuscripts II and III** demonstrate the utility of such libraries coupled to *in vitro* selection technology to discover pH-dependent antigen-binding antibodies. In manuscript II, the employment of a naïve antibody library resulted in the discovery of an antibody that bound α-cbtx in a pH-dependent manner, C08, which was devoid of histidines, thus highlighting that pH-dependent binding can at times be derived from other amino acid residues. This may be a result of the effect of the molecular microenvironment that can alter the local $pK_a$ of the amino acids at the antibody-antigen-binding interface. While a study by Sampei et al. has reported a few non-histidine mutations that further enhanced histidine derived pH-dependency of an antibody, to the best of my knowledge, no study so far has reported an antibody with pH-dependent antigen-binding properties that

is entirely devoid of histidine residues[114]. Further studies to investigate the contributing factors to the observed pH-dependent interaction between C08 and α-cbtx are planned, as the gained knowledge can potentially help advance our understanding of pH-dependent interactions. Additionally, it may help to identify amino acid residues that could find utility in engineering pH-dependent binding of other proteins. Next, in **manuscript III**, we showed that light-chain shuffling of pre-existing antibodies can be employed to enhance their pH-dependent antigen-binding properties. Unexpectedly, one of the discovered light-chain shuffled antibodies, B01, when assessed for its ability to dissociate from its cognate antigen, α-cbtx, in biolayer interferometry (BLI), only showed a sharp increase in off-rate at pH 4.5, and still behaved as a recycling antibody in a cellular recycling assay. Two reasons have been hypothesized in manuscript III that may explain the observed recycling of B01. First, it has been reported that the acidification of endosomes begins while the FcRn-bound cargo is still being sorted for lysosomal degradation or recycling[77]. It may thus be the case that B01 is rescued as a free antibody (antigen-unbound) from such later stages of the endosome. Second, B01 may have a slow on-rate at endosomal pH, which may hinder its rebinding to the antigen[88]. Studies to determine the kinetic parameters at low pH for B01, as well as other antibodies assessed in manuscript III, are planned as they may shed further light on the pH-dependent antigen-binding behaviour of these antibodies.

In summary, the work shown in this thesis has demonstrated the utility of antibody libraries with naturally occurring variable domains and light-chain shuffling to discover antibodies with pH-dependent antigen-binding properties. Further, it uncovered the observations of pH-dependency being derived from non-histidine residues and recycling behaviour of an antibody being potentially governed by factors other than its fast dissociation from the antigen in mildly acidic environment of early endosomes. In combination, this provides antibody researchers with new insight into how to discover antibodies with pH-dependent antigen-binding properties *a priori* and how to assess these properties biochemically and cellularly.

## 6.2. Possible applications of pH-dependent antibodies

The utility of pH-dependent antigen-binding antibodies has mostly been studied in the context of endogenous soluble antigens that are often overexpressed under disease conditions. Examples of antigens against which pH-dependent antibodies have been engineered include IL-6, both soluble and membrane-bound IL-6 receptor (hsIL-6, hsIL-6R), PCSK9, CXCL10, TNF-α, C5, and CEACAM5[106,108,128]. Although pH-dependent antigen-binding antibodies have shown promising results, it was found that pH-dependent antigen-binding alone may not always be able to actively eliminate the antigen from the plasma[109]. Thus, pH-dependent antigen-binding antibodies were further engineered to bind Fc receptors (FcRn or FcγRIIb) with increased affinity at neutral pH and enhance the cellular uptake of antibody-antigen complex. Such antibodies can eliminate antigen from the plasma more effectively and are referred to as sweeping antibodies[106,114,115]. Indeed, a C5-targeting sweeping antibody, ALXN1210 (ravulizumab) was able to achieve therapeutic efficacy at a lower dosing frequency (every 8 weeks) compared to the

conventional antibody eculizumab (every 2 weeks) and was approved by the FDA for the treatment of paroxysmal nocturnal hemoglobinuria (PNH)[116,117,129].

Lowering treatment doses or reducing dosing frequencies are benefits of pH-dependent antigen-binding antibodies that may also enable a reduction in the treatment cost. Snakebite envenoming is an example of a disease requiring costly and exorbitantly high doses of antivenom for its treatment[44]. Recycling antibodies may find utility in novel recombinant antivenoms that can potentially be administered at lower doses than the antivenoms based on non-recycling antibodies. Given that reducing antivenom doses for treatment has been hypothesized to translate into reduced treatment costs, this may especially aid the accessibility of the antivenoms[53].

Thus, in this thesis I have worked on discovering antibodies that bind snake toxins, α-cbtx and M-II, in a pH-dependent manner. Two such antibodies against α-cbtx and one against M-II were discovered and their recycling behaviour was validated in cellular assays. Although, these results are promising, it is important to consider the complex pharmacology and toxicokinetics involved in snakebites[130]. In contrast to endogenous antigens which are continuously produced, in the case of snakebites, high amounts of snake venom toxins can be instantaneously injected into the victim[118]. The effectivity of recycling antibodies in eliminating large amounts of fast-acting toxins from the body is not yet known. However, it is only rarely observed that snakebites result in intravenous injection of the venom, and in most cases the venom is injected intramuscularly or subcutaneously, where the toxins are first absorbed and then slowly released in circulation or the surrounding tissue due to depot effect[118]. The depot effect may have an effect on toxicity of systemically acting toxins such as α-cbtx that need to leave the site of bite and enter the bloodstream to reach their target[118]. Thus, under circumstances where toxins are released over time into the plasma and the recycling antibodies are not over-burdened, it may be possible for the recycling antibodies to effectively eliminate the toxins. Compared to systemically acting toxins, the depot effect may not be able to delay the toxic effects of locally acting muscle degrading M-II. However, it has been suggested that targeting antigens in locally diseased tissues with recycling antibodies may also be beneficial[106]. Further, muscles are highly perforated with blood vessels that show high expression levels of FcRn[131]. A scenario can thus be speculated where the recycling antibodies are able to reach the site of bite and eliminate the toxins. However, further investigations are required to understand the overall effectiveness of the recycling antibodies against snake venom toxins.

Recycling antibodies may also find utility in infectious diseases, where large amounts of harmful toxins are often produced during an active infection[119]. Indeed, a recent study by Kroetsch et al., found that pH-dependent antibodies targeting the Staphylococcal enterotoxin B (SEB) super antigen were able to eliminate the toxins significantly faster from the plasma than the non-pH-dependent antibody[119]. The findings from a study by Kroetsch et al., provide promising evidence for the potential application of recycling antibodies in treating infectious diseases as well as snakebite envenomings where the targets are also toxic.

A commonly desired feature of therapeutic antibodies is their ability to neutralize the target antigens, especially the antigens that are toxic[27,119,132]. However, Igawa et al.

reported that with sweeping antibody technology, they were able to successfully eliminate the target antigen (hsIL-6R) despite the antibody having no neutralizing activity *in vitro*[109]. Although it is uncertain whether non-neutralizing sweeping antibodies would be effective against toxins, it may be beneficial to investigate this aspect as it may make the engineering of pH-dependent antigen-binding antibodies easier.

## 6.3. Effects of Fab modulation on pH-dependent antibodies

One important feature that has made antibodies (specially IgG1s) an attractive therapeutic choice is their long plasma half-life[56,133]. The long plasma half-life of the antibodies results from the pH-dependent interaction between the Fc and FcRn[133]. However, it has been shown that this Fc-FcRn interaction and the plasma half-life of the antibodies can be affected by the Fab region[93]. Since efficient FcRn-mediated rescue of antibodies is necessary for the functioning of recycling antibodies, in manuscript III we explored the effects of the Fab on the Fc-FcRn interaction and cellular recycling of the antibodies. Indeed, varying cellular transport properties were observed for antibodies with identical Fc regions, thus demonstrating the role of Fabs. For example, two pH-dependent α-cbtx-binding antibodies, C08 and B01, that differed only in their variable light chains, showed similar cellular uptake levels, but different recycling levels, thus indicating the influence of light chain on recycling[94,100]. Further, we observed that all anti-M-II antibodies exhibited lower cellular uptake and recycling levels than the anti-α-cbtx antibodies, suggesting the distinct effects of the two different types of variable regions (α-cbtx or M-II recognizing) present in these antibodies.

Next, the cellular transport properties of the antibodies were assessed when bound to their cognate antigen. Unexpectedly, the two antigens affected the cellular behaviour of the antibodies differently. While M-II binding increased the cellular uptake of the antibodies, α-cbtx binding either reduced or did not affect the antibody cellular uptake. Since, M-II has been speculated to form large immune complexes, the observed increase in the uptake of the antibodies could probably be due to avidity-mediated enhanced interaction between the immune complex (multiple Fcs) and FcRn. However, M-II binding also resulted in higher accumulation of antibodies inside the cells, which may not be beneficial for the functioning of recycling antibodies.

In the case of α-cbtx binding, the cellular uptake and recycling levels of antibodies D11 (non-recycling) and A01 (recycling) were reduced. We speculate that binding to the α-cbtx may mask positively charged patches on the Fabs of these antibodies, which may reduce their unspecific interaction with the negatively charged plasma membrane, thus resulting in reduced uptake of the immune complexes[93]. However, reduced uptake of antibody-antigen complexes of recycling antibodies, may result in a sub-optimal recycling performance. Indeed, in a study, Sampei et al., linked the sub-optimal performance of a C5 targeting recycling antibody to the slow cellular uptake rate of its immune complexes[114]. They hypothesized that the slow uptake rate of immune complexes was partly caused by their surface charges. Remarkably, surface charge engineering of the variable regions of antibody, resulted in improved recycling performance of the antibody[114]. Thus, it may be possible to improve uptake of the recycling antibody A01 through surface charge

engineering. Further, Fc mutations reported to result in antigen sweeping activity of the antibody can be incorporated in antibody A01 to improve its performance[109,115]. Nevertheless, the assessment of recycling antibodies in a cellular assay like HERA, has shown conclusively the significant impact of Fabs and antigen-binding on the cellular transport properties of the antibodies. Such properties include, but are not limited to, enhanced cellular uptake, increased recycling, or accumulation inside the cells. These observations are crucial to take into account before progressing to *in vivo* models[78].

## 6.4. Looking into the future – the evolving field of recycling antibodies

Antibodies with pH-dependent antigen-binding properties, such as recycling or sweeping antibodies, present an ingenious approach to achieving efficient treatments. The engineering of pH-dependent antigen-binding antibodies was first reported about 12 years ago[105]. Since then, one pH-dependent antigen-binding antibody has already been approved by FDA, and another is in clinical trials, indicating the high therapeutic potential of such antibodies[114,116,129]. Moreover, exploring the application of such antibodies against a wide range of targets, as well as their coupling to other antibody engineering strategies are contributing to the fast evolution of this field[108]. An impressive example of this is illustrated in a recent study by Bogen et al., where a bispecific antibody was engineered to target two crucial markers of cancer, CEACAM5, and CEACAM6, in a pH-dependent and non-pH-dependent manner respectively[128]. Since CEACAM5 is often shed from tumors, it intercepts the non-pH-dependent anti-CEACAM5 antibodies in the bloodstream and hinders them from targeting the tumor. The bispecific antibody developed by Bogen et al. may enable the elimination of soluble CEACAM5 via pH-dependent binding, and facilitate an improved reach of the antibody to tumors where both the markers, CEACAM5 and CEACAM6, can be targeted by the bispecific antibody[128]. Importantly, the bispecific antibody with only one Fab arm showing pH-dependent antigen-binding property was achieved via light chain engineering. The same histidine-doped variable light chain ($V_L$) was paired with two different variable heavy chains ($V_H$), which resulted in conferring pH-dependent binding to CEACAM5-targeting $V_H/V_L$ pair, but not to the CEACAM6-targeting $V_H/V_L$ pair[128]. This explicitly demonstrates the influence that the light chain can have on pH-dependent antigen-binding, which has been directly observed in the work presented in this thesis. Thus, light chain engineering is a potential strategy, and should be considered when incorporating pH-dependent antigen-binding properties in an antibody.

An alternative modality for recycling antibodies that has been proposed is the use of antibodies that bind antigens in the presence of high levels of calcium ions in the bloodstream and release them in endosomes where the calcium ion concentration is about 650-fold lower[113]. In contrast to pH-dependent antibodies that often rely on the $pK_a$ of histidine and require a positive epitope, calcium-dependent antibodies circumvent this requirement and thus, may find utility in targeting a wider range of antigens. However, calcium-binding motifs are rarely found in human antibodies[113]. Consequently, the development of calcium-dependent recycling antibodies may require incorporation of calcium-binding motifs in the antibody scaffold, the result of which remains to be seen[113].

*In vitro* display technologies present an attractive approach to discovering antibodies with desired binding characteristics, as it is possible to select antibodies at various conditions, including non-physiological ones, such as low pH environments. Indeed, several studies have employed phage display or yeast display technology to discover recycling antibodies[106]. While these techniques have proven successful in discovering recycling antibodies, the antibody formats used in these techniques are often scFvs or Fabs, which typically require reformatting into full-length antibodies for their further investigation and final application[134]. As antibody reformatting can at times result in loss or alterations in binding characteristics and activity, it is sometimes beneficial to employ alternative antibody display systems, which allow for the selection of full-length antibodies, i.e., the final desired antibody format[135,136]. In this regard, yeast display system can be further explored for selection of full-length antibodies pH-dependent antibodies with pH-dependent antigen-binding properties. Mammalian display technology is another promising option to explore as it provides a favourable expression apparatus for full-length antibodies and has also been coupled to FACS and microfluidic sorting systems for high-throughput antibody selections[120,137]. However, since selections for recycling antibodies will probably require exposing antibody-displaying mammalian cells to low pH conditions, and given that cells can be more susceptible to alterations in their environment than phages, it would thus be important to explore which pH ranges do not negatively impact the viability and behaviour of the employed cells. Alternatively, the natural selection-mimicking technique of directed evolution is another promising avenue that may find utility in the discovery of pH-dependent antigen-binding antibodies[134,138]. This technique involves successive rounds of genetic variation and selection of antibodies with desired properties[138]. Although, directed evolution is already being applied in the field of antibodies, it is so far unexplored in the context of pH-dependent antibody discovery.

While the field of recycling antibodies is quickly evolving, the work presented in this thesis has contributed to its advancement in several ways. By combining antibody libraries with naturally occurring variable domains, light chain engineering, *in vitro* (phage) display selection strategies, biophysical techniques, and cellular assays, this thesis presents the successful discovery of recycling antibodies against antigens (snake toxins) that have not been explored in this context before. Additionally, the studies conducted in this thesis have explored the effects of Fab region and antigen-binding on the cellular transport properties of the recycling antibodies, which can influence their performance as recycling antibodies. The protocols developed, and the knowledge generated in the work behind this thesis will enable further research and development of recycling antibodies against various targets, including the ones of neglected diseases such as snakebite envenoming, where biotechnological revolutions are highly needed.

# References


1. Snakebite envenoming [Internet]. [cited 2023 Jan 5]. Available from: https://www.who.int/news-room/fact-sheets/detail/snakebite-envenoming

2. Gutiérrez JM, Calvete JJ, Habib AG, Harrison RA, Williams DJ, Warrell DA. Snakebite envenoming. Nat Rev Dis Primers. 2017 Sep 14;3(1):1–21.

3. Fox S, Rathuwithana AC, Kasturiratne A, Lalloo DG, de Silva HJ. Underestimation of snakebite mortality by hospital statistics in the Monaragala District of Sri Lanka. Trans R Soc Trop Med Hyg. 2006 Jul;100(7):693–5.

4. Chippaux JP. Estimate of the burden of snakebites in sub-Saharan Africa: a meta-analytic approach. Toxicon. 2011 Mar 15;57(4):586–99.

5. Mohapatra B, Warrell DA, Suraweera W, Bhatia P, Dhingra N, Jotkar RM, et al. Snakebite mortality in India: a nationally representative mortality survey. PLoS Negl Trop Dis. 2011 Apr 12;5(4):e1018.

6. Kasturiratne A, Wickremasinghe AR, Silva N de, Gunawardena NK, Pathmeswaran A, Premaratna R, et al. The Global Burden of Snakebite: A Literature Analysis and Modelling Based on Regional Estimates of Envenoming and Deaths. PLOS Medicine. 2008 Nov 4;5(11):e218.

7. Snakebite envenoming | Nature Reviews Disease Primers [Internet]. [cited 2023 Jan 6]. Available from: https://www.nature.com/articles/nrdp201763

8. Harrison RA, Hargreaves A, Wagstaff SC, Faragher B, Lalloo DG. Snake Envenoming: A Disease of Poverty. PLoS Negl Trop Dis. 2009 Dec 22;3(12):e569.

9. Gutiérrez JM, Theakston RDG, Warrell DA. Confronting the Neglected Problem of Snake Bite Envenoming: The Need for a Global Partnership. PLOS Medicine. 2006 Jun 6;3(6):e150.

10. Habib AG, Kuznik A, Hamza M, Abdullahi MI, Chedi BA, Chippaux JP, et al. Snakebite is Under Appreciated: Appraisal of Burden from West Africa. PLoS Negl Trop Dis. 2015 Sep;9(9):e0004088.

11. Hasan SMK, Basher A, Molla AA, Sultana NK, Faiz MA. The impact of snake bite on household economy in Bangladesh. Trop Doct. 2012 Jan;42(1):41–3.

12. Chippaux JP. Snakebite envenomation turns again into a neglected tropical disease! J Venom Anim Toxins Incl Trop Dis. 2017 Aug 8;23:38.

13. Warrell DA. Snake bite. The Lancet. 2010 Jan 2;375(9708):77–88.

14. Tasoulis T, Isbister GK. A Review and Database of Snake Venom Proteomes. Toxins (Basel). 2017 Sep 18;9(9):290.

15. Lauridsen LP, Laustsen AH, Lomonte B, Gutiérrez JM. Exploring the venom of the forest cobra snake: Toxicovenomics and antivenom profiling of Naja melanoleuca. Journal of Proteomics. 2017 Jan 6;150:98–108.

16. Laustsen AH, Lomonte B, Lohse B, Fernández J, Gutiérrez JM. Unveiling the nature of black mamba (Dendroaspis polylepis) venom through venomics and antivenom immunoprofiling: Identification of key toxin targets for antivenom development. Journal of Proteomics. 2015 Apr;119:126–42.

17. Rao WQ, Kalogeropoulos K, Allentoft ME, Gopalakrishnan S, Zhao WN, Workman CT, et al. The rise of genomics in snake venom research: recent advances and future perspectives. GigaScience. 2022;11(giac024).

18. Casewell NR, Jackson TNW, Laustsen AH, Sunagar K. Causes and Consequences of Snake Venom Variation. Trends in Pharmacological Sciences. 2020 Aug 1;41(8):570–81.

19. Calvete JJ, Sanz L, Cid P, de la Torre P, Flores-Díaz M, Dos Santos MC, et al. Snake venomics of the Central American rattlesnake Crotalus simus and the South American Crotalus durissus complex points to neurotoxicity as an adaptive paedomorphic trend along Crotalus dispersal in South America. J Proteome Res. 2010 Jan;9(1):528–44.

20. Calvete JJ, Sanz L, Pérez A, Borges A, Vargas AM, Lomonte B, et al. Snake population venomics and antivenomics of Bothrops atrox: Paedomorphism along its transamazonian dispersal and implications of geographic venom variability on snakebite management. J Proteomics. 2011 Apr 1;74(4):510–27.

21. Madrigal M, Sanz L, Flores-Díaz M, Sasa M, Núñez V, Alape-Girón A, et al. Snake venomics across genus Lachesis. Ontogenetic changes in the venom composition of Lachesis stenophrys and comparative proteomics of the venoms of adult Lachesis melanocephala and Lachesis acrochorda. J Proteomics. 2012 Dec 21;77:280–97.

22. Bermúdez-Méndez E, Fuglsang-Madsen A, Føns S, Lomonte B, Gutiérrez JM, Laustsen AH. Innovative Immunization Strategies for Antivenom Development. Toxins (Basel). 2018 Nov 2;10(11):452.

23. Nirthanan S. Snake three-finger α-neurotoxins and nicotinic acetylcholine receptors: molecules, mechanisms and medicine. Biochem Pharmacol. 2020 Nov;181:114168.

24. Borges RJ, Lemke N, Fontes MRM. PLA2-like proteins myotoxic mechanism: a dynamic model description. Sci Rep. 2017 Nov 14;7(1):15514.

25. Francis B, Gutierrez JM, Lomonte B, Kaiser II. Myotoxin II from Bothrops asper (terciopelo) venom is a lysine-49 phospholipase A2. Archives of Biochemistry and Biophysics. 1991 Feb 1;284(2):352–9.

26. Laustsen AH, Engmark M, Clouser C, Timberlake S, Vigneault F, Gutiérrez JM, et al. Exploration of immunoglobulin transcriptomes from mice immunized with three-finger toxins and phospholipases A2 from the Central American coral snake, Micrurus nigrocinctus. PeerJ. 2017;5:e2924.

27. Ledsgaard L, Laustsen AH, Pus U, Wade J, Villar P, Boddum K, et al. In vitro discovery of a human monoclonal antibody that neutralizes lethality of cobra snake venom. MAbs. 14(1):2085536.

28. Kini RM, Doley R. Structure, function and evolution of three-finger toxins: mini proteins with multiple targets. Toxicon. 2010 Nov;56(6):855–67.

29. de Paula RC, Castro HC, Rodrigues CR, Melo PA, Fuly AL. Structural and pharmacological features of phospholipases A2 from snake venoms. Protein Pept Lett. 2009;16(8):899–907.

30. Gutiérrez JM, Escalante T, Hernández R, Gastaldello S, Saravia-Otten P, Rucavado A. Why is Skeletal Muscle Regeneration Impaired after Myonecrosis Induced by Viperid Snake Venoms? Toxins. 2018 May;10(5):182.

31. Montecucco C, Gutiérrez JM, Lomonte B. Cellular pathology induced by snake venom phospholipase A2 myotoxins and neurotoxins: common aspects of their mechanisms of action. Cell Mol Life Sci. 2008 Sep;65(18):2897–912.

32. Lomonte B. Lys49 myotoxins, secreted phospholipase A2-like proteins of viperid venoms: A comprehensive review. Toxicon. 2023 Jan 9;224:107024.

33. Gutiérrez JM, Ownby CL. Skeletal muscle degeneration induced by venom phospholipases A2: insights into the mechanisms of local and systemic myotoxicity. Toxicon. 2003 Dec 15;42(8):915–31.

34. Fernandes CAH, Borges RJ, Lomonte B, Fontes MRM. A structure-based proposal for a comprehensive myotoxic mechanism of phospholipase A2-like proteins from viperid snake venoms. Biochimica et Biophysica Acta (BBA) - Proteins and Proteomics. 2014 Dec 1;1844(12):2265–76.

35. Guidelines for the Production, Control and Regulation of Snake Antivenom Immunoglobulins [Internet]. WHO - Prequalification of Medical Products (IVDs, Medicines, Vaccines and Immunization Devices, Vector Control). 2022 [cited 2023 Jan 5]. Available from: https://extranet.who.int/pqweb/vaccines/guidelines-production-control-and-regulation-snake-antivenom-immunoglobulins

36. Gutiérrez JM, León G, Lomonte B, Angulo Y. Antivenoms for snakebite envenomings. Inflamm Allergy Drug Targets. 2011 Oct;10(5):369–80.

37. León G, Segura Á, Gómez A, Hernandez A, Navarro D, Villalta M, et al. Industrial Production and Quality Control of Snake Antivenoms. In: Gopalakrishnakone P, Calvete JJ, editors. Toxinology: Venom Genomics and Proteomics [Internet]. Dordrecht: Springer Netherlands; 2021 [cited 2023 Jan 5]. p. 1–22. Available from: https://doi.org/10.1007/978-94-007-6649-5_24-3

38. Pucca MB, Cerni FA, Janke R, Bermúdez-Méndez E, Ledsgaard L, Barbosa JE, et al. History of Envenoming Therapy and Current Perspectives. Frontiers in Immunology [Internet]. 2019 [cited 2023 Jan 5];10. Available from: https://www.frontiersin.org/articles/10.3389/fimmu.2019.01598

39. Hawgood BJ. Doctor Albert Calmette 1863-1933: founder of antivenomous serotherapy and of antituberculous BCG vaccination. Toxicon. 1999 Sep;37(9):1241–58.

40. Knudsen C, Ledsgaard L, Dehli RI, Ahmadi S, Sørensen CV, Laustsen AH. Engineering and design considerations for next-generation snakebite antivenoms. Toxicon. 2019 Sep;167:67–75.

41. Laustsen AH, Engmark M, Milbo C, Johannesen J, Lomonte B, Gutiérrez JM, et al. From Fangs to Pharmacology: The Future of Snakebite Envenoming Therapy. Curr Pharm Des. 2016;22(34):5270–93.

42. de Silva HA, Ryan NM, de Silva HJ. Adverse reactions to snake antivenom, and their prevention and treatment. Br J Clin Pharmacol. 2016 Mar;81(3):446–52.

43. Rawat S, Laing G, Smith DC, Theakston D, Landon J. A new antivenom to treat eastern coral snake (Micrurus fulvius fulvius) envenoming. Toxicon. 1994 Feb;32(2):185–90.

44. Laustsen AH, Johansen KH, Engmark M, Andersen MR. Recombinant snakebite antivenoms: A cost-competitive solution to a neglected tropical disease? PLoS Negl Trop Dis. 2017 Feb 3;11(2):e0005361.

45. Silva A, Isbister GK. Current research into snake antivenoms, their mechanisms of action and applications. Biochem Soc Trans. 2020 Apr 29;48(2):537–46.

46. Laustsen AH. Antivenom in the Age of Recombinant DNA Technology [Internet]. Handbook of Venoms and Toxins of Reptiles. CRC Press; 2021 [cited 2023 Jan 5]. Available from: https://www.taylorfrancis.com/chapters/edit/10.1201/9780429054204-38/antivenom-age-recombinant-dna-technology-andreas-laustsen

47. Laustsen AH, Karatt-Vellatt A, Masters EW, Arias AS, Pus U, Knudsen C, et al. In vivo neutralization of dendrotoxin-mediated neurotoxicity of black mamba venom by oligoclonal human IgG antibodies. Nat Commun. 2018 Oct 2;9(1):3928.

48. Ahmadi S, Pucca MB, Jürgensen JA, Janke R, Ledsgaard L, Schoof EM, et al. An in vitro methodology for discovering broadly-neutralizing monoclonal antibodies. Sci Rep. 2020 Jul 1;10(1):10765.

49. Kini RM, Sidhu SS, Laustsen AH. Biosynthetic Oligoclonal Antivenom (BOA) for Snakebite and Next-Generation Treatments for Snakebite Victims. Toxins (Basel). 2018 Dec 13;10(12):534.

50. Laustsen AH. Recombinant Antivenoms. University of Copenhagen; 2016.

51. Laustsen AH, María Gutiérrez J, Knudsen C, Johansen KH, Bermúdez-Méndez E, Cerni FA, et al. Pros and cons of different therapeutic antibody formats for recombinant antivenom development. Toxicon. 2018 May 1;146:151–75.

52. Hamza M, Knudsen C, Gnanathasan CA, Monteiro W, Lewin MR, Laustsen AH, et al. Clinical management of snakebite envenoming: Future perspectives. Toxicon: X. 2021 Sep 1;11:100079.

53. Jenkins TP, Laustsen AH. Cost of Manufacturing for Recombinant Snakebite Antivenoms. Frontiers in Bioengineering and Biotechnology [Internet]. 2020 [cited 2023 Jan 5];8. Available from: https://www.frontiersin.org/articles/10.3389/fbioe.2020.00703

54. Cassidy JT, Nordby GL. Human serum immunoglobulin concentrations: prevalence of immunoglobulin deficiencies. J Allergy Clin Immunol. 1975 Jan;55(1):35–48.

55. Sankar K, Hoi KH, Hötzel I. Dynamics of heavy chain junctional length biases in antibody repertoires. Commun Biol. 2020 May 1;3(1):1–10.

56. Kaplon H, Chenoweth A, Crescioli S, Reichert JM. Antibodies to watch in 2022. MAbs. 2022;14(1):2014296.

57. Morell A, Terry WD, Waldmann TA. Metabolic properties of IgG subclasses in man. J Clin Invest. 1970 Apr;49(4):673–80.

58. Vidarsson G, Dekkers G, Rispens T. IgG Subclasses and Allotypes: From Structure to Effector Functions. Frontiers in Immunology [Internet]. 2014 [cited 2023 Jan 5];5. Available from: https://www.frontiersin.org/articles/10.3389/fimmu.2014.00520

59. Mankarious S, Lee M, Fischer S, Pyun KH, Ochs HD, Oxelius VA, et al. The half-lives of IgG subclasses and specific antibodies in patients with primary immunodeficiency who are receiving intravenously administered immunoglobulin. J Lab Clin Med. 1988 Nov;112(5):634–40.

60. Salfeld JG. Isotype selection in antibody engineering. Nat Biotechnol. 2007 Dec;25(12):1369–72.

61. Tang Y, Cain P, Anguiano V, Shih JJ, Chai Q, Feng Y. Impact of IgG subclass on molecular properties of monoclonal antibodies. mAbs. 2021 Jan 1;13(1):1993768.

62. Ghetie V, Hubbard JG, Kim JK, Tsen MF, Lee Y, Ward ES. Abnormally short serum half-lives of IgG in beta 2-microglobulin-deficient mice. Eur J Immunol. 1996 Mar;26(3):690–6.

63. Junghans RP, Anderson CL. The protection receptor for IgG catabolism is the beta2-microglobulin-containing neonatal intestinal transport receptor. Proceedings of the National Academy of Sciences. 1996 May 28;93(11):5512–6.

64. Israel EJ, Wilsker DF, Hayes KC, Schoenfeld D, Simister NE. Increased clearance of IgG in mice that lack beta 2-microglobulin: possible protective role of FcRn. Immunology. 1996 Dec;89(4):573–8.

65. Raghavan M, Bonagura VR, Morrison SL, Bjorkman PJ. Analysis of the pH dependence of the neonatal Fc receptor/immunoglobulin G interaction using antibody and receptor variants. Biochemistry. 1995 Nov 14;34(45):14649–57.

66. Ghetie V, Popov S, Borvak J, Radu C, Matesoi D, Medesan C, et al. Increasing the serum persistence of an IgG fragment by random mutagenesis. Nat Biotechnol. 1997 Jul;15(7):637–40.

67. Vaughn DE, Bjorkman PJ. Structural basis of pH-dependent antibody binding by the neonatal Fc receptor. Structure. 1998 Jan 15;6(1):63–73.

68. Martin WL, West AP, Gan L, Bjorkman PJ. Crystal structure at 2.8 A of an FcRn/heterodimeric Fc complex: mechanism of pH-dependent binding. Mol Cell. 2001 Apr;7(4):867–77.

69. Simister NE, Mostov KE. An Fc receptor structurally related to MHC class I antigens. Nature. 1989 Jan 12;337(6203):184–7.

70. Kim JK, Firan M, Radu CG, Kim CH, Ghetie V, Ward ES. Mapping the site on human IgG for binding of the MHC class I-related receptor, FcRn. Eur J Immunol. 1999 Sep;29(9):2819–25.

71. Burmeister WP, Huber AH, Bjorkman PJ. Crystal structure of the complex of rat neonatal Fc receptor with Fc. Nature. 1994 Nov 24;372(6504):379–83.

72. Oganesyan V, Damschroder MM, Cook KE, Li Q, Gao C, Wu H, et al. Structural Insights into Neonatal Fc Receptor-based Recycling Mechanisms. J Biol Chem. 2014 Mar 14;289(11):7812–24.

73. Gan Z, Ram S, Vaccaro C, Ober RJ, Ward ES. Analyses of the recycling receptor, FcRn, in live cells reveal novel pathways for lysosomal delivery. Traffic. 2009 May;10(5):600.

74. Lencer WI, Blumberg RS. A passionate kiss, then run: exocytosis and recycling of IgG by FcRn. Trends Cell Biol. 2005 Jan;15(1):5–9.

75. Ward ES, Martinez C, Vaccaro C, Zhou J, Tang Q, Ober RJ. From sorting endosomes to exocytosis: association of Rab4 and Rab11 GTPases with the Fc receptor, FcRn, during recycling. Mol Biol Cell. 2005 Apr;16(4):2028–38.

76. Ober RJ, Martinez C, Lai X, Zhou J, Ward ES. Exocytosis of IgG as mediated by the receptor, FcRn: an analysis at the single-molecule level. Proc Natl Acad Sci U S A. 2004 Jul 27;101(30):11076–81.

77. Ober RJ, Martinez C, Vaccaro C, Zhou J, Ward ES. Visualizing the Site and Dynamics of IgG Salvage by the MHC Class I-Related Receptor, FcRn1. The Journal of Immunology. 2004 Feb 15;172(4):2021–9.

78. Grevys A, Nilsen J, Sand KMK, Daba MB, Øynebråten I, Bern M, et al. A human endothelial cell-based recycling assay for screening of FcRn targeted molecules. Nat Commun. 2018 Feb 12;9(1):621.

79. Zalevsky J, Chamberlain AK, Horton HM, Karki S, Leung IWL, Sproule TJ, et al. Enhanced antibody half-life improves in vivo activity. Nat Biotechnol. 2010 Feb;28(2):157–9.

80. Acqua WFD, Woods RM, Ward ES, Palaszynski SR, Patel NK, Brewah YA, et al. Increasing the Affinity of a Human IgG1 for the Neonatal Fc Receptor: Biological Consequences1. The Journal of Immunology. 2002 Nov 1;169(9):5171–80.

81. Nnane IP, Han C, Jiao Q, Tam SH, Davis HM, Xu Z. Modification of the Fc Region of a Human Anti-oncostatin M Monoclonal Antibody for Higher Affinity to FcRn Receptor and Extension of Half-life in Cynomolgus Monkeys. Basic Clin Pharmacol Toxicol. 2017 Jul;121(1):13–21.

82. Ko S, Park S, Sohn MH, Jo M, Ko BJ, Na JH, et al. An Fc variant with two mutations confers prolonged serum half-life and enhanced effector functions on IgG antibodies. Exp Mol Med. 2022 Nov;54(11):1850–61.

83. Maeda A, Iwayanagi Y, Haraya K, Tachibana T, Nakamura G, Nambu T, et al. Identification of human IgG1 variant with enhanced FcRn binding and without increased binding to rheumatoid factor autoantibody. mAbs. 2017 Jul 4;9(5):844–53.

84. Kang TH, Jung ST. Boosting therapeutic potency of antibodies by taming Fc domain functions. Exp Mol Med. 2019 Nov;51(11):1–9.

85. Dall'Acqua WF, Kiener PA, Wu H. Properties of human IgG1s engineered for enhanced binding to the neonatal Fc receptor (FcRn). J Biol Chem. 2006 Aug 18;281(33):23514–24.

86. Borrok MJ, Wu Y, Beyaz N, Yu XQ, Oganesyan V, Dall'Acqua WF, et al. pH-dependent Binding Engineering Reveals an FcRn Affinity Threshold That Governs IgG Recycling. J Biol Chem. 2015 Feb 13;290(7):4282–90.

87. Ng CM, Fielder PJ, Jin J, Deng R. Mechanism-Based Competitive Binding Model to Investigate the Effect of Neonatal Fc Receptor Binding Affinity on the Pharmacokinetic of Humanized Anti-VEGF Monoclonal IgG1 Antibody in Cynomolgus Monkey. AAPS J. 2016 Jul;18(4):948–59.

88. Ward ES, Ober RJ. Targeting FcRn to generate antibody-based therapeutics. Trends Pharmacol Sci. 2018 Oct;39(10):892–904.

89. Robbie GJ, Criste R, Dall'acqua WF, Jensen K, Patel NK, Losonsky GA, et al. A novel investigational Fc-modified humanized monoclonal antibody, motavizumab-YTE, has an extended half-life in healthy adults. Antimicrob Agents Chemother. 2013 Dec;57(12):6147–53.

90. Carter PJ, Lazar GA. Next generation antibody drugs: pursuit of the 'high-hanging fruit'. Nat Rev Drug Discov. 2018 Mar;17(3):197–223.

91. Jain T, Sun T, Durand S, Hall A, Houston NR, Nett JH, et al. Biophysical properties of the clinical-stage antibody landscape. Proc Natl Acad Sci U S A. 2017 Jan 31;114(5):944–9.

92. Wang W, Lu P, Fang Y, Hamuro L, Pittman T, Carr B, et al. Monoclonal antibodies with identical Fc sequences can bind to FcRn differentially with pharmacokinetic consequences. Drug Metab Dispos. 2011 Sep;39(9):1469–77.

93. Gjølberg TT, Frick R, Mester S, Foss S, Grevys A, Høydahl LS, et al. Biophysical differences in IgG1 Fc-based therapeutics relate to their cellular handling, interaction with FcRn and plasma half-life. Commun Biol. 2022 Aug 18;5(1):1–17.

94. Grevys A, Frick R, Mester S, Flem-Karlsen K, Nilsen J, Foss S, et al. Antibody variable sequences have a pronounced effect on cellular transport and plasma half-life. iScience. 2022 Feb 18;25(2):103746.

95. Brinkhaus M, Pannecoucke E, van der Kooi EJ, Bentlage AEH, Derksen NIL, Andries J, et al. The Fab region of IgG impairs the internalization pathway of FcRn upon Fc engagement. Nat Commun. 2022 Oct 14;13(1):6073.

96. Schoch A, Kettenberger H, Mundigl O, Winter G, Engert J, Heinrich J, et al. Charge-mediated influence of the antibody variable domain on FcRn-dependent pharmacokinetics. Proc Natl Acad Sci U S A. 2015 May 12;112(19):5997–6002.

97. Schlothauer T, Rueger P, Stracke JO, Hertenberger H, Fingas F, Kling L, et al. Analytical FcRn affinity chromatography for functional characterization of monoclonal antibodies. MAbs. 2013;5(4):576–86.

98. Piche-Nicholas NM, Avery LB, King AC, Kavosi M, Wang M, O'Hara DM, et al. Changes in complementarity-determining regions significantly alter IgG binding to the neonatal Fc receptor (FcRn) and pharmacokinetics. MAbs. 2018 Jan;10(1):81–94.

99. Jensen PF, Schoch A, Larraillet V, Hilger M, Schlothauer T, Emrich T, et al. A Two-pronged Binding Mechanism of IgG to the Neonatal Fc Receptor Controls Complex Stability and IgG Serum Half-life *. Molecular & Cellular Proteomics. 2017 Mar 1;16(3):451–6.

100. Jensen PF, Larraillet V, Schlothauer T, Kettenberger H, Hilger M, Rand KD. Investigating the Interaction between the Neonatal Fc Receptor and Monoclonal Antibody Variants by Hydrogen/Deuterium Exchange Mass Spectrometry *. Molecular & Cellular Proteomics. 2015 Jan 1;14(1):148–61.

101. Sun Y, Estevez A, Schlothauer T, Wecksler AT. Antigen physiochemical properties allosterically effect the IgG Fc-region and Fc neonatal receptor affinity. MAbs. 2020;12(1):1802135.

102. Weiner LM, Surana R, Wang S. Monoclonal antibodies: versatile platforms for cancer immunotherapy. Nat Rev Immunol. 2010 May;10(5):317–27.

103. Makowski EK, Kinnunen PC, Huang J, Wu L, Smith MD, Wang T, et al. Co-optimization of therapeutic antibody affinity and specificity using machine learning models that generalize to novel mutational space. Nat Commun. 2022 Jul 1;13(1):3788.

104. Bostrom J, Lee CV, Haber L, Fuh G. Improving Antibody Binding Affinity and Specificity for Therapeutic Development. In: Dimitrov AS, editor. Therapeutic Antibodies: Methods and Protocols [Internet]. Totowa, NJ: Humana Press; 2009 [cited 2023 Jan 5]. p. 353–76. (Methods in Molecular Biology™). Available from: https://doi.org/10.1007/978-1-59745-554-1_19

105. Igawa T, Ishii S, Tachibana T, Maeda A, Higuchi Y, Shimaoka S, et al. Antibody recycling by engineered pH-dependent antigen-binding improves the duration of antigen neutralization. Nat Biotechnol. 2010 Nov;28(11):1203–7.

106. Igawa T, Haraya K, Hattori K. Sweeping antibody as a novel therapeutic antibody modality capable of eliminating soluble antigens from circulation. Immunological Reviews. 2016;270(1):132–51.

107. Devanaboyina SC, Lynch SM, Ober RJ, Ram S, Kim D, Puig-Canto A, et al. The effect of pH dependence of antibody-antigen interactions on subcellular trafficking dynamics. mAbs. 2013 Nov 1;5(6):851–9.

108. Klaus T, Deshmukh S. pH-responsive antibodies for therapeutic applications. Journal of Biomedical Science. 2021 Jan 22;28(1):11.

109. Igawa T, Maeda A, Haraya K, Tachibana T, Iwayanagi Y, Mimoto F, et al. Engineered Monoclonal Antibody with Novel Antigen-Sweeping Activity In Vivo. PLOS ONE. 2013 May 7;8(5):e63236.

110. Watkins JM, Watkins JD. An Engineered Monovalent Anti–TNF-α Antibody with pH-Sensitive Binding Abrogates Immunogenicity in Mice following a Single Intravenous Dose. The Journal of Immunology. 2022 Aug 15;209(4):829–39.

111. Bonvin P, Venet S, Fontaine G, Ravn U, Gueneau F, Kosco-Vilbois M, et al. De novo isolation of antibodies with pH-dependent binding properties. mAbs. 2015 Mar 4;7(2):294–302.

112. Fukuzawa T, Sampei Z, Haraya K, Ruike Y, Shida-Kawazoe M, Shimizu Y, et al. Long lasting neutralization of C5 by SKY59, a novel recycling antibody, is a potential therapy for complement-mediated diseases. Sci Rep. 2017 Apr 24;7(1):1080.

113. Hironiwa N, Ishii S, Kadono S, Iwayanagi Y, Mimoto F, Habu K, et al. Calcium-dependent antigen-binding as a novel modality for antibody recycling by endosomal antigen dissociation. MAbs. 2015 Oct 23;8(1):65–73.

114. Sampei Z, Haraya K, Tachibana T, Fukuzawa T, Shida-Kawazoe M, Gan SW, et al. Antibody engineering to generate SKY59, a long-acting anti-C5 recycling antibody. PLOS ONE. 2018 Dec 28;13(12):e0209509.

115. Iwayanagi Y, Igawa T, Maeda A, Haraya K, Wada NA, Shibahara N, et al. Inhibitory FcγRIIb-Mediated Soluble Antigen Clearance from Plasma by a pH-Dependent Antigen-Binding Antibody and Its Enhancement by Fc Engineering. J Immunol. 2015 Oct 1;195(7):3198–205.

116. Lee JW, Sicre de Fontbrune F, Wong Lee Lee L, Pessoa V, Gualandro S, Füreder W, et al. Ravulizumab (ALXN1210) vs eculizumab in adult patients with PNH naive to complement inhibitors: the 301 study. Blood. 2019 Feb 7;133(6):530–9.

117. Sheridan D, Yu ZX, Zhang Y, Patel R, Sun F, Lasaro MA, et al. Design and preclinical characterization of ALXN1210: A novel anti-C5 antibody with extended duration of action. PLOS ONE. 2018 Apr 12;13(4):e0195909.

118. Laustsen AH. How can monoclonal antibodies be harnessed against neglected tropical diseases and other infectious diseases? Expert Opinion on Drug Discovery. 2019 Nov 2;14(11):1103–12.

119. Kroetsch A, Qiao C, Heavey M, Guo L, Shah DK, Park S. Engineered pH-dependent recycling antibodies enhance elimination of Staphylococcal enterotoxin B superantigen in mice. MAbs. 2018 Dec 11;11(2):411–21.

120. Fernández-Quintero ML. Assessing developability early in the discovery process for novel biologics. Manuscript in preparation.

121. Strohl WR, Strohl LM, editors. 16 - Development issues: antibody stability, developability, immunogenicity, and comparability. In: Therapeutic Antibody Engineering [Internet]. Woodhead Publishing; 2012 [cited 2022 Nov 18]. p. 377–595. (Woodhead Publishing Series in Biomedicine). Available from: https://www.sciencedirect.com/science/article/pii/B9781907568374500166

122. Schofield DJ, Pope AR, Clementel V, Buckell J, Chapple SD, Clarke KF, et al. Application of phage display to high throughput antibody generation and characterization. Genome Biol. 2007;8(11):R254.

123. Smith GP. Filamentous fusion phage: novel expression vectors that display cloned antigens on the virion surface. Science. 1985 Jun 14;228(4705):1315–7.

124. McCafferty J, Griffiths AD, Winter G, Chiswell DJ. Phage antibodies: filamentous phage displaying antibody variable domains. Nature. 1990 Dec 6;348(6301):552–4.

125. Ledsgaard L, Kilstrup M, Karatt-Vellatt A, McCafferty J, Laustsen AH. Basics of Antibody Phage Display Technology. Toxins (Basel). 2018 Jun 9;10(6):236.

126. Ledsgaard L, Ljungars A, Rimbault C, Sørensen CV, Tulika T, Wade J, et al. Advances in antibody phage display technology. Drug Discovery Today. 2022 Aug 1;27(8):2151–69.

127. Igawa T, Mimoto F, Hattori K. pH-dependent antigen-binding antibodies as a novel therapeutic modality. Biochimica et Biophysica Acta (BBA) - Proteins and Proteomics. 2014 Nov 1;1844(11):1943–50.

128. Bogen JP, Hinz SC, Grzeschik J, Ebenig A, Krah S, Zielonka S, et al. Dual Function pH Responsive Bispecific Antibodies for Tumor Targeting and Antigen Depletion in Plasma. Frontiers in Immunology [Internet]. 2019 [cited 2023 Jan 12];10. Available from: https://www.frontiersin.org/articles/10.3389/fimmu.2019.01892

129. Research C for DE and. FDA approves ravulizumab-cwvz for paroxysmal nocturnal hemoglobinuria. FDA [Internet]. 2019 Dec 20 [cited 2023 Jan 11]; Available from: https://www.fda.gov/drugs/resources-information-approved-drugs/fda-approves-ravulizumab-cwvz-paroxysmal-nocturnal-hemoglobinuria

130. Sanhajariya S, Duffull SB, Isbister GK. Pharmacokinetics of Snake Venom. Toxins (Basel). 2018 Feb 7;10(2):73.

131. Latvala S, Jacobsen B, Otteneder MB, Herrmann A, Kronenberg S. Distribution of FcRn Across Species and Tissues. Journal of Histochemistry and Cytochemistry. 2017 Jun;65(6):321.

132. Ledsgaard L. Discovery and optimization of a broadly-neutralizing human monoclonal antibody against long-chain α-neurotoxins from snakes. Accepted. Nature Communiations.

133. Roopenian DC, Akilesh S. FcRn: the neonatal Fc receptor comes of age. Nat Rev Immunol. 2007 Sep;7(9):715–25.

134. Klemm J, Pekar L, Krah S, Zielonka S. Antibody Display Systems. In: Rüker F, Wozniak-Knopp G, editors. Introduction to Antibody Engineering [Internet]. Cham: Springer International Publishing; 2021 [cited 2023 Jan 14]. p. 65–96. (Learning Materials in Biosciences). Available from: https://doi.org/10.1007/978-3-030-54630-4_4

135. Steinwand M, Droste P, Frenzel A, Hust M, Dübel S, Schirrmann T. The influence of antibody fragment format on phage display based affinity maturation of IgG. MAbs. 2014 Jan 1;6(1):204–18.

136. Xiao X, Douthwaite JA, Chen Y, Kemp B, Kidd S, Percival-Alwyn J, et al. A high-throughput platform for population reformatting and mammalian expression of phage display libraries to enable functional screening as full-length IgG. mAbs. 2017 Aug 18;9(6):996–1006.

137. Valldorf B, Hinz SC, Russo G, Pekar L, Mohr L, Klemm J, et al. Antibody display technologies: selecting the cream of the crop. Biological Chemistry. 2022 Apr 1;403(5–6):455–77.

138. Wellner A, McMahon C, Gilman MSA, Clements JR, Clark S, Nguyen KM, et al. Rapid generation of potent antibodies by autonomous hypermutation in yeast. Nat Chem Biol. 2021 Oct;17(10):1057–64.